

**DIRECT-PUSH EC PROFILING TO DEFINE BRINE-IMPACTED  
GROUNDWATERS**

A thesis submitted to the College of Graduate Studies and Research in partial fulfillment  
of the requirements for the Degree of Master of Science in the Department of Geological

Sciences

University of Saskatchewan

Saskatoon

by

Kristian J. Hermann

© Copyright Kristian J. Hermann, April 2015. All rights reserved

## PERMISSION TO USE

In presenting this thesis in partial fulfilment of the requirements for a Postgraduate degree from the University of Saskatchewan, I agree that the Libraries of this University may make it freely available for inspection. I further agree that permission for copying of this thesis in any manner, in whole or in part, for scholarly purposes may be granted by the professor or professors who supervised my thesis work or, in their absence, by the Head of the Department or the Dean of the College in which my thesis work was done. It is understood that any copying or publication or use of this thesis or parts thereof for financial gain shall not be allowed without my written permission. It is also understood that due recognition shall be given to me and to the University of Saskatchewan in any scholarly use which may be made of any material in my thesis.

Requests for permission to copy or to make other use of material in this thesis in whole or part should be addressed to:

Head of the Department of Geological Sciences  
University of Saskatchewan  
114 Science Place  
Saskatoon, Saskatchewan  
Canada

## ABSTRACT

Delineating the extent of brine contamination in shallow groundwater systems using piezometers is costly and does not provide adequate data resolution. Direct-push (D-P) electrical conductivity (EC) profiling enables rapid *in situ* measurements of bulk soil EC ( $EC_a$ ) at the cm scale. Previous studies using D-P EC profiling to detect contaminant plumes have solely relied on  $EC_a$  measurements, and where attempts were made to isolate pore-water salinity variations from changes in  $EC_a$  they were accomplished using simple linear methods. In this study D-P EC profiling was used to define groundwater salinity distributions using an established soil conductance model and estimate the timing of groundwater contamination at a long-term potash mine in south-central Saskatchewan, Canada. The site was dominated by fine-grained postglacial and glacial sediments with known Na-K-Cl brine impacts resulting from mining activities. Coreholes (n=22) were drilled to 7.6-12.2 m below ground (mbg) to obtain continuous cores for detailed geologic descriptions and measurements of index parameters (n=522) below the water table. Pore-water EC ( $EC_w$ ) and Cl<sup>-</sup> results from squeezed core samples (n=142) at 12 locations were compared to  $EC_a$  measurements collected using a D-P probe adjacent to each corehole. Measured  $EC_w$  and pore-water Cl<sup>-</sup> results ranged from 1.94-55.1 mS/cm and 87-20,700 mg/L, respectively. *In situ* D-P EC values from logs collected adjacent to all 22 coreholes ranged from 2-8 mS/cm within the oxidized zone (5-6 mbg) and decreased to background values of 0.3-2 mS/cm within the underlying unoxidized zone. Significant linear  $EC_a$ - $EC_w$  regressions established for four lithological groups ( $r^2=0.78-0.95$ ) were used with porosity and dry density measurements to generate high-resolution depth profiles of  $EC_w$  from D-P EC measurements. A significant linear  $EC_w$ -Cl regression ( $r^2=0.92$ ) further enabled the generation of pore-water Cl<sup>-</sup> depth profiles from  $EC_w$  predictions. Observed 1D vertical profiles of Cl<sup>-</sup>,  $EC_w$ , and  $EC_a$  at three locations were modeled. Results suggested solute transport can be described as diffusion-dominated below depths of 3-5 mbg and that groundwater contamination began shortly after the onset of mining. Based on the results attained, this method can generate high-resolution depth profiles of pore-water salinity that can be used to define the lateral and vertical extent of brine contamination, dominant solute transport mechanisms, and timing of groundwater contamination.

## ACKNOWLEDGMENTS

I would like to thank my supervisor Dr. M. Jim Hendry for his guidance, patience, and most importantly for his continued support during my graduate research. Jim's unwavering enthusiasm and passion for research inspired me greatly during this project. I would also like to thank the members of my committee Dr. S. Lee Barbour, Dr. Matt Lindsay, and Dr. Jim Merriam for their interest in my research and their support and encouragement.

A special thanks to the Saskatchewan Potash Producers Association, NSERC, and the University of Saskatchewan for their financial support, without which this thesis would not have been possible. I would also like to acknowledge the staff and consultants at the unnamed potash mine where this research took place for their support and assistance and for providing technical reports referenced in this research.

A special thanks to Adrienne Bangsund for her assistance with field and laboratory work during this project. Many thanks to Erin Schmeling, Fina Nelson, and Virginia Chostner for their assistance with laboratory analysis, equipment training, and technical support. I would also like to thank Jonathan Turchenek and Laura Smith for their help with core sampling and summer students Ryley, Marcie, and Warren for helping with laboratory analysis. Thanks to Len Wassenaar and Geoff Koehler at Environment Canada and Jianzhong Fan at the University of Saskatchewan for their technical support with laboratory analysis.

Most of all, thanks to my wife and love of my life Janelle for supporting me through this long experience. Without her support this thesis would not have been possible.

# TABLE OF CONTENTS

	<u>page</u>
PERMISSION TO USE .....	i
ABSTRACT .....	ii
ACKNOWLEDGMENTS .....	iii
TABLE OF CONTENTS .....	iv
LIST OF TABLES .....	vi
LIST OF FIGURES .....	vii
1. INTRODUCTION .....	1
2. THEORY AND BACKGROUND .....	5
2.1 EC of Unconsolidated Sediments .....	5
2.2 Direct-push EC Profiling .....	8
2.3 Potash Mining in Saskatchewan .....	10
2.4 Quaternary Geology of Saskatchewan .....	13
2.5 Hydrogeology of Tills .....	15
2.6 Groundwater Transport Processes .....	16
2.6.1 Advective transport .....	17
2.6.2 Diffusive transport .....	17
2.7 Depth Profiles of Conservative Tracers .....	18
2.8 Prairie Wetland Hydrology .....	19
3. SITE DESCRIPTION .....	22
4. FIELD AND LABORATORY METHODS .....	25
4.1 Drilling and Piezometer Installation .....	25
4.2 EC Profiling .....	26
4.3 Core Sampling and Storage .....	27
4.4 Sediment Properties and Pore-Water Chemistry .....	27
4.5 Surface and Groundwater Hydrology .....	29
4.6 Water Sampling and Chemical Analysis .....	29
5. RESULTS AND DISCUSSION .....	32
5.1 Geology and Sediment Properties .....	32
5.2 Hydraulic Conductivity .....	35
5.3 Surface and Groundwater Hydrology .....	37
5.4 Surface Water Chemistry .....	40
5.5 Subsurface Physical and Chemical Heterogeneity .....	43
5.6 Bulk Soil and Pore-water Salinity .....	47
5.7 Predicting Pore-water EC from Direct-push EC .....	53

5.8 Relationship of Pore-water Cl <sup>-</sup> to Pore-water Salinity.....	59
5.9 Timing of Brine Release.....	61
6. CONCLUSIONS AND IMPLICATIONS.....	67
REFERENCES .....	69
APPENDIX A - CORING LOGS.....	82
APPENDIX B - DIRECT-PUSH EC LOGS .....	118
APPENDIX C - SEDIMENT PROPERTIES.....	153
APPENDIX D - PORE-WATER CHEMISTRY .....	173
APPENDIX E - HYDRAULIC CONDUCTIVITY RESULTS.....	179
APPENDIX F - GROUNDWATER HYDROGRAPHS.....	190
APPENDIX G - SURFACE WATER CHEMISTRY .....	205
APPENDIX H - GROUNDWATER CHEMISTRY .....	218

## LIST OF TABLES

<u>Table</u>	<u>page</u>
<b>Table 4-1.</b> Completion details of MW1, MW2, and 10 piezometers installed by others [unpublished consultant data 2008, 2011] and instrumented with pressure transducers. ....	30
<b>Table 5-1.</b> Mean index parameters from water-saturated samples across 22 core locations (a) and 12 squeeze locations (b).....	34
<b>Table 5-2.</b> Summary of slope and intercept terms of $EC_w$ versus $EC_a$ functions from linear regression analysis for glaciolacustrine and till lithologies and saturation extract ( $EC_e$ ) versus $EC_a$ functions for surface soils of the Northern Great Plains from Halvorson et al. 1977, Figure 1†. ....	51
<b>Table 5-3.</b> Measured (*) and empirically determined parameters used in equation (2.1) to predict $EC_w$ in Figure 5-10.....	53
<b>Table 5-4.</b> Paired sample $t$ -test results for comparisons between measured and calculated $EC_w$ and pore-water Cl <sup>-</sup> for each major lithological group using equation (2.1), and across all data using linear relations from Figures 5-8b and 5-12.. ....	55
<b>Table 5-5.</b> Paired sample $t$ -test results for comparisons between measured and calculated $EC_w$ and pore-water Cl <sup>-</sup> for BH5, BH6, and BH14 using equation (2.1), and linear relations from Figures 5-8b and 5-13.. ....	59

## LIST OF FIGURES

<u>Figure</u>	<u>page</u>
<b>Figure 2-1.</b> Schematic (A) and model (B) representation of electrical conduction through three pathways in soil [after Rhoades et al. 1989].	7
<b>Figure 2-2.</b> Schematic of Geoprobe Systems <sup>®</sup> direct-push rig and electrical conductivity logging equipment [after Direct Image 2015].	10
<b>Figure 2-3.</b> Isopach map of the Prairie Evaporite Formation within the Elk Point Basin [after Fuzesy 1982].	12
<b>Figure 2-4.</b> Illustrative cross-section through the Prairie Evaporite Formation [after Fuzesy 1982].	13
<b>Figure 2-5.</b> Stratigraphic chart of Pleistocene deposits in the Saskatoon area [after Christiansen 1992].	14
<b>Figure 2-6.</b> Groundwater flow under a recharge wetland (a); groundwater flow under a wetland complex of recharge, flow-through, and discharge wetlands (b) [after van der Kamp and Hayashi 2009].	20
<b>Figure 3-1.</b> Location of the study area within south-central Saskatchewan, Canada and the semiarid glaciated plains region of North America (shaded area) [redrawn after Winter 1989 and Fulton 1995].	22
<b>Figure 3-2.</b> Surface elevation map (masl; 5 m LiDAR raster, 15 m pixel size) of the study area...	23
<b>Figure 5-1.</b> Cross section A-A' showing surface topography, major geological boundaries, wetlands, and the seasonal high and low water table elevation in July and October, respectively, during the ice-free months of 2012.	33
<b>Figure 5-2.</b> Hydraulic conductivity results from laboratory triaxial permeameter tests and bail testing of piezometers located across the site versus depth below ground (a) and length of screen intake zone (b).	36
<b>Figure 5-3.</b> Daily precipitation in Saskatoon [Environment Canada 2014] and surface water hydrographs of six wetlands (Figure 3-2) along the longitudinal axis of the brine plume for the ice-free months of 2012.	37
<b>Figure 5-4.</b> Piper plot of ions in surface waters and potash mill outflow.	41
<b>Figure 5-5.</b> Cl/Br ratios in surface water samples collected from wetlands.	43
<b>Figure 5-6.</b> Depth profiles of D-P EC, $EC_w$ (relative to 25°C), pore-water Cl, and $n$ at BH6 located within the brine plume (a) and BH5 located the southern edge of the brine plume (b).	46

<b>Figure 5-7.</b> Depth profiles of D-P EC measured adjacent to BH1 in 2011 and 2012.....	48
<b>Figure 5-8.</b> D-P EC values plotted as a function of $EC_w$ for the four major lithologies encountered in the study area (a) and for all lithologies together (b).....	50
<b>Figure 5-9.</b> D-P EC versus $EC_w$ for sand samples. ....	52
<b>Figure 5-10.</b> Predicted $EC_w$ values using equation (2.1) over a continuous range of D-P EC (solid line) compared to measured data (diamonds) for each major lithology. ....	54
<b>Figure 5-11.</b> Predicted $EC_w$ values using equation (2.1) (solid line) compared to measured data (diamonds) for glaciolacustrine from Figure 5-10.....	56
<b>Figure 5-12.</b> Measured and predicted $EC_w$ and pore-water Cl <sup>-</sup> profiles for BH6 (a), BH5 (b), and BH14 (c).....	58
<b>Figure 5-13.</b> Pore-water EC (relative to 25°C) values plotted as a function of pore-water Cl <sup>-</sup> concentrations for all samples.....	60
<b>Figure 5-14.</b> Simulated and measured vertical profiles of $EC_a$ (BH21 and BH13), $EC_w$ , and pore-water Cl <sup>-</sup> (BH6) for three drill locations along the length of the brine plume.....	66

## 1. INTRODUCTION

Produced water resulting from oil and gas production and salt tailings associated with potash mining in Western Canada present risks to underlying groundwater resources and adjacent agricultural lands because of the quantity and quality of the water produced. On a worldwide average, the ratio of produced water to oil from oil well production is 2-3, while the ratio of produced water to gas is usually higher for gas wells [Veil 2011; Neff et al. 2011]. Furthermore, because water production increases as oil and gas production decreases [Veil 2011], production from older wells may be as high as 98% produced water [Stephenson 1992]. Produced water is typically dominated by  $\text{Na}^+$  and  $\text{Cl}^-$  with mean  $\text{Cl}^-$  concentrations ranging from 46,100 to 141,000 ppm [Collins 1975] and is commonly referred to as brine. Large quantities of NaCl-rich brine are also produced during potash processing in Saskatchewan, Canada with 1-2  $\text{m}^3$  of brine generated for every tonne of KCl that is produced [Tallin et al. 1990]. Typical potash tailings brine has  $\text{Cl}^-$  concentrations on the order of 185,000 mg/L [Yang & Barbour 1992].

Releases of saline water contribute to salinization of arable soils, reducing their fertility and productivity, and degrade groundwater supplies by lowering their potability [Ghassemi et al. 1995]. Brine-impacted soils as a consequence of legacy contamination, pipeline breaks, or spills are a widespread environmental problem facing the upstream oil and gas industry in Western Canada. As of 2012, the Government of Alberta reported more than 52,000 abandoned but not yet reclaimed well sites in the province, 32% of which were abandoned between 1963 and 2002 [ESRD 2014]. Oil and Gas Conservation Regulations in Alberta were not amended to require that earthen drilling sumps be lined to prevent the leaching of  $\text{Cl}^-$  from drilling mud and that drilling waste be properly treated and disposed of until 2002 [Government of Alberta 2014]. Similarly, the leaching of tailings brine from above-ground storage areas is a major environmental concern for the potash mining industry in Saskatchewan [Tallin et al. 1990].

A four-year study was commissioned by the Saskatchewan Potash Producers Association in 1989 to define the extent of brine migration from tailings storage areas since the onset of mining and to develop methods to monitor and reliably predict long-term brine migration. The study found that brine had migrated 5-10 m vertically in 20-25 years at seven mine sites and that the extent of migration was dependent upon local- and regional-scale hydrogeology and depended most critically upon the bulk hydraulic conductivity ( $K$ ) of glacial material underlying tailings areas

[Maathuis and van der Kamp 1994]. The study further concluded that brine migration would continue long after mine closure due to diffusive and density-driven transport necessitating long-term models to adequately predict brine fate and transport.

Delineating brine impacts in groundwater for assessment purposes with piezometers is time-intensive and data resolution is often poor due to cost constraints. While fine-scale soil sampling and analysis of soil extracts has been used to generate detailed vertical profiles of brine concentrations [Maathuis and van der Kamp 1994], without prior knowledge of brine distributions many samples are needed to adequately reproduce concentration changes which can occur over short distances. Generating pore-water concentrations from extracts of dried and crushed core samples involves a calculation from mass percent to concentration using gravimetric water content measurements and is thus more susceptible to errors in final concentrations than directly measured pore-water concentrations obtained from piezometers or squeezing of cores.

While non-intrusive surface geophysical techniques such as electromagnetic induction (EM) have proven to be very effective in spatial mapping of groundwater salinity [Greenhouse and Slaine 1983; Goldstein et al. 1990; Monier-Williams et al. 1990], vertical delineation is often challenging and typically requires the use of more involved time and frequency domain EM methods or electrical resistivity imaging methods. Borehole logging using EM induction tools is effective for defining high-resolution vertical brine distributions [Maathuis and van der Kamp 1991], however it requires pre-existing boreholes and therefore is not well suited for reconnaissance or directing soil sampling during initial site assessment, making it better suited to temporal monitoring of lateral and vertical brine migration using cased boreholes.

Direct-push EC profiling is an intrusive technique that enables *in situ* measurements of subsurface EC at the cm scale permitting rapid vertical [i.e. one-dimensional (1D)] visualization of subsurface EC in real-time [Direct Image 2014]. This approach also allows directed soil sampling and piezometer installation with the same D-P drilling equipment during the same site visit. Demands for accurate contaminant transport models at the local scale require fine-scale geological and pore-water chemistry data to provide meaningful predictions [Kessler et al. 2013; Harrington and Hendry 2006]. This assertion is particularly true for clay-rich glacial tills and

glaciolacustrine deposits that dominate the surficial geology of the Canadian Prairies [Meyboom 1967], are typically fractured near surface [D'Astous et al. 1989; McKay et al. 1993a; McKay and Fredericia 1995], and commonly contain geological heterogeneities such as sand lenses [Gerber et al. 2001; Kessler et al. 2012], which have both been shown to provide preferential pathways for contaminant transport [McKay et al. 1993b; McKay et al. 1999; Harrington et al. 2007].

The high-resolution measurement capabilities of D-P EC profiling make the technique particularly well suited to detailed lithologic characterization of unconsolidated alluvial sands, silts, and clays [Christy et al. 1994; McCall 1996], for defining fine-scale hydrostratigraphic features in highly stratified alluvial deposits [Schulmeister et al. 2003], and for identifying sand lenses in clayey till aquitards [Harrington and Hendry 2006]. While the primary application of D-P EC profiling has been geological characterization, the method has also proved useful for detecting and mapping contaminant plumes [Johnson et al. 1999; Zume et al. 2006] and pore-water salinity variations [Harrington and Hendry 2006].

Most studies that employed D-P EC profiling for detecting contaminant plumes solely made use of  $EC_a$  measurements for delineation, while few [e.g. Harrington and Hendry 2006] attempted to predict pore-water salinity from measurements of  $EC_a$ . In saturated sediments  $EC_a$  is primarily a function of geology and pore-water salinity. Therefore, an understanding of both properties is required in order to distinguish  $EC_a$  variations caused by changes in pore-water salinity from changes in geology. Developments in high-resolution sampling methodologies within clay-rich media consisting of continuous coring and high-pressure mechanical squeezing [e.g. Hendry et al. 2013] have significantly reduced the cost of obtaining fine-scale chemical profiles of pore-waters from low  $K$  geologic materials including clayey till aquitards.

The goal of this study was to establish a high-resolution method for characterizing groundwater salinity using D-P EC profiling at a brine-impacted site associated with potash mining activities. The objectives of the study were to: (1) characterize the surface and groundwater hydrology to explain the current distribution of brine at the site; (2) define the lateral and vertical distribution of  $EC_a$ ,  $EC_w$ , and pore-water  $Cl^-$  variations in brine-impacted groundwater using D-P EC profiling combined with high-resolution core sampling; (3) predict  $EC_w$  and  $Cl^-$  from  $EC_a$

measurements using an established soil conductance model; (4) evaluate the accuracy of model predictions by comparing calculated  $EC_w$  and  $Cl^-$  concentrations to measured values determined from squeezing of cores collected adjacent to D-P EC log locations; and, (5) estimate the timing of brine release using solute transport modelling to reproduce observed EC and  $Cl^-$  profiles. The data generated from this study will be used in subsequent groundwater studies to predict the fate and transport of  $Cl^-$  resulting from the brine plume and to define the dominant controls on water and solute transport.

## 2. THEORY AND BACKGROUND

### 2.1 EC of Unconsolidated Sediments

The EC of a material is a numerical expression of its ability conduct electric current [Rhoades et al. 1999]. The measurement of EC involves passing current ( $I$ ) through a material and measuring the resulting potential difference ( $V$ ) across two points. Resistance ( $R$ ) in ohms can then be determined using Ohm's Law where  $R=V/I$ . The EC of the material is expressed by  $K/R$ , where  $K$  is a constant that relates length to the cross-sectional area of the material measured. The value  $K$ , sometimes referred to as a cell constant, is a function of the EC measuring device. More specifically, the distance/cross-sectional area between electrodes. Electrical conductivity is conventionally reported in siemens (S) per metre (S/m), mS/cm, or dS/m.

The EC in free water,  $EC_w$ , depends upon the relative concentration, mobility, and valence of the specific ions present, as well as temperature [Rhoades et al. 1999]. However, since  $EC_w$  is closely related to the total solute concentration, it is commonly used as an indicator for total dissolved solids (TDS) or salinity of aqueous solutions. In unconsolidated sediments  $EC_a$  is a function of water content ( $\theta_w$ ), physical porosity ( $n$ ),  $EC_w$ , temperature, and properties of the sediment including particle shape, orientation, particle-size distribution, cation exchange capacity (CEC; a function of clay content and mineralogy), and organic matter content [Friedman 2005; Rhoades et al. 1999]. To control for temperature dependence,  $EC_w$  and  $EC_a$  measurements are commonly expressed at a reference temperature; typically 25°C.

Due to the many factors controlling  $EC_a$ , predicting  $EC_w$  variations from measurements of  $EC_a$  requires discrete resistor network models. The complex nature of these models limits their practical use for  $EC_w$  predictions, and thus most of the models in use have been developed using mean field theory to simplify a 3D problem into an idealized geometry [Friedman 2005]. Mean field theories also attempt to reduce the number of input parameters to enable models to be easily applied in field studies. This is most commonly accomplished by consolidating parameters that are difficult to measure, such as sediment properties, into fewer terms.

In saline soils, the dominant factors controlling  $EC_a$  are  $EC_w$  and  $\theta_w$ , since air-filled pores and soil particles are generally regarded as non-conducting [Friedman 2005]. Conduction through a volume of moist soil therefore occurs primarily through the pore-water containing charged ions.

Clays modify soil conduction by providing a secondary pathway for current to pass along their charged mineral surfaces. A commonly applied simplifying assumption to account for conduction along clay surfaces is to consider conduction through two parallel pathways, one being the pore-water and one being the charged clay surfaces [e.g. Rhoades et al. 1976]. Through this simplifying assumption, the relationship between  $EC_a$  and  $EC_w$  (or saturation extract;  $EC_e$ ) has been shown to be linear for many saline soils around the world [e.g. Halvorson et al. 1977; Loveday 1980; Rhoades 1980; Bohn et al. 1982].

However, at values of  $EC_w < 4$  mS/cm in clayey soils the  $EC_a$ - $EC_w$  relation becomes non-linear [Shainberg et al. 1980] and cannot be adequately described with linear methods. To account for the nonlinear relationship between  $EC_a$  and  $EC_w$  at low values of  $EC_w$ , Rhoades et al. [1989] proposed an updated two parallel-pathway conductance model for salinity appraisal:

$$EC_a = (\theta_w - \theta_{ws})EC_{wc} + \left[ \frac{(\theta_s + \theta_{ws})^2 EC_{ws} EC_s}{(\theta_s) EC_{ws} + (\theta_{ws}) EC_s} \right] \quad (2.1)$$

where  $\theta_{ws}$  is the volumetric water content of the series-coupled solid-liquid pathway,  $(\theta_w - \theta_{ws})$  is the volumetric water content of the continuous liquid pathway,  $\theta_s$  is volumetric content of the solid phase,  $EC_{wc}$  and  $EC_{ws}$  are the conductivities of the continuous and series-coupled pathways, respectively, and  $EC_s$  the conductivity of the solid phase. The model presumes that  $EC_a$  of a soil can be described by conductance through two pathways acting in parallel: (1) a continuous liquid pathway comprising connected pores (i.e.  $\theta_w - \theta_{ws}$ ), and (2) a series-coupled pathway comprising conductance along soil particle surfaces (clays) coupled with isolated pores that bridge adjacent particles (i.e.  $\theta_{ws}$ ) (**Figure 2-1**). Originally conceived as a three-pathway model, Rhoades et al. [1989] determined that the solid phase contribution was negligible due to the inability of direct particle-to-particle contact to provide a continuous current pathway and proposed the two-pathway model above.

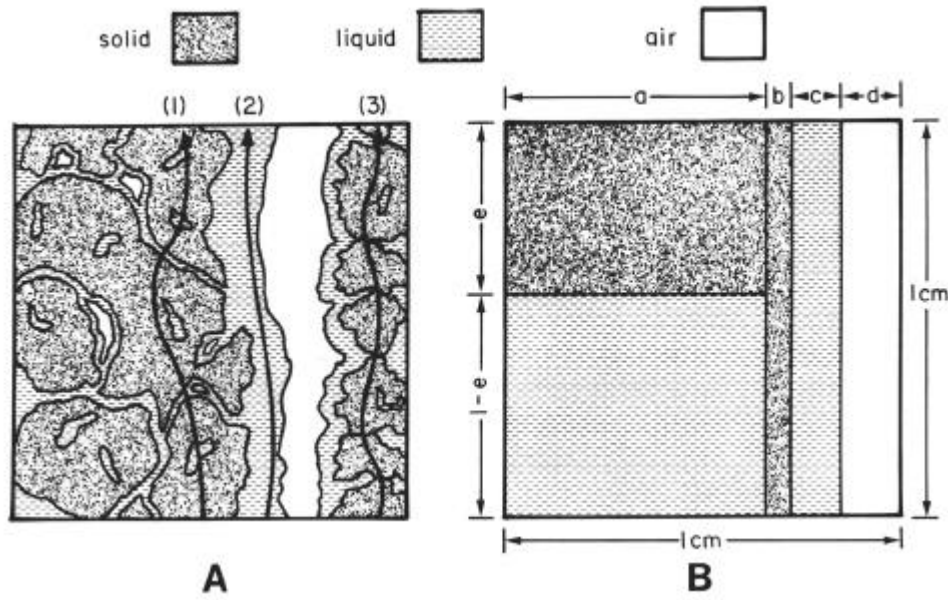


**Figure 2-1.** Schematic (A) and model (B) representation of electrical conduction through three pathways in soil [after Rhoades et al. 1989].

As a result of diffusion of dissolved salts,  $EC_{ws}$  and  $EC_{wc}$  are assumed to be equivalent under steady-state conditions, and therefore equal to  $EC_w$ . Rhoades et al. [1989] further showed that under conditions of  $EC_{ws} > 2$  mS/cm and  $EC_s \leq 1.5$  mS/cm, the product  $(\theta_s)EC_{ws} \gg (\theta_{ws})EC_{ws}$  such that the latter can be neglected resulting in the linear equation:

$$EC_a = (\theta_w - \theta_{ws})EC_w + \left[ \frac{(\theta_s + \theta_{ws})^2}{\theta_s} EC_s \right] \quad (2.2)$$

where  $(\theta_w - \theta_{ws})$  represents the slope and  $[(\theta_s + \theta_{ws})^2 / \theta_s] EC_s$  represents the intercept term on a plot of  $EC_w$  plotted as a function of  $EC_a$ . Because of the linear relation between  $EC_a$  and  $EC_w$  under saline conditions (i.e.  $EC_w > 2-4$  mS/cm), if  $\theta_w$  and  $\theta_s$  are known,  $\theta_{ws}$  and  $EC_s$  can be determined from equation (2.2) by fitting a linear regression line to  $EC_a - EC_w$  measurements at a fixed  $\theta_w$  for a given soil type. Under the assumption that  $EC_{ws} = EC_{wc}$ , equation (2.1) can then be solved for  $EC_w$  as a quadratic equation:

$$EC_w = \frac{-b \pm \sqrt{b^2 - 4ac}}{2a} \quad (2.3)$$

where  $a = (\theta_s)(\theta_w - \theta_{ws})$ ,  $b = (\theta_s + \theta_{ws})^2(EC_s) + (\theta_w - \theta_{ws})(\theta_{ws}EC_s) - (\theta_s EC_a)$ , and  $c = -(\theta_{ws}EC_s EC_a)$ . The additional parameters within the intercept term of equation (2.1) are needed to adequately describe  $EC_a$  under conditions of lower salinity due to the curvilinear relation between  $EC_a$  and  $EC_w$ . Equation (2.2) however, can be used to describe  $EC_a$  under saline conditions.

The model of Rhoades et al. [1989] was developed for use in surface soils that are not typically saturated (i.e.  $\theta_w < n$ ). While  $EC_w$  has been shown to increase proportionally with decreases in  $\theta_w$  as long as salt losses are minimal (i.e.  $EC_w \theta_w$  is constant), changes in  $\theta_w$  do affect  $EC_a$  by altering the partitioning of pore-water between continuous and series-couple pathways [Rhoades 1993]. Therefore  $EC_a-EC_w$  calibrations need to be made at a fixed  $\theta_w$ ; typically field capacity. Field capacity is defined as the water content retained in soil at 33 kPa suction, and is naturally reached once excess water drains following an irrigation cycle [Biswas and Mukherjee 1995]. However, in saturated sediments (i.e.  $\theta_w = n$ ) the water content in each pathway is fixed since all of the pores are filled. Therefore at any point below the water table,  $EC_a-EC_w$  calibrations for a given sediment type can be readily made to determine  $\theta_{ws}$  and  $EC_s$ . Furthermore,  $\theta_w$  and  $\theta_s$  can be determined from lab measurements of  $n$  and dry density ( $\rho_d$ ), where  $\theta_s = \rho_d/\rho_s$  and  $\rho_s$  is a measured or assumed particle density.

To employ equations (2.1) or (2.2) for  $EC_w$  determinations from measurements of  $EC_a$  in saturated sediments,  $\theta_{ws}$ ,  $\theta_s$ , and  $EC_s$  must be known. These three parameters vary with soil type as a result of differences in sediment properties (i.e.  $n$ , CEC, soil structure etc.). Therefore the general approach is to establish  $EC_a-EC_w$  calibrations and parameter determinations for each sediment type encountered. This approach was taken in the present study in order to separate geological effects from  $EC_w$  variations to assess  $EC_a$  measurements obtained by D-P EC profiling as a predictive tool for defining groundwater salinity.

## 2.2 Direct-push EC Profiling

Direct-push EC profiling is a technique similar to borehole resistivity logging, but it differs primarily in the probe design and advancement technique. Borehole resistivity tools are designed to be used with open or cased boreholes and typically have greater electrode spacing to enable current to penetrate beyond the casing and borehole fluids. In contrast, D-P probes have direct

contact with soil. This allows for smaller electrode spacing that has the benefit of enhanced vertical resolution at the cost of lateral penetration. As implied by the name, D-P tools are directly pushed or advanced using oscillating forces. This form of advancement has the benefit of not requiring pre-existing boreholes at the cost of depth of investigation. Due to the advancement technique and probe design, D-P EC profiling is limited to unconsolidated sediments. Depths of investigation depend entirely on the geological conditions encountered, and range from ~10 mbg in clayey tills [Harrington and Hendry 2006] to 30 mbg in alluvial deposits [Schulmeister et al. 2003].

The first D-P EC probe that incorporated electrode rings mounted onto a single probe for  $EC_a$  measurements of soils was that of Rhoades and van Schilfgaarde [1976]. Their probe was designed to be manually pushed into surface soils to depths of <1 m. Advancements from the early 1990's to present have vastly improved the penetration and logging abilities of D-P EC probes, while also improving probe strength and robustness to withstand static weight and percussion forces. There are presently two main types of D-P EC probes: those designed for use with cone penetration testing (CPT) equipment, and percussion probes. Whereas CPT probes are advanced under the static weight of the rig [Robertson et al. 1996], percussion probes are advanced with a hydraulically driven percussion hammer [Christy et al. 1994]. This study focuses on the latter type produced by Geoprobe Systems<sup>®</sup>.

In D-P EC profiling, a sensor probe is attached to a hollow steel rod and driven into the ground vertically. The probe houses a series of isolated electrodes that are connected to a controller and data acquisition system at surface by wiring routed through the steel rods (**Figure 2-2**). As the probe is advanced, electric current is provided to two electrodes by the controller at surface and voltage is recorded by two electrodes (**Figure 2-2**). Electrodes can be configured in different arrays depending on the electrode spacing and which electrodes are acting as current sources and which are measuring electrical potential. Depth and rate of advancement are measured by a potentiometer attached to the drill mast and recorded by the acquisition system. Once the percussion hammer reaches its maximum length of travel, it can be raised and additional steel rods can be added to increase probe depth.

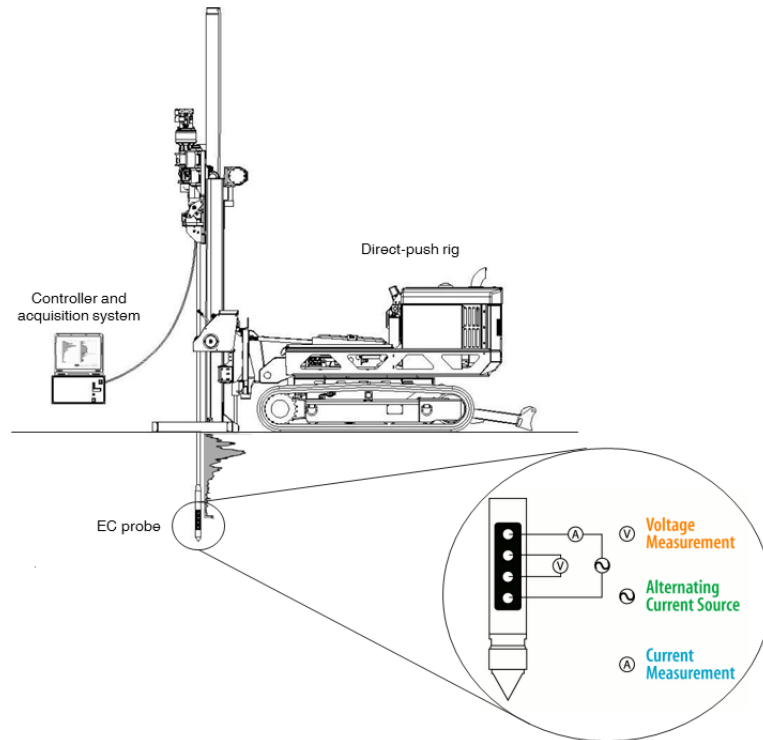


**Figure 2-2.** Schematic of Geoprobe Systems<sup>®</sup> direct-push rig and electrical conductivity logging equipment [after Direct Image 2015].

Based on the supplied current and measured voltage, measurements of  $EC_a$  are computed to produce a log of  $EC_a$  versus depth. This information is displayed alongside logging speed versus depth and is viewable in real-time from a portable computer connected to the acquisition system. When combined with geological information obtained from an adjacent corehole,  $EC_a$  depth profiles viewable in real-time are particularly useful for on-site decision-making. Logs of  $EC_a$  and logging speed can also be saved and exported for further analysis. Not cuttings are generated during D-P EC logging, which reduces waste management costs and the small diameter (~30-60 mm depending on tooling diameter) open probe holes remaining after the completion of logging can easily be filled with traditional well sealing materials.

### 2.3 Potash Mining in Saskatchewan

Potash deposits in Saskatchewan consist of potassium salts mined from the Middle Devonian Prairie Evaporite Formation in the southern portion of the province. The name potash is derived from an alkali substance made from leaching the ashes of woody plants. The leachate was then dried within iron pots for use in glass, soap, and cloth making, hence the term ‘pot ash’ [Fuzesy

1982]. The term potash is now commonly used to describe naturally occurring potassium salts and the products derived from them. The primary use of potash worldwide is in agricultural fertilizer production, as potassium along with phosphorus and nitrogen is an important plant nutrient. Potash deposits were discovered in Saskatchewan in 1942 during drilling for oil exploration. Once the value of the deposit was realized, ten mines were soon constructed with production commencing between 1958 and 1970 [Fuzesy 1982]. Saskatchewan is a large producer of potash on the global stage. The province currently produces nearly one-third of the world's potash with known mineable reserves estimated at almost half the total world reserves [SMER 2014].

The Prairie Evaporite Formation was formed by the evaporation of an inland seaway within the Elk Point Basin about 400 Ma (**Figure 2-3**). Potash-bearing deposits exist within four groups of diagonally lying beds within the formation termed the Esterhazy, White Bear, Belle Plaine, and Patience Lake Members (**Figure 2-4**). The ore from potash-bearing members is comprised primarily of halite (NaCl) with lesser quantities of sylvite (KCl) and carnallite ( $\text{KClMgCl}_2 \cdot 6\text{H}_2\text{O}$ ) [Fuzesy 1982]. Insolubles comprising dolomite, anhydrite, hematite, silica, gypsum, and clay minerals typically make up 1-8% of the ore [Wist et al. 2009]. Although occurring in only small quantities, iron-containing minerals (e.g. hematite) are responsible for giving the ore its characteristic pink to red colour. The ten current mines in Saskatchewan all target the Esterhazy and Patience Lake Members for their higher KCl content relative to carnallite, which yields higher-grade ore [Perucca 2003].

Of the currently operating potash mines, eight employ conventional mining techniques involving extracting the ore with boring equipment and returning it to surface for processing. Two mines employ solution mining methods whereby heated NaCl brine is injected to preferentially dissolve KCl and then pumped back to surface for processing [Wist et al. 2009]. Processing involves liberating KCl from the potash ore through crushing, desliming, flotation, and crystallization methods. The NaCl and insolubles remaining after processing are slurried with process brine and pumped to large tailings ponds adjacent to each mine [Tallin et al. 1990]. Although some NaCl is sold for use as road salt at several mines, the majority is stored as tailings.

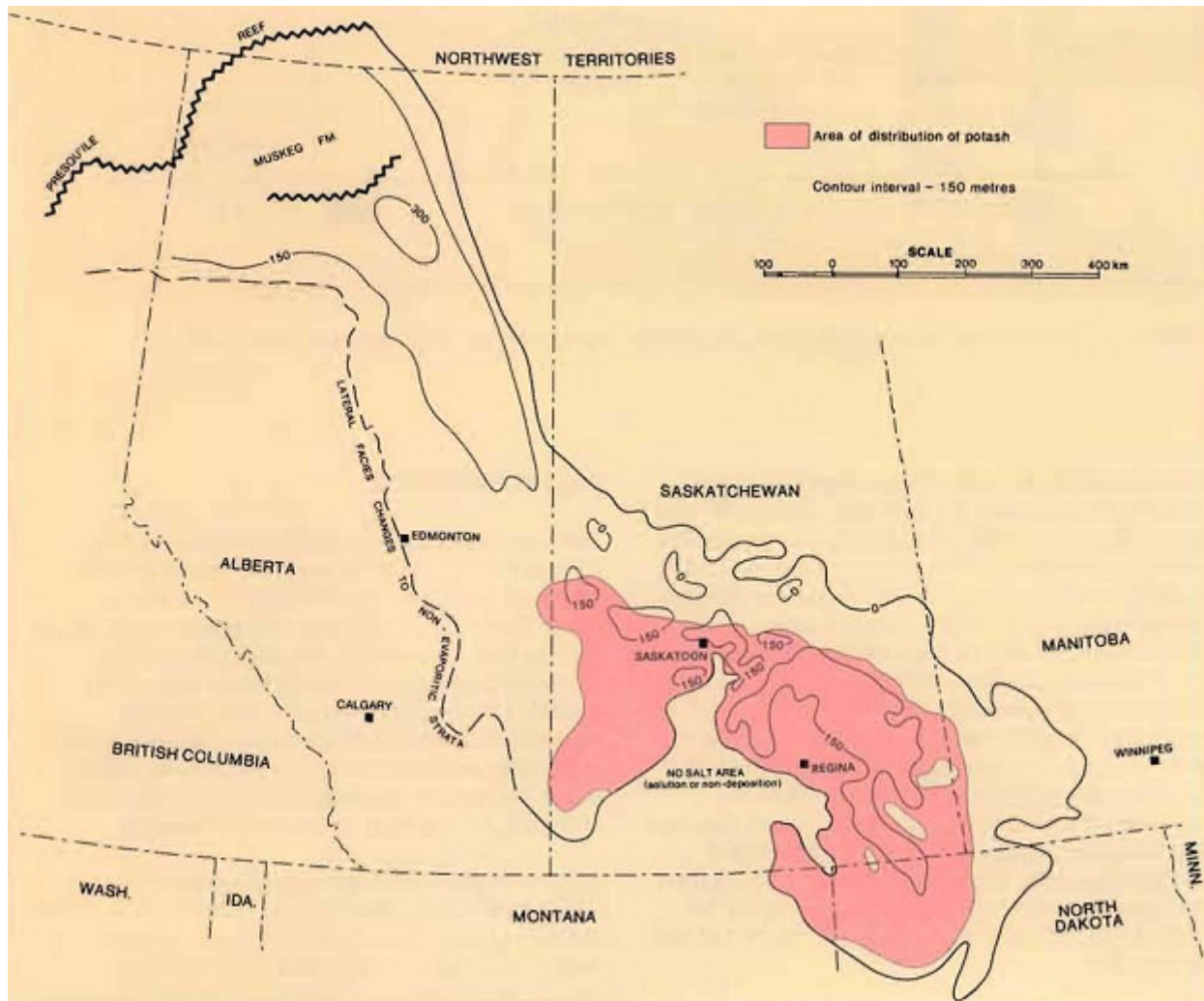


**Figure 2-3.** Isopach map of the Prairie Evaporite Formation within the Elk Point Basin [after Fuzesy 1982].

As a consequence of the initial ore composition, 2 t of NaCl and 1-2 m<sup>3</sup> of brine are generated for every 1 t of KCl produced [Tallin et al. 1990], resulting in large quantities of tailings that present challenges for waste management. The leaching of tailings brine poses the main environmental concern for the potash industry. The investment of \$14 billion dollars by current potash producers to nearly double total productive capacity by 2023 combined with almost a dozen potash exploration/development projects currently underway [SMER 2014] stress the importance for adequate waste management systems and a clear understanding of the role of surficial glacial aquitards in controlling brine transport.

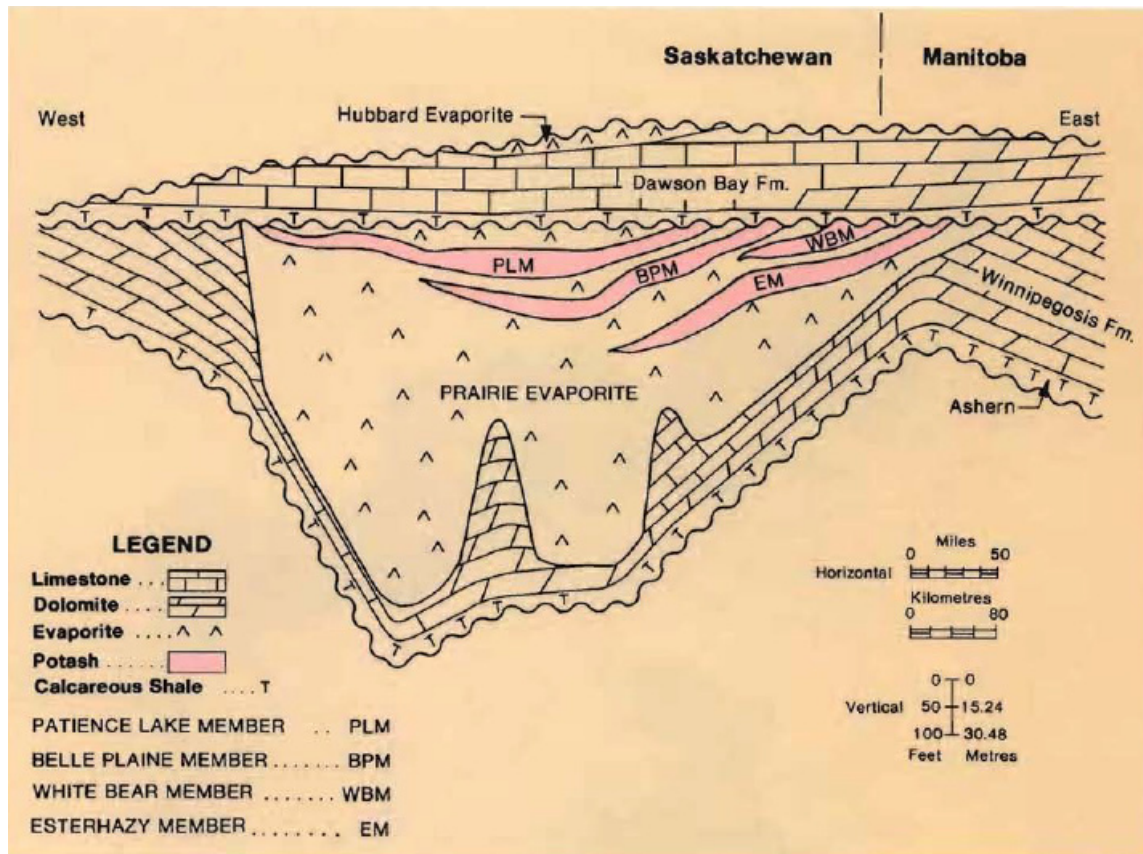


**Figure 2-4.** Illustrative cross-section through the Prairie Evaporite Formation [after Fuzesy 1982].

#### 2.4 Quaternary Geology of Saskatchewan

Glacial deposits comprised of clay-rich glacial till, glaciolacustrine silt and clay, and glaciofluvial sand and gravel dominate the Quaternary geology of southern Saskatchewan [Lennox et al. 1988]. These deposits were formed by successive glaciations during the Pleistocene and retreat of the Laurentide ice sheet during the early Holocene. Holocene deposits comprise glaciolacustrine, outwash, ice-contact sediments and postglacial alluvium, colluvium, eolian, and landslide deposits found between Late Pleistocene till and present ground surface [Christiansen 1992]. Of these recent deposits, glaciolacustrine silts and clays are the most common, with outwash sands and gravels forming less than one percent of surficial deposits [Meyboom 1967].

The stratigraphy of Pleistocene deposits in the Saskatoon area has been described in detail by Christiansen [1992], in which six separate and distinct glaciations were differentiated based on

till lithology (**Figure 2-5**). Five separate till formations are described belonging to either Sutherland or Saskatoon Groups and are differentiated based on carbonate content, weathering, preconsolidation pressure, jointing, borehole geophysical logs, stratigraphic position, and relationships to intertill deposits. Tills are brown in colour when oxidized, dark grey when unoxidized, and are poorly sorted containing a range of particle sizes. The term diamict or diamicton is sometimes used to describe the massive, poorly sorted texture of tills. A diamicton is defined as sediment containing sand or larger clasts within a fine-grained matrix [Dreimanis 1976].

TIME UNITS		STRATIGRAPHIC UNITS	ENVIRONMENT	SASKATOON AREA	
QUATERNARY	LATE PLEISTOCENE	SASKATOON GROUP	POSTGLACIAL	SOIL + STRATIFIED DEPOSITS	
			DEGLACIAL		
			BATTLEFORD FM.	GLACIAL	BATTLEFORD FORMATION till
			FLORAL FORMATION	PROGLACIAL	2 WEATHERED ZONE
				PROGLACIAL	1 WEATHERED ZONE
	GLACIAL	FLORAL FORMATION upper till			
	EARLY AND MIDDLE PLEISTOCENE	SUTHERLAND GROUP	PRE-ILLINOIAN	PROGLACIAL	RIDDELL MEMBER
				PROGLACIAL	
				GLACIAL	FLORAL FORMATION lower till
				PROGLACIAL	
				PROGLACIAL	
	TERTIARY	PLIOGENE	EMPRESS GROUP	NONGLACIAL	WEATHERED ZONE
				PROGLACIAL	
				GLACIAL	WARMAN FORMATION till
PROGLACIAL					
NONGLACIAL				WEATHERED ZONE	
PROGLACIAL					
GLACIAL				DUNDURN FORMATION till(s)	
PROGLACIAL					
NONGLACIAL				WEATHERED ZONE	
PROGLACIAL					
		GLACIAL	MENNON FORMATION till(s)		
		PROGLACIAL			
		PREGLACIAL	STRATIFIED DEPOSITS		

**Figure 2-5.** Stratigraphic chart of Pleistocene deposits in the Saskatoon area [after Christiansen 1992].

The texture of Saskatchewan tills is characterized by roughly equivalent amounts of sand, silt, and clay [Scott 1976; Christiansen 1992]. Saskatchewan tills are commonly characterized as silty or clayey as a result of the siltstone and shale bedrock they are derived from [Scott 1976]. The

fine-grained texture of prairie tills is distinct from sandier and more gravely tills found elsewhere in Canada. Unoxidized prairie tills are rich in carbonate and pyrite that strongly influences groundwater [Hendry et al. 1986; Keller et al. 1991] and surface water chemistry [van der Kamp and Hayashi 2009] across the Prairies.

Sutherland and Saskatoon Group tills, as described by Christiansen [1992], have been identified throughout southern Saskatchewan, however formations are sometimes absent either due to non-deposition or erosion by subsequent glacial advances. For example, Shaw and Hendry [1998] characterized 80 m of Battleford till (deposited 12-18 ka) disconformably overlying late Cretaceous marine clay (deposited 70-72 Ma). Intertill sands and gravels, indicated as proglacial deposits in **Figure 2-5** (e.g. Riddell Member), occur as extensive sheets, long narrow channel deposits, or small deposits of local extent. These coarse-grained deposits constitute local and regional aquifers from which nearly all of Saskatchewan groundwater wells draw their water [van der Kamp and Hayashi 1998].

### 2.5 Hydrogeology of Tills

The low  $K$  ( $<10^{-9}$  m/s) associated with fine-grained tills and glaciolacustrine deposits is influenced by the presence of fractures and sand streaks that can provide more permeable pathways for water and solutes to move. In surficial aquitards, the upper several metres is commonly oxidized and highly fractured, with fracture density decreasing with depth [McKay et al. 1993a]. Some studies have shown evidence for hydraulically conductive fractures extending many metres into the unoxidized zone [Keller et al. 1986; Ruland et al. 1991; McKay and Fredericia 1995], however generally fractures most commonly associated with weathered zones. Grisak et al. [1976] proposed a series of possible mechanisms to explain fractures in till. In the case of surficial aquitards however, the most likely explanation for fracturing is desiccation above the water-saturated zone and past periods of low water table [McKay and Fredericia 1995].

Fracturing within the oxidized zone of surficial glacial aquitards results in bulk  $K$  values that are typically one to three orders of magnitude greater than underlying unoxidized material [Hendry 1982; Keller et al. 1989; D'Astous et al. 1989; McKay et al. 1993a]. The parameter  $K$  is defined as the ease with which groundwater can move through a geologic medium and is dependent on

the properties of the porous medium and the density and viscosity of groundwater [Freeze and Cherry 1979]. Fractures add a secondary porosity to surficial aquitards that permit higher rates of water and solute transport than would normally be possible. Typical values of  $K$  for unoxidized and unfractured glacial deposits are on the order of  $10^{-10}$  to  $10^{-11}$  m/s [Grisak et al. 1976; Hendry 1982; Keller et al. 1989]. This range in  $K$  equates to appreciably slow rates of groundwater flow (e.g. under a unit hydraulic gradient ( $i$ ) and  $n$  of 0.3, average linear groundwater velocity ( $v$ ) would range from 0.01 to 0.001 m/year).

Sand layers, both continuous sheet-like deposits and discontinuous lenses or streaks, are sometimes encountered within surficial aquitards [Gerber et al. 2001; Kessler et al. 2012] and commonly exist between till formations as proglacial deposits [Christiansen 1992]. When sufficiently thick, sand layers can yield groundwater at rates sufficient to constitute aquifers for domestic consumption. However, even thin sand layers (cm scale) can cause deviations from diffusive 1D solute transport in aquitards [Gerber et al. 2001; Harrington et al. 2007]. The  $K$  of sand layers, typically ranging from  $10^{-2}$  to  $10^{-5}$  (Freeze and Cherry 1979), can permit rates of groundwater flow much greater than those measured within unfractured glacial deposits. Harrington et al. [2007] estimated  $v$  within a sand layer in unoxidized till to be  $\sim 1000$  m/year based on a  $K$  of  $10^{-2}$  m/s for the sand and horizontal  $i$  of 0.0005.

## 2.6 Groundwater Transport Processes

The flow of groundwater through geologic media is controlled by Darcy's Law, which relates groundwater flow to a hydraulic head difference ( $dh$ ) between two ends of a flow path of length  $dl$  [Freeze and Cherry 1979], and is given by:

$$q = -Ki \tag{2.4}$$

where  $q$  is defined as specific discharge (m/s) and can be related to  $v$  (m/s), by dividing by the cross-sectional area through which flow occurs, given by  $n$ . The term  $i$  is defined as  $dh/dl$  (m/m). The negative sign indicates flow is in the direction of decreasing hydraulic head. The transport of solutes in geologic media can occur through advection, molecular diffusion, and mechanical dispersion.

### 2.6.1 Advective transport

The process whereby solutes are transported by the bulk motion of flowing groundwater is known as advection [Fetter 1999]. Since motion of the groundwater provides the transport, it follows that solutes will move in the direction of groundwater flow. The 1D transport of a conservative solute by advection is given by:

$$J_a = vnC \quad (2.5)$$

where  $J_a$  is the advective flux ( $\text{kg/m}^2\text{s}$ ) and  $C$  is the solute concentration ( $\text{kg/m}^3$ ). There is a tendency for solutes to spread during transport due to mixing with pore-water (mechanical dispersion) and molecular diffusion, and this phenomenon is termed hydrodynamic dispersion [Fetter 1999]. To account for these additional processes, the transient 1D transport of a conservative solute under steady-state flow can be further described by the advection-dispersion equation given by:

$$\frac{\partial C}{\partial t} = D \frac{\partial^2 C}{\partial x^2} - v \frac{\partial C}{\partial x} \quad (2.6)$$

where  $\partial C/\partial t$  is the change in solute concentration with time measured in the  $x$ -direction within an elementary volume. The first term in equation (2.6) describes transport by hydrodynamic dispersion and the second term describes advective transport. The term  $D$  is the coefficient of hydrodynamic dispersion ( $\text{m}^2/\text{s}$ ) and is defined by  $D = \alpha v + D_e$ , where  $\alpha$  is the dispersivity of the porous medium (m) and  $D_e$  is the effective diffusion coefficient of the solute ( $\text{m}^2/\text{s}$ ).

### 2.6.2 Diffusive transport

The transport of solutes along a concentration gradient as a result of their kinetic activity is known as molecular diffusion or simply diffusion [Freeze and Cherry 1979]. In contrast to advection, diffusion occurs both in the presence and absence of groundwater flow, permitted a concentration gradient exists. The 1D transport of a conservative solute by diffusion is governed by Fick's first law and is given by:

$$J_d = -n_e D_e \frac{dC}{dx} \quad (2.7)$$

where  $J_d$  is the diffusive flux ( $\text{kg}/\text{m}^2\text{s}$ ) and  $dC/dx$  is the concentration gradient in the  $x$ -direction ( $\text{kg}/\text{m}^3\text{m}$ ). Under transient conditions the 1D diffusive transport of a conservative solute can be described using Fick's second law and is given by:

$$\frac{\partial C}{\partial t} = D_e \frac{\partial^2 C}{\partial x^2} \quad (2.8)$$

Notice the similarity between equation (2.8) and the left side of equation (2.6). In fact, in a diffusion-dominated environment where  $v$  is very small,  $D$  in equation (2.6) is equivalent to  $D_e$  and the contribution of advection to solute transport becomes negligible. Thus the advection-dispersion equation given in equation (2.6) reduces to equation (2.8) in geologic environments where  $v$  is very small.

### 2.7 Depth Profiles of Conservative Tracers

A conservative tracer is one that does not interact with porous media or undergo biological or radioactive decay [Fetter 1999]. Tracers are useful in groundwater studies because they provide information about water and solute transport processes, groundwater residence times, and hydraulic properties of geologic media. To avoid effects other processes have on solute transport (e.g. sorption, chemical reactions), conservative tracers are often employed. Examples of conservative tracers that have been applied to the study of aquitards include  $^3\text{H}$ ,  $\delta^2\text{H}$ ,  $\delta^{18}\text{O}$ ,  $^{14}\text{C}$ ,  $^{36}\text{Cl}$ ,  $^4\text{He}$ , and  $\text{Cl}^-$  [Hendry and Wassenaar 2011].

Several features of  $\text{Cl}^-$  make it useful as a conservative solute and tracer in groundwater studies. These include: a lack of adsorption when dissolved in its anionic form; a low concentration within most rock-forming minerals; a high solubility in simple non-silicate minerals (e.g.  $\text{NaCl}$ ); low rates of bioaccumulation; and, a lack of volatility in the subsurface (excluding hydrothermal areas) [Feth 1981]. Natural sources of  $\text{Cl}^-$  in groundwater are: atmospheric deposition of aerosols; dissolution of evaporites; extrusion from compacting clays; diffusion from saline fluid inclusions and macropores; expulsion of water through recrystallization of minerals; and,

seawater intrusion [Davis et al. 1998]. Human activities further account for the redistribution of  $\text{Cl}^-$  and constitute important point sources of  $\text{Cl}^-$  in groundwater. Some examples from Feth [1981] include produced water from oil and gas production, sewage, road salt, and landfill leachates.

Depth profiles of conservative tracers are useful in groundwater studies because their 1D distribution with time reflects the mechanisms responsible for their transport. The use of numerical modelling to reproduce observed 1D vertical profiles of conservative tracers in aquitards has provided key information on groundwater flow, solute transport mechanisms,  $K$ , residence times and sources of pore-water and solutes, and the timing of climactic and geologic events [Desaulniers et al. 1981; Simpkins and Bradbury 1992; Remenda et al. 1994 and 1996; Hendry and Wassenaar 1999; Hendry et al. 2000; Hendry and Wassenaar 2011]. In the context of this study, the transport of  $\text{Cl}^-$  resulting from potash mining will be studied to estimate the timing of brine release.

## 2.8 Prairie Wetland Hydrology

Wetlands dominate the landscape of the Canadian Prairies and play an integral role in the recharge of groundwater resources [Winter 1989; van der Kamp and Hayashi 1998]. While wetlands by definition are not connected by permanent streams and are often considered isolated, they are commonly linked to one another by groundwater and occasional fill and spill events [Winter and LaBaugh 2003]. The presence of wetlands across the Prairies is largely a result of Pleistocene glaciations that deposited clay-rich sediments and left behind a hummocky landscape containing numerous topographically closed basins [Winter 1989; van der Kamp and Hayashi 2009]. On a local scale, the water table is largely unrelated to topography in contrast to accepted regional flow models [Hubbert 1940; Tóth 1963]. Rather, depressions are focal points for groundwater exchange and inter-depressional highs are largely inactive in terms of groundwater movement [Lissey 1971]. This concept of depression-focused flow has been supported by numerous studies since and is widely accepted among wetland scientists [van der Kamp and Hayashi 2009].

The water balance of wetlands is controlled by snowmelt runoff, precipitation, evapotranspiration, groundwater exchange, and infrequent overland flow events between

adjacent wetlands [Meyboom 1966; LaBaugh et al. 1987; Hayashi et al. 1998a]. The  $K$  contrast between oxidized and unoxidized glacial deposits results in the majority of shallow groundwater flow occurring laterally between wetlands and their margins in response to high evapotranspiration along margins during summer months (**Figure 2-6**). In contrast, groundwater flow through underlying unoxidized till is very slow and contributes little to the overall water balance of wetlands, but plays an important role in the hydraulic containment of salts depending on the direction of  $i$ . This  $K$  contrast results in an effective transmission zone for active groundwater exchange between wetlands. However, wetland connectivity is controlled by the thickness of the oxidized zone, position of the water table, and topography that dictates the position of wetlands in relation to one another [van der Kamp and Hayashi 2009].

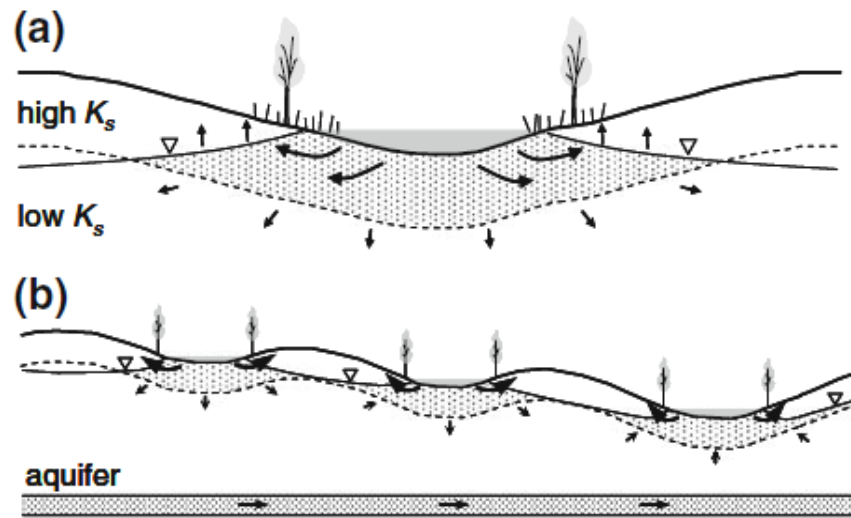


**Figure 2-6.** Groundwater flow under a recharge wetland (a); groundwater flow under a wetland complex of recharge, flow-through, and discharge wetlands (b). The effective transmission zone is indicated by the stippled areas [after van der Kamp and Hayashi 2009].

Chemistry and salinity amongst wetlands is highly variable and depends upon the position of wetlands within the groundwater flow system [Rozkowski 1967; Lissey 1971; Sloan 1972]. Wetlands on topographic highs are generally less saline as a result of groundwater recharge that transports salts away (recharge wetlands). In contrast, wetlands in topographic lows are generally more saline as a result of groundwater discharge that prevents salts from leaving (discharge wetlands). However, wetlands can also receive groundwater discharge on one end and lose water to the groundwater flow system on the other (flow-through wetlands) [Lissey 1971; Euliss et al.

2004]. However, the above classifications do not necessarily mean that groundwater is the dominant mechanism for salt transport, as overland flow can be an equally important transport mechanism [Heagle et al. 2013].

Seasonal and annual variations in water balance also influence the chemistry and salinity of wetlands. Salinity is generally lowest in the spring, increases through the summer, and reaches a maximum over winter due to dilution by runoff and precipitation, and concentration by evapotranspiration and ice cover [LaBaugh 1989]. The main sources of salts in wetlands are atmospheric deposition and groundwater input [Hayashi et al. 1998b; Heagle et al. 2013; Nachshon et al. 2013]. The major source of  $\text{SO}_4^{2-}$  and  $\text{HCO}_3^-$  in prairie wetlands is the glacial sediment that underlies the region [van der Kamp and Hayashi 2009]. The dissolution of carbonate minerals, pyrite oxidation, and cation exchange processes involving clay minerals influence the geochemistry of groundwater within glacial deposits [Hendry et al. 1986; Keller et al. 1991; Van Stempvoort et al. 1994], which in turn influences wetland chemistry.

### 3. SITE DESCRIPTION

The study area is located in south-central Saskatchewan, Canada within the semiarid glaciated plains region of North America (**Figure 3-1**), commonly referred to as the northern prairie wetland region or prairie pothole region [van der Kamp and Hayashi 2009]. The boundaries of the region are defined by climate, vegetation, and surficial geology comprising clay-rich glacial deposits resulting from Pleistocene glaciations and retreat of the continental ice sheet in late Pleistocene [Winter 1989]. The region is characterized by a cold, semi-arid climate with annual potential evapotranspiration exceeding precipitation. The combination of a cold-climate and low  $K$  of clay-rich glacial deposits produce an abundance of wetlands or sloughs which fill topographic depressions on the prairie landscape and define the region. Mean annual precipitation (1981-2010) for nearby Saskatoon is 350 mm with 90 mm falling as snow. Mean monthly air temperature ranges from  $-15.5^{\circ}\text{C}$  in January to  $18.5^{\circ}\text{C}$  in July [Environment Canada 2015].

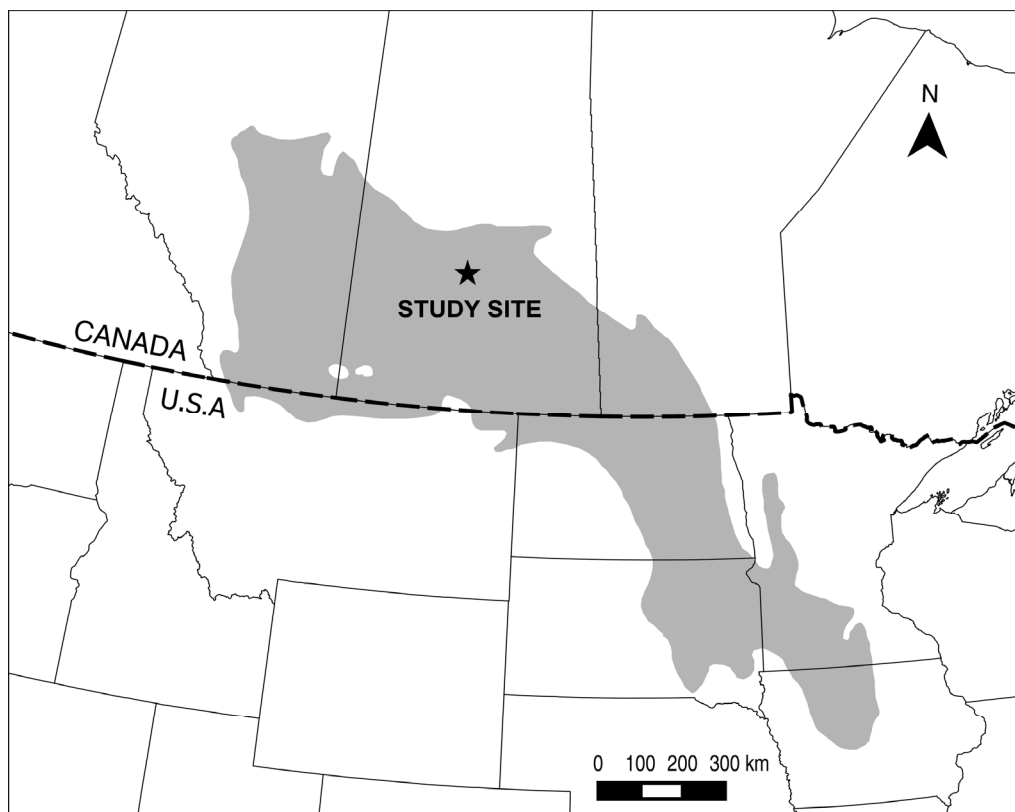


**Figure 3-1.** Location of the study area within south-central Saskatchewan, Canada and the semiarid glaciated plains region of North America (shaded area) [redrawn after Winter 1989 and Fulton 1995].

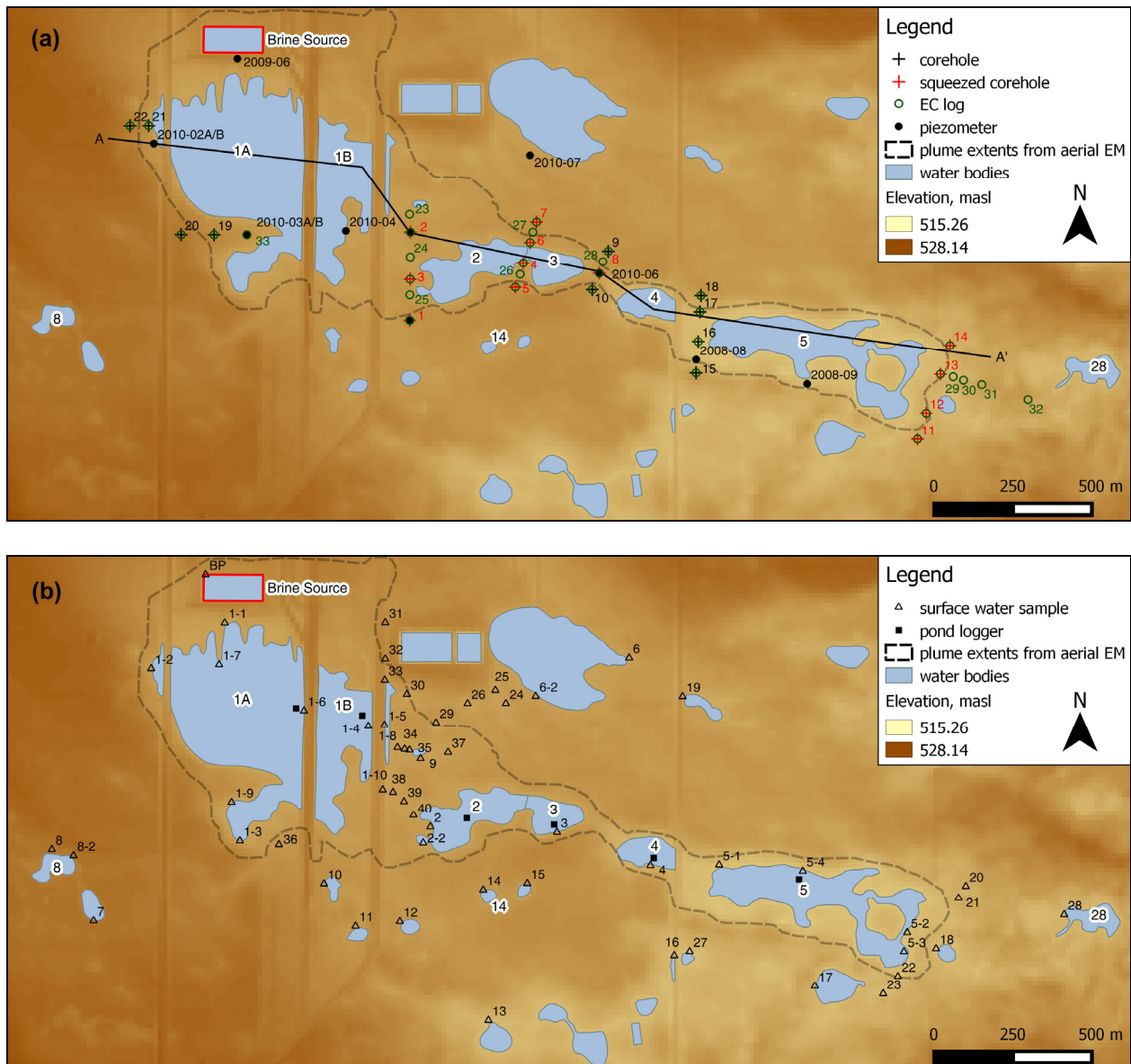


**Figure 3-2.** Surface elevation map (masl; 5 m LiDAR raster, 15 m pixel size) of the study area. The locations of coreholes and cross section A-A', D-P EC logs, piezometers, distribution of wetlands, brine source area, and approximate extent of the brine plume are presented in (a). The location of surface water samples and pond loggers in relation to wetlands and the brine plume extents are presented in (b). The extent of the brine plume was based on 2009 aerial electromagnetic (EM) survey data [unpublished consultant data 2009] and the extent of the wetland water bodies determined from satellite imagery collected September 10, 2009 [unpublished consultant data 2009]. Selected wetlands are numbered 1A through 28.

The study site is located in a regional lowland area and the surface topography is gently undulating to rolling (**Figure 3-2**). The near surface geology is dominated by stratified glaciolacustrine silt and clay deposits overlying clayey till of the Battleford and Floral Formations [Christiansen 1992]. The study area has been impacted by a brine plume resulting from mining activities at a potash mine located adjacent to the site and in continuous operation since 1968. The brine plume is centered along a series of wetlands extending southeast from the brine source in the direction of lower topographic relief (**Figure 3-2**). The brine source is dominated by  $\text{Na}^+$ ,  $\text{K}^+$ , and  $\text{Cl}^-$  reflecting the composition of tailings brine produced during potash processing. Maximum  $\text{Cl}^-$  and total dissolved solids (TDS) concentrations in shallow groundwater adjacent to the source (2009-06; **Figure 3-2a**) is 108,000 and 194,000 mg/L, respectively [unpublished consultant data 2012].

## 4. FIELD AND LABORATORY METHODS

### 4.1 Drilling and Piezometer Installation

Twenty-two coreholes (**Figure 3-2a**) were drilled August 15-19, 2011 to obtain continuous soil cores to depths below the base of brine impacts. Historical environmental investigations completed by others [unpublished consultant data 2008, 2011] and real-time  $EC_a$  measurements obtained from D-P EC profiling conducted in conjunction with drilling were used to determine the depth of investigation at each core location. At locations where this data was not available, the core sampler was advanced a minimum of 1.5 m into unoxidized sediment. Total drill depths ranged from 7.6-12.2 m. Corehole locations were positioned along seven transects placed along the length of the brine plume to permit 2D and 3D mapping of subsurface brine distributions. Where possible, transects were aligned with pre-existing piezometers to incorporate additional data pertinent to the study and to permit comparisons of pore-water chemistry data.

Drilling was completed using a Geoprobe Systems<sup>®</sup> 7822 DT direct-push rig. Cores measuring 44 mm dia. x 1.5 m long were collected using 53 mm OD x 1.52 m long PVC tubing. Cores from three locations (BH1 to BH3) and the top 1.5 m of BH4 were logged and sampled during drilling and the remaining core from BH4 and eighteen other coreholes were sealed in the field for sampling in the laboratory. The clear PVC tubing enabled visual identification of colour and basic lithology from sealed cores to aid in making decisions during drilling (e.g., oxidized versus unoxidized sediment). Sealing involved wrapping the ends of each 1.5 m core tube with multiple layers of plastic food wrap followed by a polyethylene vapour barrier sheath placed over the core tube ends, folded to cover each end, and secured with duct tape.

Two piezometers were installed following drilling of coreholes BH1 and BH2 in August 2011 to intercept sand lenses encountered at these locations, to monitor transient changes in groundwater chemistry, and to corroborate pore-water chemistry determined from analysis of soil core samples. The piezometers (MW1 and MW2) were constructed from 51 mm ID schedule 40, flush-threaded, PVC pipe with 0.30 m long slotted screens (0.254 mm slot size). Following core collection, each location was backfilled through the outer protective steel drill casing with medium sized bentonite chips to the base of sand layering. Piezometers were then placed inside

the drill casing and the annulus surrounding the intake zone was filled with silica sand (0.254-0.508 mm). The outer drill casing was incrementally removed as completion materials were placed in the annular space to ensure proper material placement. The remainder of each corehole was backfilled to surface with granular bentonite (No. 20). The length of the sandpack for each piezometer was 0.76 m and the completed diameter of each corehole was 83 mm.

#### 4.2 EC Profiling

Fifteen D-P EC logs were collected during the core drilling program in August 2011 using the method after Harrington and Hendry [2006]. An additional 18 D-P EC logs were obtained during October 10-11, 2012 after analysis of the 2011 dataset. The EC probe used was a 44 mm diameter Geoprobe Systems® model SC520 array containing four equally spaced electrodes with an inner electrode spacing of 25 mm [Direct Image 2014]. The probe was operated in Wenner array configuration, which meant current was provided to the outer electrodes and voltage measurements were recorded by the inner electrodes. Measurements of  $EC_a$  were obtained every 15 mm of probe advancement. The probe did not contain a temperature sensor and therefore all measurements were made relative to *in situ* temperature conditions. The probe calibration and electrode continuity was verified before and after the collection of each log using a factory-supplied load tester. Calibration tolerance was  $\pm 5\%$ .

The locations of D-P EC logs were selected based on the following criteria: (1) adjacent to coring locations to permit comparisons of D-P EC measurements to  $EC_w$  and pore-water Cl<sup>-</sup> values from analysis of drill core; (2) to aid in identifying geological heterogeneities and geological interpretation at coring locations; (3) additional locations were placed along four transects to provide increased lateral resolution for salinity mapping; and (4) four August 2011 locations were re-drilled in October 2012 to test for temporal D-P EC effects and to acquire complete logs where equipment problems in 2011 prevented the collection of continuous datasets. The EC probe was advanced at each location until the  $EC_a$  response remained constant with depth, until drill rig refusal, or 12 mbg. The 12 mbg maximum depth was selected to avoid penetrating a regional sand aquifer that underlies the study area [unpublished consultant data 2012]. The total depth of the logs ranged from 4.8-12 mbg.

### 4.3 Core Sampling and Storage

Cores were removed from sealed core tubes by using a dedicated tool to score the outer PVC liner twice lengthwise. Each half of the outer liner was then removed to expose the contained core. Cores were geologically described and immediately sampled at 0.15 m depth intervals to minimize evaporative losses. Samples were trimmed to remove the outer 1-4 mm of potentially contaminated core and split crosswise. One sample subset was double-bagged in re-sealable polyethylene freezer bags (Ziploc<sup>®</sup> brand), compressed and rolled to remove air, and packed tightly into coolers for storage in the manner described by Hendry et al. [2013]. In the case of cores sampled in the field during drilling, all samples were sealed and packaged in this manner.

A second sample subset from lab-sampled cores was tightly wrapped in plastic food wrap, vacuum-sealed within polyethylene bags (FoodSaver<sup>®</sup> brand), and packed tightly into separate coolers for storage. Vacuum-sealed samples were reserved for analysis of pore-water chemistry and all other analyses were performed on samples sealed in freezer bags. Samples were stored at room temperature prior to analysis. As chemistry analyses were conducted after the completion of all other analyses and required longer processing times, it was believed that vacuum sealing would minimize water loss more so than freezer bags.

The initial wet mass of all lab-sampled cores was recorded prior to storage to quantify water loss during storage from the time of sampling to analysis of sediment properties and pore-water chemistry. Mean water content loss was  $2.1 \pm 1.7\%$  and  $5.0 \pm 3.1\%$  prior to analysis of sediment properties and pore-water chemistry, respectively. Mean initial gravimetric water content was  $37.96 \pm 13.35$  g and depended on sample size after trimming and lithology. Vacuum-sealing was not found to provide further protection from water loss and core samples experienced similar, if not higher, water losses compared to double freezer-bagged cores after considering longer process times.

### 4.4 Sediment Properties and Pore-Water Chemistry

Soil index parameters including wet density, gravimetric water content,  $\rho_d$ , and  $n$ , were measured at 0.3 m intervals for all core locations ( $n=559$ ) in accordance with ASTM D2216-10 and D7263-09 [ASTM 2010a and 2009, respectively]. Soil particle density was assumed to be  $2700 \text{ kg/m}^3$  for  $n$  calculations. Grain size distributions were determined for four samples of

glaciolacustrine and four samples of till representative of the range of textures encountered across the study site using ASTM 422-6 [ASTM 2007]. Except where noted, all analyses were performed in the Aqueous and Environmental Geochemistry Laboratories, University of Saskatchewan. Four samples of undisturbed, unoxidized core from three coreholes (BH8, BH13, BH21) were collected during laboratory core sampling and immediately sealed in plastic food wrap and sealed with a minimum of three coats of paraffin wax and submitted for one-dimensional constant head triaxial permeameter testing at MDH Engineered Solutions Soils Testing Laboratory, Saskatoon, SK using ASTM D5084–10 [ASTM 2010b].

Selected core samples (n=142) from twelve locations were mechanically squeezed using hydraulic squeezers to extract pore-water samples from saturated samples for chemical analysis. Samples were selected for squeezing following review of D-P EC logs and lithological interpretations to ensure an appropriate number of samples were chosen from each lithology encountered and across the entire range of soil EC values measured. Samples measuring ~75 mm in length were weighed, removed from storage wrapping, and immediately placed inside squeeze cylinders and squeezed using the method after Hendry et al. [2013]. A 2 µm stainless steel filter was used to filter pore-water during squeezing. Pressure (~20 MPa) was maintained for up to three days until a minimum of 5 mL pore-water was collected and filtered a second time through disposable 0.45µm nylon filters into 15 mL centrifuge tubes and tightly capped until analysis.

The EC of pore-water in each centrifuge tube was measured using a Traceable® 4063 Conductivity Meter calibrated to three certified EC standards (1K, 10K, and 100K µS/cm). Measurement range and accuracy were 0.01-200,000 µS/cm and 0.3%. All EC measurements were made in automatic temperature compensation mode (2% per °C) and thus relative to 25°C. The EC probe was rinsed with deionized water and dried between measurements. Pore-water Cl<sup>-</sup> concentrations were determined by suppressed conductivity ion exchange chromatography using a Dionex™ ICS-2100 with AS9-HC exchange column in accordance with EPA Method 300.1 [Hautman et al. 1997]. Method detection limit was 0.05 mg/L and sample reproducibility better than ±10% after accounting for sample dilution. Pore-water EC and Cl<sup>-</sup> measurements were corrected for water loss during storage using mass difference measurements determined for each individual sample.

#### 4.5 Surface and Groundwater Hydrology

The water levels in six wetlands (1A, 1B, 2, 3, 4, and 5; **Figure 3-2b**) were measured from September to October 2011 and April to October 2012 to characterize seasonal water level changes and compare hydraulic heads between ponds. The term “pond” refers to the portion of each wetland containing surface water, whereas the extent of each wetland is generally greater and defined by an area having surface soils at or near saturation for the majority of the year [Heagle, et al. 2013]. Pressure transducers were affixed to weights and placed at the bottom of each pond. Each location was surveyed relative to a steel pin installed at shore and later converted to metres above sea level (masl).

Pressure transducers were also installed in 12 piezometers to record continuous pressure head data from June 2011 to November 2013 (**Figure 3-2a**). Piezometers ranged in depth from 3.4-18.3 m with screen lengths 0.3 to 4.6 m (**Table 4-1**). Pressure head data from ponds and piezometers was corrected for barometric effects using air pressure measurements recorded with an onsite barologger and then converted to hydraulic head. Bail tests were performed on ten piezometers by lowering the water level by ~0.25 m with quick removal of a clean PVC bailer slowly lowered into the water column and then measuring recovery using a pressure transducer. Saturated  $K$  of the geologic material surrounding the well screens was calculated using the method of Hvorslev [1951]. At one location the water level entered the screened interval during bail testing, therefore the Bouwer and Rice [1976] method was employed.

#### 4.6 Water Sampling and Chemical Analysis

Surface water samples from 57 locations were collected in summer and fall of 2011 and quarterly in 2012 ( $n=234$ ) during ice-free months to determine EC and Cl<sup>-</sup> distributions within wetlands and depressions temporally throughout the study area (**Figure 3-2b**). Some locations were added later in the study and thus were sampled fewer times. Furthermore, some locations were dry at certain times of the year and no samples were collected. Samples were collected in 250 mL low density polyethylene (LDPE) bottles using a 2 m sampling pole, tightly capped, and stored in a cooler at 4°C for transport to the Aqueous and Environmental Geochemistry Laboratories, University of Saskatchewan for analysis.

**Table 4-1.** Completion details of MW1, MW2, and 10 piezometers installed by others [unpublished consultant data 2008, 2011] and instrumented with pressure transducers.

Piezometer ID	Lithology screened	Screen interval (mbg)	Sandpack interval (mbg)	Ground elevation (masl)
MW1	glaciolacustrine	3.05 – 3.35	2.74 – 3.50	522.299
MW2	glaciolacustrine	3.96 – 4.27	3.66 – 4.42	522.228
2008-08	till	7.56 – 9.08	7.04 – 9.08	520.08
2008-09	till	3.38 – 4.91	3.05 – 4.91	519.62
2009-06	glaciolacustrine	2.7 – 7.3	2.4 – 7.3	523.945
2010-02A	till	11.9 – 13.4	11.0 – 13.5	522.586
2010-02B	glaciolacustrine	3.0 – 6.05	2.1 – 6.05	522.646
2010-03A	Upper Floral Aquifer	9.2 – 12.2	8.8 – 18.3	522.482
2010-03B	glaciolacustrine	6.0 – 9.04	5.5 – 9.04	522.464
2010-04	glaciolacustrine/till	4.4 – 7.5	3.4 – 7.6	522.291
2010-06	glaciolacustrine/till	2.9 – 6.0	2.4 – 6.1	522.086
2010-07	glaciolacustrine	2.8 – 5.8	2.4 – 6.1	522.045

Surface water samples were filtered through a 0.45µm membrane filter into clean 250 mL LDPE bottles, allowed to reach room temperature and measured for EC and Cl<sup>-</sup> using methods described for pore-water analysis above. Immediately following filtration, a portion was placed into clean 20mL LDPE vials and acidified to 0.2 w/w % with nitric acid for cation analysis. In the case of samples collected in August 2012 for base cations and anions, an additional 250 mL LDPE bottle was filled at each sample location, transported and stored unfiltered in the manner described above, and analyzed for pH and alkalinity using a Radiometric Titralab Tim870 Titration Manager Autoburette coupled to a TIM800 TitraLab Titration Manager in accordance with EPA Method 310.1 [EPA 1983]. Analysis for SO<sub>4</sub><sup>2-</sup> was performed by suppressed conductivity ion exchange chromatography using previously described methods. Analysis for Ca<sup>2+</sup>, Na<sup>+</sup>, K<sup>+</sup>, Mg<sup>2+</sup>, and Br<sup>-</sup> was performed by inductively coupled plasma mass spectrometry (ICP-MS) using a Perkin Elmer NexION300D ICP-MS coupled to a Perkin Elmer S10 autosampler operated in standard mode after EPA [2007] and Jenner et al. [1990]. For analysis of Br, the instrument was run in kinetic energy discrimination mode using a He collision cell to reduce interference to achieve improved detection of Br. Method detection limit was generally better than 0.01 ppm and sample reproducibility was better than ±10% after accounting for sample dilution.

Groundwater samples were collected from selected piezometers in October 2011 and June, October, and November 2012. In all cases, a clean PVC bailer was slowly lowered into the intake zone of each piezometer and ~0.5 L of groundwater retrieved. Temperature and EC were immediately measured on a portion of each sample using the abovementioned conductivity meter and EC measurements were automatically corrected to 25°C. The remaining samples were immediately passed through a 0.45 µm membrane filter using a clean 60 mL syringe into clean 20 mL LDPE vials and stored in a cooler at 4°C for transport to the Aqueous and Environmental Geochemistry Laboratories, University of Saskatchewan for Cl<sup>-</sup> analysis using methods described above. One sample subset was acidified to 0.2 w/w % with nitric acid for cation analysis.

## 5. RESULTS AND DISCUSSION

### 5.1 Geology and Sediment Properties

The geology encountered during drilling consisted of glaciolacustrine silt and clay, underlain by ablation till and subglacial till (**Figure 5-1**). Ablation or supraglacial meltout till is formed during downward melting of glacial ice during episodes of glacial retreat [Dreimanis 1988]. Subglacial or basal till refers to till deposited beneath an ice sheet by lodgement, flow, meltout, or deformation processes. No further attempts were made to distinguish subglacial tills since the aforementioned processes have been shown to coexist and are difficult to classify in field studies [van der Meer et al. 2003; Evans et al. 2006]. As a result of reworking of sediment during melting, ablation tills often exhibit some degree of stratification in contrast to the massive texture of subglacial tills. In Saskatchewan, late Pleistocene ablation tills are characterized by greater  $n$  and lower  $\rho_d$  values compared to subglacial tills subjected to greater consolidation pressures [Sauer and Christiansen 1991]. Occasionally late Pleistocene ablation tills are interbedded with Holocene glaciolacustrine sediment. According to [Sauer and Christiansen 1991], their origin can be explained by the inundation of ice marginal lakes overtop of downmelting glacial ice and the resultant mixing of englacial till with glaciolacustrine sediment.

Apart from 1.5-1.6 m of near-surface sand encountered at BH1 and BH3, the glaciolacustrine sediments were fine-grained and consisted of silt- and clay-sized fractions (0.074-0.005 and <0.005 mm, respectively). This deposit was stratified with depth across the site and ranged from 12:88% and 75:25% silt:clay ( $n=4$ ), although  $\rho_d$  and  $n$  measurements showed low variability over a greater number of samples (**Table 5-1a**). The glaciolacustrine unit thinned eastward across the study area from 11 m thick at BH22 to 0.15 m thick at BH11 (**Figure 5-1**). A thin layer of ablation till, often intercalated with glaciolacustrine material and generally about 0.5 m thick, was encountered at most corehole locations, although up to 1.8 m of ablation till was noted at several locations. The appearance of ablation till was apparent from the presence of sand and trace amounts of gravel which distinguished it from overlying glaciolacustrine sediment. Mean sand (4.75-0.074 mm), silt, and clay contents of 18, 44, and 38%, respectively, were determined for one sample of ablation till.

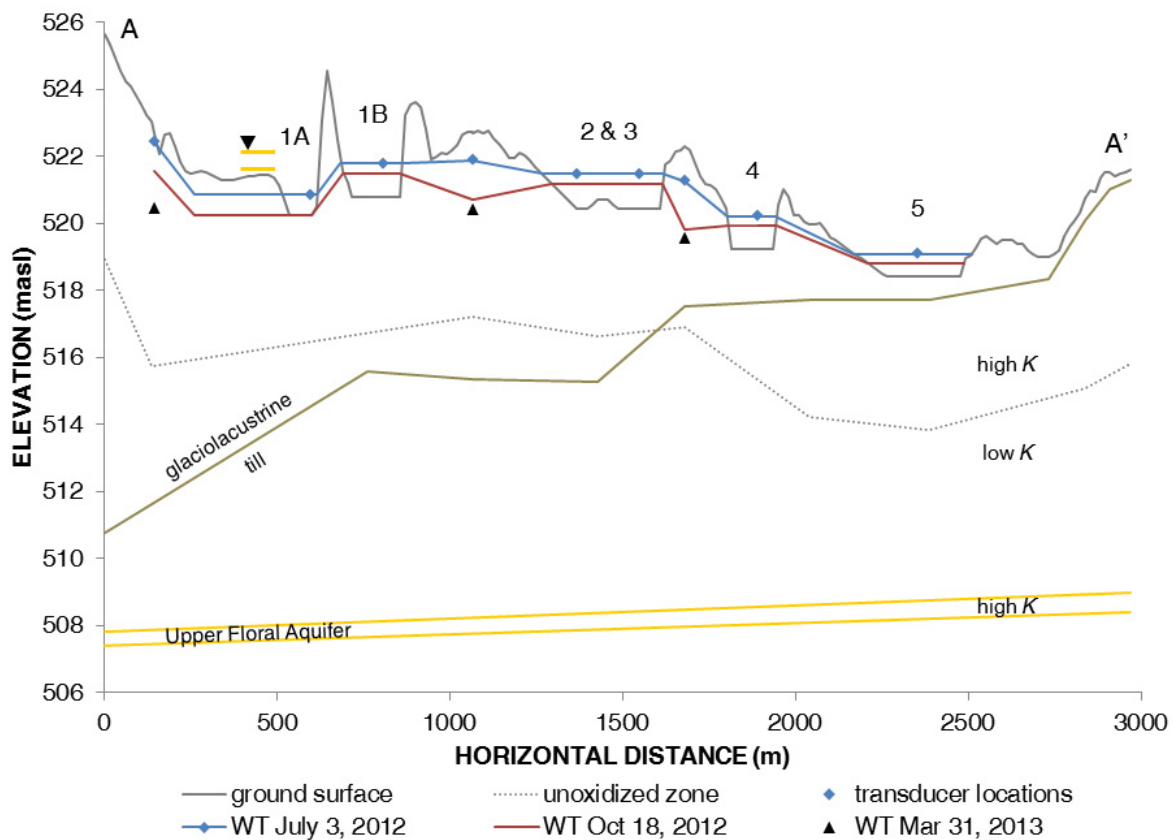


**Figure 5-1.** Cross section A-A' showing surface topography, major geological boundaries, wetlands, and the seasonal high and low water table elevation in July and October, respectively, during the ice-free months of 2012. Triangles represent the true water table low in three piezometers on March 31, 2013 (wetland ponds frozen). Orange lines beneath the inverted triangle represent the range in head within the Upper Floral Aquifer between Dec 6, 2012 and Sept 12, 2013. Geological boundaries were determined based on drilling logs from the present study and those completed by others [unpublished consultant data 2008, 2011]. Vertical exaggeration is 94.

The underlying subglacial till was distinguishable from ablation till by the absence of stratification, greater sand content, higher  $\rho_d$ , and lower  $n$  values (**Table 5-1a**). The subglacial till was massive and uniform with mean  $\pm$  standard deviation sand, silt, and clay contents of  $39\pm 2.7$ ,  $34\pm 2.5$ , and  $27\pm 0.5\%$ , respectively ( $n=3$ ). Texture and index parameters for subglacial till are in agreement those measured by others for tills in Saskatchewan [Christiansen 1992; Sauer and Christiansen 1991; Shaw and Hendry 1998] and are consistent with late Pleistocene till of the Battleford Formation. Oxidized sediments were light brown coloured and contained fractures visible in the drill core, often coated in iron oxide or crystalline precipitates. In contrast,

unoxidized sediments were olive grey coloured and free of visible fractures. The transition from oxidized to unoxidized sediments generally occurred at 5-6 mbg and was typically gradual and marked by a light brown-olive grey mottled zone.

**Table 5-1.** Mean index parameters from water-saturated samples across 22 core locations (a) and 12 squeeze locations (b).

(a)

Lithology	Dry density (kg/m <sup>3</sup> )	Physical porosity (%)
glaciolacustrine, n = 296	1389 ± 71	49 ± 3
ablation till, n = 66	1659 ± 172	39 ± 6
subglacial till, n = 150	1910 ± 77	28 ± 3
sand, n = 10	1667 ± 114	38 ± 4

(b)

Lithology	Dry density (kg/m <sup>3</sup> )	Physical porosity (%)
glaciolacustrine, n = 123	1391 ± 65	48 ± 2
ablation till, n = 27	1699 ± 178	37 ± 7
subglacial till, n = 71	1928 ± 57	29 ± 2
sand, n = 7	1657 ± 108	39 ± 4

As noted above, a sand aquifer (**Figure 5-1**) exists beneath the Battleford till within the study area [unpublished consultant data 2012]. This aquifer is defined as the Upper Floral Aquifer or Riddell Member [Christiansen 1992]. Sand layers 0.1-1.2 m thick were noted within subglacial till in three cores from the eastern part of the study area (BH11, BH12, BH14). These are not believed to be part of the Upper Floral Aquifer based on comparisons with nearby borehole logs completed by others [unpublished consultant data 2012], but rather to be sand lenses. At four locations (BH4, 11, 12, and 14) an unoxidized plastic clay up to 0.75 m thick was encountered near the bottom of each hole at depths between 7.3 and 8.4 mbg. The clay is interpreted to be glaciolacustrine that may have been deposited during an interglacial period between Battleford and Floral till formations, although the boundary between these two formations is more commonly nonconformable [Christiansen 1992]. The congruence of index parameter measurements from squeezed locations to data across all core locations (**Table 5-1a and b**)

suggests the locations selected for analysis of pore-water for later comparisons to D-P EC measurements are representative of the geology across entire study area.

## 5.2 Hydraulic Conductivity

Measurements of  $K$  on one sample of glaciolacustrine, one sample of ablation till, and two samples of subglacial till were determined in the laboratory via triaxial permeameter testing. All four samples were collected from within the unoxidized zone from 6.9 to 11.3 mbg. Lab measured  $K$  values ranged from  $6.0 \times 10^{-11}$  to  $1.0 \times 10^{-10}$  m/s. These values were consistent with those determined by others for unfractured and unoxidized Saskatchewan tills [Keller et al. 1989; Shaw and Hendry 1998] and glaciolacustrine clays in Canada [Desaulniers et al. 1981; Remenda et al. 1994]. Lab determined  $K$  values generally underestimate bulk  $K$  in fractured clays and tills as a result of sample scales too small to incorporate fracture permeability compared to larger-scale field methods [van der Kamp 2001], but can be used to establish a lower bound for  $K$  in unfractured media.

Bail testing of MW1 and MW2 and eight piezometers installed by others [unpublished consultant data 2008 and 2011] in the study area and screened from 2.1 to 13.5 mbg within glaciolacustrine and till units yielded  $K$  values ranging from  $1.2 \times 10^{-9}$  to  $5.1 \times 10^{-6}$  m/s (**Figure 5-2a**). The high variability in  $K$  above 5 m depth and the increase in  $K$  with increasing sandpack length (**Figure 5-2b**) suggests fracture flow within the oxidized zone. This suggestion is consistent with the observation of fractures during core sampling, which are common in oxidized tills. The decrease in magnitude and variability of  $K$  below 5 m is consistent with reduced fracture density in tills with increasing depth below the water table [Hendry 1982; McKay et al. 1993a]. Within the unoxidized zone,  $K$  results from slug tests exceeded those from lab testing by 1-3 orders of magnitude (**Figure 5-2a**). Similar results have been reported for other tills in Saskatchewan [e.g., Keller et al. 1986, 1988]. These authors attributed the discrepancy to fractures extending into the unoxidized zone. While fractures cannot be ruled out, piezometer 1 (**Figure 5-2a**) was screened in glaciolacustrine with a long sandpack that extended into the oxidized zone above and piezometers 2 and 3 were screened across till intervals containing intermittent sand lenses. These sand lenses could also be responsible for the greater field  $K$  values.

It was not possible to compare the  $K$  between glaciolacustrine and till units using bail test results due the lack of deep piezometers screened below the oxidized zone to exclude the effects of fracture-flow. However, the lab  $K$  measured on one sample of unoxidized glaciolacustrine clay was within the range of lab measurements made on three samples of unoxidized till, suggesting the matrix  $K$  of both lithologies may be similar. More data would be required to test this hypothesis. Overall, the decrease in  $K$  from maximum values of  $10^{-5}$  in the oxidized zone to less than  $10^{-9}$  m/s in the unoxidized zone is consistent with studies by others in the glaciated plains region [Simpkins and Bradbury 1992; Shaw and Hendry 1998; van der Kamp and Hayashi 2009]. It is this prevalent decrease in  $K$  with depth that creates an effective transmission zone, defined as the distance between the water table and the unoxidized zone [van der Kamp and Hayashi 2009], for active groundwater flow between wetlands and their margins (**Figure 5-1**).

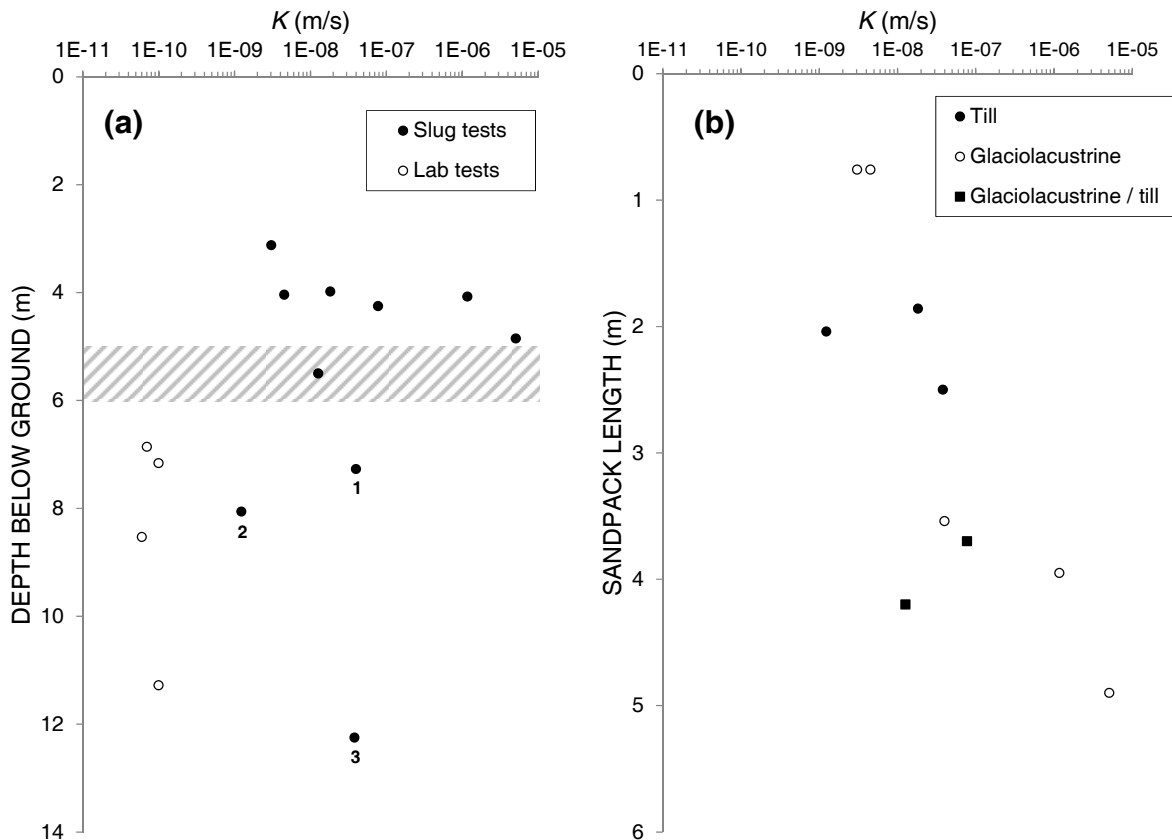


**Figure 5-2.** Hydraulic conductivity results from laboratory triaxial permeameter tests and bail testing of piezometers located across the site versus depth below ground (a) and length of screen intake zone (b). The depth to the midpoint of the sandpack and the transition between overlying oxidized and underlying unoxidized sediments (the dashed region) are presented in (a). Numbered bail tests in (a) correspond to piezometers screened within unoxidized sediment that had long screened intakes or intersected sand lenses.

### 5.3 Surface and Groundwater Hydrology

Pond water levels in wetlands located along the longitudinal axis of the brine plume generally decreased towards the southeast in the direction of lower topographic relief (**Figures 5-1 and 5-3**). The difference in average water elevation between ponds 1B and 5 from April 18 to October 18, 2012 was 2.7 m. The exception was pond 1A, which together with the brine source area and underlying Upper Floral Aquifer, was pumped from July 2011 through 2012 as part of remediation efforts. The effects of pumping are evident by a steady decrease in the water level in pond 1A during 2012 (**Figure 5-3**). Effects of pumping were pronounced in pond 1A through September and by late September it was dry. In the past, wetlands 1A and 1B would likely have comprised one large wetland. Currently, these ponds are separated by a railway track used by the nearby mine. Pumping of 1A during 2012 did not affect the water level in 1B. Rather, the overall water level trend in 1B throughout 2012 mimicked that of wetlands 2, 3, 4, and 5.

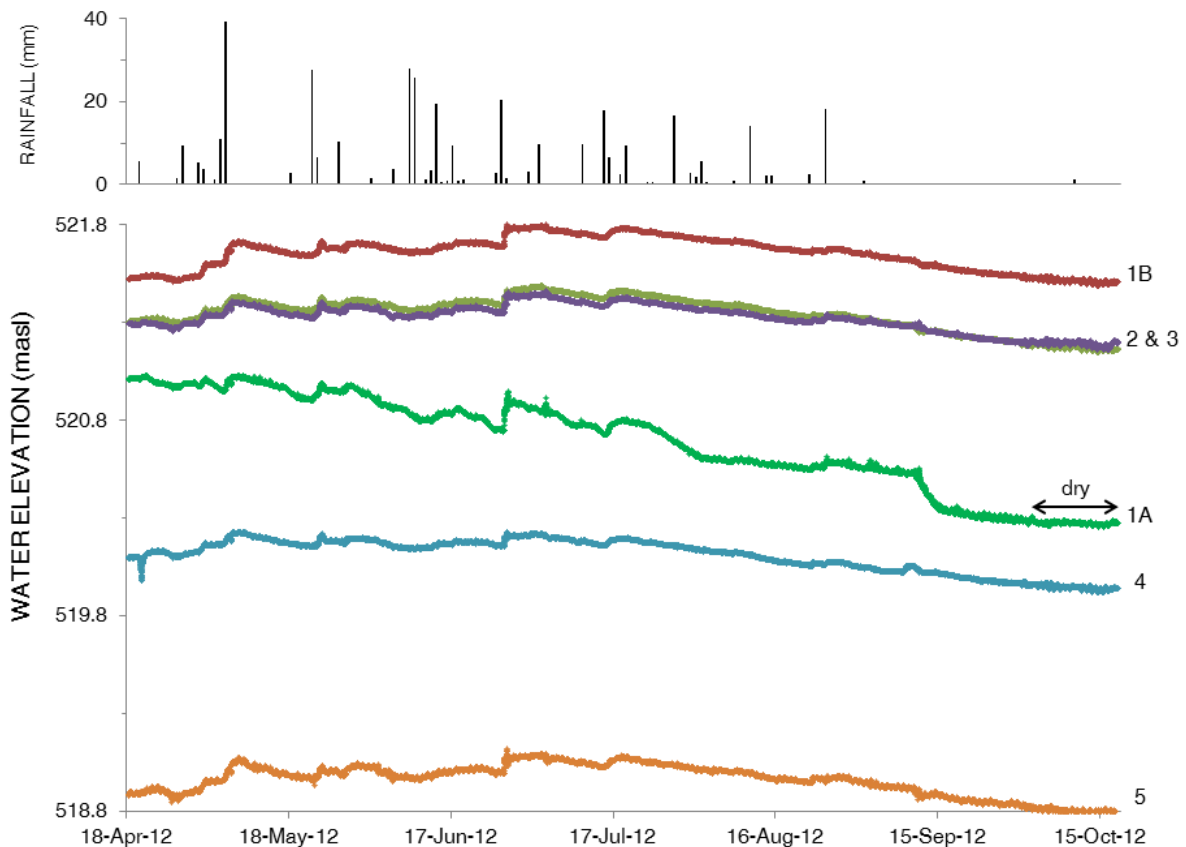


**Figure 5-3.** Daily precipitation in Saskatoon [Environment Canada 2014] and surface water hydrographs of six wetlands (Figure 3-2) along the longitudinal axis of the brine plume for the ice-free months of 2012.

Water levels in ponds 1A-5 generally peaked in late June to early July (**Figure 5-3**). Sudden increases in pond water levels of 20-180 mm occurred concomitantly with rainfall events (3-39 mm). Spring snowmelt occurred prior to the installation of pond level monitoring instrumentation in April 2012, as ice covering the wetlands did not fully retreat until snow covering the surrounding lands had melted. However, pond levels in October 2011 were comparable to levels upon re-installation of instrumentation in April 2012 (data not shown), suggesting little contribution from spring runoff to the overall water balance of wetlands 1A through 5. Wetlands 2 and 3 were connected during the study as indicated by the similarity in their pond levels in 2012 (**Figure 5-3**). The connection between ponds 2 and 3 was narrow and generally shallow, such that during dry periods it may have acted as a division between them. Topographic highs separating wetlands 1A to 5 from each other (**Figure 3-2**) reduce the likelihood of overland flow between wetlands, except possibly during very wet years. However, natural and engineered features such as a culvert beneath the road separating wetlands 4 and 5 provided migration pathways to enable surface water connection between wetlands. A dry flow channel was observed between wetlands 3 and 4, suggesting overland flow has occurred in the past. For a brief period in early July 2012 following several rain events spanning a week, 7-15 cm of standing water was observed between SW-1-10 and SW-40 (**Figure 3-2b**) within a ~30 m wide topographic low trending NW-SE. This feature may serve as a runoff channel connecting the railway ditch east of wetland 1B with wetland 2.

Overland flow aside, the size of the effective transmission zone, illustrated by the high  $K$  region between the water table and unoxidized sediments (**Figure 5-1**), was adequate to permit year-round groundwater exchange between wetlands in 2012. However, this may not always be the case since the water table will undoubtedly vary between wet and dry years, thereby controlling the size of the effective transmission zone. At the nearby St. Denis research site in Saskatchewan, van der Kamp and Hayashi [2009] observed that by November within a moderately wet year, the effective transmission zone was very thin or disconnected beneath ridges separating wetlands, thereby limiting active groundwater exchange to a short period in the spring.

Darcy's law (equation 2.4) can be used to examine groundwater exchange through the effective transmission zone between wetlands as a potential mechanism to explain the presence of brine

~2.4 km downgradient of the source area (**Figure 3-2**). Focusing on the high ground separating ponds 1B and 2, the linear distance between ponds is about 200 m (**Figure 3-2**) and the hydraulic head difference in 2012 ranged from 0.2-0.3 m (**Figure 5-3**), yielding a  $i$  on the order of 0.001-0.0015. Assuming a  $n$  of 0.5 and a  $K$  of  $10^{-5}$  m/s for the underlying glaciolacustrine sediment (**Table 5-1**; **Figure 5-2**) produces a groundwater velocity of 0.7-1 m/s. Assuming brine was present in pond 1B shortly after the start of mining in 1968, advective groundwater transport can only account for a maximum travel distance of 40 m towards pond 2 in 40 years. Due to diffusion and dispersion, the actual transport distance would be <40 m. Given the distance separating ponds 1B-2, 3-4, and 4-5 (~450 m total) groundwater transport alone cannot explain the current distribution of the brine plume. Therefore, overland flow between ponds resulting from fill and spill events during wet years must have occurred in the past to account for the presence of brine in wetlands 2-5 currently.

Groundwater levels in the oxidized glaciolacustrine and till across the study area generally ranged from <0.5 mbg from May to July to 2.5 mbg from March to April in 2011-2013. At the time of drilling in August 2011 the water table across the site ranged from 0.15-2.3 mbg. The average vertical gradient from Dec 6, 2012 to Sept 12, 2013 was calculated to be  $0.17 \pm 0.09$  upwards from the Upper Floral Aquifer to the overlying glaciolacustrine at nested piezometers 2010-03A/B (**Figure 3-2a**). Hydraulic head in the Upper Floral aquifer during this period ranged from 521.7-522.1 with a mean of 521.9 masl, suggesting that head in the aquifer may exceed heads in ponds 1A through 5 on an average annual basis (**Figure 5-1**). Hydraulic head data in the aquifer at this same location was not available in 2012; however, the average vertical gradient from Sept 15, 2011 to Sept 10, 2013 at nested piezometers 2010-02A/B (**Figure 3-2a**) also yielded a mean net upward gradient of  $0.07 \pm 0.08$ . While the deep piezometer at this location was screened in till above the Upper Floral Aquifer, the gradient remained upwards for the majority of the monitoring period and only reversed direction when the water table peaked between May and July. While upward gradients have not been shown to play a significant role in wetland water balance owing to the low  $K$  of unfractured tills limiting contributions from the deep groundwater flow system [van der Kamp and Hayashi 2009], they have been shown to play an important role in controlling wetland salinity by preventing the transport of salts to the underlying flow system [Heagle et al. 2013].

#### 5.4 Surface Water Chemistry

Surface water EC and  $\text{Cl}^-$  concentrations in wetlands within the brine plume ranged from 7230-58,000  $\mu\text{S}/\text{cm}$  and 1680-23,100  $\text{mg}/\text{L}$  between June and October of 2011 and 2012, respectively. The EC and  $\text{Cl}^-$  concentration varied seasonally with changes in pond levels, although the greatest concentrations were observed in wetland 1A adjacent to the brine source and wetland 5, furthest downgradient from the source. The relative distribution of major ions from select wetlands and mill outflow are presented in **Figure 5-4**. Wetlands 1A-5 were characterized by Na-K-Cl type waters with high  $\text{Cl}^-$  concentrations. In contrast, wetlands 8, 14, and 28, located outside the plume extents (**Figure 3-2b**), were dominated by  $\text{HCO}_3^-$  and  $\text{SO}_4^{2-}$  with  $\text{Cl}^-$  concentrations ranging from 12-184  $\text{mg}/\text{L}$  in 2011-2012. Mill outflow was dominated by Na-K-Cl with a  $\text{Cl}^-$  concentration of 179,000  $\text{mg}/\text{L}$  and was expected to be similar to the historical brine source. The most abundant anions in the majority wetlands and lakes within the semiarid glaciated plains are  $\text{SO}_4^{2-}$  and  $\text{HCO}_3^-$ , whereas  $\text{Cl}^-$  dominated wetlands and lakes are rare [LaBaugh 1989]. These data suggest that the Cl-type waters of wetlands 1A-5 are likely the result of brine inputs rather than pre-existing naturally derived  $\text{Cl}^-$ .

In a study of wetlands within the Moose Mountain area of Saskatchewan, Rozkowski [1969], found the chemistry and salinity of wetlands was dependent on their position within the landscape which influenced the amount of groundwater discharge received by a given wetland. He developed a classification scheme for wetland chemistry comprising three major wetland types: Type I wetlands consisted of  $\text{HCO}_3^-$ -Ca-Mg waters with low salinity and occupied recharge areas; Type II wetlands consisted of  $\text{HCO}_3^-$ - $\text{SO}_4^{2-}$ -Ca-Mg (or Mg-Ca) and  $\text{SO}_4^{2-}$ - $\text{HCO}_3^-$ -Ca-Mg (or Mg-Ca) waters and were subjected to increasing groundwater recharge; and Type III wetlands consisted of  $\text{SO}_4^{2-}$ -Mg-Ca waters with high salinity and occupied groundwater discharge areas. The chemical evolution scheme of wetland chemistry described by Rozkowski [1969] has been observed elsewhere within the northern prairie region [eg. LaBaugh et al. 1987; Heagle et al. 2013] and provides a means for explaining the chemistry of wetlands in the present study.

Wetlands 8 and 14 were seasonal wetlands in 2011-2012 characterized by low EC (460-1190  $\mu\text{S}/\text{cm}$ ) and can be classified as Type I (**Figure 5-4**). Wetland 28 was a permanent wetland characterized by moderate EC (1080-2240  $\mu\text{S}/\text{cm}$ ) and is classified as Type II. Wetlands 1A-5 fall on a mixing line between Type III waters and Mill outflow, suggesting they may have been

Type III wetlands prior to brine inputs. This classification is further supported by high  $\text{SO}_4/\text{HCO}_3+\text{CO}_3$  molar equivalent ratios ( $>8$ ) measured in wetlands 1A-5 in November 2011 and the upward hydraulic gradients measured adjacent to wetland 1A (section 5.3 above), suggesting groundwater discharge. According to Rozkowski [1969],  $\text{SO}_4/\text{HCO}_3+\text{CO}_3$  molar equivalent ratios  $>3$  constitute Type III wetlands. Wetlands 8, 14, and 28 also contained appreciable amounts of Na+K (39-51% of total cations). While not as common dominant cations in wetlands within the semiarid glaciated plains as compared to  $\text{Ca}^{2+}$  and  $\text{Mg}^{2+}$  [LaBaugh 1989], Na+K quantities of 40-60% of total cations have been reported and are commonly associated with recharge wetlands [LaBaugh et al. 1987].

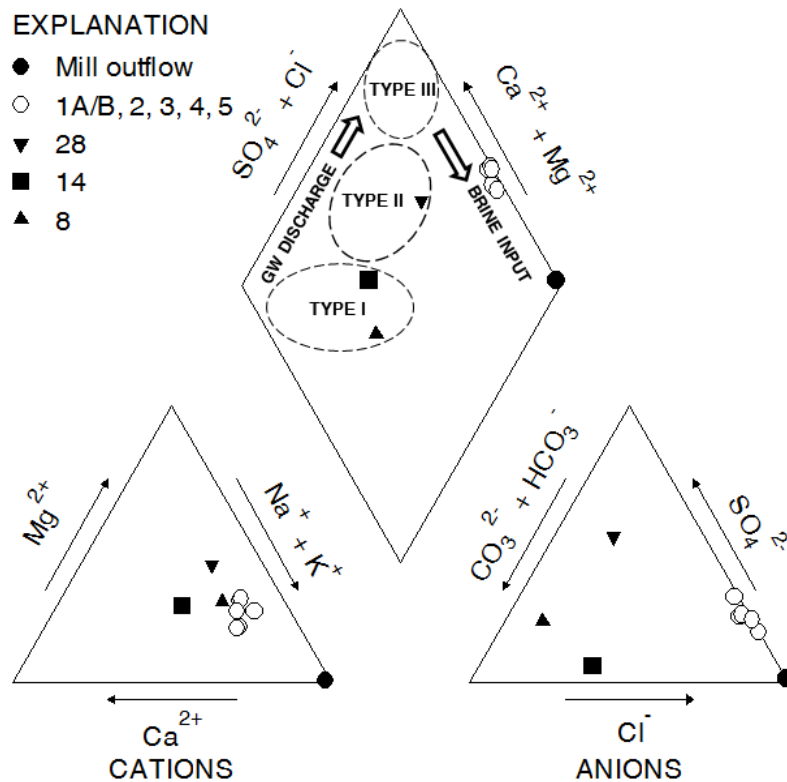


**Figure 5-4.** Piper plot of ions in surface waters and potash mill outflow. Sample locations are presented in Figure 3-2. Locations 8, 14, 28, and mill outflow were sampled August 2012. The remaining locations were sampled in November 2011 [unpublished consultant data 2011]. Type I, II, and III zones after Rozkowski [1969].

Mill outflow and wetlands 8, 14, and 28 plot as two distinct end members based on their Cl/Br mass ratios of 1758 and  $391 \pm 17$ , respectively, in 2011 and 2012 (**Figure 5-5**). Wetlands 1A-5 had Cl/Br ratios ranging from 975-1157 in October 2011 and plotted between these end members. Evaporites have high Cl/Br ratios relative to the seawater from which they are derived as a result of the lower solubility of Cl in relation to Br. Seawater has a Cl/Br ratio of about 290 [Morris and Riley 1966], whereas sylvite (KCl) and halite (NaCl) from the Patience Lake Member of the Prairie Evaporite Formation in Saskatchewan have average Br contents of 61 ppm and 410 ppm [Fuzesy 1983], yielding Cl/Br ratios on the order of 1160 and 9950, respectively. Ore from the Patience Lake Member that is currently mined for potash contains approximately 36% sylvite, 58.5% halite, and 5.5% insoluble minerals by weight [Perucca 2003]. In contrast, atmospheric precipitation in North America from which wetlands receive the majority of their water has Cl/Br ratios on the order of 50 to 150 [Davis et al. 1998]. The average Cl/Br ratio of wetlands 8, 14, and 28 is above this range. The cause of these elevated ratios is not clear. They may be due to windblown dust from the tailings pile of the nearby potash mine, which is comprised primarily of halite separated from ore during processing [Tallin et al. 1990].

The  $\text{Cl}^-$  concentration for a given wetland is dependent on its unique hydrologic conditions and will vary seasonally with changes in water balance, however its Cl/Br ratio will only vary if the source of these species changes since  $\text{Cl}^-$  and  $\text{Br}^-$  are generally considered to be conservative [Feth 1981; Fuge 1969]. While the data plotted on **Figure 5-5** is sparse and does not provide insight into seasonal variability within each wetland, the difference in Cl/Br ratios between wetlands within and outside the brine plume is apparent. The hypothetical mixing lines in **Figure 5-5** also illustrate that relatively small quantities of brine can produce sharp increases in the Cl/Br ratio of 1 L of surface water assuming an initial Cl/Br ratio of 400 or approximately that of wetlands 8, 14, and 28. The initial salinity of wetlands 1A-5 must have been greater than current levels within wetlands 8, 14, and 28 prior to the release of brine since a tenfold greater initial  $\text{Cl}^-$  concentration is needed to reproduce the current Cl/Br ratios measured in wetlands 1A-5 (mixing line B). However, wetlands 1A-5 were sampled in October when their water levels were at a seasonal low. Their  $\text{Cl}^-$  concentrations were 20-40% lower the following April to June, which would yield an initial  $\text{Cl}^-$  concentration of 600-800 mg/L along mixing line B, assuming an equivalent Cl/Br ratio in spring 2012 compared to fall 2011.

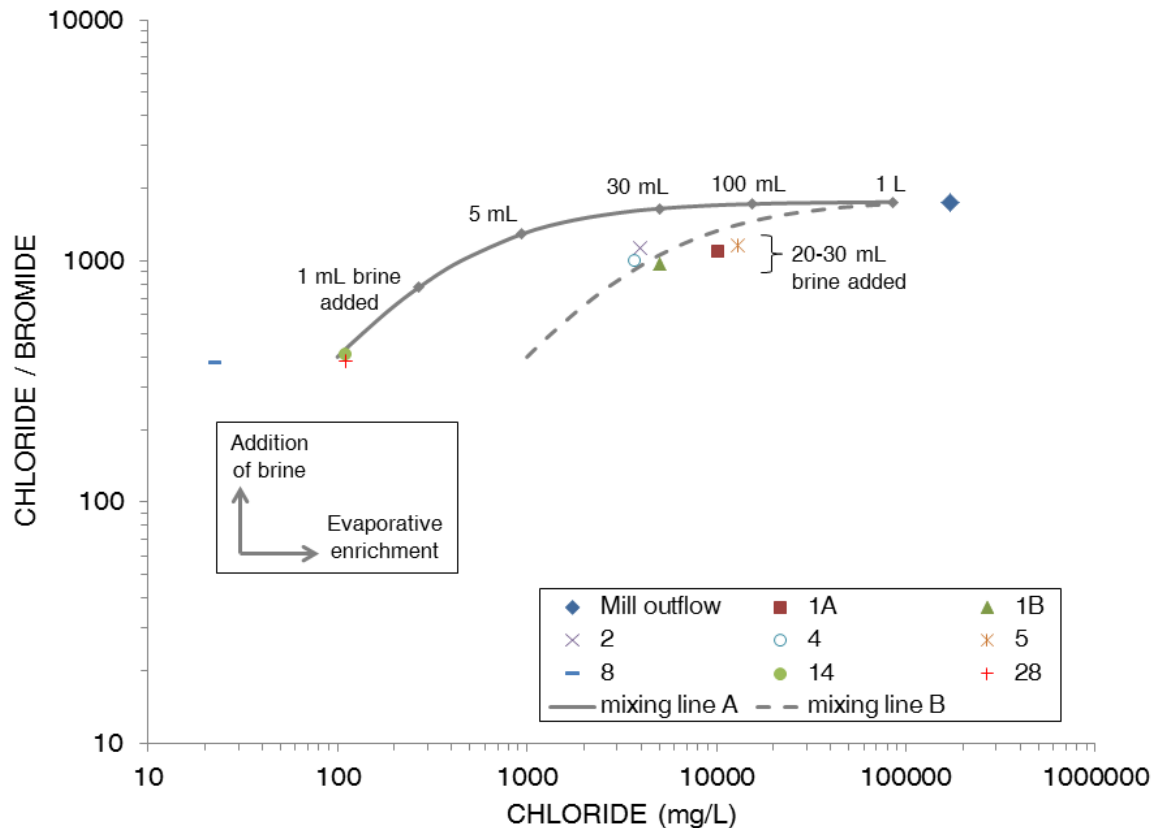


**Figure 5-5.** Cl/Br ratios in surface water samples collected from wetlands. Locations 1A, 1B, 2, 4, 5, 8 were sampled in October 2011, mill outflow in June 2012, and locations 14 and 28 in August 2012. Hypothetical mixing lines represent the addition of increasing amounts of brine up to an equivalent volume of surface water with an initial Cl/Br ratio of 400 and Cl- concentrations of 100 and 1000 mg/L for mixing lines A and B, respectively.

### 5.5 Subsurface Physical and Chemical Heterogeneity

Direct-push EC logs generally displayed a similar trend with depth. From surface, D-P EC increased with depth approaching the water table beyond which the greatest values were recorded. Peak EC values within the oxidized zone generally ranged from 2-6 mS/cm, with the greatest value of 8 mS/cm recorded adjacent to wetland 1A at BH21 within glaciolacustrine clayey silt. The magnitude of D-P EC values within the oxidized zone was dependent on proximity to the brine front with locations within the brine plume and adjacent to wetlands affected by brine inputs having the highest values. Values of  $EC_a$  remained high through the oxidized zone to about 4-5 mbg before decreasing and following a diffusion-like trend with depth to background values within the unoxidized zone of 0.3-0.5 mS/cm for subglacial till and 1-2 mS/cm for glaciolacustrine silt and clay. Background values were reached when  $EC_a$  values

stopped decreasing and remained constant with depth. Background values were not achieved at several locations due to drilling refusal or the maximum depth of investigation being reached.

At many locations peak D-P EC values only extended to 2-3 mbg before decreasing towards background values. These locations were situated further from wetland margins and it is thought that the EC upper boundary condition may be transient depending on pond extent between wet and dry years. Shallow groundwater flow between wetlands and their margins is a dynamic process strongly influenced by pond level and evapotranspiration along wetland margins [Meyboom 1966; Hayashi et al. 1998; van der Kamp and Hayashi 2009]. Furthermore, salt accumulation within the unsaturated zone of wetland margins provides an alternate source of salt that can be remobilised with increases in water table position [Nachshon et al. 2013].

Background  $EC_a$  values were similar to those reported by Maathuis and van der Kamp [1991] who reported values of 0.5-1 mS/cm for till and  $\sim 2$  mS/cm for Regina Clay from Saskatchewan measured using a Geonics EM-39 induction tool; however, values of subglacial till were greater than those recorded by Harrington and Hendry [2006] who reported values of 0.1-0.15 mS/cm for unoxidized Battleford till at the nearby King site in Saskatchewan. Regina Clay is a regional name referring to glaciolacustrine silty clay deposits originating from Glacial Lake Regina during the Wisconsin deglaciation of southern Saskatchewan [Mermut and Acton 1985; Christiansen 1979]. These surficial deposits are similar in texture, age, and depositional environment to those in the current study. As such, the ranges quoted are comparable despite differences in locale. However, differences in the proportion of silt:clay undoubtedly have an effect on  $EC_a$  and are likely the reason for the 1-2 mS/cm range in  $EC_a$  observed, with lower values indicative of less clay and higher values indicative of more clay. Textures of background glaciolacustrine core from the present study ranged from clay to silt with some clay based on geologic descriptions. The difference between background  $EC_a$  values of subglacial till to those reported by others cannot be as easily explained given the similarity in texture,  $n$ , and  $\rho_d$  to Battleford till from the King site and texture amongst Saskatoon Group tills in general [Christiansen 1992]. It is important to note that the background values stated above are *in situ* values and are dependent upon the temperature at which they are measured. Therefore they should only be used as an indication to values one might expect for similar sediments unaffected by brine impacts or natural salinity.

Pore-water EC and  $\text{Cl}^-$  from squeezed core samples from 12 locations displayed a similar trend to the D-P EC data. Values were greatest in the oxidized zone, typically immediately below the water table, and then decreased with depth continuing through the unoxidized zone and reaching stable values at depths of 6-8 mbg. As with D-P EC, the magnitude of  $EC_w$  and pore-water  $\text{Cl}^-$  values within the oxidized zone was dependent on proximity to the brine front and wetlands affected by brine inputs. Pore-water EC and  $\text{Cl}^-$  results from squeezing ranged from 1.94-55.1 mS/cm and 86.7-20,700 mg/L, respectively, with background values of unoxidized subglacial till beneath the brine plume ranging from 2-5 mS/cm and 80-150 mg/L, respectively. Harrington and Hendry [2006] reported  $EC_w$  values of 4-6 mS/cm for unoxidized Battleford till at a nearby site in Saskatchewan unaffected by brine inputs, suggesting values less than 5-6 mS/cm are representative of natural pore-water salinity in unoxidized till.

Several important observations can be made from a comparison of the D-P EC profiles to pore-water chemistry, lithological descriptions, and  $n$  profiles. These data are presented for a representative location within the brine plume (BH6) and at the southern edge of the brine plume (BH5) in **Figure 5-6**. Overall, the shape of the individual D-P EC logs and the associated EC and  $\text{Cl}^-$  results are consistent and do not correlate with lithology, even for the low D-P EC values at BH5. The correlation between the D-P EC logs and the squeezed data at both profiles suggest that pore-water concentrations define the D-P EC response. Minor shifts in the D-P EC response at BH6 between the water table and 4.5 mbgs were likely attributed to changes in texture and clay content, evidenced by shifts in  $n$  from 47 to 50%. Furthermore, transitions from silt to clay at 4.5 mbg in BH6 and 5.3 mbg in BH5 results in a decrease in D-P EC response. This trend is counterintuitive to what would be expected under homogeneous pore-water conditions as clays typically produce higher EC responses relative to coarser sediments [McNeill 1980; Schulmeister et al. 2003].

The clay layer at 2.5 m depth at BH5 (**Figure 5-6**) and described during core sampling was not reflected in the  $n$  profile, possibly due to the 30 cm sampling frequency being too great to characterize this thin layer. Oddly,  $EC_w$  and pore water  $\text{Cl}^-$  increases in response to the clay layer do not result in increases to D-P EC response. For pore-water conditions within and adjacent to the brine plume, lithological boundaries clearly played an important hydrostratigraphic role in

controlling brine transport, evidenced by decreases in  $EC_w$  and pore-water  $Cl^-$  in response to the presence of the clay layer from 4.5-5.3 mbg at BH06 and BH05, respectively.

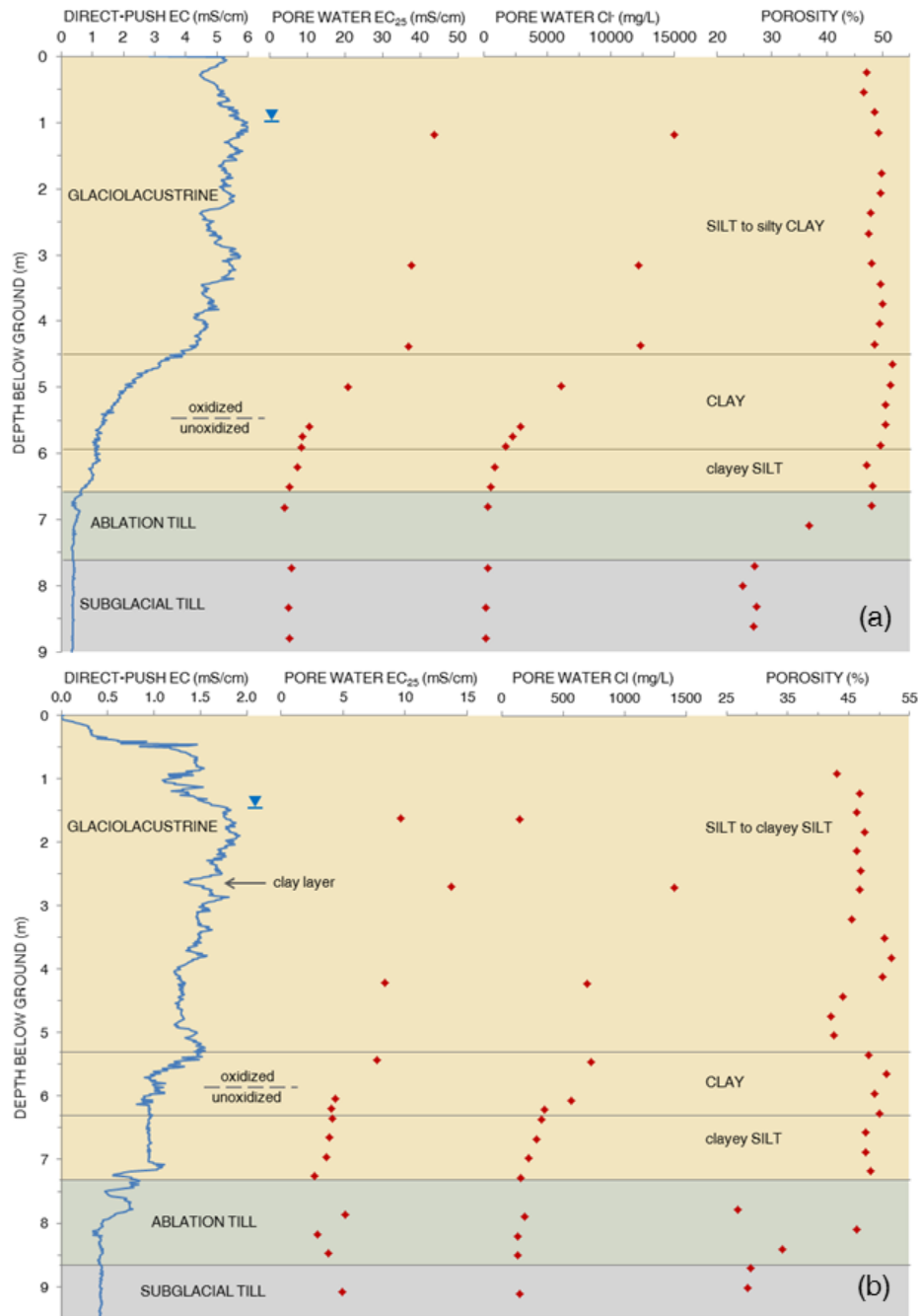


**Figure 5-6.** Depth profiles of D-P EC,  $EC_w$  (relative to 25°C), pore-water  $Cl^-$ , and  $n$  at BH6 located within the brine plume (a) and BH5 located the southern edge of the brine plume (b). The inverted triangle represents the location of the water table at time of coring.

## 5.6 Bulk Soil and Pore-water Salinity

To examine the relationship between bulk soil and pore-water salinity, D-P EC logs were compared to EC results from squeezing of cores collected in adjacent squeezed core locations. To ensure equivalency of scale between EC results obtained from squeezing ~7.5 cm long cores to higher resolution D-P EC measurements, D-P EC data were smoothed using a moving five-point average. Additionally, D-P EC data collected at *in situ* temperature conditions were corrected to 25°C to ensure equivalent comparisons to  $EC_w$  data. The  $EC_a$  of moist soils increases at approximately the same rate as  $EC_w$  (i.e. 2% per 1°C; [Rhoades et al. 1999]). The same can be expected for coarse-textured sediments [Friedman 2005], however in clay-rich media the  $EC_a$ -temperature relationship is actually more complex due to surface conduction and the mobility of counterions [Sen and Goode 1992]. Temperature conversions were made using a linear relationship after Sorensen and Glass [1987]:

$$EC_{25} = \frac{EC_T}{[1+k(T-25)]} \quad (5.1)$$

where  $EC_{25}$  is the EC at 25°C,  $EC_T$  is the EC at *in situ* temperature  $T$ , and  $k$  is the temperature compensation factor (°C<sup>-1</sup>). A  $k$  value of 0.02 was used to ensure consistency with compensation of pore-water measurements. It was within the range determined for natural saline waters [Hayashi 2004]. A geometric mean groundwater temperature of 5.4°C obtained from temperature measurements recorded by water level instrumentation from eight piezometers located across the study area and screened between 2.1 and 13.5 mbg on October 10-11, 2012 was used to represent *in situ* temperature conditions for all D-P EC logs collected.

Temperature variations with depth below the water table could not be easily accounted for during drilling because the Geoprobe Systems<sup>®</sup> instrument used to collect  $EC_a$  measurements lacked a built-in temperature sensor. While temperature variations with depth below the water table in fine-grained glacial materials are generally small ( $\leq 3-4^\circ\text{C}$ ), temporal variations near a shallow water table can be greater ( $>7^\circ\text{C}$ ) as a result of seasonal fluctuations at surface [Hayley et al. [2007]. However, with increasing depth, temporal variations become negligible. For example, Hendry and Woodbury [2007] did not observe any seasonal temperature fluctuations beyond 12 mbg in a clay-rich till aquitard in Saskatchewan.

Temporal variations in subsurface temperature conditions were considered to be minimal between August 2011 and October 2012 drilling campaigns for several reasons. In October 2012 groundwater temperatures ranging from 3.4-7.8°C were measured with the majority of measurements ~5°C. Temperatures measured at two piezometers during the August 15-19, 2011 drilling program were 4.5°C. Furthermore, D-P EC logs collected at BH1 in 2011 and 2012 were nearly identical (**Figure 5-7**), suggesting that differences in groundwater temperatures between the two drilling events were negligible. The strong similarity in D-P EC logs at BH1 also suggest that temporal changes in  $EC_w$  and pore-water  $Cl^-$  over the period of one year were small, therefore suggesting that a comparison of 2011 drill core to the D-P EC logs collected the following year were valid.

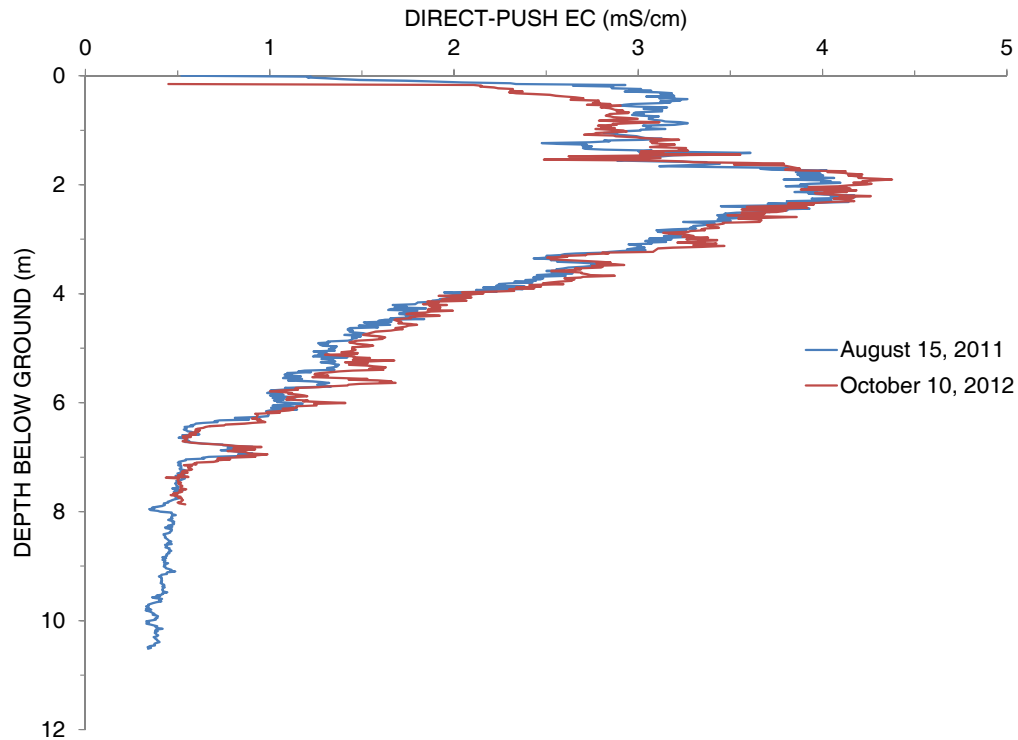


**Figure 5-7.** Depth profiles of D-P EC measured adjacent to BH1 in 2011 and 2012.

Pore-water EC data obtained for each of the major lithologies encountered during drilling were plotted as a function of D-P EC and are presented in **Figure 5-8**. To empirically determine the slope and intercept terms in equation (2.2) it was necessary to exclude a number of low EC data points from the regression analyses, since (2.2) is a linear equation and is only applicable for

conditions when  $EC_w \geq 2-4$  mS/cm. After plotting  $EC_a$  as a function of  $EC_w$  which made it easier to identify deviation from linearity at low values of  $EC_w$  (data not shown), a total of 12 and 31 data points were excluded from glaciolacustrine and grouped comparisons, respectively. Significant agreements between  $EC_a$  and  $EC_w$  were obtained for each lithology using least-squares linear regression with coefficients of determination greater than 0.91 for glaciolacustrine and till lithologies (**Figure 5-8a**). Grouping samples from all four lithologies as one population also produced a significant linear relationship  $EC_a$  and  $EC_w$  at the 0.05 probability level (**Figure 5-8b**), suggesting that values of  $EC_a$  are largely controlled by  $EC_w$  when D-P EC  $>1-1.5$  mS/cm. At lower  $EC_a$  values the relationship becomes nonlinear, as documented for surface soils [Rhoades 1981; Shainberg et al. 1980].

One outlier with a D-P EC of about 8 mS/cm was also excluded from the ablation till regression analysis (**Figure 5-8a**). Because ablation till was observed to be intercalated with glaciolacustrine sediment, this sample was likely dominated by glaciolacustrine material as it plots near the top of the glaciolacustrine regression line. Since these intercalations often occurred on a scale too small to be adequately captured by sampling, where observed the entire interval was considered ablation till. Despite differences in the squeezing methods used in this study to obtain  $EC_w$  compared to the more conventional saturation extract method, slope and intercept terms for glaciolacustrine and till lithologies obtained by linear regression analysis of measured  $EC_w$  versus  $EC_a$  data (**Table 5-2**) were comparable to those determined by Halvorson et al. [1977] for surface soils from Montana and North Dakota that ranged from clay to sandy loam. Their study used three different methods to obtain  $EC_a$ , including an EC probe similar to the one employed in this study.

As predicted by equations (2.1) and (2.2), the slope of the  $EC_a-EC_w$  relationship increased as a result of increases in  $n$  between subglacial till, ablation till, and glaciolacustrine (**Figure 5-8a**). This is because at values of  $EC_w >2-4$  mS/cm, pore-water salinity is the dominant contributor to  $EC_a$  [Rhoades et al. 1993]. A higher  $n$  means a greater proportion of pore-water to sediment on a volume basis, and thus increases in  $n$  translate to increased  $EC_a$  response. Similarly the y-intercept, which is strongly controlled by  $EC_s$  since the  $[(\theta_s + \theta_{ws})^2 / \theta_s]$  term in equation (2.2) is typically close to 1 [Rhoades et al. 1989], increased with clay content.

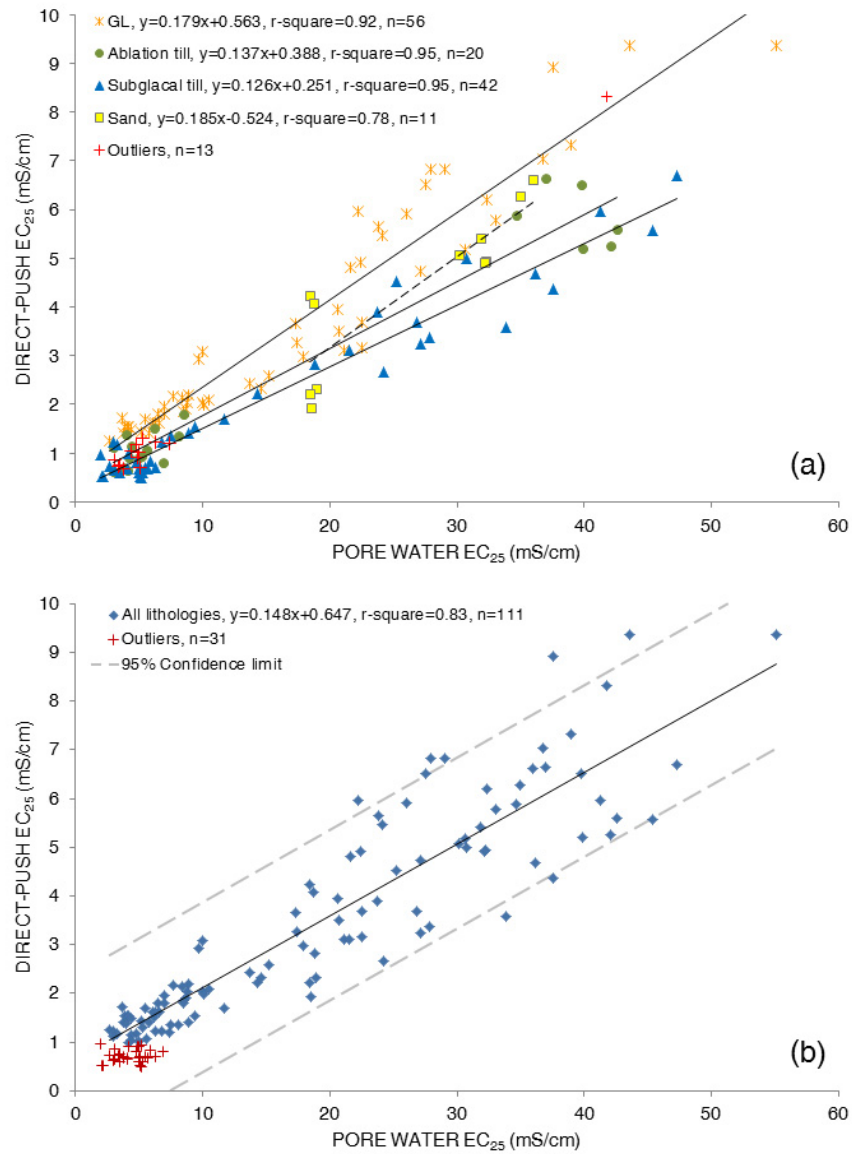


**Figure 5-8.** D-P EC values plotted as a function of  $EC_w$  for the four major lithologies encountered in the study area (a) and for all lithologies together (b). Linear regression lines are drawn in black with a probability level of 0.05 and sand line is dashed. GL denotes glaciolacustrine. All data expressed relative to 25°C.

**Table 5-2.** Summary of slope and intercept terms of  $EC_w$  versus  $EC_a$  functions from linear regression analysis for glaciolacustrine and till lithologies and saturation extract ( $EC_e$ ) versus  $EC_a$  functions for surface soils of the Northern Great Plains from Halvorson et al. 1977, Figure 1†.

Lithology or Texture	$EC_w$ (or $EC_e$ ) – $EC_a$ function
glaciolacustrine	$EC_w = 5.10EC_a - 1.44$
ablation till	$EC_w = 6.91EC_a - 1.91$
subglacial till	$EC_w = 7.50EC_a - 1.09$
silty clay, clay†	$EC_e = 3.48EC_a - 1.07$
silty clay loam, clay loam, sandy clay loam, loam†	$EC_e = 5.47EC_a - 0.47$
sandy loam†	$EC_e = 7.36EC_a - 0.87$

The steepest slope measured was for sand (**Figure 5-8a**), despite it having a  $n$  of 38% and was generally equivalent to that of ablation till. Furthermore, the  $y$ -intercept term for sand was negative compared to the positive terms determined for glaciolacustrine, ablation till, and subglacial till. While sand and silt grains are considered to be insulating and have the effect of reducing the ability of pore-water to conduct current at sufficiently low values of  $EC_w$  [McNeill 1980], a negative  $y$ -intercept is not possible because it implies a negative  $EC_s$ . According to the regression results presented for sand in **Figure 5-8a**, D-P EC should reach zero at values of  $EC_w$  below about 2.8 mS/cm. Schulmeister et al. [2003] reported D-P EC values on the order of 0.2 mS/cm for a Kansas River Floodplain alluvial sand and gravel unit with groundwater EC values ranging from 0.5-0.8 mS/cm using similar D-P drilling equipment, suggesting that low  $EC_w$  values should yield measureable D-P EC values. Sand was only encountered in a limited number of core locations within the study area, thus limiting the sample size and range of EC measurements attainable for sand.

The great variability in D-P EC observed between two groups of sand data at a  $EC_w$  of about 18 mS/cm (**Figure 5-9**) can be explained by differences in  $n$  using Archie's Law [Archie 1942]:

$$\frac{EC_a}{EC_w} = n^m \quad (5.2)$$

where  $m$  is a material-dependent empirical exponent. Originally derived from conductivity measurements on unconsolidated sands and consolidated sandstones, Archie's Law is applicable to sediments containing little or no clay. The two data points at location 1 (**Figure 5-9**) represent fine sand with some silt with an  $n$  of about 0.35 from BH11. The three data points at location 2 represent a poorly sorted fine and medium-grained sand with trace gravel from BH14. Porosity could not be determined for the sand from BH14 as the core lacked the cohesiveness needed for testing, however gravimetric water content was determined to be about 14% compared to about 21% for samples from BH11. This suggests the  $n$  for sand from BH14 is lower than that measured for BH11. Rearranging equation (5.2) to solve for  $EC_a$  and plotting over a continuous range of  $EC_w$  with an  $m$  value of 1.4 for quartz sand [Friedman 2005], the data at points 1 and 2 in **Figure 5-9** are indeed reproducible assuming an  $n$  of 0.35 and 0.22 for BH11 and BH14, respectively.

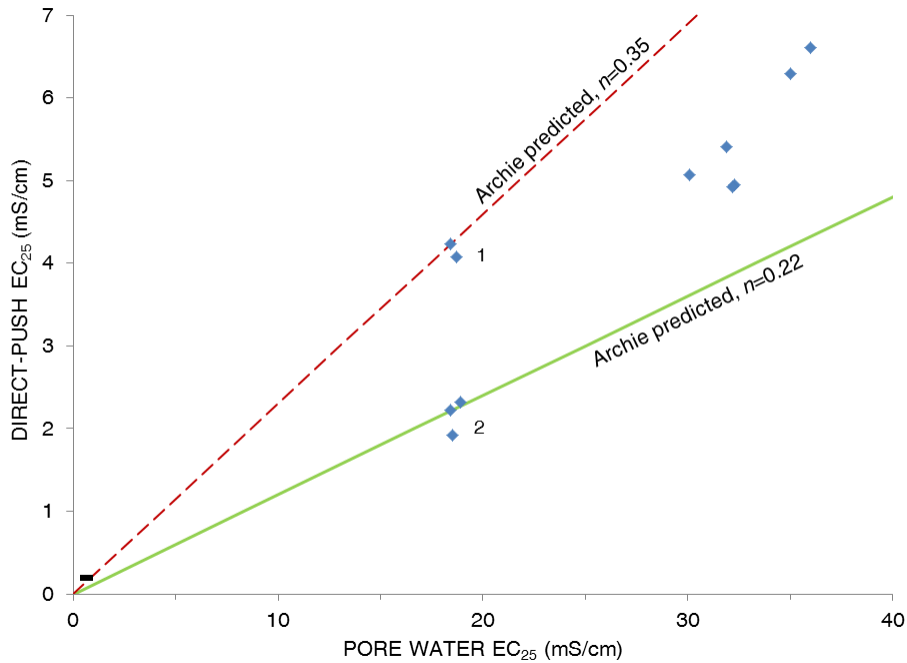


**Figure 5-9.** D-P EC versus  $EC_w$  for sand samples. Diamonds represent measured data and solid and dashed lines represent predicted D-P EC using Archie's law over a continuous range of  $EC_w$  using an  $m$  value of 1.4 for quartz sand. The solid rectangle represents the range in  $EC_w$  values measured by Schulmeister et al. [2003] for alluvial sand and gravel. All data expressed relative to 25°C.

### 5.7 Predicting Pore-water EC from Direct-push EC

The empirically determined slope and intercept terms for each lithology from **Figure 5-8a** were used with measured  $\rho_d$  and  $n$  values presented in **Table 5-1a** to calculate  $EC_w$  as a function of D-P EC using equation (2.3), where  $\theta_s = \rho_d/\rho_s$  and  $\rho_s$  is an assumed soil particle density of 2700 kg/m<sup>3</sup>. Given the limited sample size for sand and considerable spread in the measured data, a best-fit slope of 0.17, determined assuming a  $y$ -intercept of zero in the linear regression, was used. A summary of the parameters used to solve equation (2.1) are presented in **Table 5-3**. A good overall fit was achieved between measured and calculated  $EC_w$  for the four lithologies encountered within the linear portion of the Rhoades model (i.e.  $EC_w$  values >2 mS/cm) (**Figure 5-10**). However, the model under approximated  $EC_w$  for glaciolacustrine at values of  $EC_w < 5-7$  mS/cm.

**Table 5-3.** Measured (\*) and empirically determined parameters used in equation (2.1) to predict  $EC_w$  in Figure 5-10.

Parameter	Glaciolacustrine	Ablation till	Subglacial till	Sand
$\theta_w^* \dagger$	0.49	0.39	0.28	0.38
$\theta_{ws}$	0.31	0.25	0.16	0.21 ‡
$\theta_s^*$	0.51	0.61	0.71	0.62
$EC_s$	0.43	0.32	0.24	0

† values from Table 5-1a.

‡ calculated from a best-fit slope of 0.17 on  $EC_a$  versus  $EC_w$  plot assuming  $EC_s$  is zero.

To evaluate the accuracy of model predictions, paired sample  $t$ -tests were performed on measured and calculated  $EC_w$  values by individual sample location for each major lithological group and across all data. Predictions using equation (2.1) which accounted for lithological changes were also compared to predictions across all data using the simple linear relation developed in **Figure 5-8b**. While this method cannot account for differences in  $n$ , clay content and mineralogy, and sediment structure between sediment types shown to influence  $EC_a$  [Rhoades and Corwin 1990; Friedman 2005], it may be appropriate for sites with simple geology or where geologic knowledge is limited. Results of statistical comparisons are presented in **Table 5-4**.

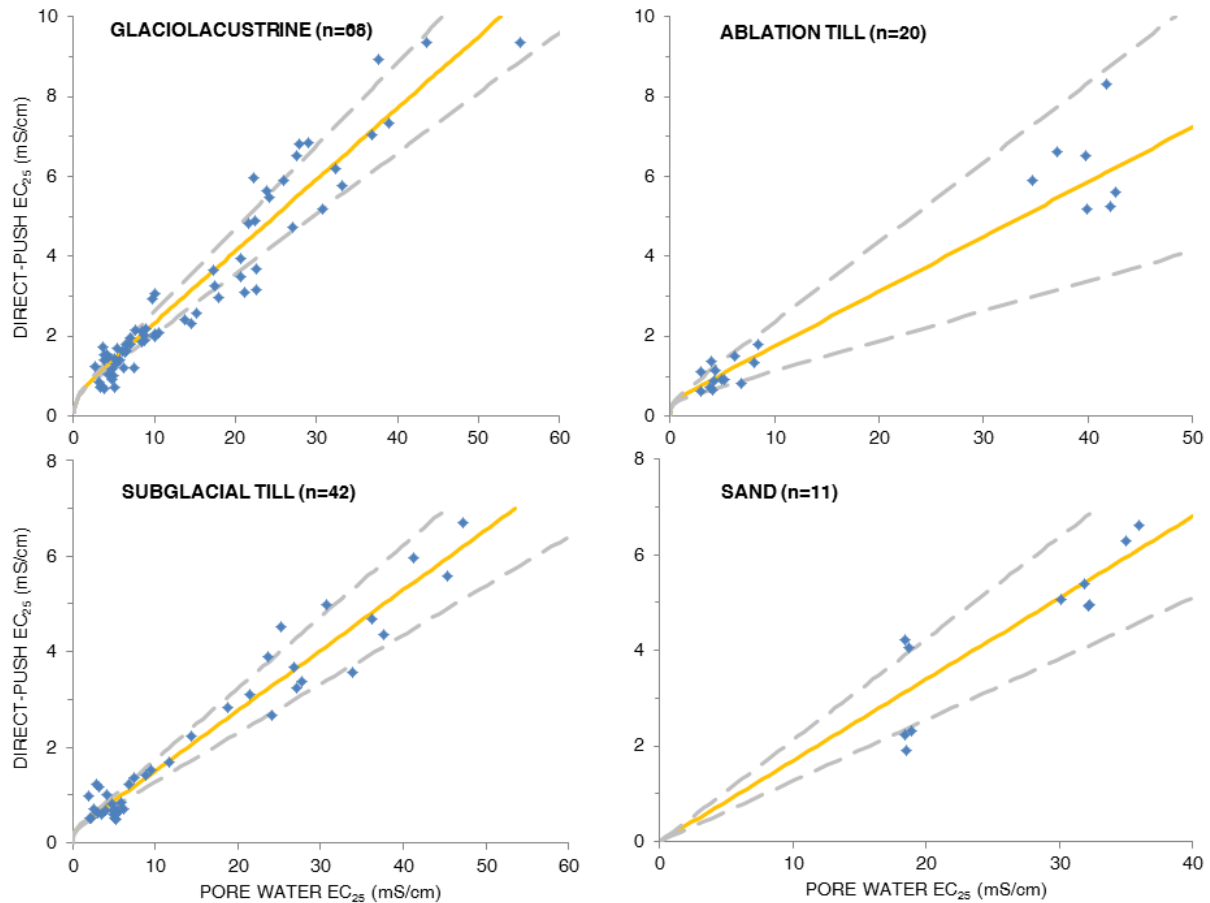


**Figure 5-10.** Predicted  $EC_w$  values using equation (2.1) over a continuous range of D-P EC (solid line) compared to measured data (diamonds) for each major lithology. Dashed lines represent  $\pm 1$  standard deviation of the measured  $n$  for each sediment type (Table 5-1a). All data expressed relative to 25°C.

A paired sample  $t$ -test compares the mean difference between two populations of paired samples whose differences are normally distributed. In comparisons where the assumption of normality was not fully met, which tended to be those with small sample sizes, statistical outcomes of  $t$ -tests were confirmed using Wilcoxon signed-rank tests. The Wilcoxon signed-rank test is a nonparametric alternative to a paired sample  $t$ -test that uses the sign and magnitude of the rank of differences between pairs of measurements without the assumption of normally distributed differences [Ott 1977]. In all cases, statistical outcomes did not differ between paired sample  $t$ -tests and Wilcoxon signed-rank tests and so  $t$ -test results are presented for consistency. There was no statistical difference between measured and calculated  $EC_w$  values determined using equation (2.1) for each lithological group (Table 5-4). While  $EC_w$  predictions were not as

statistical significant for glaciolacustrine at measured  $EC_w < 7$  mS/cm versus  $EC_w \geq 7$  mS/cm, evidenced by lower  $p$ -values, measured and predicted  $EC_w$  values were still statistically equivalent. Pore-water EC predictions were better across all data using the Rhoades model ( $p=0.85$ ) versus the simple linear relation from **Figure 5-8b** ( $p=0.70$ ), however compositing all data still enabled statistically accurate predictions of  $EC_w$ .

**Table 5-4.** Paired sample  $t$ -test results for comparisons between measured and calculated  $EC_w$  and pore-water  $Cl^-$  for each major lithological group using equation (2.1), and across all data using linear relations from Figures 5-8b and 5-12. Samples paired by location and depth with a significance level of 0.05 (two-tailed).

Comparison	$t$ -statistic	Degrees of freedom	$p$ -value	Result
glaciolacustrine $EC_w$	0.70	67	0.49	no difference
glaciolacustrine $EC_w \geq 7$ mS/cm	0.35	41	0.73	no difference
glaciolacustrine $EC_w < 7$ mS/cm	1.20	25	0.24	no difference
ablation till $EC_w$ †	0.12	19	0.91	no difference
sand $EC_w$	0.54	10	0.60	no difference
subglacial till $EC_w$	0.07	41	0.95	no difference
$EC_w$ all data equation (2.1)	0.19	141	0.85	no difference
$EC_w$ all data linear	0.38	141	0.70	no difference
$Cl^-$ all data linear ‡	0.75	98	0.46	no difference

† one outlier from Figure 5-8a excluded from comparison.

‡ all negative  $Cl^-$  predictions and eight outliers from Figure 5-12 excluded from comparison.

The ability of equation (2.1) to predict  $EC_w$  at values  $< 2$  mS/cm could not be evaluated for the four lithologies encountered because background pore-water salinities were above this concentration (**Figure 5-10**). This suggests that the simplified linear form of the Rhoades model given by equation (2.2) may be appropriate for other sites elsewhere in the glaciated northern plains region, as the additional complexity of the  $y$ -intercept term in equation (2.1) is only needed to predict  $EC_w$  at values  $< 2$  mS/cm [Rhoades 1993]. The general increase in variability of measured data with increasing  $EC_w$  may be attributed to  $n$  variations within each lithological unit. As illustrated by the grey lines in **Figure 5-10**,  $n$  variations produce more pronounced deviations in  $EC_a$  at higher values of  $EC_w$ .

Based on the linear relationship established between measured  $EC_a$  and  $EC_w$  at values of  $EC_w > 5$  mS/cm for glaciolacustrine in **Figure 5-8a**, every 1 mS/cm increase in  $EC_a$  corresponds to a 5 mS/cm increase in  $EC_w$ . Maathuis and van der Kamp [1991] reported the same ratio between  $EC_a$  and  $EC_w$  for similar postglacial silt and clay deposits at other potash mining sites in southern Saskatchewan. For comparison, their data is presented in **Figure 5-11** together with data from the present study. In their report they compared  $EC_a$  measurements obtained by running a EM-39 induction tool down existing piezometers to  $EC_w$  measurements of groundwater samples collected from the same piezometers screened within silt and clay at two potash mining sites located about 70 km west and 180 km southeast of the present study area, respectively. While a reference temperature for  $EC_a$  measurements was not explicitly stated in their study, the EM-39 instrument they used can be calibrated by taking apparent EC measurements of fluids of known temperature and EC, such as lakes [Taylor et al. 1989] or by simply measuring the temperature of groundwater from piezometers logged and applying a correction as in equation (5.1).

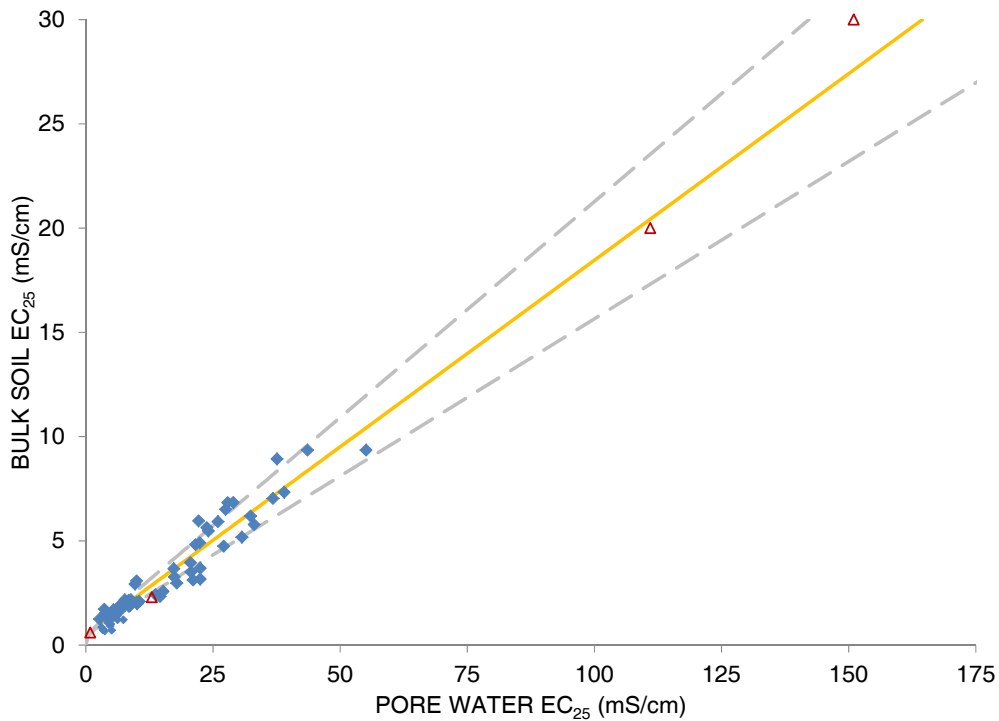
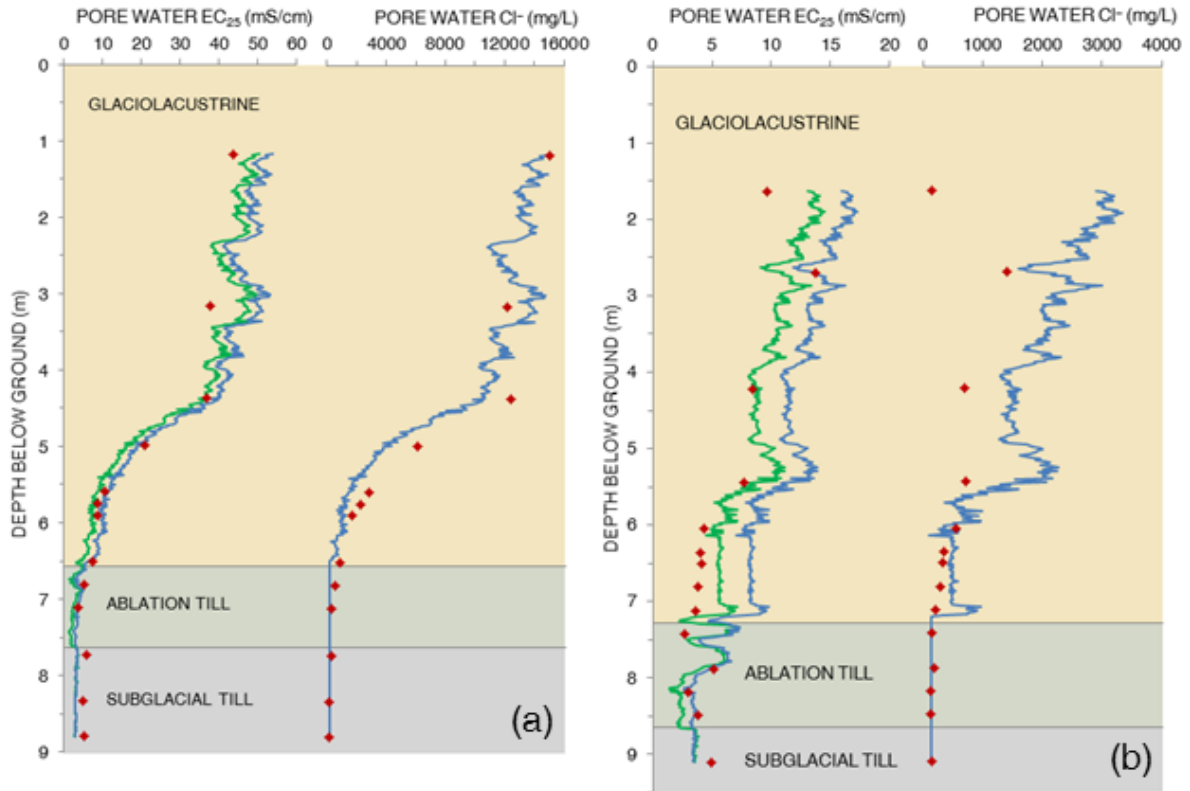


**Figure 5-11.** Predicted  $EC_w$  values using equation (2.1) (solid line) compared to measured data (diamonds) for glaciolacustrine from Figure 5-10. Open triangles represent data from Maathuis and van der Kamp [1991] for similar Saskatchewan postglacial silt and clay deposits. Dashed lines represent  $\pm 1$  standard deviation of the measured  $n$  (Table 5-1a). All data expressed relative to 25°C.

Although the dataset of Maathuis and van der Kamp [1991] is small, it spans a much greater range of EC values than data from the current study and plots nearly on top of the  $EC_a-EC_w$  line predicted for glaciolacustrine using equation (2.1) (**Figure 5-11**). The similarity between datasets suggests that the parameters established for glaciolacustrine sediment at the present study area (**Table 5-3**) may be applicable for other sites in southern Saskatchewan containing similar postglacial sediments. More site specific data from other regions would need to be compared, including index parameter measurements to confirm lithologic equivalency, to support this indication.

In order to assess model predictions on the scale of individual profiles, predicted and measured  $EC_w$  were compared for three core locations representative of the lithologies and varying levels of relative brine concentrations encountered across the study area (**Figure 5-12 and Table 5-5**). There was no significant difference between predicted values of  $EC_w$  using equation (2.1) and measured values for all three depth profiles assessed. Slight over and under approximations within glaciolacustrine and till lithologies were expected given the natural variations in  $n$  and clay content; however, overall trends in pore-water salinity even under low relative brine impact (i.e. BH5) are reproducible from  $EC_a$  measurements. The poorest fits between predicted and measured  $EC_w$  were obtained for sand, undoubtedly due to  $n$  differences between sands encountered across the site.

Using the linear relation developed in **Figure 5-8b** to predict  $EC_w$ , in which all lithologic data were grouped together, resulted in a statistically equivalent fit to measured data for BH6, but not for BH5 and BH14 (**Table 5-5**). Since the surficial geology of the study area was dominated by glaciolacustrine, which resulted in a greater proportion of glaciolacustrine to till samples, predictions using the linear relation for locations underlain primarily by till (i.e. BH14) were less accurate. The linear relation was also less accurate at predicting  $EC_w$  under low relative brine impact (i.e. BH5) compared to equation (2.1). Overall, by controlling for lithology type and differences in index parameters in equation (2.1), better fits can be achieved than by simply grouping data across all sediment types together. However, if the area of investigation was focused over a smaller portion of the site such as the western portion that is underlain primarily by glaciolacustrine sediment, the simpler approach could produce accurate predictions.



◆ measured — Rhoades equation (1) — all lithologies empirical

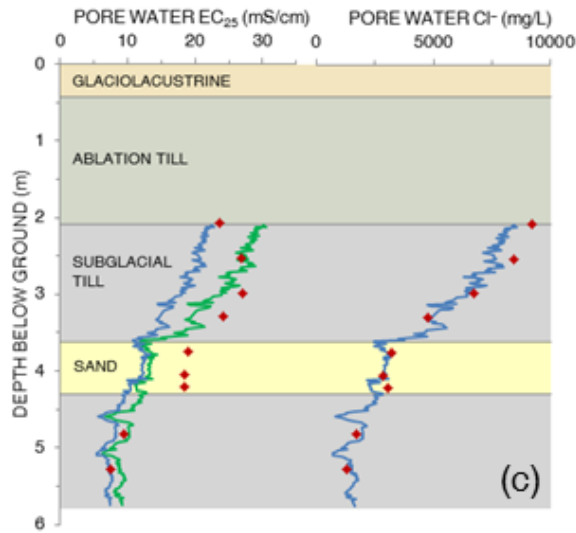


**Figure 5-12.** Measured and predicted  $EC_w$  and pore-water  $Cl^-$  profiles for BH6 (a), BH5 (b), and BH14 (c). All data presented was collected below the water table.

**Table 5-5.** Paired sample *t*-test results for comparisons between measured and calculated  $EC_w$  and pore-water  $Cl^-$  for BH5, BH6, and BH14 using equation (2.1), and linear relations from Figures 5-8b and 5-13. Samples paired by location and depth with a significance level of 0.05 (two-tailed). Negative  $Cl^-$  predictions and paired measured values excluded from comparisons.

Comparison	<i>t</i> -statistic	Degrees of freedom	<i>p</i> -value	Result
BH5 $EC_w$ equation (2.1)	1.28	13	0.22	no difference
BH5 $EC_w$ all data linear	3.85	13	0.002	different
BH5 $Cl^-$ all data linear	2.37	8	0.04	different
BH6 $EC_w$ equation (2.1)	0.68	12	0.51	no difference
BH6 $EC_w$ all data linear	1.10	12	0.29	no difference
BH6 $Cl^-$ all data linear	1.68	6	0.14	no difference
BH14 $EC_w$ equation (2.1)	1.24	8	0.25	no difference
BH14 $EC_w$ all data linear	4.47	8	0.002	different
BH14 $Cl^-$ all data linear	1.70	8	0.13	no difference

### 5.8 Relationship of Pore-water $Cl^-$ to Pore-water Salinity

For the majority of locations at which core samples were squeezed, depth profiles of pore-water  $Cl^-$  were observed to mirror those of  $EC_w$  (**Figure 5-6**), suggesting that  $EC_w$  may be used to predict pore-water  $Cl^-$  at this brine impacted site. To examine the relationship further, pore-water  $Cl^-$  was plotted as a function of  $EC_w$  for squeezed samples. Results yielded a significant regression ( $r^2=0.92$ ; **Figure 5-13**) and suggested that  $Cl^-$  changes in the subsurface were attributed to the presence of the brine plume across the study area and that the plume was responsible for changes in  $EC_w$  and  $EC_a$ . Linear regression analysis of D-P EC versus pore-water  $Cl^-$  also produced significant outcomes with coefficients of determination ranging from 0.84-0.94 for glaciolacustrine and till lithologies (data not presented).

Eight outliers from the top 2 m of BH12 and BH13 were excluded from the linear regression analysis in **Figure 5-13**, as these data clearly stood apart from the rest of the data. Although squeezed pore-water samples were only analyzed for  $Cl^-$ , it is likely that changes in relative proportions of other dissolved chemical species (e.g.,  $SO_4^{2-}$ ) may be responsible for the lower  $EC_w$  values observed amongst these outliers. Shallow groundwater in glacial tills within the glaciated plains region of North America is typically dominated by  $SO_4^{2-}$  resulting from pyrite oxidation, with groundwater  $SO_4^{2-}$  concentrations within unleached tills commonly in the

thousands to tens of thousands of mg/L [Hendry et al. 1986; Keller et al. 1991; Van Stempvoort et al. 1994].

Applying the empirical equation developed in **Figure 5-13** to calculated  $EC_w$  depth profiles using equation (2.1) for squeezed cores yielded significant fits between calculated and measured pore-water  $Cl^-$  across all data (**Table 5-4**). Greater discrepancies between calculated and measured  $Cl^-$  data were noted in areas of low relative brine impact (**Figure 5-12b**), likely due to greater influence from other dissolved charged species. Paired  $t$ -test results indicated no significant difference between measured and calculated pore water  $Cl^-$  at BH6 and BH14, however results at BH5 differed significantly (**Table 5-5**). It is important to note that  $EC_w$  values  $\geq 5$  mS/cm are needed for  $Cl^-$  approximations using the linear equation in **Figure 5-13**. Below this concentration, the predicted  $Cl^-$  values approach zero. As such, the limit for  $Cl^-$  approximations for BH6 and BH5 was attained at depths of 6.5 and 7.3 m, respectively (**Figure 5-12**).

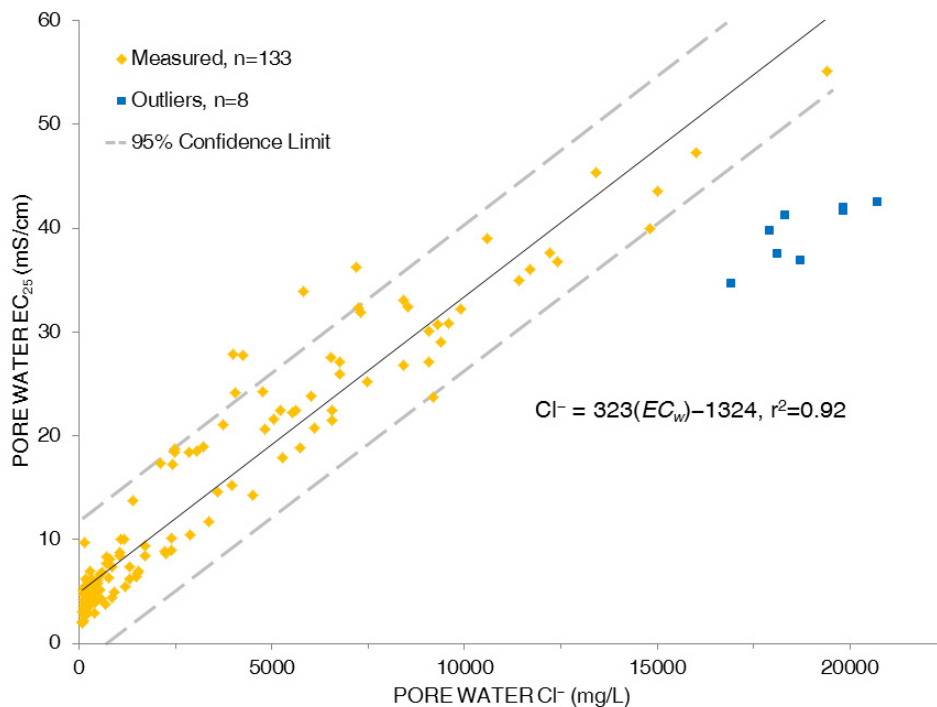


**Figure 5-13.** Pore-water EC (relative to 25°C) values plotted as a function of pore-water  $Cl^-$  concentrations for all samples. Linear regression line is drawn in black at a probability level of 0.05. Outliers shown were excluded from the regression analysis.

### 5.9 Timing of Brine Release

The diffusion-shaped depth profiles of  $EC_a$  observed in the vicinity of the brine plume in response to pore-water  $Cl^-$  variations associated with brine migration suggested that vertical brine transport was likely diffusion-controlled. Short-term solute transport (i.e. <50 years) [Johnson et al. 1989] and long-term solute transport [Desaulniers et al. 1981; Remenda et al. 1994; Hendry and Wassenaar 1999; Hendry et al. 2000] in similar low  $K$  clay-rich glacial deposits has also shown to be diffusion-dominated. The upward hydraulic gradients measured near wetland 1A further suggested that downward brine transport could not have occurred by advection under present-day conditions. To estimate the timing of brine introduction into wetlands 1A-5, D-P EC profiles from three drill locations along the length of the brine plume were modeled assuming 1D vertical  $Cl^-$  transport by diffusion only. BH21 was located nearest the brine source and adjacent to pond 1A, BH6 was located approximately half-way down the length of the plume and adjacent to ponds 2 and 3, and BH13 was located at the downgradient end of the plume and adjacent to pond 5 (**Figure 3-2a**).

Vertical diffusive transport with time is governed by Fick's second law (equation 2.8). A numerical solution to (equation 2.8) for 1D transport of a conservative solute ( $Cl^-$  in this case) downward through a surficial aquitard after Appelo and Postma [2005] is given by:

$$\frac{C(x,t) - C_i}{C_0 - C_i} = \operatorname{erfc}\left(\frac{x}{\sqrt{4D_e t}}\right) \quad (5.3)$$

where  $C(x,t)$  is the pore-water  $Cl^-$  concentration at distance  $x$  from the upper boundary at time  $t > 0$ ,  $C_i$  is the initial pore-water  $Cl^-$  concentration of the glacial material prior to diffusion, and  $C_0$  is the pore-water  $Cl^-$  concentration at the upper boundary after the introduction of brine at  $t=0$ . The model assumes that  $C_0$  is constant with time. This is a simplifying assumption that does not account for changes in the  $Cl^-$  concentration of each wetland in response to seasonal or annual changes in water balance or  $Cl^-$  losses with time. However, presuming fill and spill events are the main source of brine inputs into wetlands 2-5,  $Cl^-$  mass losses are comparatively small with time, and long-term average annual  $Cl^-$  concentration variations in groundwater at the upper boundary are sufficiently small, this assumption is considered valid. The model further assumes that the initial  $Cl^-$  concentration of the glacial material prior to brine diffusion is constant with depth.

The upper boundary for each D-P EC profile was chosen as the depth below which  $EC_a$  began to decrease from consistent near-maximum values within the oxidized zone towards background values within the unoxidized zone. The upper boundary for BH21, BH6, and BH13 was selected at depths of 4.75, 4.33, and 3.17 mbg, respectively. These depths occurred 1.2-2.8 m above the unoxidized zone and corresponded to the appearance of clay (BH6), interbedded silt and clay (BH21), or subglacial till (BH13) (**Appendix A**). The lower boundary for each profile (i.e.  $C_i$ ) was defined as a constant  $EC_a$  concentration attained with increasing depth.

Diffusion coefficients for diffusion through saturated porous media depend upon properties of the sediment, temperature and viscosity of the pore fluid, chemistry of the source solution, and interactions between diffusing species and sorbed or aqueous species present in the saturated media [Shackelford 1991]. Solutes diffuse at slower rates in porous media than in free-solution as a result of tortuous migration pathways caused by the complex arrangement of soil particles. The free-solution diffusion coefficient ( $D_0$ ) of  $Cl^-$  is  $2 \times 10^{-10} \text{ m}^2/\text{s}$  at  $25^\circ\text{C}$  [Li and Gregory 1974], however the  $D_e$  of  $Cl^-$  through glacial till can be up to 1 order of magnitude less than this value.

Values of  $D_e$  are most commonly determined by laboratory diffusion tests on soil cores from the geologic unit of interest. Hendry et al. [2000] reported lab  $D_e$  values for  $Cl^-$  of  $2.1 \times 10^{-10} \text{ m}^2/\text{s}$  for pore-water from three samples of unoxidized Battleford till from the King Site in Saskatchewan. Maathuis and van der Kamp [1994] determined  $D_e$  values for  $Cl^-$  on the order of  $2 \times 10^{-10}$  to  $4 \times 10^{-10} \text{ m}^2/\text{s}$  from lab diffusion tests of potash brine through samples of unoxidized Floral and Sutherland till from Saskatchewan. Crooks and Quigley [1984] reported  $D_e$  values for  $Cl^-$  of  $4.4 \times 10^{-10}$  to  $7.3 \times 10^{-10} \text{ m}^2/\text{s}$  from lab diffusion tests of NaCl solutions through remolded and compacted oxidized Sarnia clay till from Ontario. Barone et al. [1989] determined  $D_e$  values for  $Cl^-$  of  $5.9 \times 10^{-10} \text{ m}^2/\text{s}$  and  $7.5 \times 10^{-10} \text{ m}^2/\text{s}$  for lab diffusion tests of NaCl and landfill leachate, respectively, through unoxidized Sarnia clay till. All of the  $D_e$  values quoted above were measured at or corrected to *in situ* pore water temperatures of  $5\text{-}10^\circ\text{C}$ .

Values of  $D_e$  can also be approximated by fitting a solute transport model such as equation (5.3) to measured data, provided remaining parameters and boundary conditions are well constrained and  $D_e$  values are representative for the geologic unit of interest. This approach was employed in

the current study. Using this approach, Desaulniers et al. [1981] obtained good agreement between model outcomes and observed values for  $\text{Cl}^-$  using a  $D_e$  of  $3 \times 10^{-10} \text{ m}^2/\text{s}$  to reproduce solute transport over a 10-15 ka period at four southwestern Ontario sites underlain by clayey till and glaciolacustrine clay. In a study of diffusive transport beneath a five-year-old Ontario landfill, Johnson et al. [1989] was able to reproduce observed  $\text{Cl}^-$  values using  $D_e$  values of  $4 \times 10^{-10}$  to  $6 \times 10^{-10} \text{ m}^2/\text{s}$  within clayey till. In both of the above studies, groundwater advection was not found to provide a major influence on  $\text{Cl}^-$  transport and measured  $\text{Cl}^-$  distributions were attributed to diffusion.

A possible explanation for the greater  $D_e$  values reported for Sarnia clay tills studied by Crooks and Quigley [1984], Barone et al. [1989], and Johnson et al. [1989] in comparison to Saskatchewan tills studied by Maathuis and van der Kamp [1994] and Hendry et al. [2000] is a difference in  $\rho_d$  and  $n$  values due to different consolidation histories. Van Loon et al. [2007] determined that increasing  $\rho_d$  by compacting samples to 1300-1900  $\text{kg}/\text{m}^3$  resulted in a decrease of both the  $D_e$  and  $n_e$  for  $\text{Cl}^-$  in bentonite clays and attributed it to decreasing interlayer porosity. Values of  $\rho_d$  and  $n$  for Sarnia clay till and Battleford till are about 1700  $\text{kg}/\text{m}^3$  and 39% [Barone et al. 1989] and 1900  $\text{kg}/\text{m}^3$  and 30% [Sauer and Christiansen 1991; Shaw and Hendry 1998], each respectively. The greater reported  $\rho_d$  and lower  $n$  for Battleford till is consistent with lower published  $D_e$  values compared to Sarnia Clay till and suggests higher rates of consolidation by glacial ice. Since subglacial till in the present study was found to be consistent with Battleford till, a  $D_e$  range of  $2 \times 10^{-10}$  to  $4 \times 10^{-10} \text{ m}^2/\text{s}$  for  $\text{Cl}^-$  is considered more representative than the higher published values for Ontario tills.

The glaciolacustrine sediment across the study area had average  $\rho_d$  and  $n$  values of about 1400  $\text{kg}/\text{m}^3$  and 49%, respectively (**Table 5-1a**). The lower  $\rho_d$  and higher  $n$  for glaciolacustrine in comparison to Battleford till are consistent with minimal consolidation as a result of deposition during glacial retreat as opposed to beneath glacial ice. Based on the findings of Van Loon et al. [2007] and upon the discussions above,  $D_e$  values for  $\text{Cl}^-$  can be expected to be greater for glaciolacustrine sediment than for till. Without lab determined  $D_e$  values for  $\text{Cl}^-$  for glaciolacustrine sediment from Saskatchewan for comparison, an approximate range of  $5 \times 10^{-10}$  to  $7.5 \times 10^{-10} \text{ m}^2/\text{s}$  was deemed representative based on the findings of Crooks and Quigley [1984] and Barone et al. [1989].

Since  $D_e$  and  $t$  are within the same term in equation (5.3), different combinations of each could yield the same model fit to observed data. To ensure realistic estimates for the timing of brine release, a sensitivity study was conducted by varying  $D_e$  within the acceptable ranges for  $\text{Cl}^-$  quoted above for glaciolacustrine and subglacial till given different values of  $t$  until a best fit was achieved. Since mining operations began in 1968, it was assumed any brine releases would have occurred after this date. Therefore,  $t$  was limited to 44 years representing the time between the start of mining and the study. An alternative approach would have been to achieve a best fit to the observed data using a single parameter represented by  $(D_e \cdot t)$ . Combinations of  $D_e$  and  $t$  that yielded a value equivalent to this parameter could then have been explored.

In the case of BH21 and BH13, the sediment between upper and lower model boundaries (i.e. the diffusive zone) comprised one lithology and therefore changes in  $EC_a$  could be attributed predominantly to pore-water  $\text{Cl}^-$  changes with depth. At BH6 however, the diffusive zone comprised glaciolacustrine, ablation till, and subglacial till lithologies. To separate geological effects on  $EC_a$  from pore-water  $\text{Cl}^-$  variations, equation (2.1) was used generate an  $EC_w$  profile from  $EC_a$  measurements for BH6. The resulting  $EC_w$  profile was then modeled alongside the pore-water  $\text{Cl}^-$  profile generated from squeeze measurements to compare model outcomes. Modeled diffusion profiles for BH21, BH13, and BH6 are presented alongside measured  $EC_a$ ,  $EC_w$ ,  $\text{Cl}^-$ , reported in relative concentration (i.e.  $C/C_0$ ) in **Figure 5-14**.

At BH21 located nearest the brine source, a reasonable model fit was achieved using a  $D_e$  of  $7.5 \times 10^{-10} \text{ m}^2/\text{s}$  and a  $t$  of 44 years (**Figure 5-14**). This  $D_e$  value was high but within the expected range for  $\text{Cl}^-$  in glaciolacustrine sediment. Reasonable model fits using smaller  $D_e$  values could not be achieved for BH21 without longer diffusion times, which would imply diffusion of  $\text{Cl}^-$  began prior to mining operations. Conversely, shorter diffusion times would have required  $D_e$  values  $>7.5 \times 10^{-10} \text{ m}^2/\text{s}$ . For example, a  $D_e$  of  $1.1 \times 10^{-9} \text{ m}^2/\text{s}$  was required to fit the model to measured data assuming a  $t$  of 30 years (data not shown). This value is unrealistically high since it is equivalent to the  $D_0$  value of  $\text{Cl}^-$  at  $5^\circ\text{C}$  after applying a temperature and viscosity correction after Li and Gregory [1974]. An average annual groundwater temperature of  $5^\circ\text{C}$  obtained from measurements down piezometer 2010-02A near BH21 suggested this value was representative of *in situ* temperatures. These findings suggested that releases of brine into wetland 1A must have occurred shortly after the mine began operation.

At BH6 the glaciolacustrine sediment was underlain by ablation and subglacial till (**Figure 5-14**), however the majority of the relative concentration changes occurred within the glaciolacustrine sediment. Therefore a  $D_e$  range considered representative of glaciolacustrine was used to constrain the model. At BH6, the same model fits to the measured  $Cl^-$  profile were achieved using  $D_e$  and  $t$  values of  $7.5 \times 10^{-10} \text{ m}^2/\text{s}$  and 20 years and  $5.0 \times 10^{-10} \text{ m}^2/\text{s}$  and 30 years, respectively (**Figure 5-14**). This range in diffusion time suggests brine was introduced into wetlands 2 and 3 about 14-24 years after the mine began operation (i.e. ~1982-1992). A reasonable fit to the  $EC_w$  profile was achieved using the same best-fit model parameters as for the  $Cl^-$  profile, suggesting that geological effects on  $EC_a$  could be suitably controlled for using equation (2.1) to enable solute transport modelling of predicted  $EC_w$  variations from measurements of  $EC_a$ . Attempts to model the  $EC_a$  profile at BH6 were inconsistent with fits achieved from  $Cl^-$  and  $EC_w$  profiles as a result of a lithological changes occurring with depth that made choosing an appropriate lower boundary impossible.

At BH13, nearly identical model fits to the measured  $EC_a$  profile were achieved using  $D_e$  and  $t$  values of  $4 \times 10^{-10} \text{ m}^2/\text{s}$  and 20 years and  $3 \times 10^{-10} \text{ m}^2/\text{s}$  and 30 years, respectively (**Figure 5-14**). This range in  $D_e$  values was consistent with the expected range for subglacial till. A diffusion time of 20-30 years is consistent with the onset of brine diffusion at BH6 and suggests brine was introduced into wetland 5 at about the same time as wetlands 2 and 3. This scenario is consistent with a fill and spill event, possibly during a single wet year, that may have resulted in a cascade of brine-impacted water from pond 1A or 1B into ponds 2-5. Model fits using smaller values of  $D_e$  could not be achieved without diffusion times >30 years, which was unrealistic given the 20-30 year diffusion times predicted upgradient at BH6.

To investigate fill and spill as the principal mechanism for brine transport between wetlands further, historical climate records were consulted for nearby Saskatoon. The year of 1991 was a particularly wet year, in fact the wettest year between 1982 and 1992. Annual precipitation in 1991 (546 mm) exceeded the 1981-2010 average of 340 mm [Environment Canada 2015]. Precipitation during the months of April, May, and June of 1991 exceeded their respective monthly averages by 2.2-2.6 times and totaled 296 mm (160 mm in June alone), which is nearly equivalent to the annual average for Saskatoon. Since pond levels were found to peak by late June (**Figure 5-3**), excessive rainfall during the months leading up to and including June would

more likely to lead to a fill and spill event occurring than at other times of the year. The above-average rainfall in 1991 is consistent with the onset of brine diffusion at BH6 and BH13, which suggested brine could have been introduced into wetlands 2-5 between 1982 and 1992.

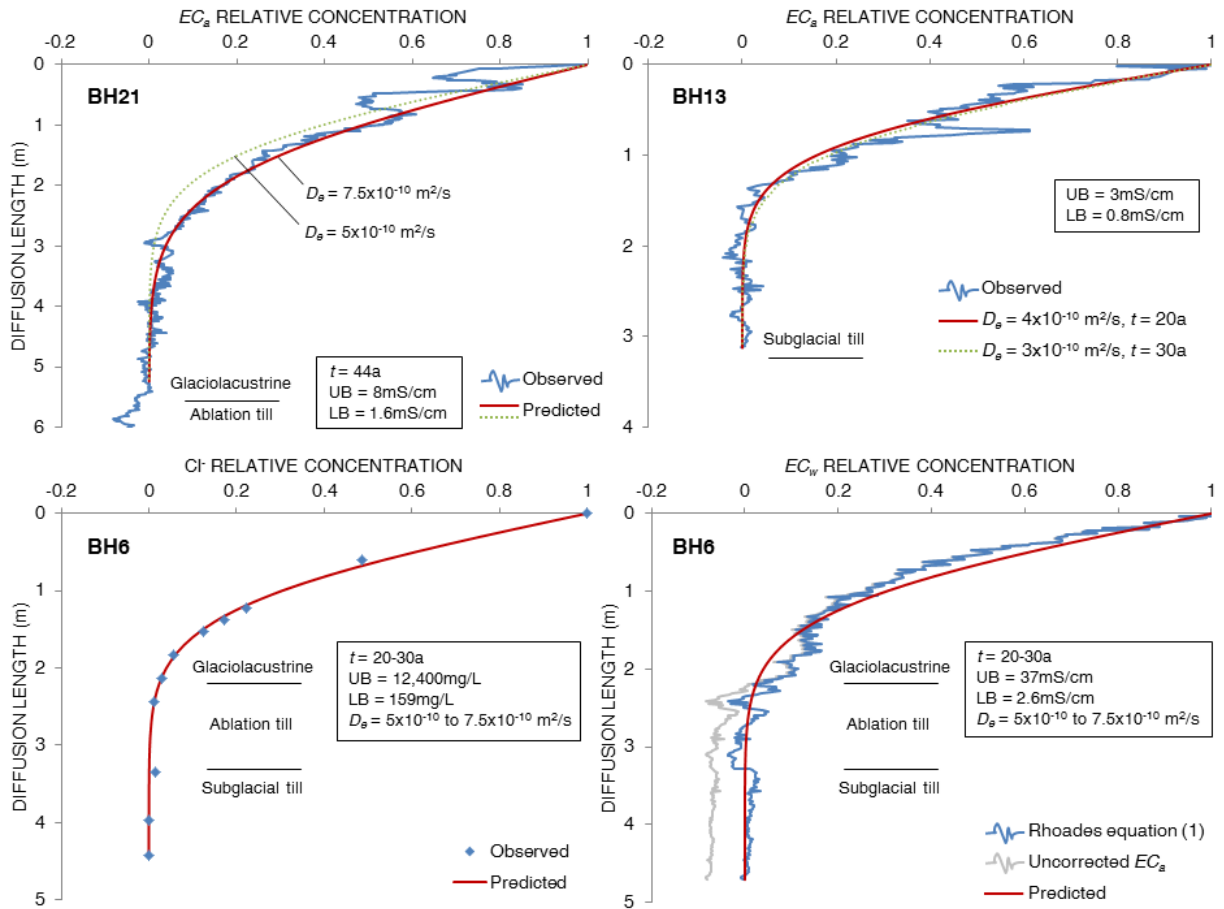


**Figure 5-14.** Simulated and measured vertical profiles of  $EC_a$  (BH21 and BH13),  $EC_w$ , and pore-water  $Cl^-$  (BH6) for three drill locations along the length of the brine plume. UB and LB denote upper and lower boundary concentrations, respectively. The uncorrected  $EC_a$  profile is shown alongside the calculated  $EC_w$  (modeled) profile for BH6 to illustrate the effects of geological changes.

## 6. CONCLUSIONS AND IMPLICATIONS

Measurements of  $EC_a$  using D-P EC profiling can be used to rapidly delineate brine-impacted groundwaters and guide groundwater sampling efforts, provided pore-water salinity contrasts are sufficiently high and geology is simplistic. However, changes in  $n$  as a result of lithological changes exert a strong influence on  $EC_a$  by altering the volume fraction of pore-water to sediment. Changes in clay content further alter  $EC_a$  by influencing the relative flow of current along clay surfaces as opposed to through dissolved salts present in the pore-water. By defining lithological changes and associated differences in sediment properties and texture, fine-scale (2 cm) depth profiles of  $EC_w$  and pore-water  $Cl^-$  can be deduced from measurements of D-P EC using an appropriate conductance model. This study showed the soil conductance model of Rhoades et al. [1989] could accurately reproduce measured values of  $EC_w$  at a site dominated by glaciolacustrine and till sediments and affected by brine inputs resulting from potash mining. A significant linear  $EC_w-Cl^-$  regression ( $r^2=0.92$ ) further enabled the generation of pore-water  $Cl^-$  depth profiles from  $EC_w$  predictions. This significant relation also suggested that  $Cl^-$  changes in the subsurface resulting from brine transport were responsible for changes in  $EC_w$  and  $EC_a$ . Observed vertical profiles of  $Cl^-$ ,  $EC_w$ , and  $EC_a$  could be explained by diffusion alone by simulating 1D  $Cl^-$  transport at three locations along the length of the brine plume, suggesting vertical solute transport within the surficial aquitard was diffusion-dominated below depths of 3-5 mbg. Numerical modelling further suggested that the release of brine began shortly after the onset of mining and that brine had travelled  $\sim 2.4$  km downgradient from the source 20-30 years after the initial release, likely as a result of overland flow between wetlands during wet years.

To successfully employ D-P EC profiling to characterize the distribution of groundwater salinity, a detailed understanding of site geology, and site-specific measurements of D-P EC, pore-water chemistry, and sediment properties are needed. The benefit of using a soil conductance model is that the influence of  $n$ , clay content, and  $EC_a-EC_w$  calibrations can be quantified. Presuming a similar geology is encountered at another site, there is potential for predetermined parameters to be applied. This is particularly true of the semiarid glaciated plains region of North America that is dominated by fine-grained glacial deposits. However, site-specific measurements of the above properties should be made to confirm parameter applicability. Temperature and water table position also need to be accounted for due to their effect on EC. The depth of investigation must

also be considered given anticipated geological conditions. In fine-grained glacial sediments D-P EC profiling is limited to shallow depths (i.e. 10-15 m) because of the high plasticity of these clayey sediments and increasing stiffness with depth.

As a mapping tool for groundwater salinity, the usefulness of D-P EC profiling is dependent on the spacing between individual EC log locations. Although vertical resolution is high, lateral sensing abilities are limited making this technique better suited to vertical visualization for assessment and remediation purposes. However, by pairing  $EC_a$  measurements obtained with D-P EC profiling with those obtained by established spatial geophysical methods such as surface EM surveying, it could be possible to characterize the vertical and spatial extent of groundwater brine impacts at the local scale in a cost-effective manner. Due to the higher resolution results attainable as compared to conventional soil and groundwater sampling techniques, D-P EC profiling can generate fine-scale depth profiles of pore-water salinity. These profiles can be used to define the lateral and vertical extent of brine contamination, dominant solute transport mechanisms, and timing of groundwater contamination.

## 7. REFERENCES

- Appelo, C.A.J. and D. Postma. 2005. *Geochemistry, groundwater and pollution*, second edition. A.A. Balkema Publishers, Netherlands: 649 pp.
- Archie, G.E. 1942. The electrical resistivity log as an aid in determining some reservoir characteristics. *Transactions of the American Institute of Mining and Metallurgical Engineers* 146: 54–62.
- ASTM Standard D2216-10. 2010a. Standard test methods for laboratory determination of water (moisture) content of soil and rock by mass. ASTM International, West Conshohocken, PA, DOI: 10.1520/D2216-10, [www.astm.org](http://www.astm.org).
- ASTM Standard D5084-10. 2010b. Standard test methods for measurement of hydraulic conductivity of saturated porous materials using a flexible wall permeameter. ASTM International, West Conshohocken, PA, DOI: 10.1520/ D5084-10, [www.astm.org](http://www.astm.org).
- ASTM Standard D7263-09. 2009. Standard test methods for laboratory determination of density (unit weight) of soil specimens. ASTM International, West Conshohocken, PA, DOI: 10.1520/D7263-09, [www.astm.org](http://www.astm.org).
- Barone, F.S., E.K. Yanful, R.M. Quigley, and R.K. Rowe. Effect of multiple contaminant migration on diffusion and adsorption of some domestic waste contaminants in a natural clayey soil. *Canadian Geotechnical Journal* 26: 189-198.
- Biswas, T.D. and S.K. Mukherjee. 1995. *Textbook of soil science*, second edition. Tata McGraw-Hill, New Delhi: 433 pp.
- Bohn, H.L., J. Ben-Asher, H.S. Tabbara, and M. Marwan. 1982. Theories and tests of electrical conductivity in soils. *Soil Science Society of America Journal* 46: 1143-1146.
- Christiansen, E.A. 1979. The Wisconsinan deglaciation of southern Saskatchewan and adjacent areas. *Canadian Journal of Earth Sciences* 16: 913-938.
- Christiansen, E.A. 1992. Pleistocene stratigraphy of the Saskatoon area, Saskatchewan, Canada. *Canadian Journal of Earth Sciences* 29: 1767-1778.

Christy, C.D., T.M. Christy, and V. Wittig. 1994. A percussion probing tool for the direct sensing of soil conductivity. Geoprobe Systems, Salina, Kansas, Technical Paper No. 94-100.

Collins A.G. 1975. Geochemistry of oilfield waters. Elsevier, New York: 496 pp.

Crooks, V.E. and R.M. Quigley. 1984. Saline leachate migration through clay: a comparative laboratory and field investigation. Canadian Geotechnical Journal 21: 349-362.

Davis, S.N., D.O. Whittmore, and J. Fabryka-Martin. 1998. Uses of chloride/bromide ratios in studies of potable water. Groundwater 36 (2): 338-350.

D'Astous, A.Y., W.W. Ruland, J.R.G. Bruce, J.A. Cherry, and R.W. Gillham. 1989. Fracture effects in the shallow groundwater zone in weathered Sarnia-area clay. Canadian Geotechnical Journal 26: 43-56.

Desaulniers, D.E., J.A. Cherry, and P. Fritz. 1981. Origin, age and movement of pore water in argillaceous Quaternary deposits at four sites in southwestern Ontario. Journal of Hydrology 50: 231-257.

Direct Image. 2014. [http://files.geoprobe.com/pdfs/e-ec\\_conductivity\\_0.pdf](http://files.geoprobe.com/pdfs/e-ec_conductivity_0.pdf). Accessed October 2014.

Direct Image. 2015. <http://geoprobe.com/ec-electrical-conductivity>. Accessed April 2015.

Dreimanis, A. 1976. Tills: their origin and properties. In Glacial till, an inter-disciplinary study. Edited by R.F. Legget. The Royal Society of Canada, Special Publication 12: 11-49.

Dreimanis, A. 1988. Tills: their genetic terminology and classification. In: Genetic Classification of Glacigenic Deposits. Edited by R.P. Goldthwait and C.L. Matsch C.L., Balkema, Rotterdam: 17-83.

Environment Canada. 2015. National climate data archive: 1981-2010 Canadian climate normals and monthly climate records. [http://climate.weather.gc.ca/data\\_index\\_e.html](http://climate.weather.gc.ca/data_index_e.html). Accessed March 2015.

EPA [U.S. Environmental Protection Agency]. 1983. Method 310.1, alkalinity (titrimetric). In: Methods for Chemical Analysis of Water and Wastes. EPA-600/4-79-020. U.S. Environmental Protection Agency, Environmental Monitoring and Support Laboratory, Cincinnati, Ohio.

EPA [U.S. Environmental Protection Agency]. 2007. Test methods for evaluating solid waste, physical/chemical methods. EPA SW-846, Revision 4. U.S. Environmental Protection Agency, Environmental Monitoring and Support Laboratory, Cincinnati, Ohio.

ESRD [Environment and Sustainable Resource Development]. 2014. <http://esrd.alberta.ca/focus/state-of-the-environment/land/response-indicators/oil-and-gas-wells-reclamation.aspx>. Accessed November 2014.

Euliss, N.H., J.W. LaBaugh, L.H. Fredrickson, D.M. Mushet, M.K. Laubhan, G.A. Swanson, T.C. Winter, D.O. Rosenberry, and R.D. Nelson. 2004. The wetland continuum: a conceptual framework for interpreting biological studies. *Wetlands* 24(2): 448-458.

Evans, D.J.A., E.R. Phillips, J.F. Hiemstra, and C.A. Auton. 2006. Subglacial till: formation, sedimentary characteristics and classification. *Earth Science Reviews* 78: 115-176.

Feth, J.H. 1981. Chloride in natural continental water—a review. United States Geological Survey Water-Supply Paper 2176: 29 pp.

Fetter, C.W. 1999. Contaminant hydrogeology, second edition. Prentice Hall, NJ: 500 pp.

Friedman, S.P. 2005. Soil properties influencing apparent electrical conductivity: a review. *Computers and Electronics in Agriculture* 46(1): 45-70.

Freeze, R.A. and J.A. Cherry. 1979. Groundwater. Prentice Hall, NJ: 604 pp.

Fuge, R. 1969. Bromine. In: Handbook of Geochemistry, Vol. 2. Edited by K.H. Wedepohl, Springer-Verlag, 35-B1 to 35-I6, Berlin.

Fuzesy, A. 1982. Potash in Saskatchewan. Saskatchewan Energy and Mines, Report 181. 44 pp.

Fuzesy, L.M. 1983. Petrology of the Middle Devonian Prairie Evaporite potash ore in Saskatchewan. Saskatchewan Geological Survey, Misc. Report 83-4: 138-143.

Fulton, R.J., compiler. 1995. Surficial materials of Canada, map 1880A, scale 1:5,000,000. Geological Survey of Canada.

Gerber, R.E., J.I. Boyce, and K.W.F. Howard. 2001. Evaluation of a heterogeneity and field scale groundwater flow regime in a leaky till aquitard. *Hydrogeology Journal* 9: 60-78.

Ghassemi, F., A.J. Jakeman, and H.A. Nix. 1995. Salinisation of land and water resources—human causes, extent, management and case studies. CAB International, Wallingford, U.K. 526 pp.

Government of Alberta. 2014. Oil and gas conservation rules. Alberta Regulation 151/1971, amended 2014. Alberta Queen's Printer, Edmonton, AB: 140 pp.

Goldstein, N.E., S.M. Benson, and D. Alumbough. 1990. Saline groundwater plume mapping with electromagnetics. In: *Geotechnical and Environmental Geophysics, Vol.2: Environmental and Groundwater*, Edited by S.H. Ward. Society of Exploration Geophysicists, Tulsa, Oklahoma: 17-25.

Greenhouse, J.P. and D.D. Slaine. 1983. The use of reconnaissance electromagnetic methods to map contaminant migration. *Groundwater Monitoring & Remediation* 3(2): 47-59.

Grisak, G.E., J.A. Cherry, J.A. Vonhof, and J.P. Blumele. 1976. Hydrogeologic and hydrochemical properties of fractured till in the interior plains region. In *Glacial till, an interdisciplinary study*. Edited by R.F. Legget. The Royal Society of Canada, Special Publication 12: 304-335.

Halvorson, A.D., J.D. Rhoades, and C.A. Reule. 1977. Soil salinity—four-electrode conductivity relationships for soils of the Northern Great Plains. *Soil Science Society of America Journal* 41: 966-971.

Harrington, G.A. and M.J. Hendry. 2006. Using direct-push EC logging to delineate heterogeneity in a clay-rich aquitard. *Groundwater Monitoring & Remediation* 26(1): 92-100.

- Harrington, G.A., M.J. Hendry, and N.I. Robinson. 2007. Impact of permeable conduits on solute transport in aquitards: Mathematical models and their application. *Water Resources Research* 43(5): W05441.
- Hautman, D.P., D. Munch, and J.D. Pfaff. 1997. Method 300.1, determination of inorganic anions in drinking water by ion chromatography. U.S. Environmental Protection Agency, National Exposure Research Laboratory, Office of Research and Development, Cincinnati, Ohio 45268: 40 pp.
- Hayashi, M. 2004. Temperature-electrical conductivity relation of water for environmental monitoring and geophysical data inversion. *Environmental Monitoring and Assessment* 96:119-128.
- Hayashi, M., G. van der Kamp, and D.L. Rudolph. 1998a. Water and solute transfer between a prairie wetland and adjacent uplands, 1. Water balance. *Journal of Hydrology* 207:42-55.
- Hayashi, M., G. van der Kamp, and D.L. Rudolph. 1998b. Water and solute transfer between a prairie wetland and adjacent uplands, 2. Chloride cycle. *Journal of Hydrology* 207(1): 56-67.
- Hayley, K., L.R. Bentley, M. Gharibi, and M. Nightingale. 2007. Low temperature dependence of electrical resistivity: implications for near surface geophysical monitoring. *Geophysical Research Letters* 34: L18402.
- Heagle, D., M. Hayashi, and G. van der Kamp. 2013. Surface-subsurface salinity distribution and exchange in a closed-basin prairie wetland. *Journal of Hydrology* 478: 1-14.
- Hendry, M.J. 1982. Hydraulic conductivity of a glacial till in Alberta. *Groundwater* 20(2): 162-169.
- Hendry, M.J. and L.I. Wassenaar. 1999. Implications of the distribution of  $\delta D$  in pore waters for groundwater flow and the timing of geologic events in a thick aquitard system. *Water Resources Research* 35(6): 1751-1760.

Hendry, M.J. and L.I. Wassenaar. 2011. Millennial-scale diffusive migration of solutes in thick clay-rich aquitards: evidence from multiple environmental tracers. *Hydrogeology Journal* 19(1): 259-270.

Hendry, M.J. and A.D. Woodbury. 2007. Clay aquitards as archives of Holocene paleoclimate:  $\delta^{18}\text{O}$  and thermal profiling. *Groundwater* 45(6): 683-691.

Hendry, M.J., S.L. Barbour, K. Novakowski, and L.I. Wassenaar. 2013. Paleohydrogeology of the Cretaceous sediments of the Williston Basin using stable isotopes of water. *Water Resources Research* 49: 4580-4592.

Hendry, M.J., J.A. Cherry, and E.I. Wallick. 1986. Origin and distribution of sulfate in a fractured till in Southern Alberta, Canada. *Water Resources Research* 22(1): 45-61.

Hendry, M.J., L.I. Wassenaar, and T. Kotzer. 2000. Chloride and chlorine isotopes ( $^{36}\text{Cl}$  and  $\delta^{37}\text{Cl}$ ) as tracers of solute migration in a thick, clay-rich aquitard system. *Water Resources Research* 36(1): 285-296.

Hubbert, M.K. 1940. The theory of groundwater motion. *Journal of Geology* 48(8): 785-944.

Hvorslev, M.J. 1951. Time lag and soil permeability in groundwater observations. U.S. Army Corps of Engineers, Waterways Experiment Station, Vicksburg, MS, Bulletin No. 36: 51 pp.

Jenner, G.A., H.P. Longerich, S.E. Jackson, and B.J. Fryer. 1990. ICP-MS—a powerful tool for high-precision trace-element analysis in earth sciences: evidence from analysis of selected USGS reference samples. *Chemical Geology* 83(1): 133-148.

Johnson, R.L., J.A. Cherry, and J.F. Pankow. 1989. Diffusive contaminant transport in natural clay: a field example and implications for clay-lined waste disposal sites. *Environmental Science and Technology* 23: 340-349.

Johnson, B., B. Hopkins, and W. McCall. 1999. Direct-push electrical logging for rapid site assessment and definition of brine plumes. In: *Proceedings of the 6<sup>th</sup> International Petroleum Environmental Conference*, Edited by K.L. Sublette, G. Thoma, and T.J. Ward. Integrated Petroleum Environmental Consortium, Houston, Texas.

- Keller, C.K., G. van der Kamp, and J.A. Cherry. 1986. Fracture permeability and groundwater flow in a clayey till near Saskatoon, Saskatchewan. *Canadian Geotechnical Journal* 23: 229-240.
- Keller, C.K., G. van der Kamp, and J.A. Cherry. 1988. Hydrogeology of two Saskatchewan tills, I. Fractures, bulk permeability, and spatial variability of downward flow. *Journal of Hydrology* 101: 97-121.
- Keller, C.K., G. van der Kamp, and J.A. Cherry. 1989. A multi-scale study of the permeability of a thick clayey till. *Water Resources Research* 25(11): 2299-2317.
- Keller, C.K., G. van der Kamp, and J.A. Cherry. 1991. Hydrogeochemistry of a clayey till, 1. spatial variability. *Water Resources Research* 27(10): 2543-2554.
- Kessler, T.C., K.E.S. Klint, B. Nilsson, and P.L. Bjerg. 2012. Characterization of sand lenses embedded in tills. *Quaternary Science Reviews* 53: 55-71.
- LaBaugh, J.W., T.C. Winter, V.A. Adomaitis, and G.A. Swanson. 1987. Hydrology and chemistry of selected prairie wetlands in the Cottonwood Lake area, Stutsman County, North Dakota, 1979-1982. U.S. Geological Survey Professional Paper 1431: 26 pp.
- LaBaugh, J.W. 1989. Chemical characteristics of northern prairie wetlands. In: *Northern Prairie Wetlands*, Edited by A. van der Valk. Iowa State University Press, Ames, Iowa: 56-90.
- Lennox, D.H., H. Maathuis, and D. Pederson. 1988. Region 13, western glaciated plains. In: *The Geology of North America, Vol. 0-2, Hydrogeology*. Edited by W. Back, J.S. Rosenshein, and P.R. Seaber. The Geological Society of America, CO: 115-128.
- Lissey, A. 1971. Depression-focused transient groundwater flow patterns in Manitoba. Geological Association of Canada, Special Paper 9: 333-341.
- Loveday, J. 1980. Experiences with the 4-electrode resistivity technique for measuring soil salinity. CSIRO Division of Soils (Australia), Divisional Report No. 51.

Maathuis, H. and G. van der Kamp. 1991. Subsurface brine migration at potash waste disposal sites in Saskatchewan, Appendix C: coring and EM-39 logging. Prepared for the Saskatchewan Potash Producers Association. Saskatchewan Research Council, No. R-1210-1-E-91.

Maathuis, H. and G. van der Kamp. 1994. Subsurface brine migration at potash waste disposal sites in Saskatchewan, final report. Prepared for the Saskatchewan Potash Producers Association. Saskatchewan Research Council, No. R-1220-10-E-94.

McCall, W. 1996. Electrical conductivity logging to determine control of hydrocarbon flow paths in alluvial sediments. In: Proceedings of the 10<sup>th</sup> National Outdoor Action Conference, National Ground Water Association, Westerville, Ohio: 461-477.

McKay, L.D. and J. Fredericia. 1995. Distribution, origin, and hydraulic influence of fractures in a clay-rich glacial deposit. *Canadian Geotechnical Journal* 32: 957-975.

McKay, L.D., J.A. Cherry, and R.W. Gillham. 1993a. Field experiments in a fractured clay till, 1. Hydraulic conductivity and fracture aperture. *Water Resources Research* 29(4): 1149-1162.

McKay, L.D., R.W. Gillham, and J.A. Cherry. 1993b. Field experiments in a fractured clay till, 1. Solute and colloid transport. *Water Resources Research* 29(12): 3879-3890.

McKay, L., J. Fredericia, M. Lenczewski, J. Morthorst, and K.E.S. Klint. 1999. Spatial variability of contaminant transport in a fractured till, Avedøre Denmark. *Nordic Hydrology* 30(4/5): 333-360.

McNeill, J.D. 1980. Electrical conductivity of soils and rocks. Geonics Limited, Mississauga, Ontario, Canada, Technical Note TN-5: 22 pp.

Mermut, A.R. and D.F. Acton. 1985. Surficial rearrangement and cracking in swelling clay soils of the Glacial Lake Regina basin in Saskatchewan. *Canadian Journal of Soil Science* 65: 317-327.

Meyboom, P. 1966. Unsteady groundwater flow near a willow ring in hummocky moraine. *Journal of Hydrology* 4:38-62.

- Meyboom, P. 1967. Interior plains hydrogeological region. In: Groundwater in Canada. Edited by I.C. Brown. Geological Survey of Canada, Economic Geology Report No. 24: 131-158.
- Monier-Williams, M.E., J.P. Greenhouse, J.M. Mendes, and N. Ellert. 1990. Terrain conductivity mapping with topographic corrections at three waste disposal sites in Brazil. In: Geotechnical and Environmental Geophysics, Vol.2: Environmental and Groundwater, Edited by S.H. Ward. Society of Exploration Geophysicists, Tulsa, Oklahoma: 41-55.
- Morris, A.W. and J.P. Riley. 1966. The bromide/chlorinity and sulphate/chlorinity ratios in sea water. Deep-Sea Research and Oceanographic Abstracts 13(4): 699-705.
- Nachshon, U. 2013. Sulfate salt dynamics in the glaciated plains of North America. Journal of Hydrology 499:188-199.
- Neff, J., K. Lee, and E.M. DeBlois. 2011. Produced water: overview of composition, fates, and effects. In: Produced Water, Environmental Risks and Advances in Mitigation Technologies. Edited by K. Lee and J. Neff. Springer, New York: 3-54.
- Ott, L. 1977. An introduction to statistical methods and data analysis. Duxbury Press, North Scituate, Massachusetts: 730 pp.
- Perucca, C.F. 2003. Potash processing in Saskatchewan—a review of process technologies. CIM Bulletin 96(1070): 61-65.
- Remenda, V.H., J.A. Cherry, and T.W.D. Edwards. 1994. Isotopic composition of old groundwater from Lake Agassiz: implications for late Pleistocene climate. Science 266: 1975-1978.
- Remenda, V.H., G. van der Kamp, and J.A. Cherry. 1996. Use of vertical profiles of  $\delta^{18}\text{O}$  to constrain estimates of hydraulic conductivity in a thick, unfractured aquitard. Water Resources Research 32(10): 2979-2987.
- Rhoades, J.D., P.A.C. Raats, and R.J. Prather. 1976. Effects of liquid-phase electrical conductivity, water content, and surface conductivity on bulk soil electrical conductivity. Soil Science Society of America Journal 40: 651-655.

- Rhoades, J.D. 1980. Determining leaching fraction from field measurements of soil electrical conductivity. *Agricultural Water Management* 3: 205-215.
- Rhoades, J.D. 1981. Predicting bulk soil electrical conductivity versus saturation paste extract electrical conductivity calibrations from soil properties. *Soil Science Society of America Journal* 45: 42-44.
- Rhoades, J.D. 1993. Electrical conductivity methods for measuring and mapping soil salinity. *Advances in Agronomy* 49: 201-251.
- Rhoades, J.D. and D.L. Corwin. 1990. Soil electrical conductivity: effects of soil properties and application to soil salinity appraisal. *Communications in Soil Science and Plant Analysis* 21(11&12): 837-860.
- Rhoades, J.D. and J. van Schilfgaarde. 1976. An electrical conductivity probe for determining soil salinity. *Soil Science Society of America Journal* 40(5): 647-651.
- Rhoades, J.D., N.A. Manteghi, P.J. Shouse, and W.J. Alves. 1989. Soil electrical conductivity and soil salinity: new formulations and calibrations. *Soil Science Society of America Journal* 53: 433-439.
- Rhoades, J.D., F. Chanduvi, and S.M. Lesch. 1999. Soil salinity assessment: methods and interpretation of electrical conductivity measurements. Food and Agriculture Organization (FAO) of the United Nations, Rome, Italy, FAO Irrigation and Drainage Paper No. 57: 150 pp.
- Robertson, P.K., T. Lunne, and J. Powell. 1996. Applications of penetration tests for geo-environmental purposes. In: *Advances in Site Investigation Practice*, Edited by C. Craig. Thomas Telford Publishing, London: 407-420.
- Rozkowski, A. 1967. The origin of hydrochemical patterns in hummocky moraine. *Canadian Journal of Earth Science* 4: 1065–1092.
- Rozkowski, A. 1969. Chemistry of ground and surface waters in the Moose Mountain area, southern Saskatchewan. *Geological Survey of Canada Paper* 67-9: 111 pp.

- Ruland, W.W., J.A. Cherry, and S. Feenstra. 1991. The depth of fractures and active ground-water flow in a clayey till plain in southwestern Ontario. *Ground Water* 29(3): 405-417.
- Sauer, E.K. and E.A Christiansen. 1991. Preconsolidation pressures in the Battleford Formation, southern Saskatchewan, Canada. *Canadian Journal of Earth Sciences* 28: 1613-1623.
- Schulmeister, M.K., J.J. Butler, J.M. Healey, L. Zheng, D.A. Wysocki, and G.W. McCall. 2003. Direct-push electrical conductivity logging for high-resolution hydrostratigraphic characterization. *Groundwater Monitoring & Remediation* 23(3): 52-62.
- Scott, J.S. 1976. Geology of Canadian tills. In: *Glacial till, an inter-disciplinary study*. Edited by R.F. Legget. The Royal Society of Canada, Special Publication 12: 50-66.
- Sen, P.N. and P.A. Goode. 1992. Influence of temperature on electrical conductivity of shaly sands. *Geophysics* 57(1): 89-96.
- Shainberg, I., J.D. Rhoades, and R.J. Prather. 1980. Effect of exchangeable sodium percentage, cation-exchange capacity, and soil solution concentration on soil electrical conductivity. *Soil Science of America Journal* 44(3): 469-473.
- Shakelford, C.D. 1991. Diffusion in saturated soil, I: background. *Journal of Geotechnical Engineering* 117 (3): 467-484.
- Shaw, J.R. and M.J. Hendry. 1998. Hydrogeology of a thick clay till and Cretaceous clay sequence, Saskatchewan, Canada. *Canadian Geotechnical Journal* 35: 1041-1052.
- Simpkins, W.W. and K.R. Bradbury. 1992. Groundwater flow, velocity, and age in a thick, fine-grained till unit in southeastern Wisconsin. *Journal of Hydrology* 132: 283-319.
- Sloan, C.E. 1972. Ground-water hydrology of prairie potholes in North Dakota. US Geological Survey, Professional Paper 585-C:28.
- Saskatchewan Ministry of Energy and Resources (SMER). 2014. Saskatchewan exploration and development highlights 2014. Available online at: <http://www.economy.gov.sk.ca/SEDH2014>. Accessed April 2015.

- Sorensen, J.A. and G.E. Glass. 1987. Ion and temperature dependence of electrical conductance for natural waters. *Analytical Chemistry* 59: 1594-1597.
- Stephenson, M.T. 1992. A survey of produced water studies. In: *Produced Water, Technological/Environmental Issues and Solutions*. Edited by J.P. Ray and F.R. Engelhardt, Plenum Press, New York: 1–11.
- Tallin, J.E., D.E. Pufahl, and S.L. Barbour. 1990. Waste management schemes of potash mines in Saskatchewan. *Canadian Journal of Civil Engineering* 17: 528-542.
- Taylor, K.C., J.W. Hess, and A. Mazzela. 1989. Field evaluation of a slim-hole borehole induction tool. *Groundwater Monitoring & Remediation* 9(1): 100-104.
- Tóth, J. 1963. A theoretical analysis of groundwater flow in small drainage basins. *Journal of Geophysical Research* 68(16): 4795-4812.
- Unpublished consultant data. 2008, 2009, 2011, 2012, 2013.
- van der Kamp, G. 2001. Methods for determining in situ hydraulic conductivity of shallow aquitards—an overview. *Hydrogeology Journal* 9: 5-16.
- van der Kamp, G. and M. Hayashi. 1998. The groundwater recharge function of small wetlands in the semi-arid northern prairies. *Great Plains Research* 8(1): 39-56.
- van der Kamp, G. and M. Hayashi. 2009. Groundwater-wetland ecosystem interaction in the semiarid glaciated plains of North America. *Hydrogeology Journal* 17: 203-214.
- van der Meer, J.J.M., J. Menzies, and J. Rose. 2003. Subglacial till: the deforming glacier bed. *Quaternary Science Reviews* 22: 1659-1685.
- Van Loon, L.R., M.A. Glaus, and W. Muller. 2007. Anion exclusion effects in compacted bentonites: towards a better understanding of anion diffusion. *Applied Geochemistry* 22: 2536-2552.

Van Stempvoort, D.R., M.J. Hendry, J.J. Schoenau, and H.R. Krouse. 1994. Sources and dynamics of sulfur in weathered till, western glaciated plains of North America. *Chemical Geology* 111: 35-56.

Veil, J.A. 2011. Produced water management options and technologies. In: *Produced Water, Environmental Risks and Advances in Mitigation Technologies*. Edited by K. Lee and J. Neff. Springer, New York: 537-571.

Winter, T.C. 1989. Hydrologic studies of wetlands in the northern prairie. In: *Northern Prairie Wetlands*, Edited by A. van der Valk. Iowa State University Press, Ames, Iowa: 16-54.

Winter, T.C. and J.W. LaBaugh. 2003. Hydrologic considerations in defining isolated wetlands. *Wetlands* 23(3): 532–540.

Wist, W., J.H. Lehr, and R. McEachern. 2009. Water softening with potassium chloride: Process, health, and environmental benefits. John Wiley and Sons, NJ: 240 pp.

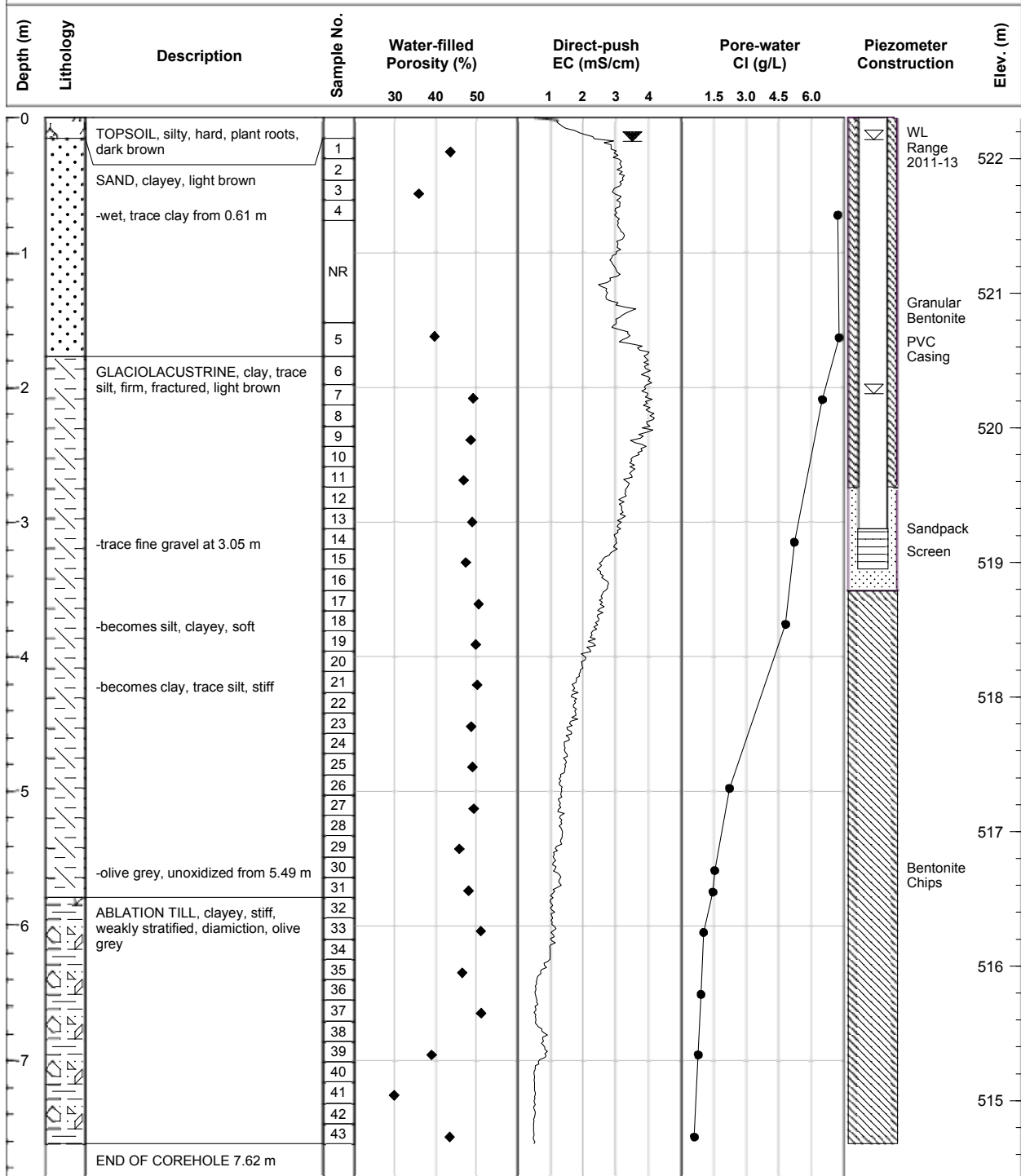
Zume, J.T., A. Tarhule, and S. Christenson. 2006. Subsurface imaging of an abandoned solid waste landfill site in Norman, Oklahoma. *Groundwater Monitoring & Remediation* 26(2): 62-69.

APPENDIX A  
CORING LOGS

Drill Method: Direct-push continuous core  
 Drill Rig: Geoprobe 7822 DT  
 EC Probe: SC520 wenner array

### CORING LOG: BH1

Coring Date: 15-Aug-2011  
 EC Logging Date: 15-Aug-2011  
 Ground Elevation (masl): 522.30

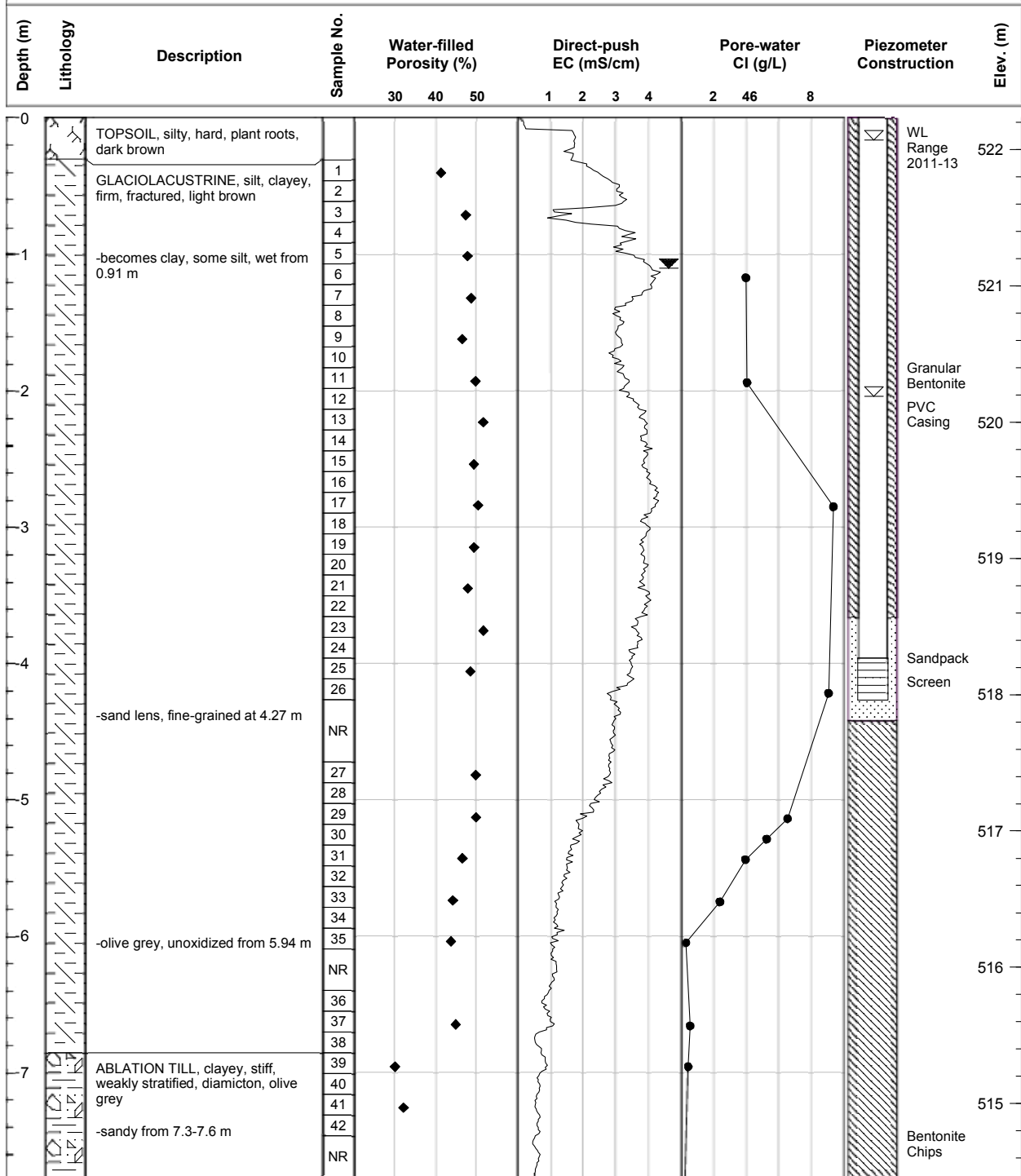


NOTE:  
 NR No recovery

Drill Method: Direct-push continuous core  
 Drill Rig: Geoprobe 7822 DT  
 EC Probe: SC520 wenner array

### CORING LOG: BH2

Coring Date: 16-Aug-2011  
 EC Logging Date: 15-Aug-2011  
 Ground Elevation (masl): 522.23



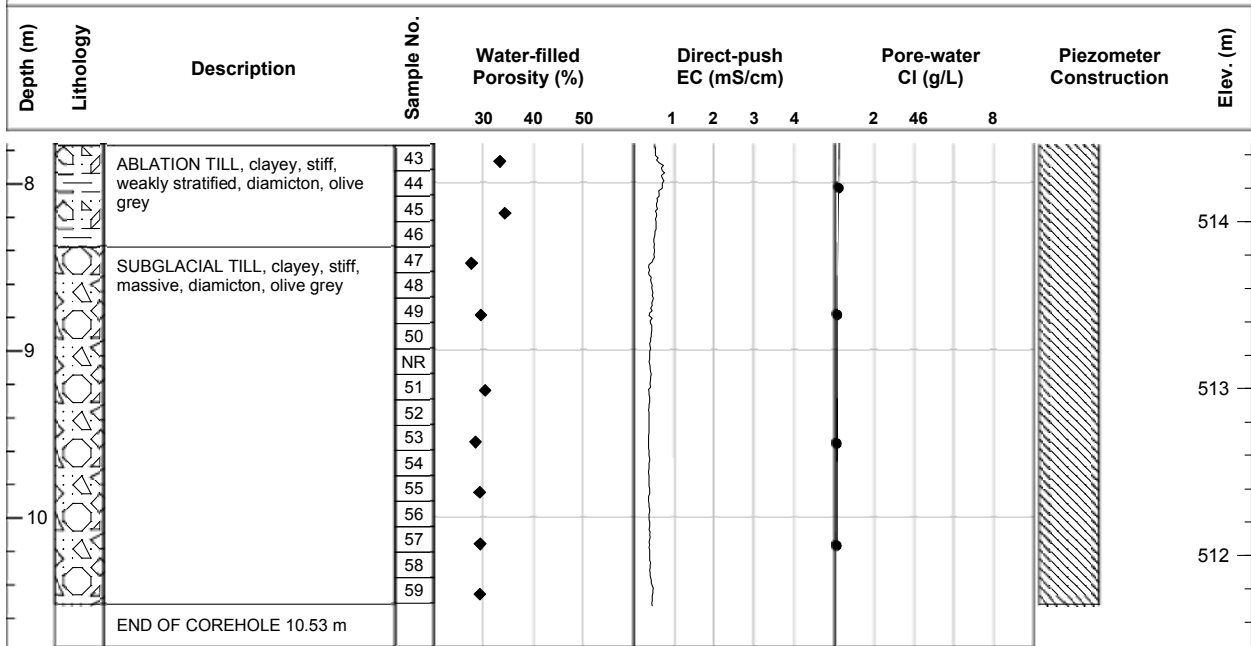
**NOTE:**  
 NR No recovery

Sheet 1 of 2

Drill Method: Direct-push continuous core  
 Drill Rig: Geoprobe 7822 DT  
 EC Probe: SC520 wenner array

### CORING LOG: BH2

Coring Date: 16-Aug-2011  
 EC Logging Date: 15-Aug-2011  
 Ground Elevation (masl): 522.23

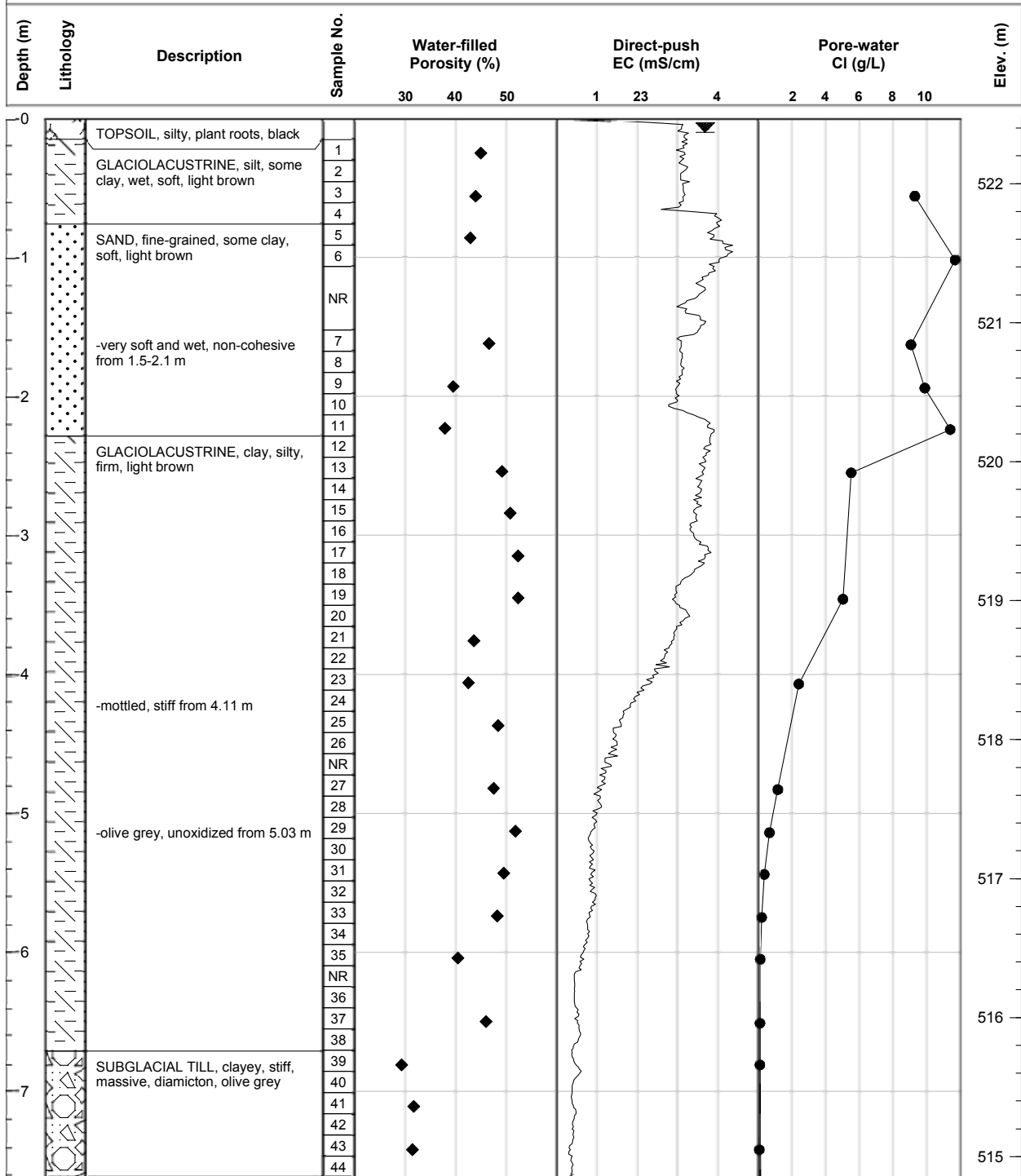


**NOTE:**  
 NR No recovery

Drill Method: Direct-push continuous core  
 Drill Rig: Geoprobe 7822 DT  
 EC Probe: SC520 wenner array

### CORING LOG: BH3

Coring Date: 16-Aug-2011  
 EC Logging Date: 15-Aug-2011  
 Ground Elevation (masl): 522.47

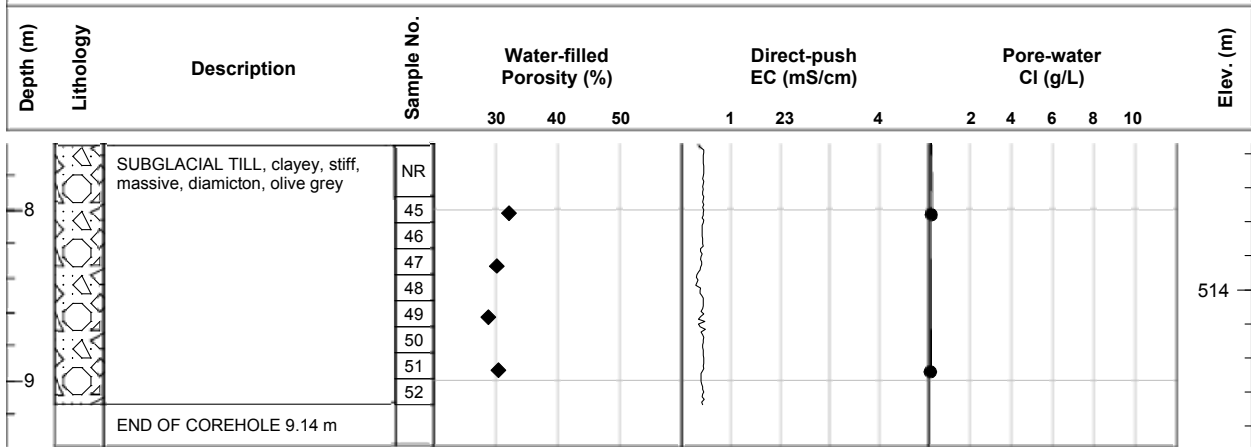


NOTE:  
 NR No recovery

Drill Method: Direct-push continuous core  
 Drill Rig: Geoprobe 7822 DT  
 EC Probe: SC520 wenner array

### CORING LOG: BH3

Coring Date: 16-Aug-2011  
 EC Logging Date: 15-Aug-2011  
 Ground Elevation (masl): 522.47

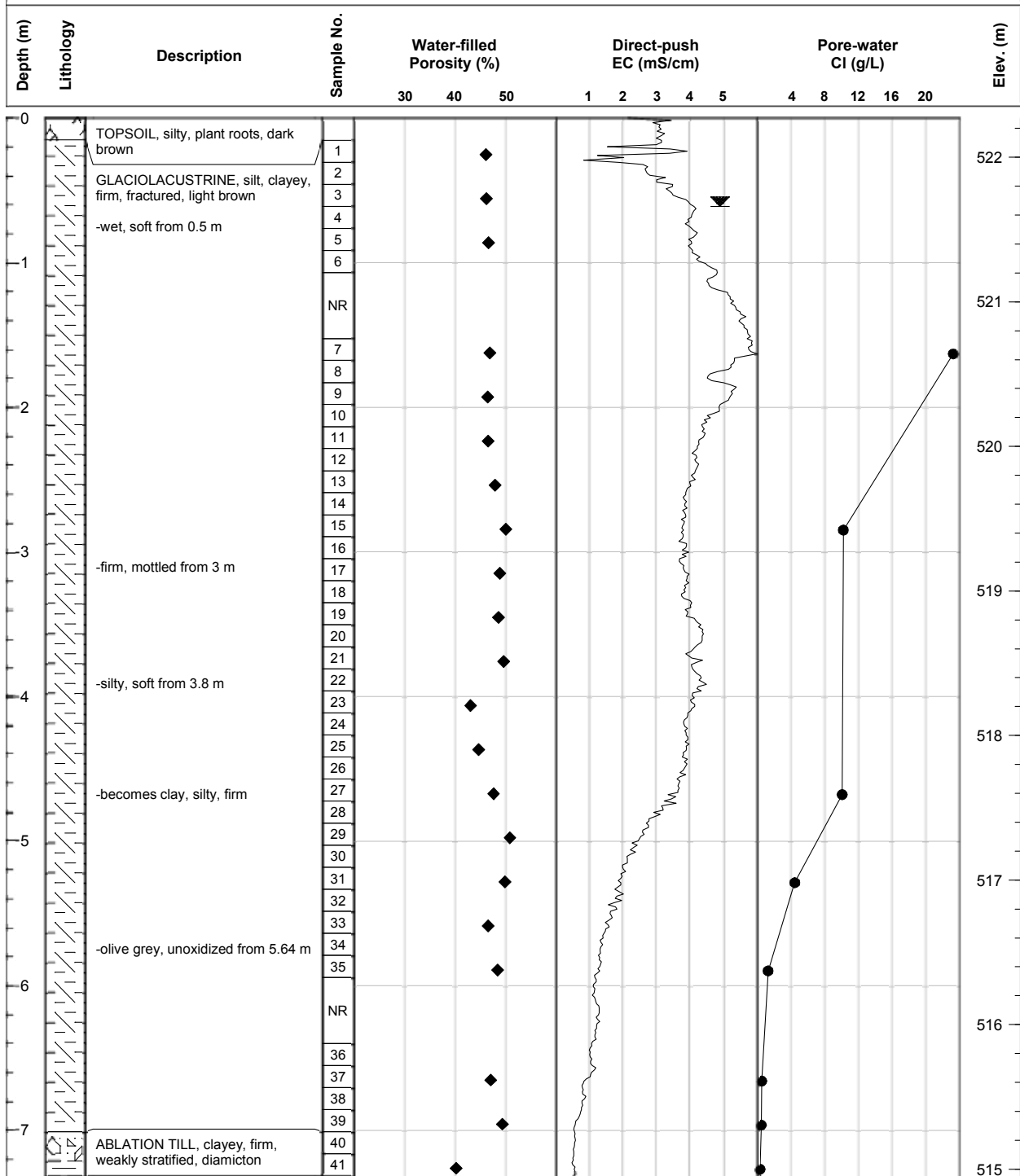


**NOTE:**  
 NR No recovery

Drill Method: Direct-push continuous core  
 Drill Rig: Geoprobe 7822 DT  
 EC Probe: SC520 wenner array

### CORING LOG: BH4

Coring Date: 16-Aug-2011  
 EC Logging Date: 16-Aug-2011  
 Ground Elevation (masl): 522.27

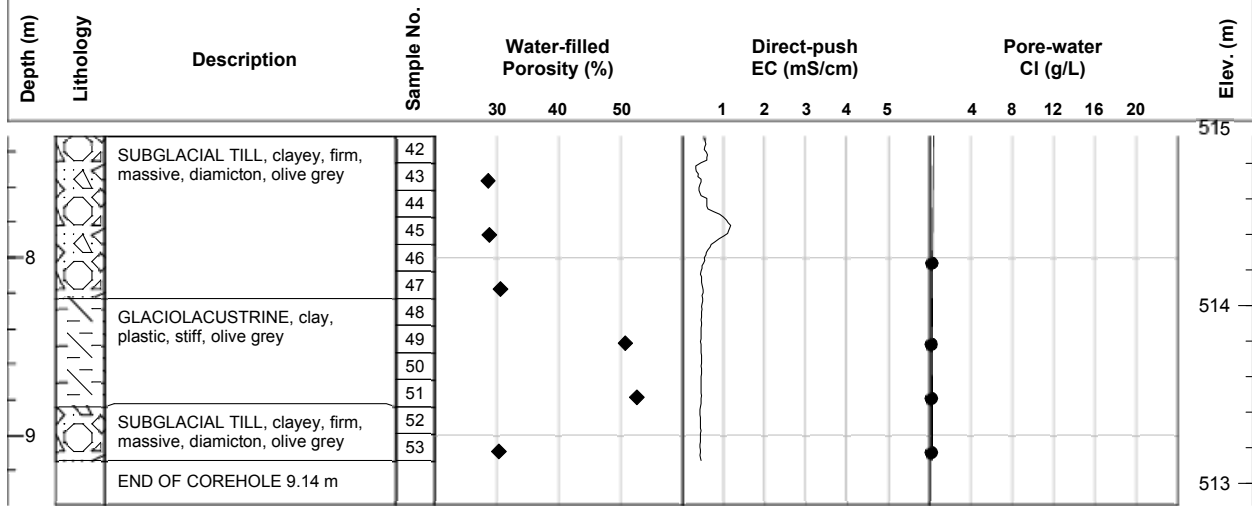


NOTE:  
 NR No recovery

Drill Method: Direct-push continuous core  
 Drill Rig: Geoprobe 7822 DT  
 EC Probe: SC520 wenner array

### CORING LOG: BH4

Coring Date: 16-Aug-2011  
 EC Logging Date: 16-Aug-2011  
 Ground Elevation (masl): 522.27



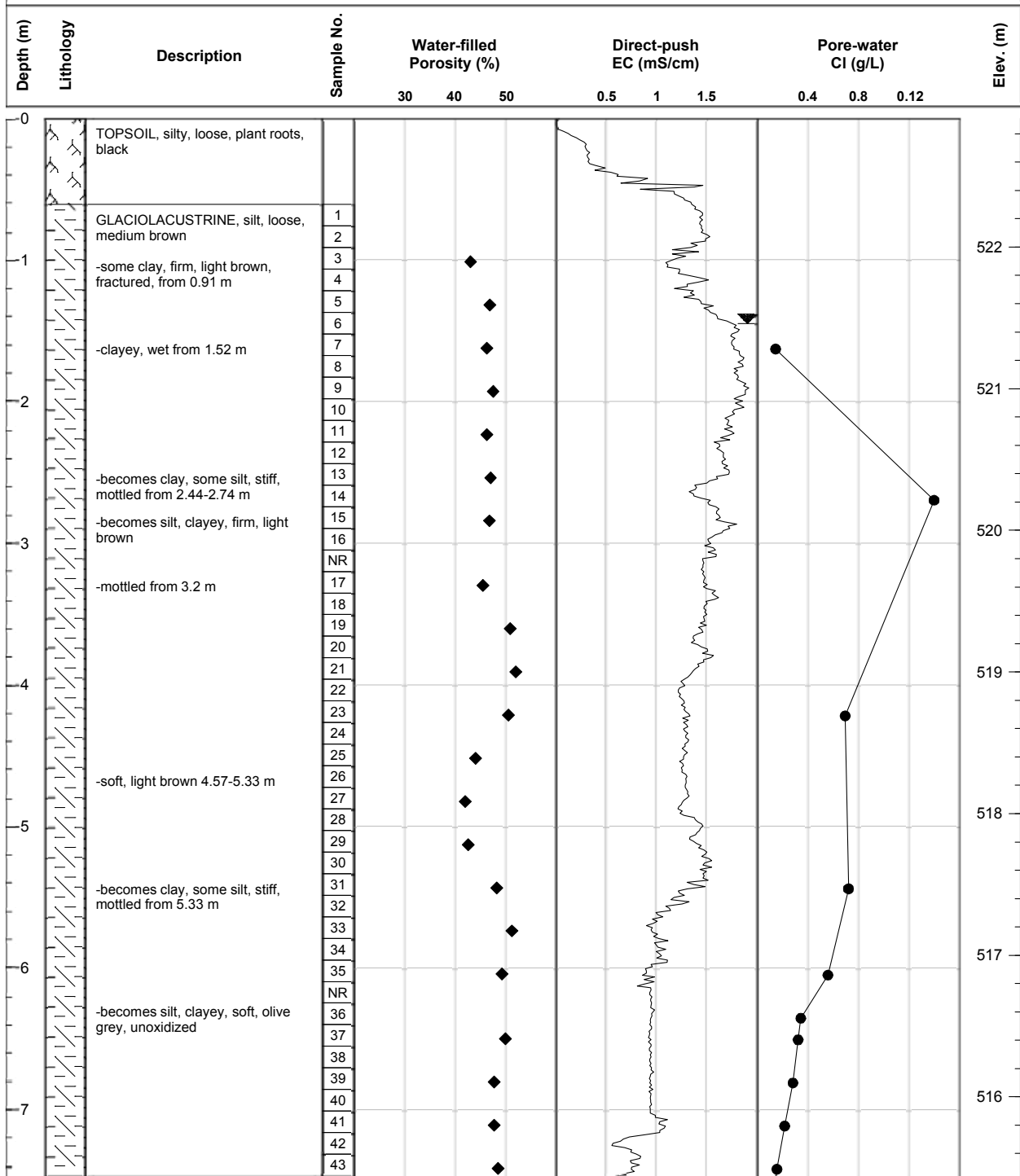
**NOTE:**

NR No recovery

Drill Method: Direct-push continuous core  
 Drill Rig: Geoprobe 7822 DT  
 EC Probe: SC520 wenner array

### CORING LOG: BH5

Coring Date: 16-Aug-2011  
 EC Logging Date: 16-Aug-2011  
 Ground Elevation (masl): 522.91

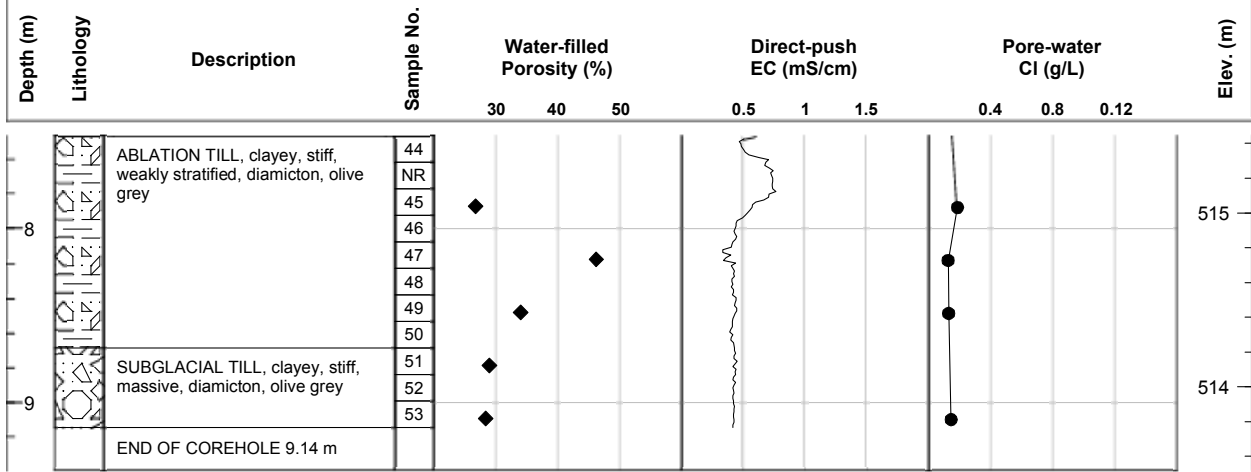


**NOTE:**  
 NR No recovery

Drill Method: Direct-push continuous core  
 Drill Rig: Geoprobe 7822 DT  
 EC Probe: SC520 wenner array

### CORING LOG: BH5

Coring Date: 16-Aug-2011  
 EC Logging Date: 16-Aug-2011  
 Ground Elevation (masl): 522.91



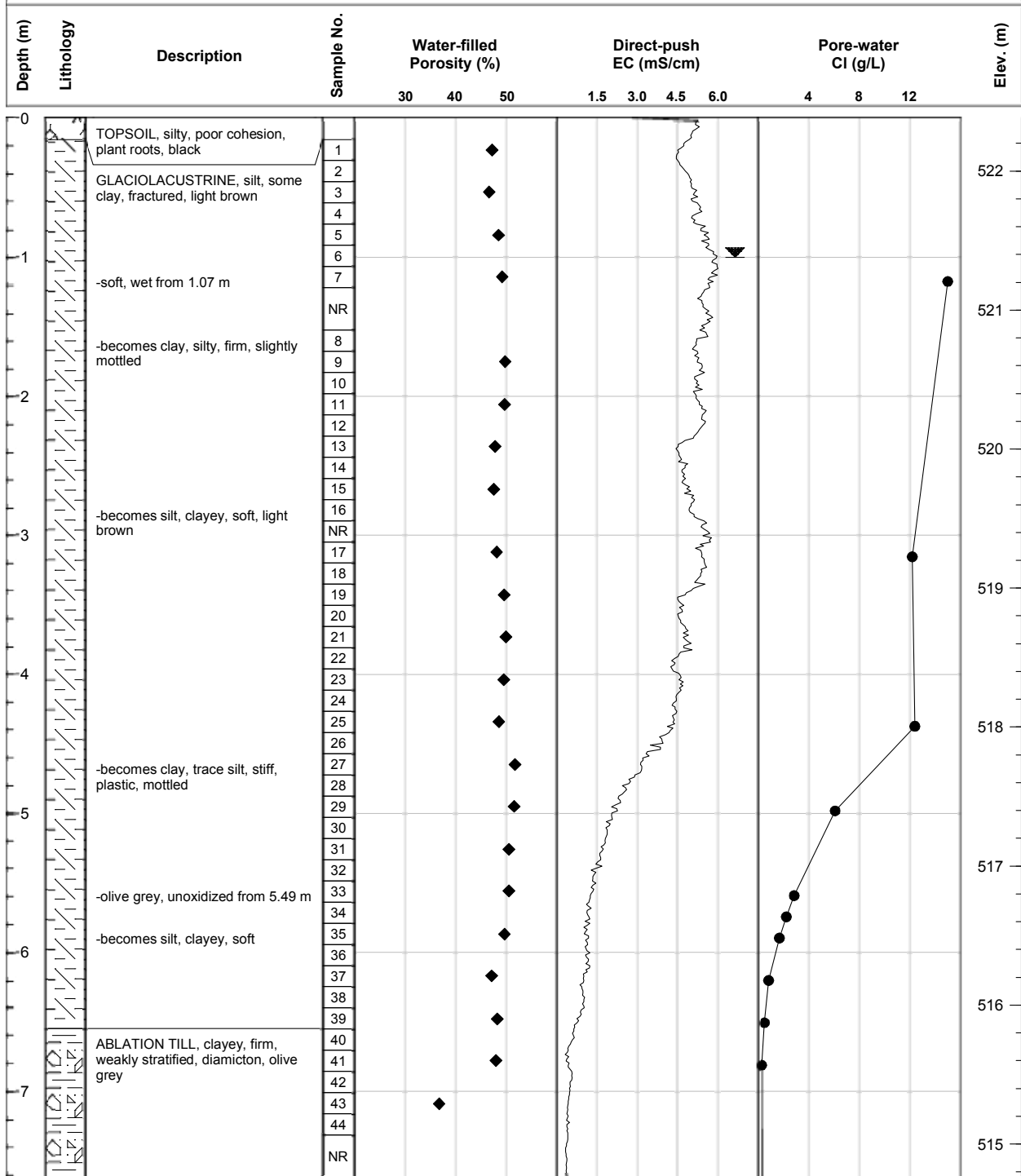
**NOTE:**

NR No recovery

Drill Method: Direct-push continuous core  
 Drill Rig: Geoprobe 7822 DT  
 EC Probe: SC520 wenner array

### CORING LOG: BH6

Coring Date: 17-Aug-2011  
 EC Logging Date: 16-Aug-2011  
 Ground Elevation (masl): 522.38

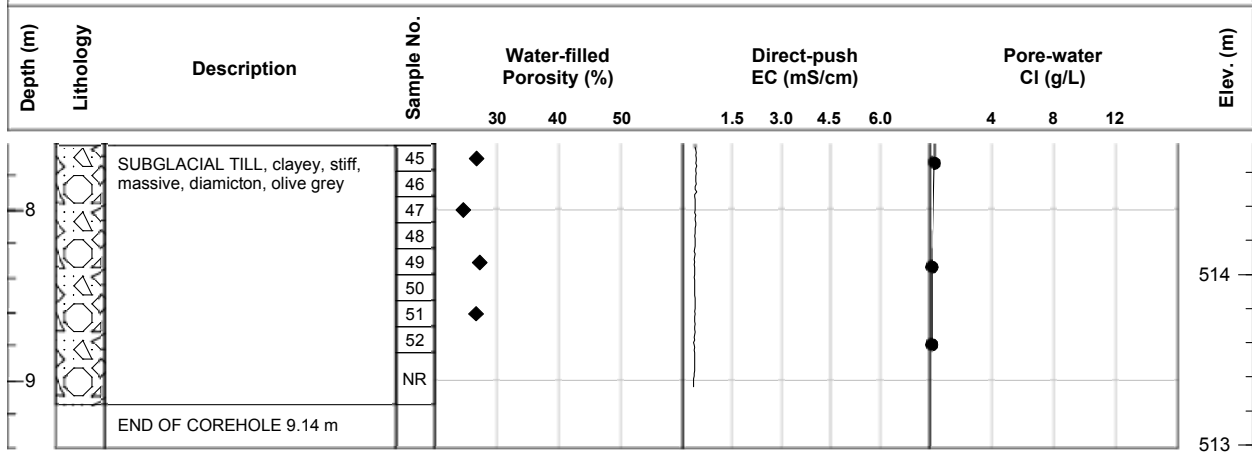


**NOTE:**  
 NR No recovery

Drill Method: Direct-push continuous core  
 Drill Rig: Geoprobe 7822 DT  
 EC Probe: SC520 wenner array

### CORING LOG: BH6

Coring Date: 17-Aug-2011  
 EC Logging Date: 16-Aug-2011  
 Ground Elevation (masl): 522.38

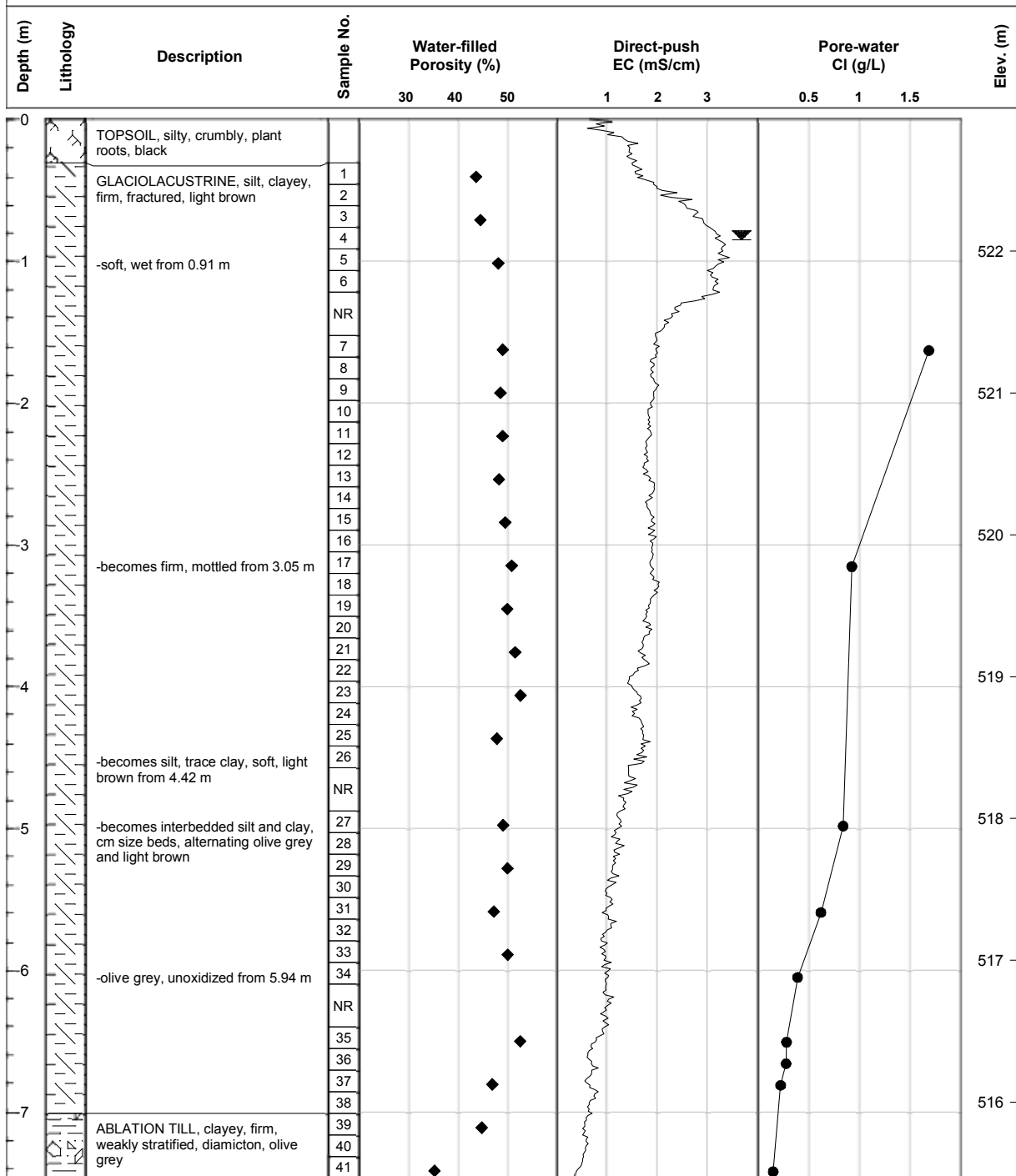


**NOTE:**  
 NR No recovery

Drill Method: Direct-push continuous core  
 Drill Rig: Geoprobe 7822 DT  
 EC Probe: SC520 wenner array

### CORING LOG: BH7

Coring Date: 17-Aug-2011  
 EC Logging Date: 17-Aug-2011  
 Ground Elevation (masl): 522.93



**NOTE:**

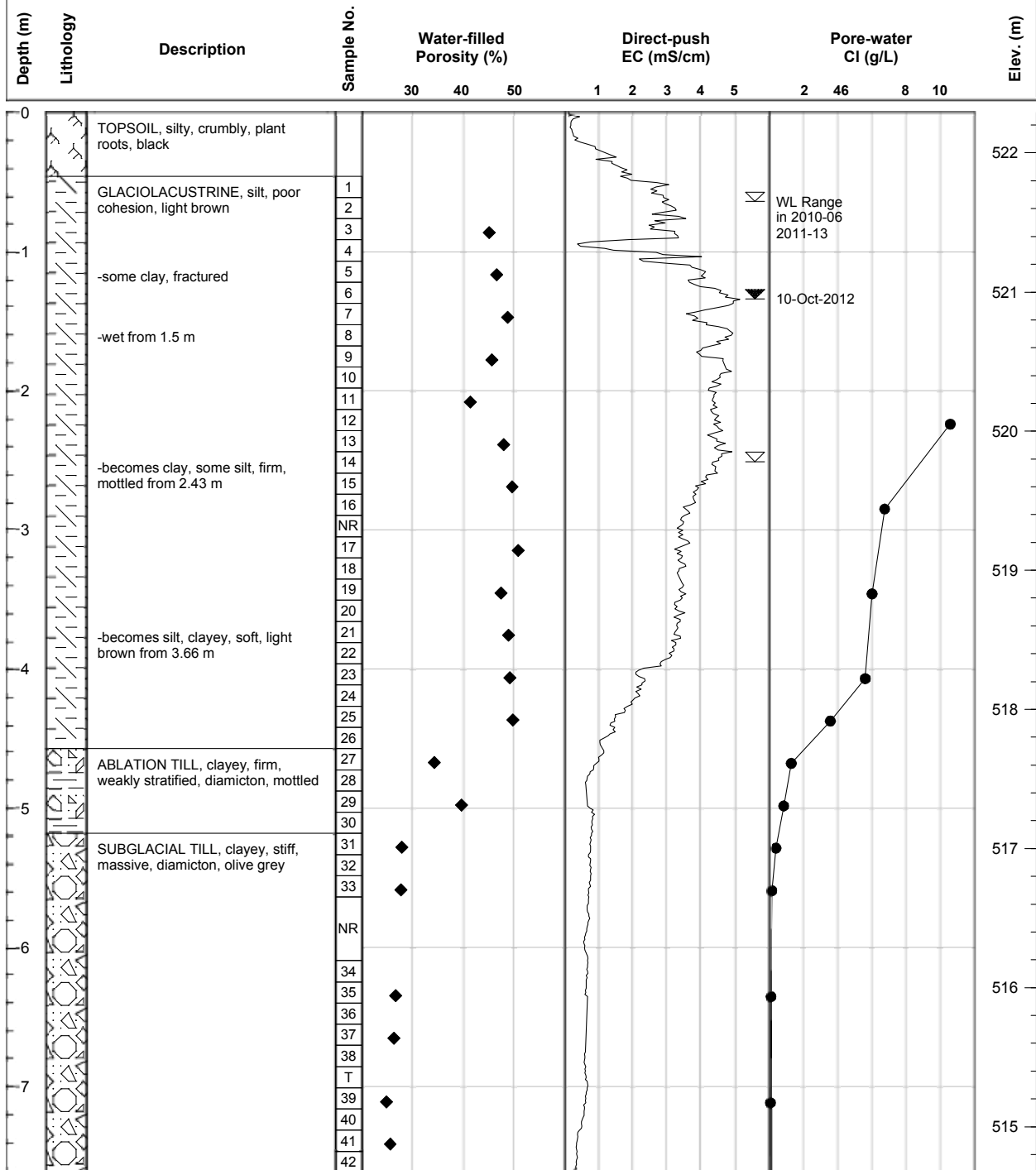
NR No recovery



Drill Method: Direct-push continuous core  
 Drill Rig: Geoprobe 7822 DT  
 EC Probe: SC520 wenner array

### CORING LOG: BH8

Coring Date: 17-Aug-2011  
 EC Logging Date: 10-Oct-2012  
 Ground Elevation (masl): 522.29



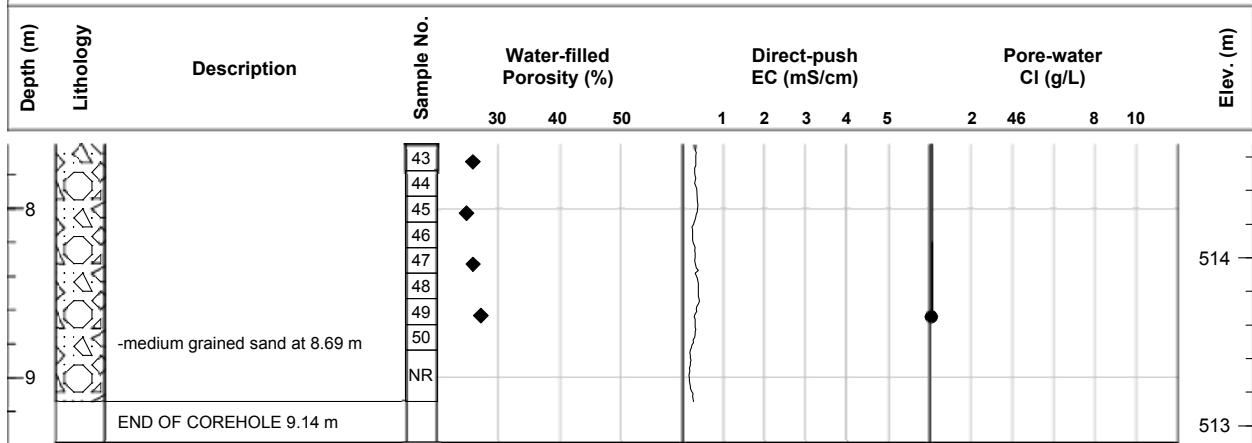
**NOTE:**

NR No recovery  
 T Triaxial permeameter test sample

**Drill Method:** Direct-push continuous core  
**Drill Rig:** Geoprobe 7822 DT  
**EC Probe:** SC520 wenner array

### CORING LOG: BH8

**Coring Date:** 17-Aug-2011  
**EC Logging Date:** 10-Oct-2012  
**Ground Elevation (masl):** 522.29



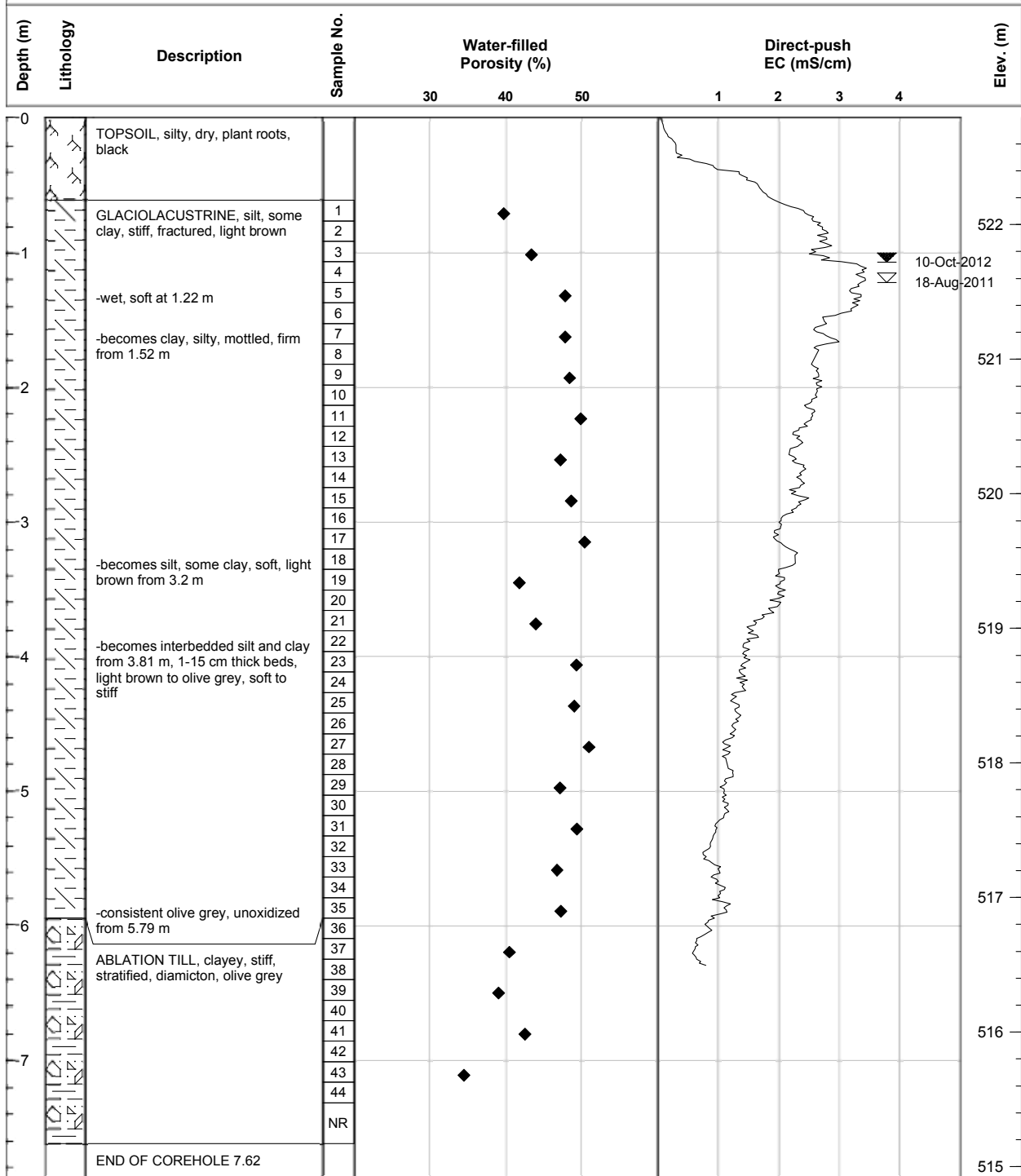
**NOTE:**

- NR No recovery
- T Triaxial permeameter test sample

Drill Method: Direct-push continuous core  
 Drill Rig: Geoprobe 7822 DT  
 EC Probe: SC520 wenner array

### CORING LOG: BH9

Coring Date: 18-Aug-2011  
 EC Logging Date: 10-Oct-2012  
 Ground Elevation (masl): 522.79



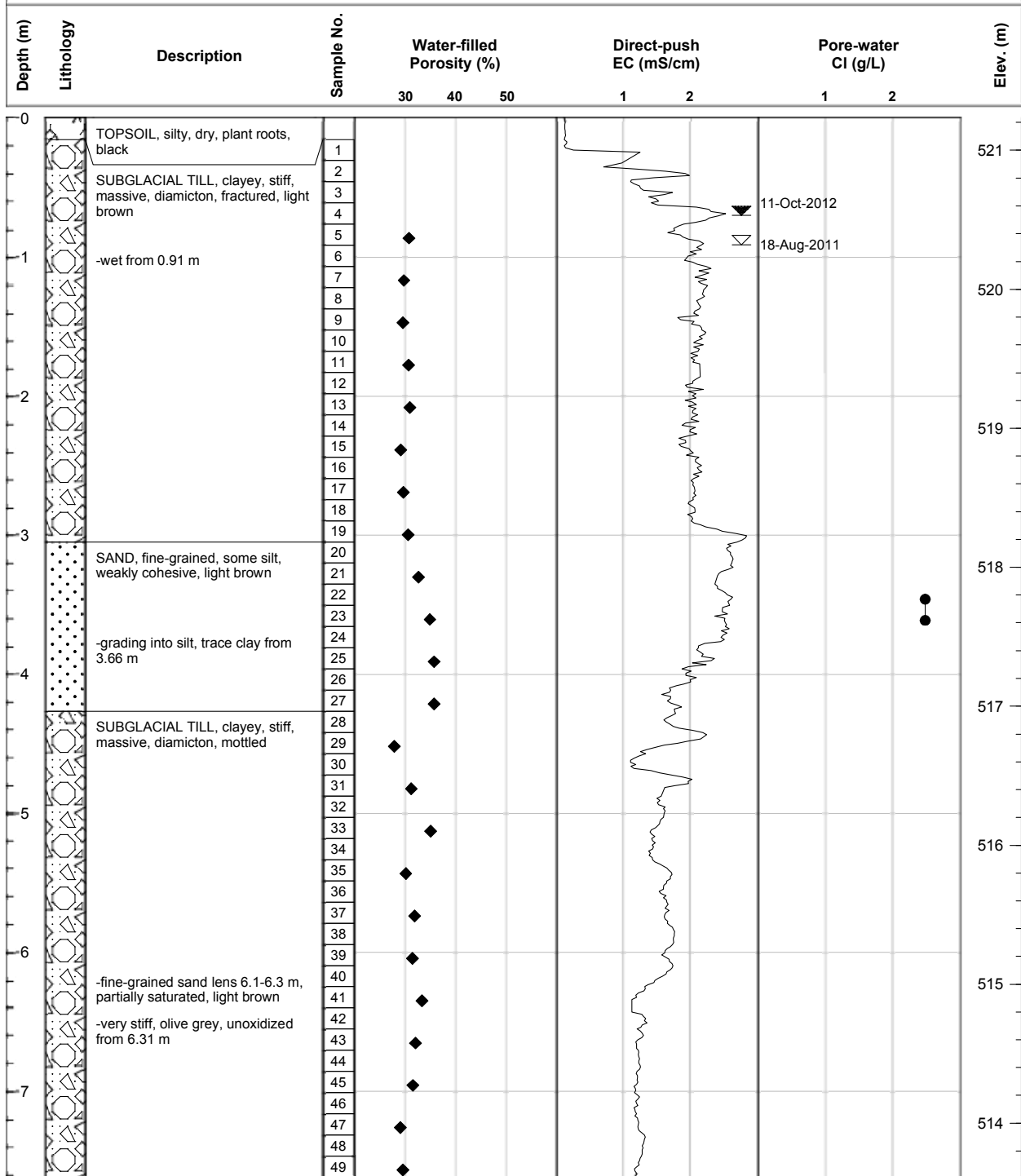
**NOTE:**  
 NR No recovery



Drill Method: Direct-push continuous core  
 Drill Rig: Geoprobe 7822 DT  
 EC Probe: SC520 wenner array

### CORING LOG: BH11

Coring Date: 18-Aug-2011  
 EC Logging Date: 11-Oct-2012  
 Ground Elevation (masl): 521.23

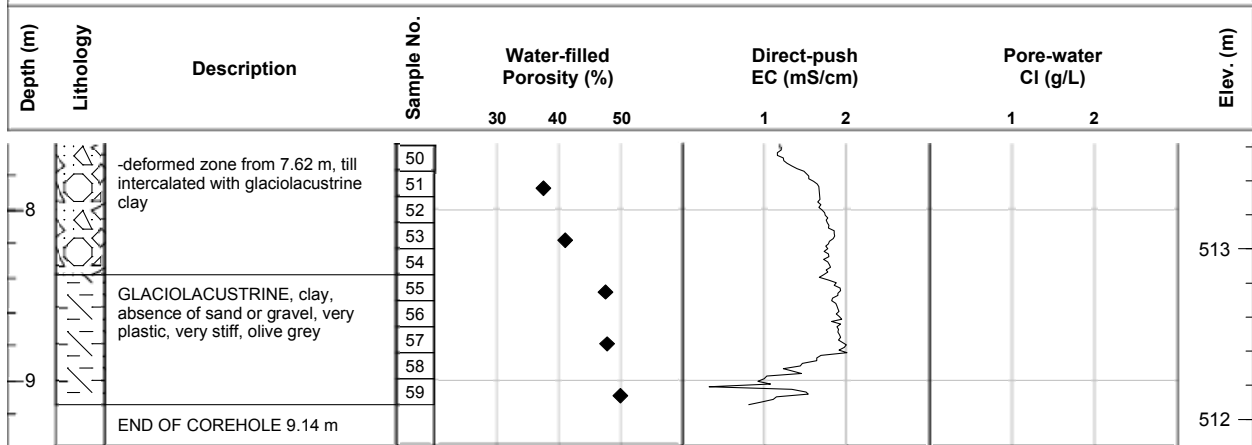


NOTE:  
 NR No recovery

**Drill Method:** Direct-push continuous core  
**Drill Rig:** Geoprobe 7822 DT  
**EC Probe:** SC520 wenner array

### CORING LOG: BH11

**Coring Date:** 18-Aug-2011  
**EC Logging Date:** 11-Oct-2012  
**Ground Elevation (masl):** 521.23



**NOTE:**  
 NR No recovery

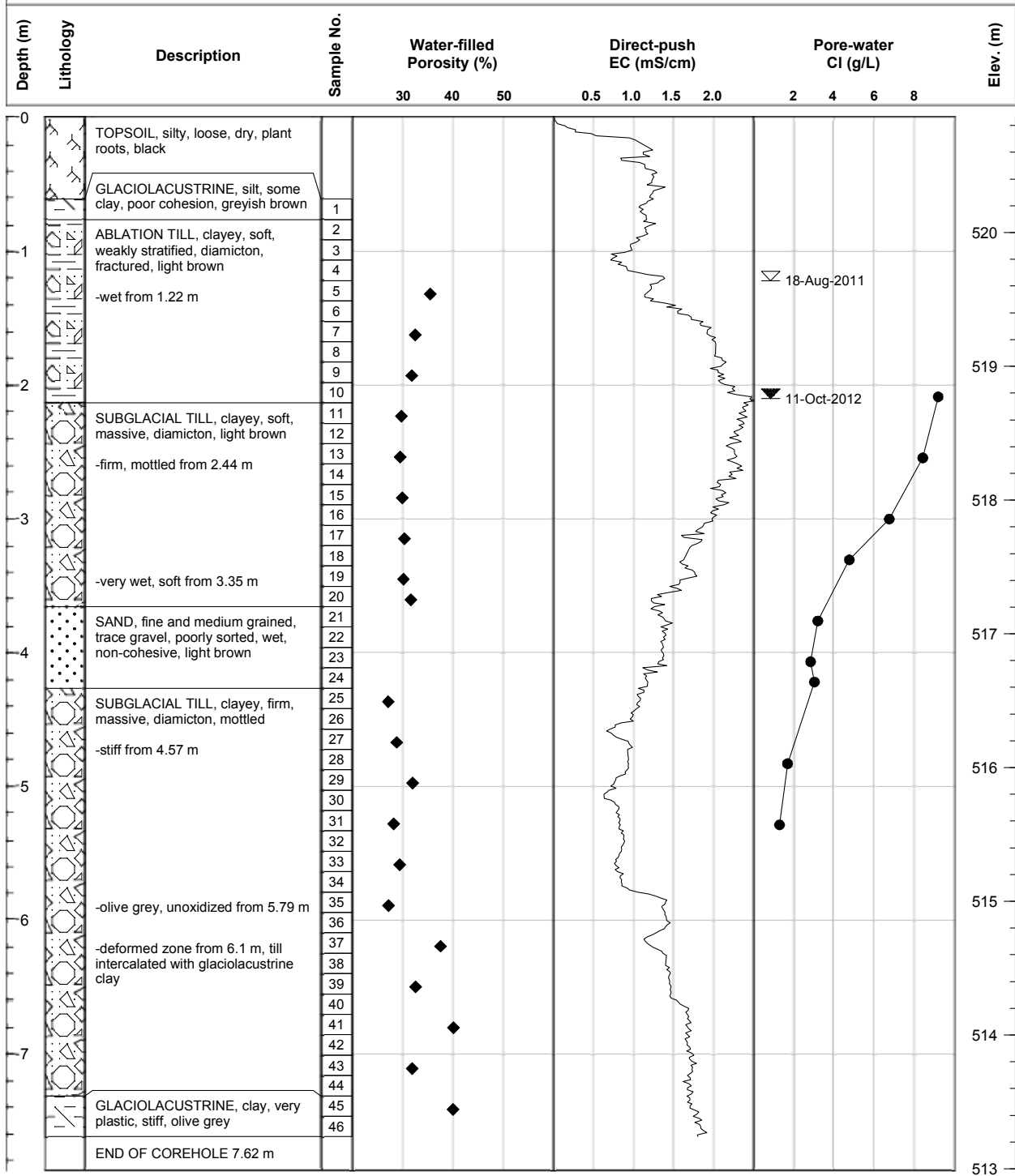




Drill Method: Direct-push continuous core  
 Drill Rig: Geoprobe 7822 DT  
 EC Probe: SC520 wenner array

### CORING LOG: BH14

Coring Date: 18-Aug-2011  
 EC Logging Date: 11-Oct-2012  
 Ground Elevation (masl): 520.86

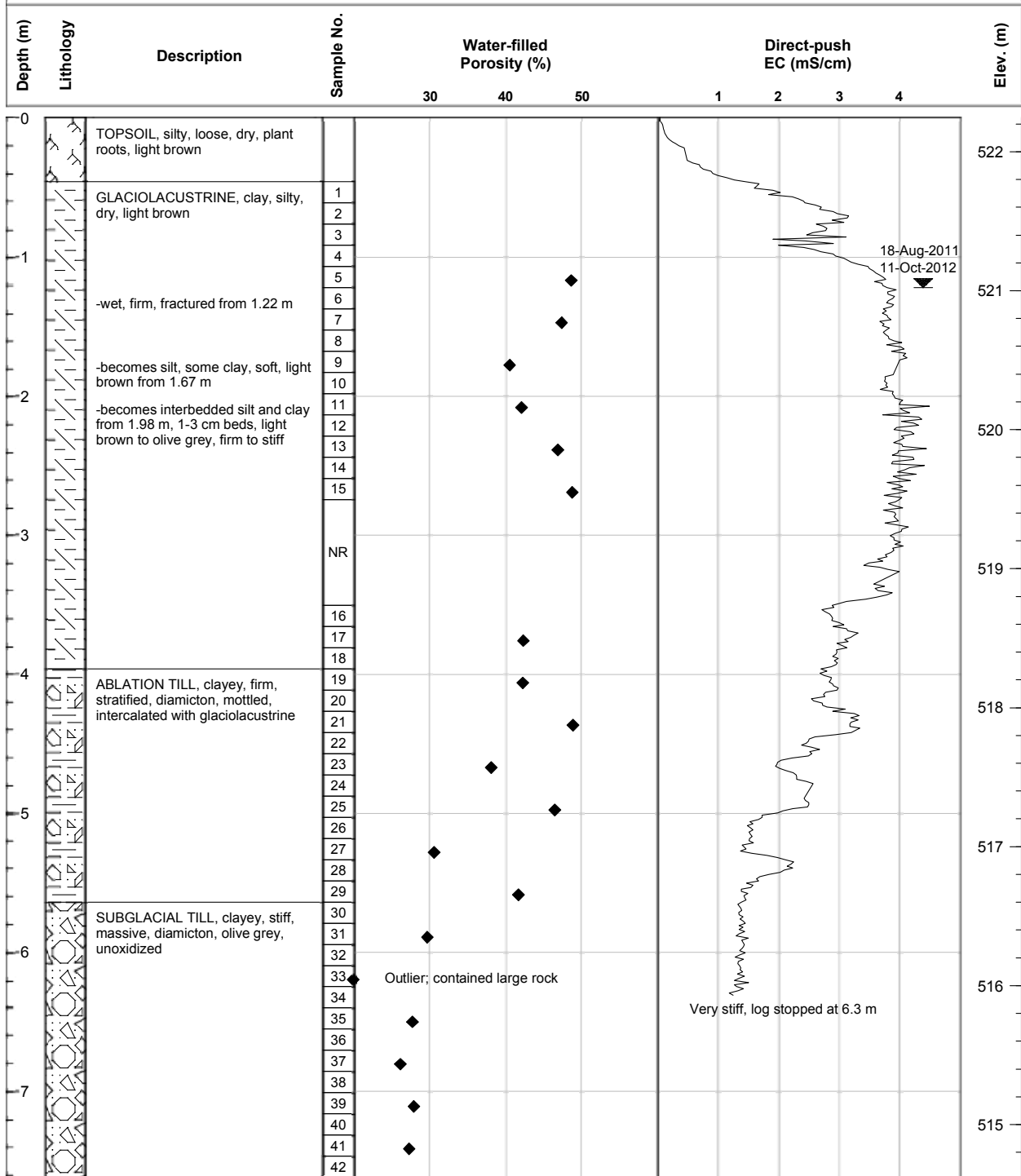


NOTE:  
 NR No recovery

Drill Method: Direct-push continuous core  
 Drill Rig: Geoprobe 7822 DT  
 EC Probe: SC520 wenner array

### CORING LOG: BH15

Coring Date: 18-Aug-2011  
 EC Logging Date: 11-Oct-2012  
 Ground Elevation (masl): 522.24



NOTE:  
 NR No recovery

Drill Method: Direct-push continuous core  
 Drill Rig: Geoprobe 7822 DT  
 EC Probe: SC520 wenner array

### CORING LOG: BH15

Coring Date: 18-Aug-2011  
 EC Logging Date: 11-Oct-2012  
 Ground Elevation (masl): 522.24

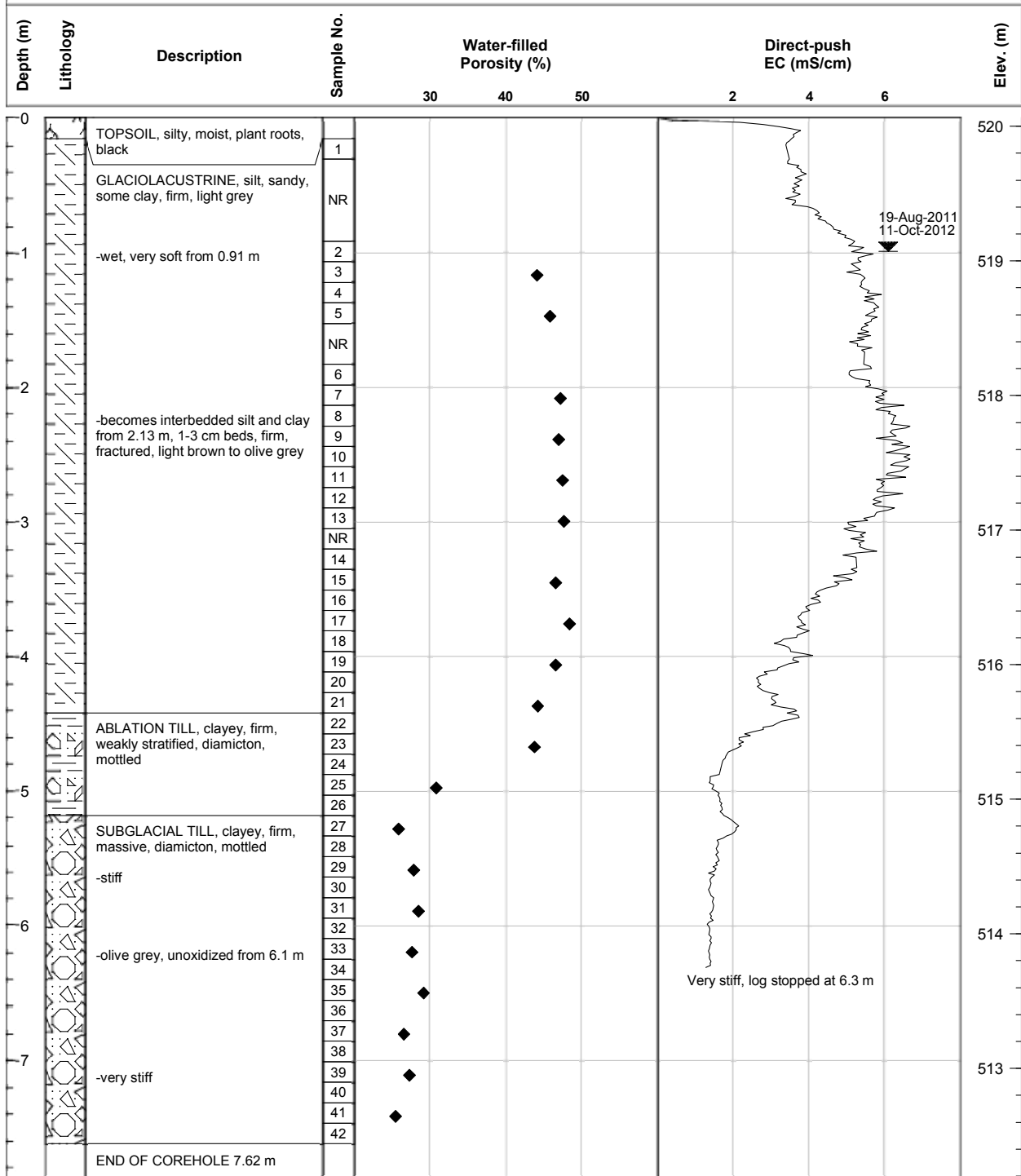
Depth (m)	Lithology	Description	Sample No.	Water-filled Porosity (%)			Direct-push EC (mS/cm)				Elev. (m)	
				30	40	50	1	2	3	4		
8		-very stiff from 7.62 m, broken rock at 7.78 m	43	◆								514
			44									
			45	◆								
			46									
			47	◆								
			48									
			49	◆								
			50									
			51	◆								
			52									
9		END OF COREHOLE 9.14 m									513	

**NOTE:**  
 NR No recovery

Drill Method: Direct-push continuous core  
 Drill Rig: Geoprobe 7822 DT  
 EC Probe: SC520 wenner array

### CORING LOG: BH16

Coring Date: 19-Aug-2011  
 EC Logging Date: 11-Oct-2012  
 Ground Elevation (masl): 520.06



**NOTE:**

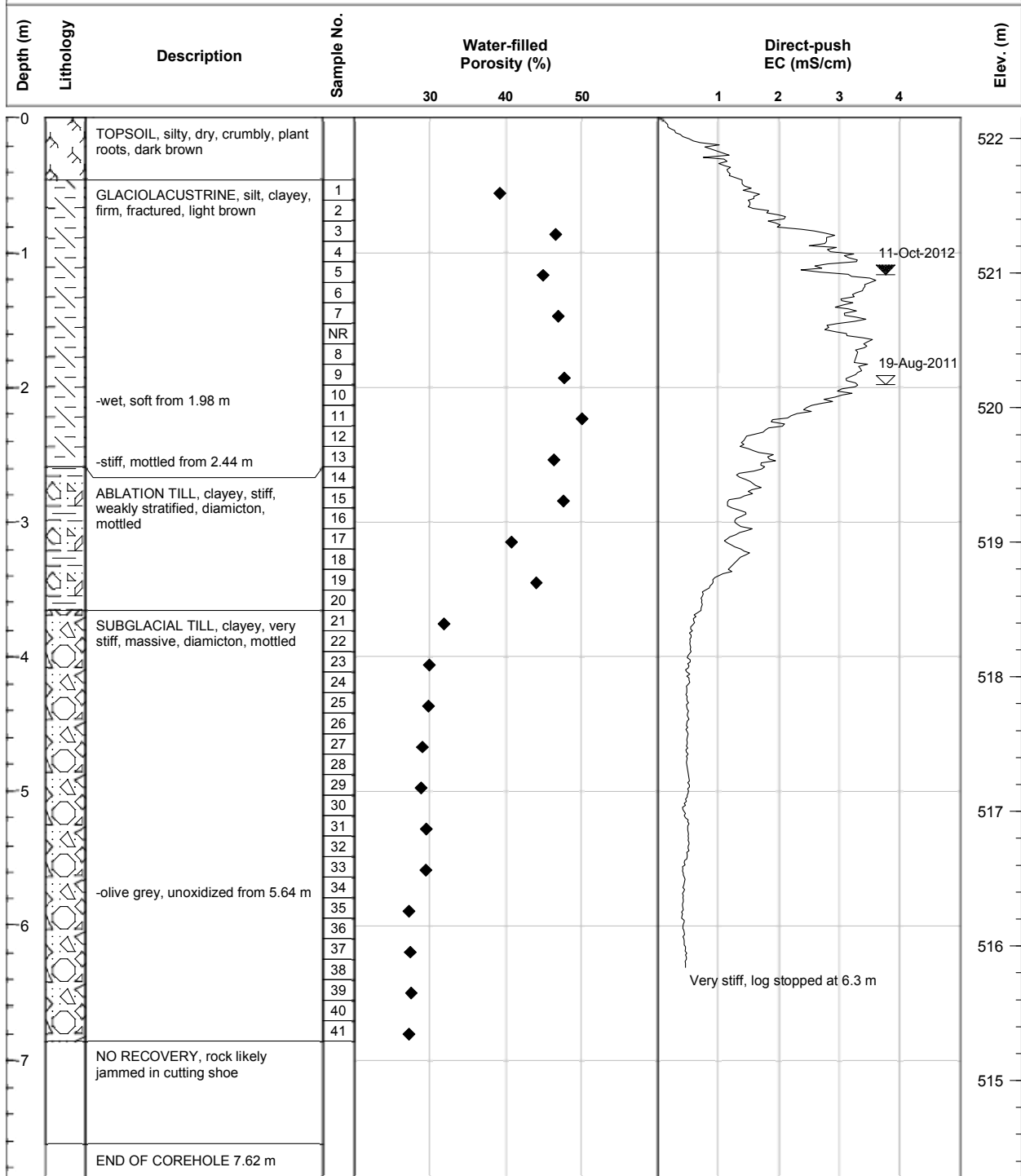
NR No recovery



Drill Method: Direct-push continuous core  
 Drill Rig: Geoprobe 7822 DT  
 EC Probe: SC520 wenner array

### CORING LOG: BH18

Coring Date: 19-Aug-2011  
 EC Logging Date: 11-Oct-2012  
 Ground Elevation (masl): 522.15

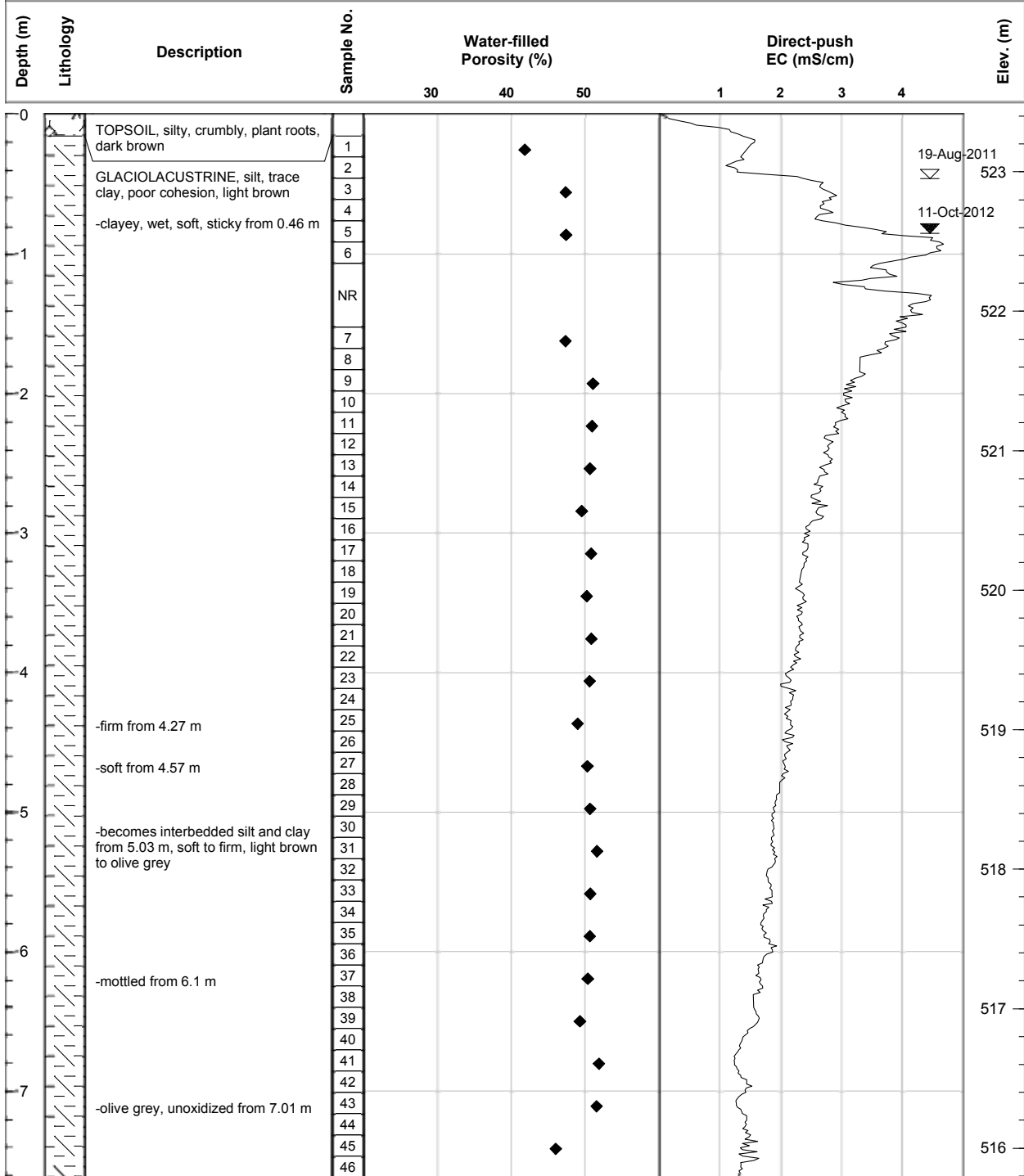


NOTE:  
 NR No recovery

Drill Method: Direct-push continuous core  
 Drill Rig: Geoprobe 7822 DT  
 EC Probe: SC520 wenner array

### CORING LOG: BH19

Coring Date: 19-Aug-2011  
 EC Logging Date: 11-Oct-2012  
 Ground Elevation (masl): 523.41

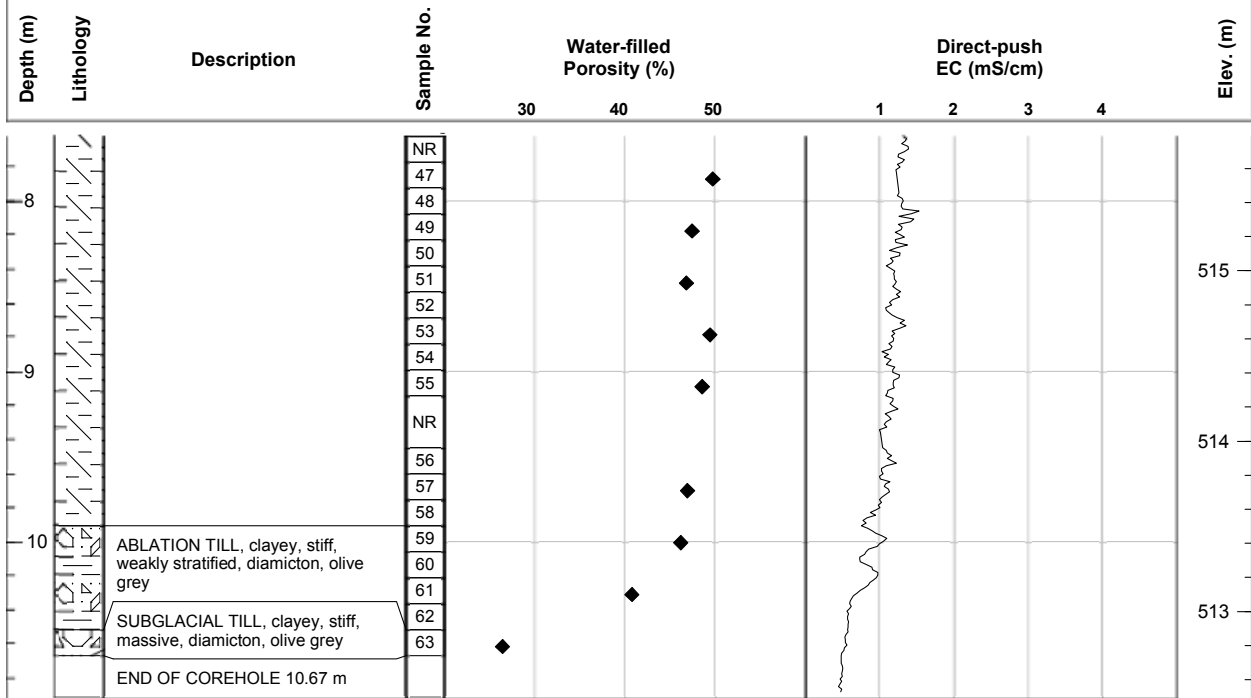


NOTE:  
 NR No recovery

Drill Method: Direct-push continuous core  
 Drill Rig: Geoprobe 7822 DT  
 EC Probe: SC520 wenner array

### CORING LOG: BH19

Coring Date: 19-Aug-2011  
 EC Logging Date: 11-Oct-2012  
 Ground Elevation (masl): 523.41



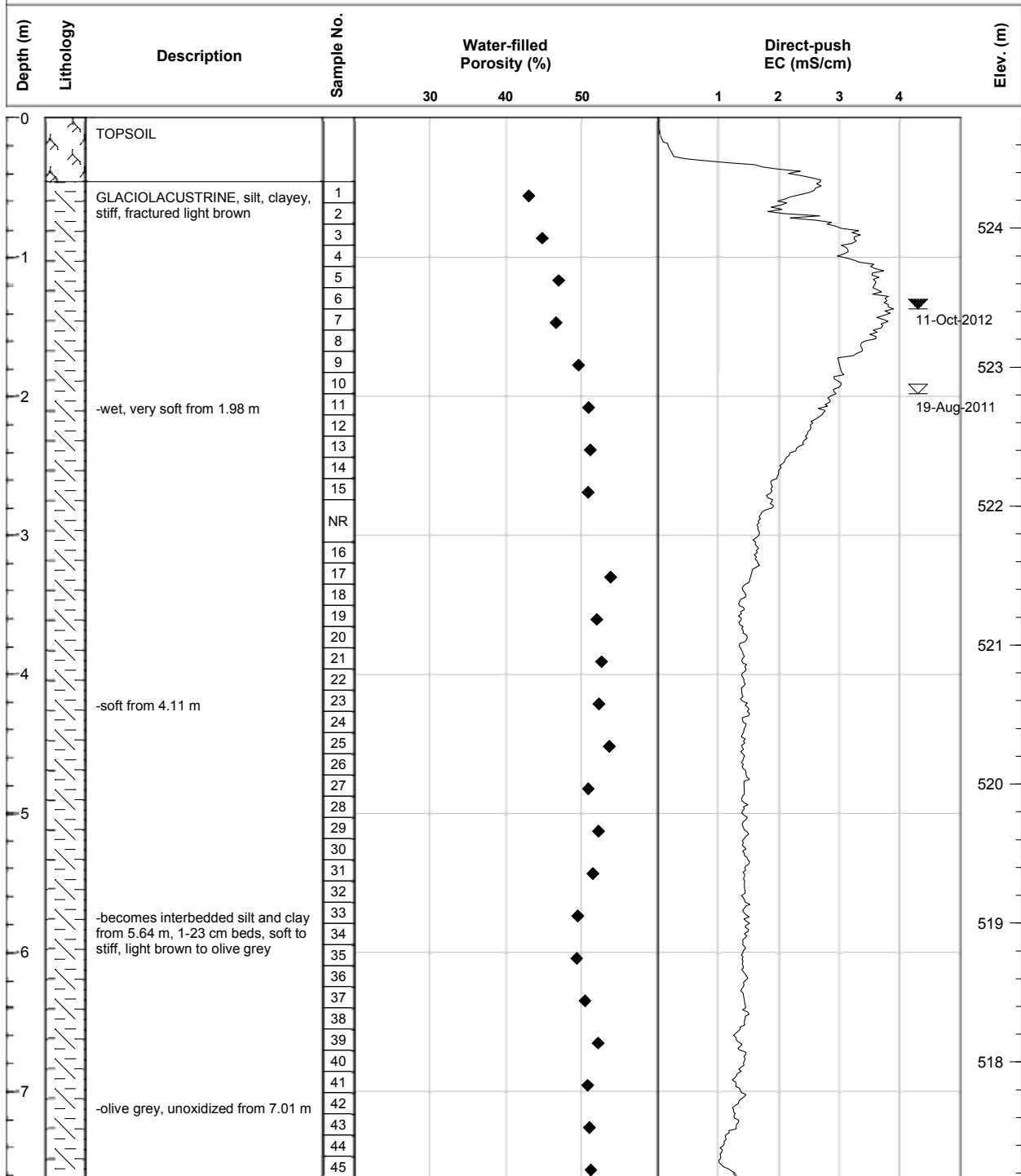
**NOTE:**  
 NR No recovery

Sheet 2 of 2

Drill Method: Direct-push continuous core  
 Drill Rig: Geoprobe 7822 DT  
 EC Probe: SC520 wenner array

### CORING LOG: BH20

Coring Date: 19-Aug-2011  
 EC Logging Date: 11-Oct-2012  
 Ground Elevation (masl): 524.79

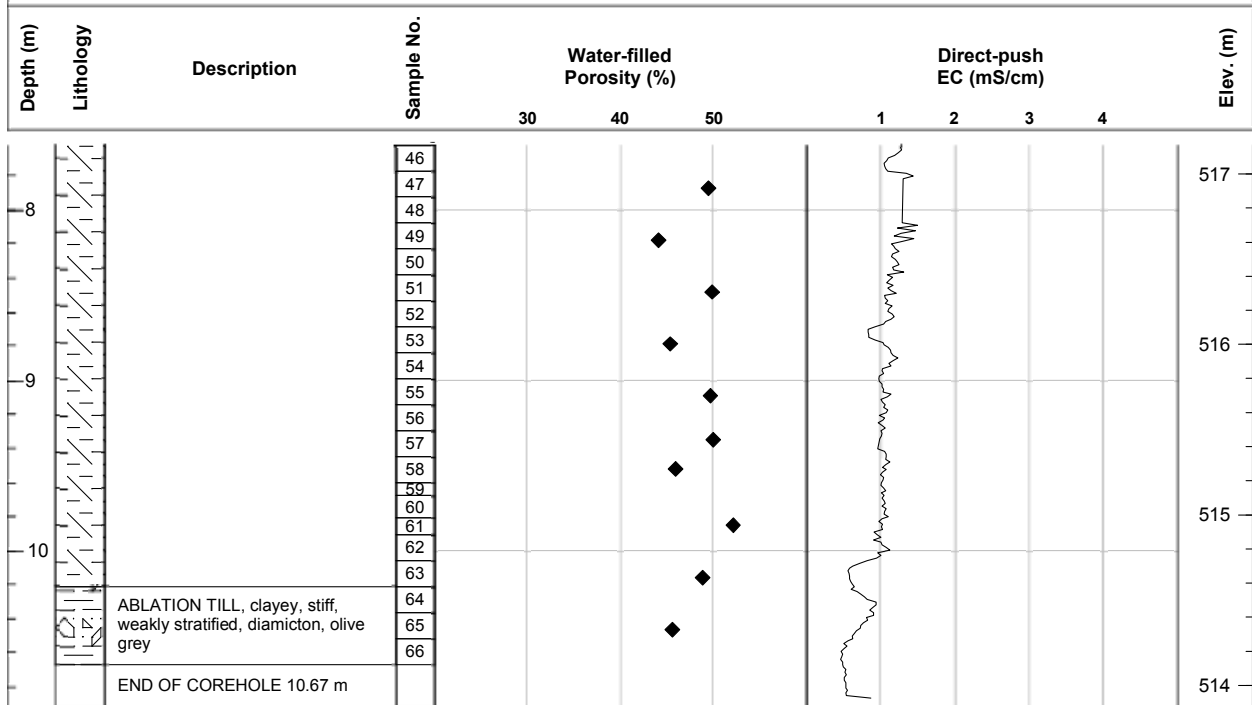


**NOTE:**  
 NR No recovery

**Drill Method:** Direct-push continuous core  
**Drill Rig:** Geoprobe 7822 DT  
**EC Probe:** SC520 wenner array

### CORING LOG: BH20

**Coring Date:** 19-Aug-2011  
**EC Logging Date:** 11-Oct-2012  
**Ground Elevation (masl):** 524.79



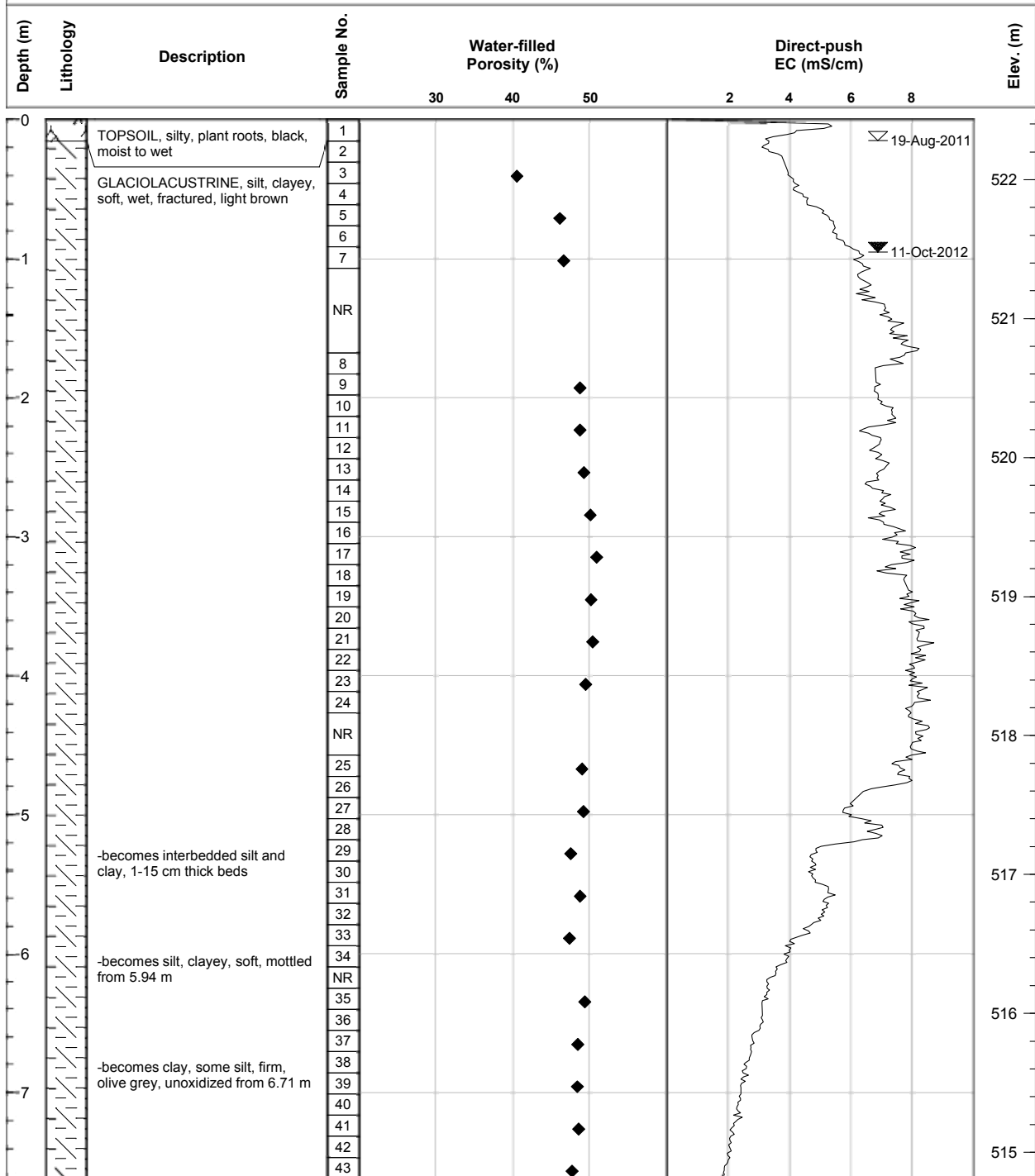
**NOTE:**

NR No recovery

Drill Method: Direct-push continuous core  
 Drill Rig: Geoprobe 7822 DT  
 EC Probe: SC520 wenner array

### CORING LOG: BH21

Coring Date: 19-Aug-2011  
 EC Logging Date: 11-Oct-2012  
 Ground Elevation (masl): 522.43



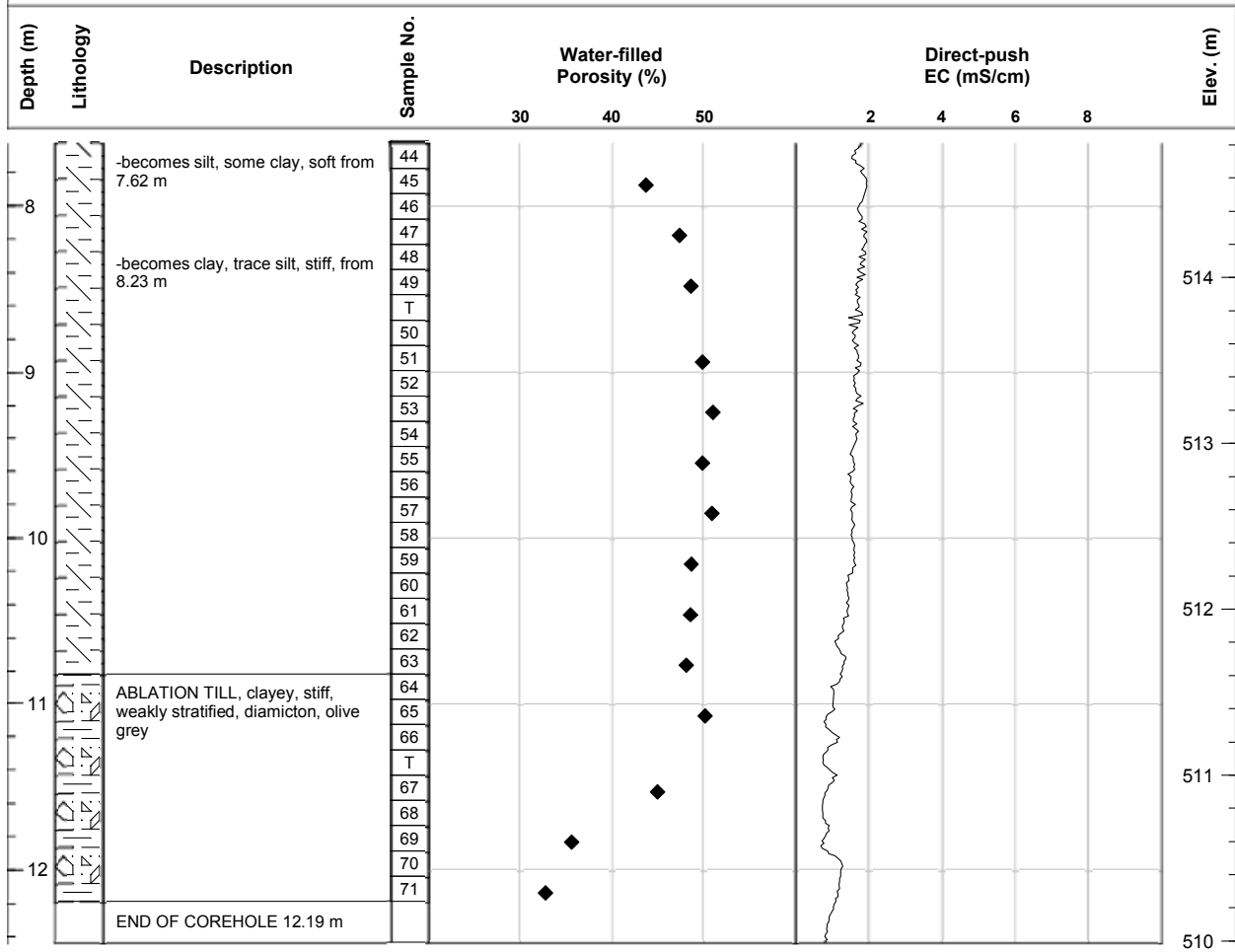
**NOTE:**

NR No recovery  
 T Triaxial permeameter test sample

Drill Method: Direct-push continuous core  
 Drill Rig: Geoprobe 7822 DT  
 EC Probe: SC520 wenner array

### CORING LOG: BH21

Coring Date: 19-Aug-2011  
 EC Logging Date: 11-Oct-2012  
 Ground Elevation (masl): 522.43



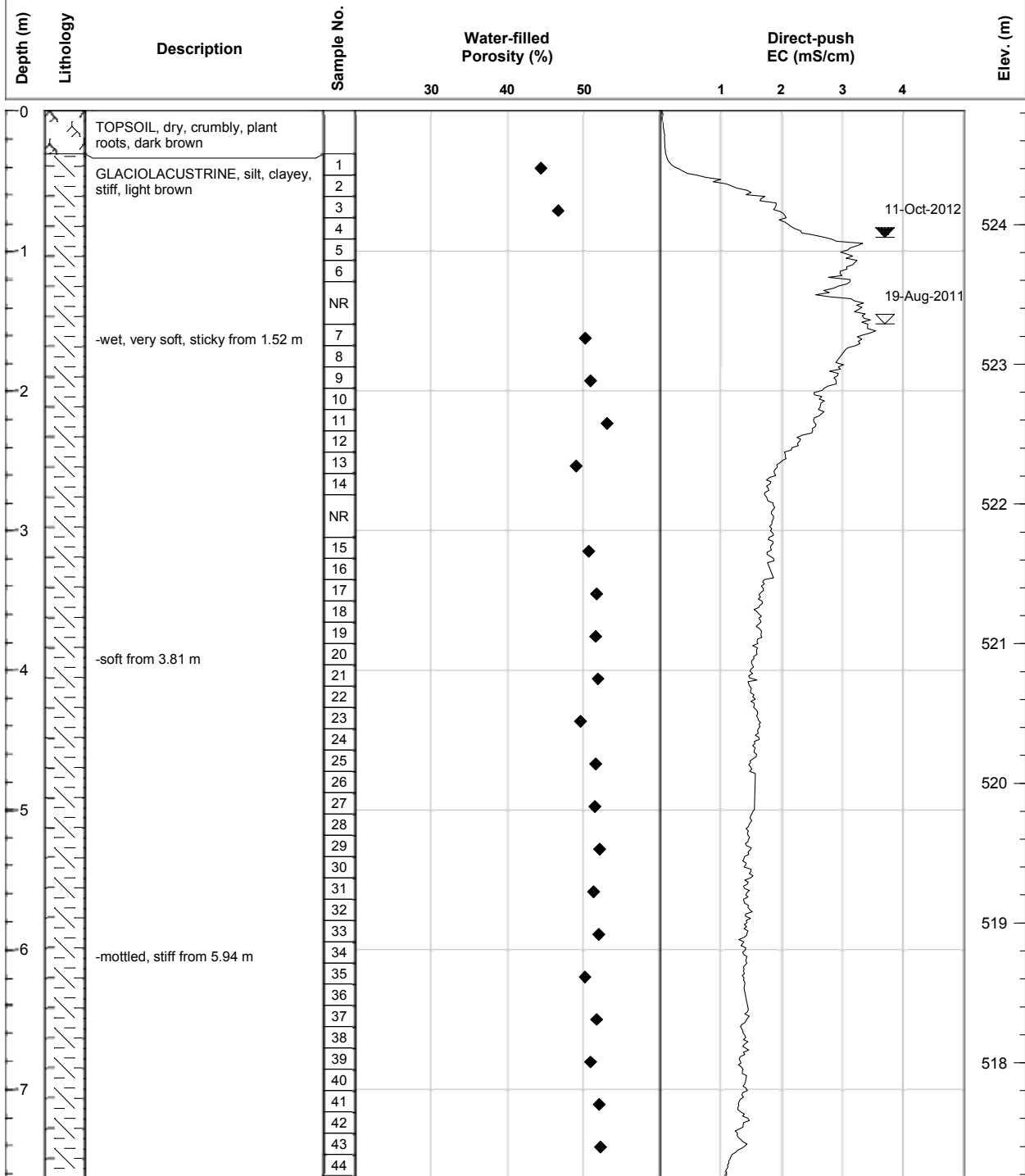
**NOTE:**

NR No recovery  
 T Triaxial permeameter test sample

Drill Method: Direct-push continuous core  
 Drill Rig: Geoprobe 7822 DT  
 EC Probe: SC520 wenner array

### CORING LOG: BH22

Coring Date: 19-Aug-2011  
 EC Logging Date: 11-Oct-2012  
 Ground Elevation (masl): 524.81



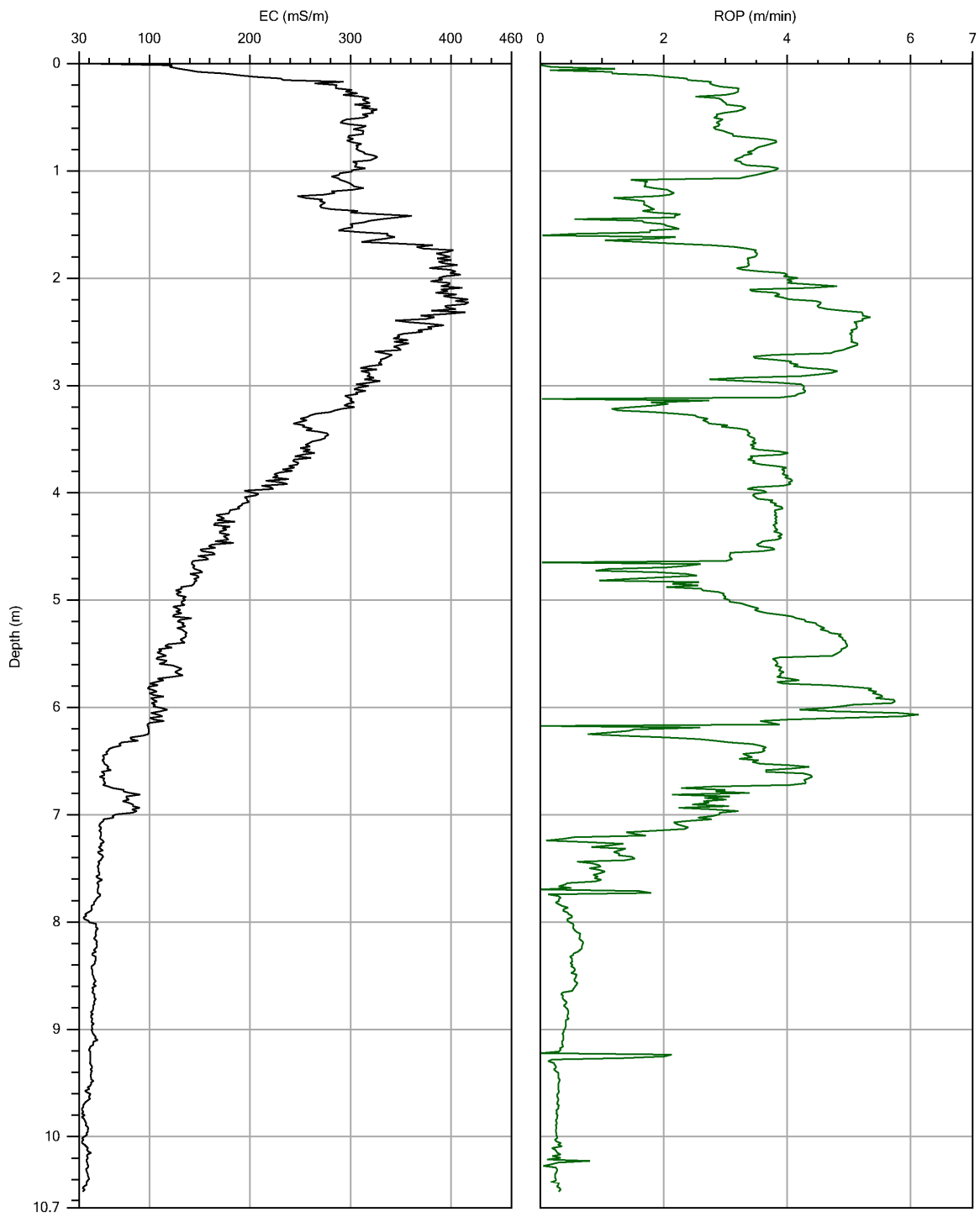
NOTE:  
 NR No recovery



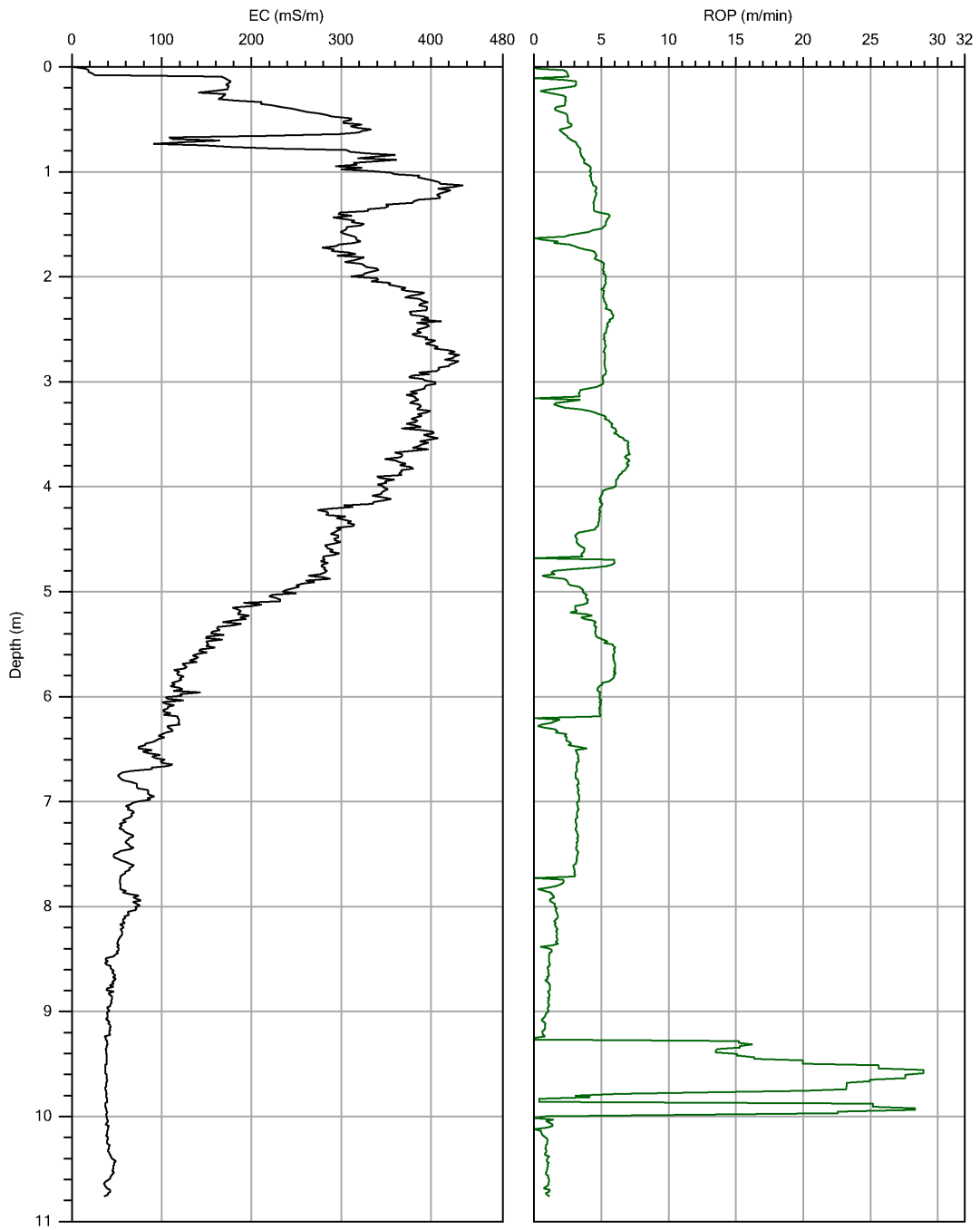
APPENDIX B  
DIRECT-PUSH EC LOGS

**Table B1:** Direct-push EC log identification.

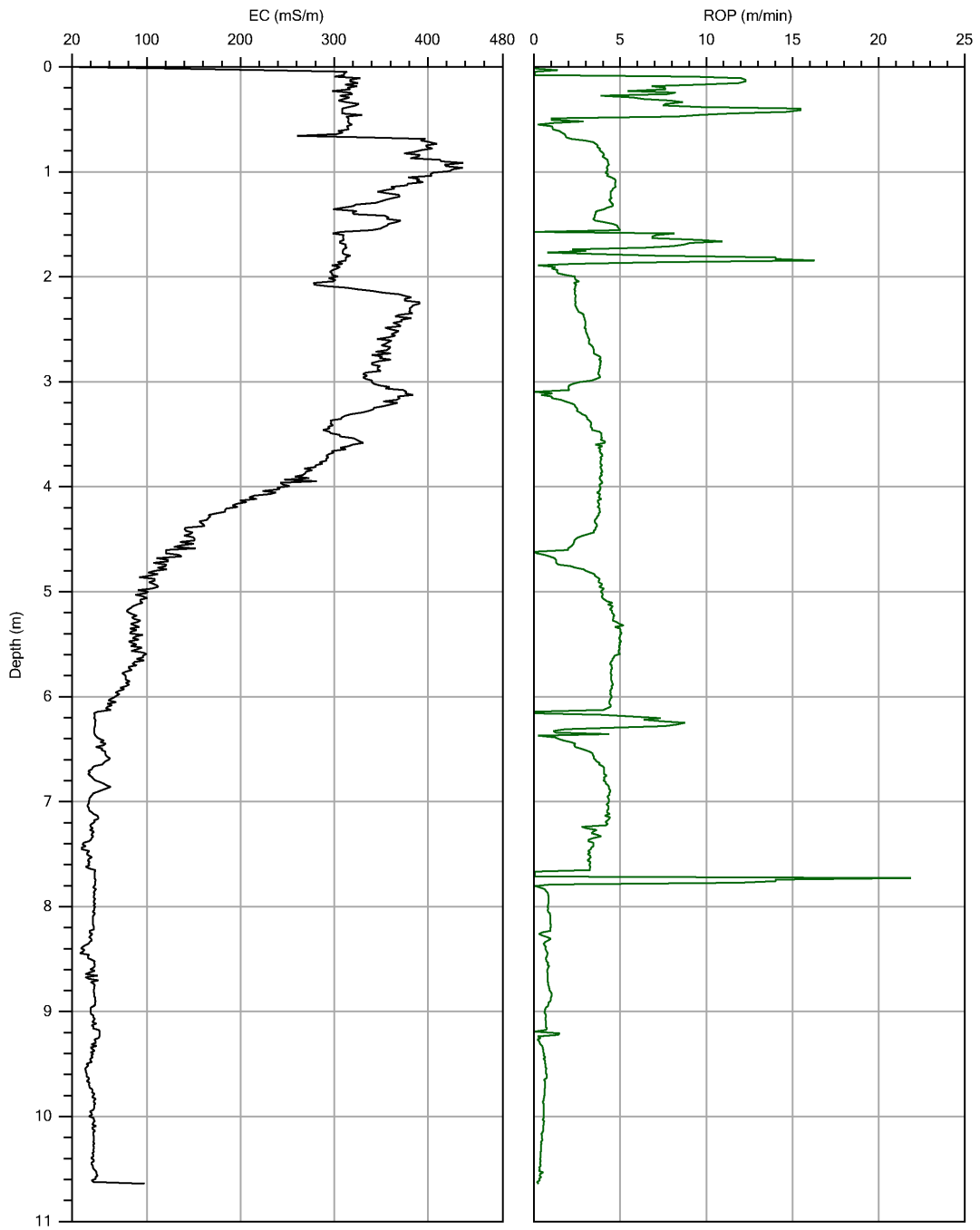
Revised log name on Figure 2a	Adjacent corehole name	Appendix B log filename
EC1	BH1	EC06-2
EC2	BH2	EC02
EC3	BH3	EC04
EC4	BH4	EC07
EC5	BH5	EC09
EC6	BH6	EC10
EC7	BH7	EC12
EC8	BH8	EC-13
EC9	BH9	EC-15-2
EC10	BH10	EC-17
EC11	BH11	EC-24
EC12	BH12	EC-26
EC13	BH13	EC-28
EC14	BH14	EC-30
EC15	BH15	EC-23
EC16	BH16	EC-21
EC17	BH17	EC-19
EC18	BH18	EC-18
EC19	BH19	EC-36
EC20	BH20	EC-38
EC21	BH21	EC-39
EC22	BH22	EC-41
EC23	none	EC-01-2
EC24	none	EC03
EC25	none	EC05
EC26	none	EC08
EC27	none	EC11
EC28	none	EC14
EC29	none	EC-31
EC30	none	EC-32
EC31	none	EC-44
EC32	none	EC-33
EC33	2010-03A/B	EC-34



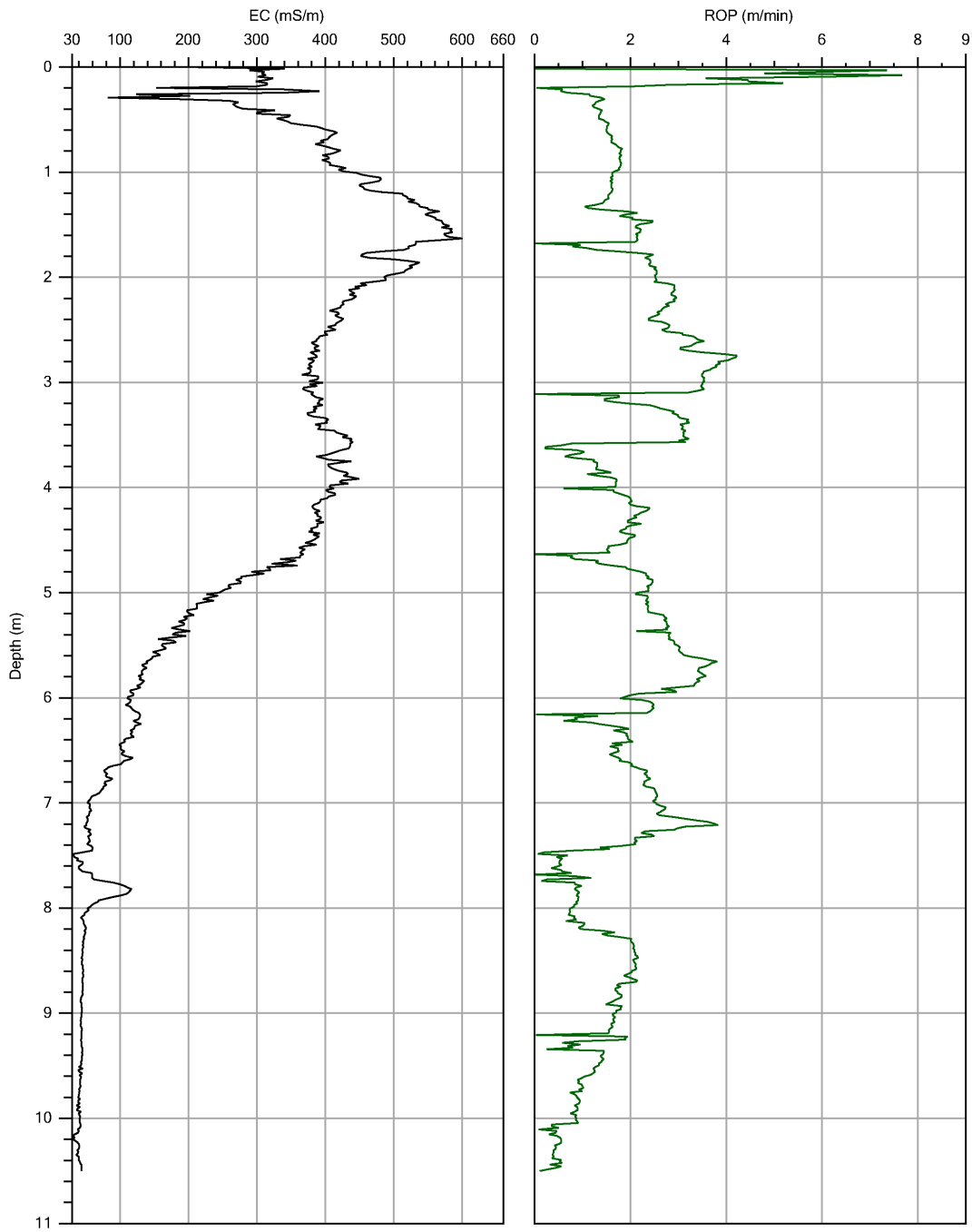
Company:	Intercore	Operator:	Deter	File:	EC06-2.EC
Project ID:	KJH study site	Client:	U of S	Date:	15/08/2011
				Location:	



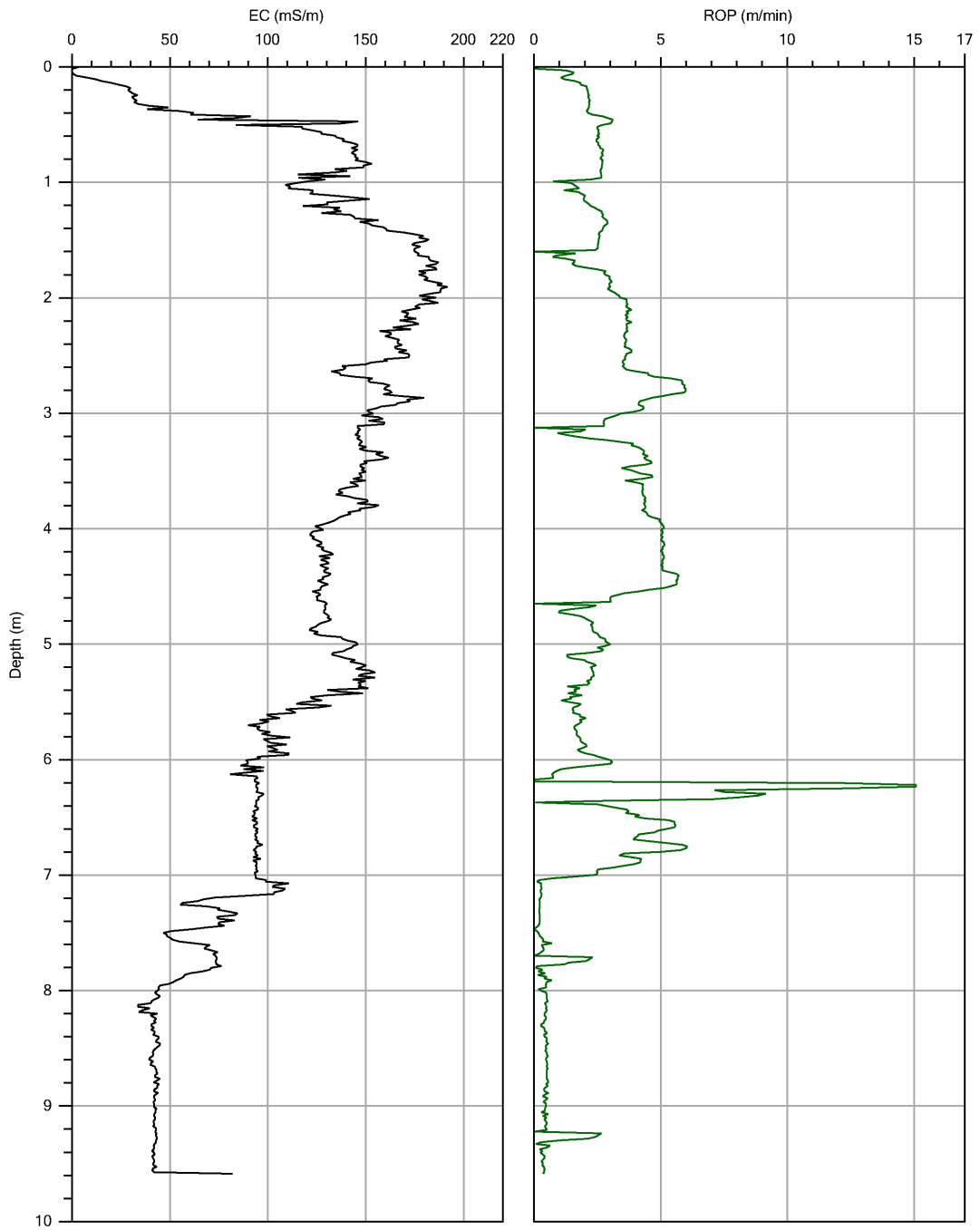
Company:	Intercore	Operator:	Deter	File:	EC02.EC
Project ID:	KJH study site	Client:	U of S	Date:	15/08/2011
				Location:	



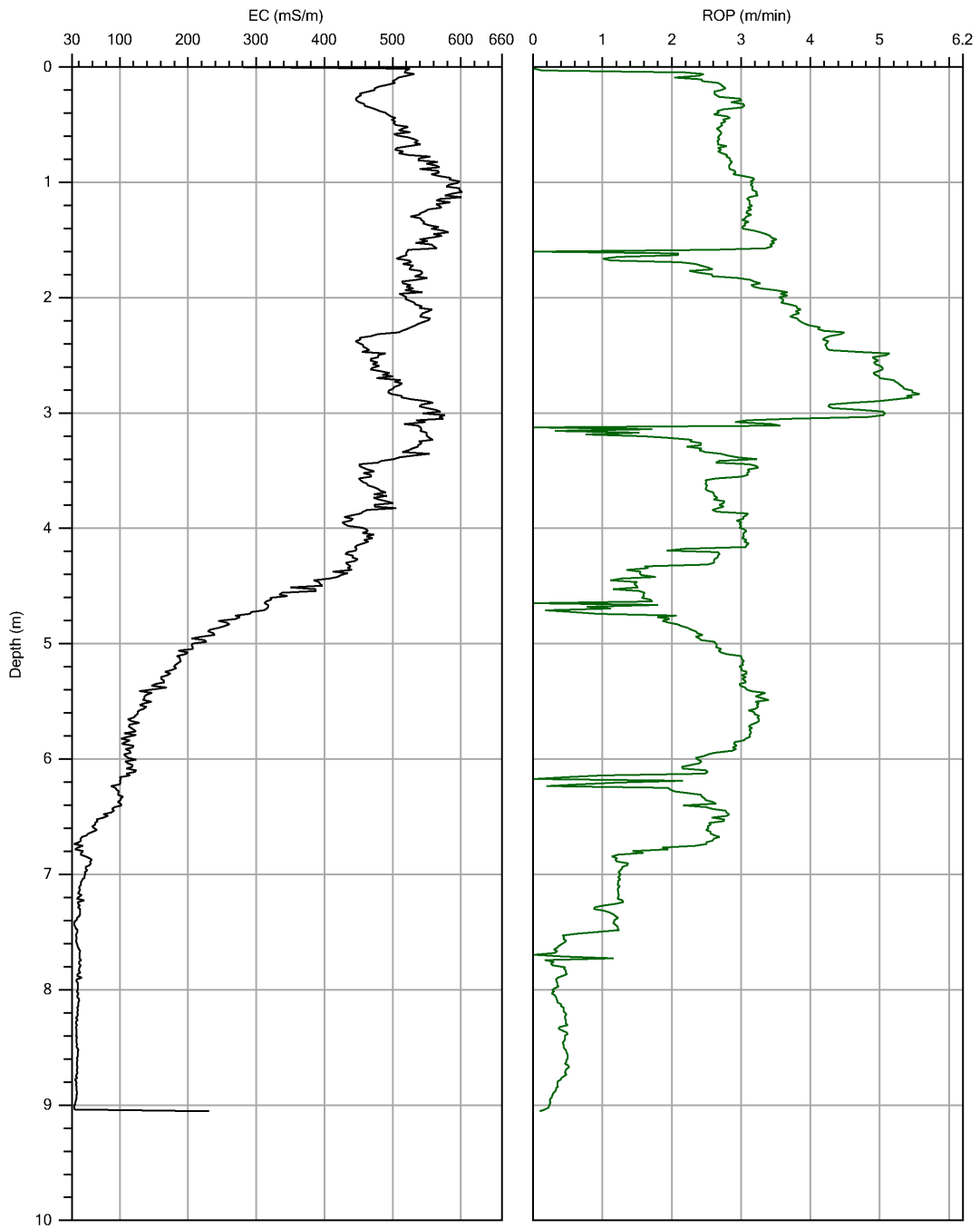
Company:	Intecore	Operator:	Deter	File:	EC04.EC
Project ID:	KJH study site	Client:	U of S	Date:	15/08/2011
				Location:	



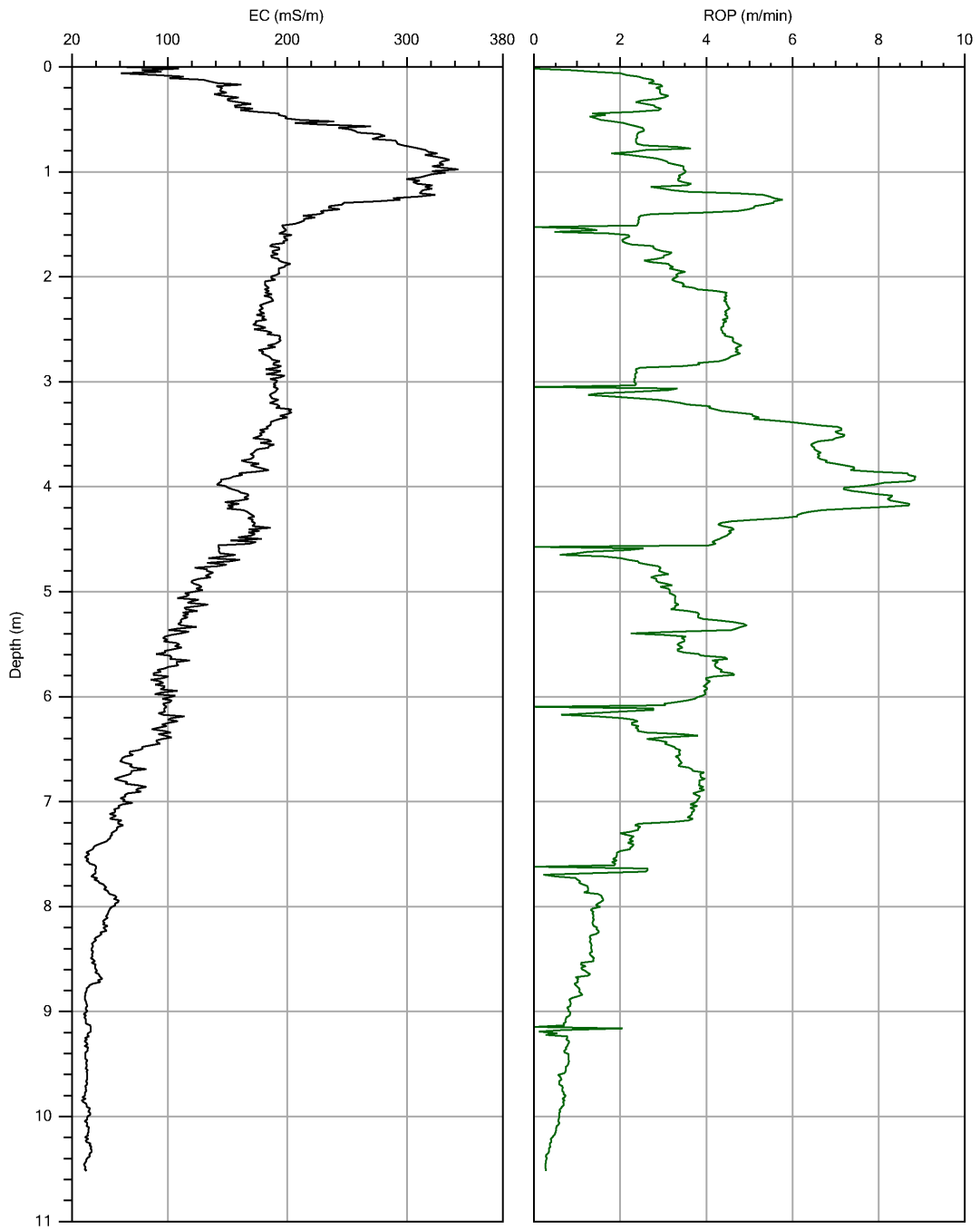
Company:	Intecore	Operator:	Deter	File:	EC07.EC
Project ID:	KJH study site	Client:	U of S	Date:	16/08/2011
				Location:	



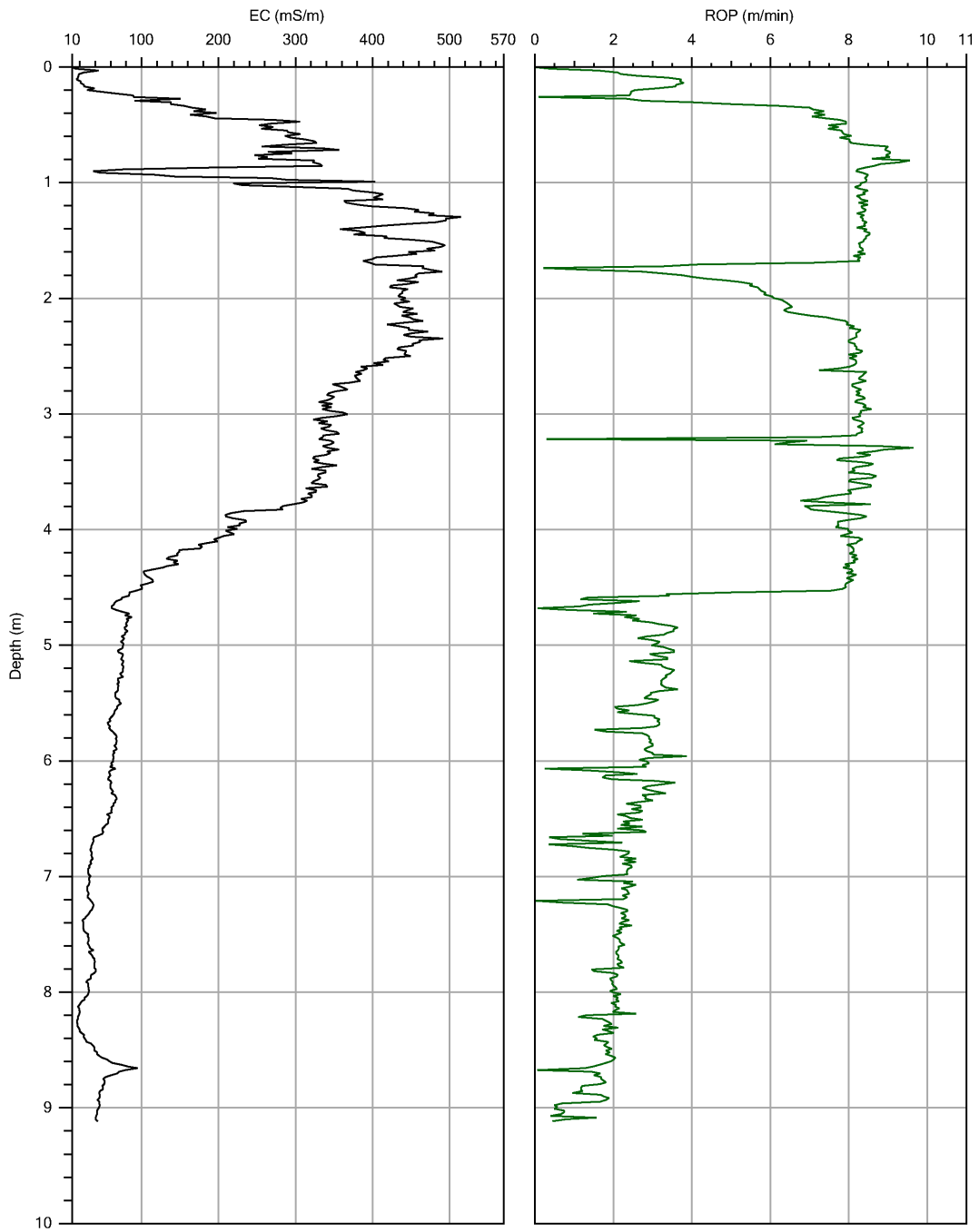
Company:	Intercore	Operator:	Deter	File:	EC09.EC
Project ID:	KJH study site	Client:	U of S	Date:	16/08/2011
				Location:	



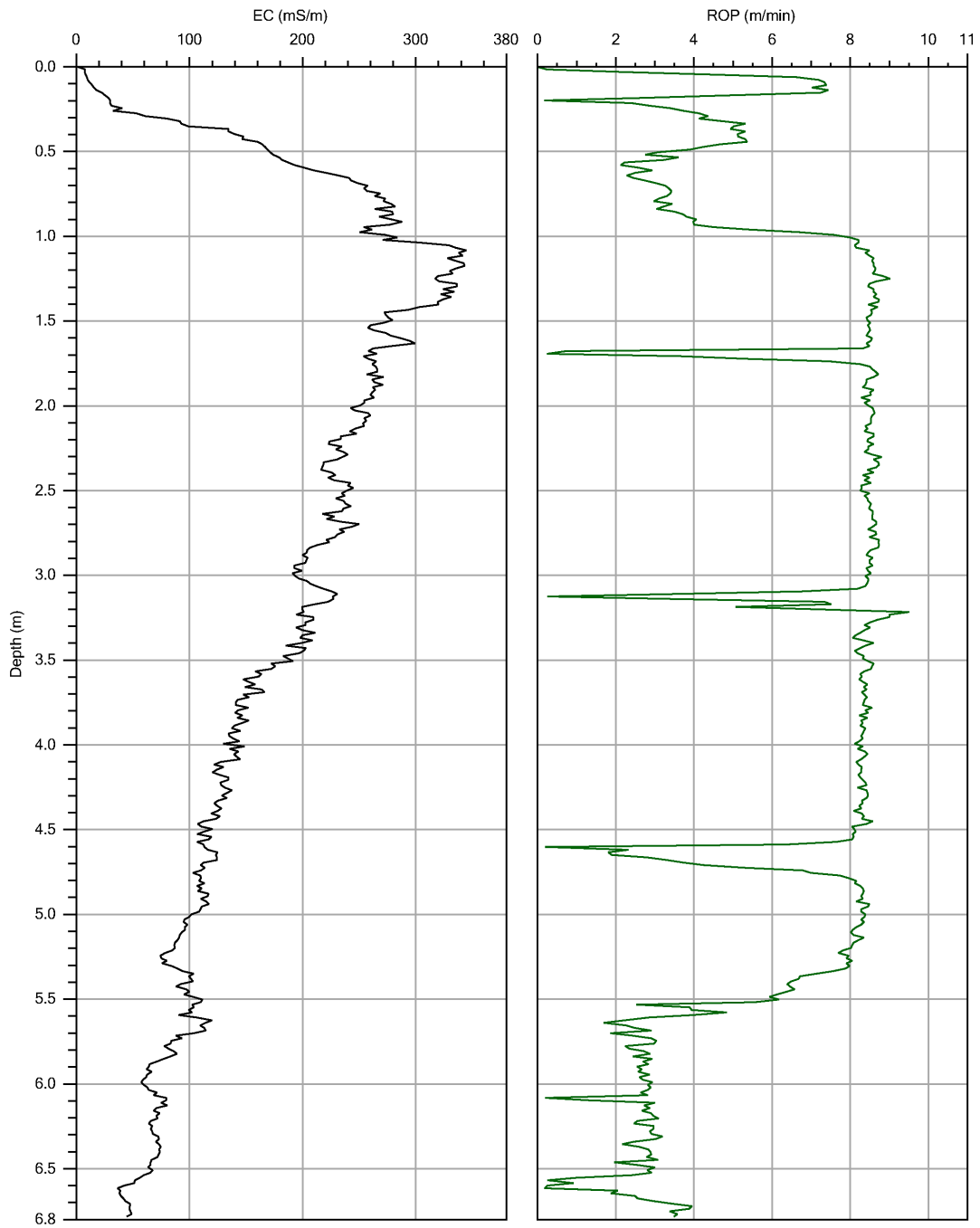
Company:	Intercore	Operator:	Deter	File:	EC10.EC
Project ID:	KJH study site	Client:	U of S	Date:	16/08/2011
				Location:	



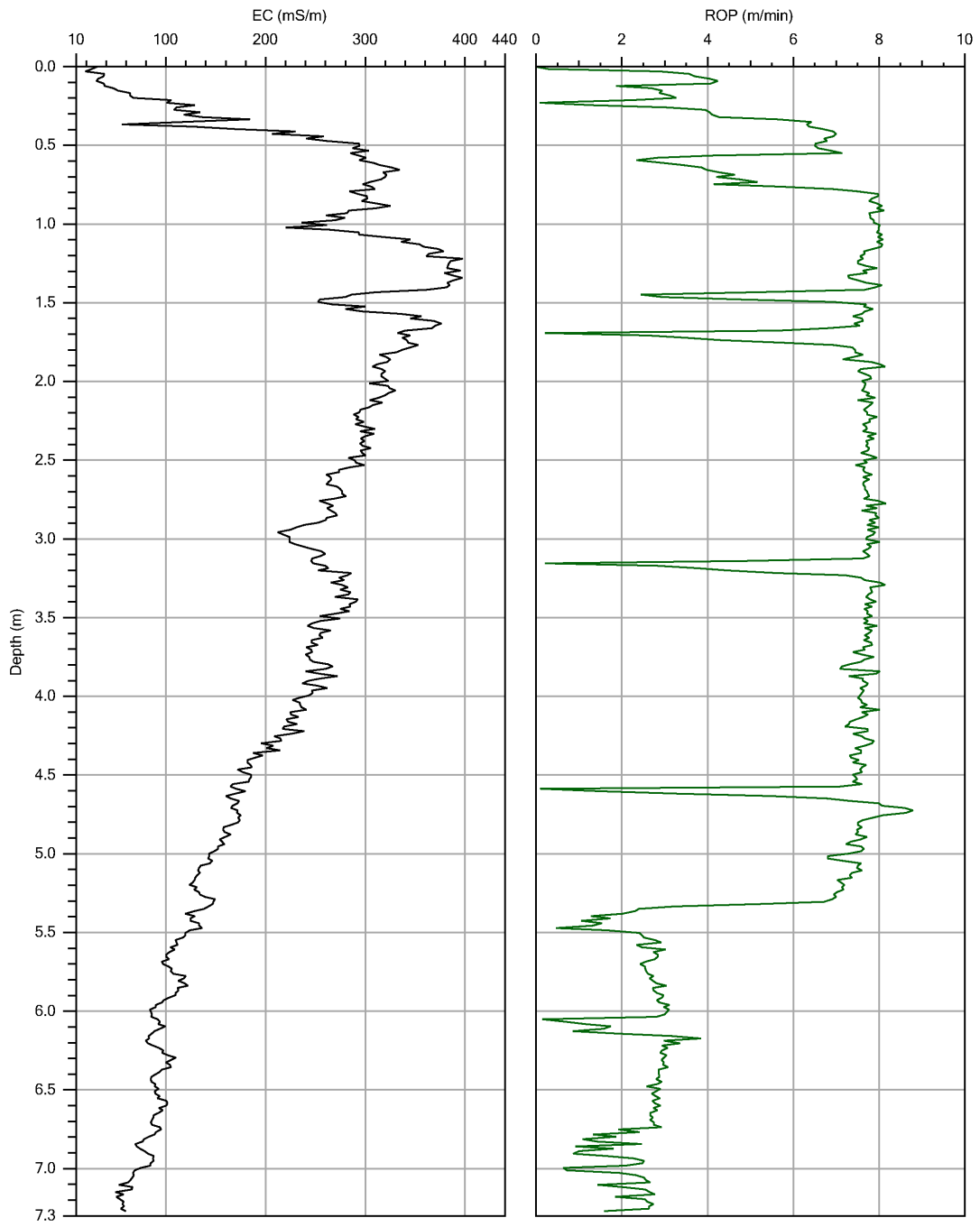
Company:	Intercore	Operator:	Deter	File:	EC12.EC
Project ID:	KJH study site	Client:	U of S	Date:	17/08/2011
				Location:	



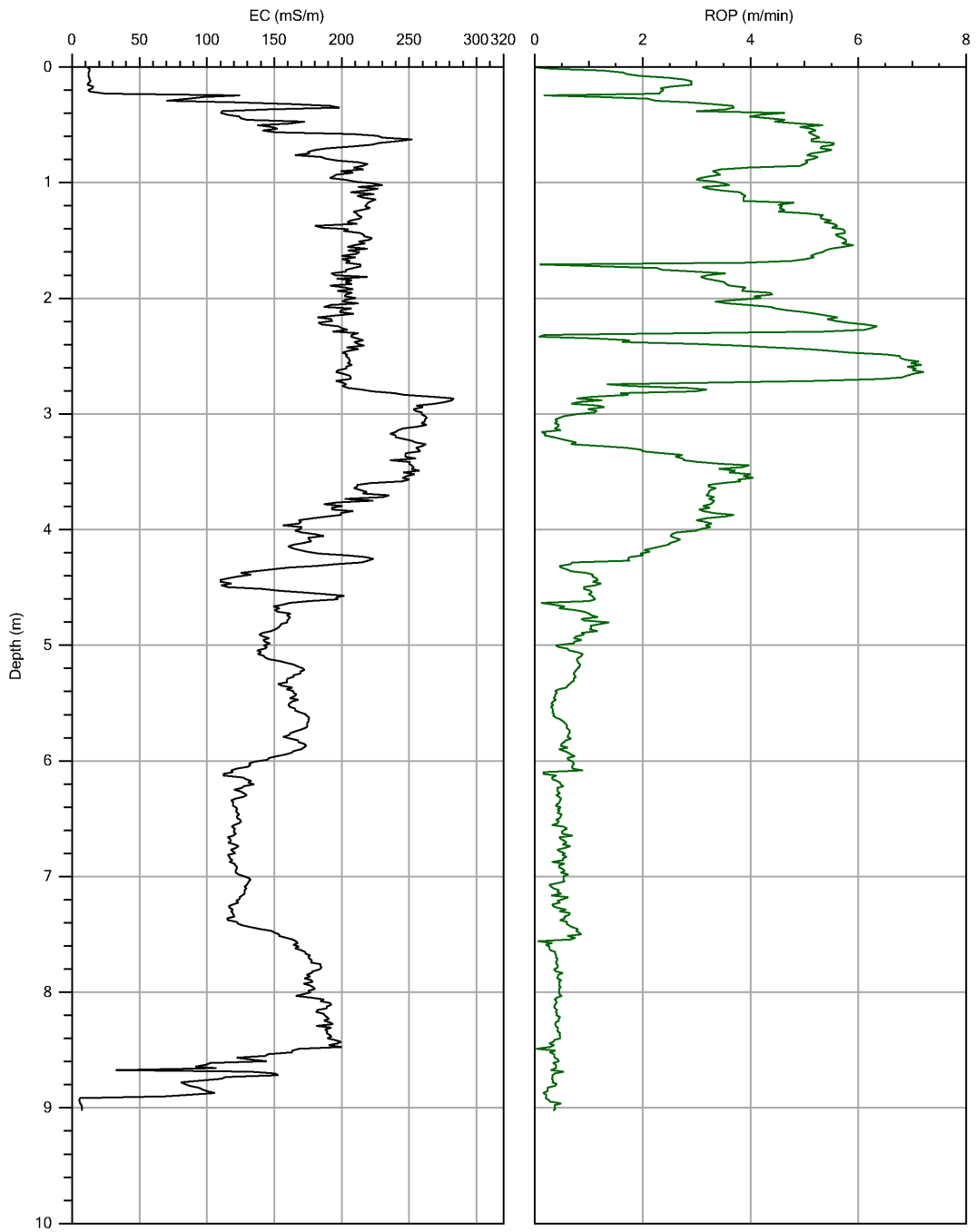
Company:	Intercore	Operator:	Deter	File:	EC-13.EC
Project ID:	KJH study site	Client:	U of S	Date:	10/10/2012
				Location:	



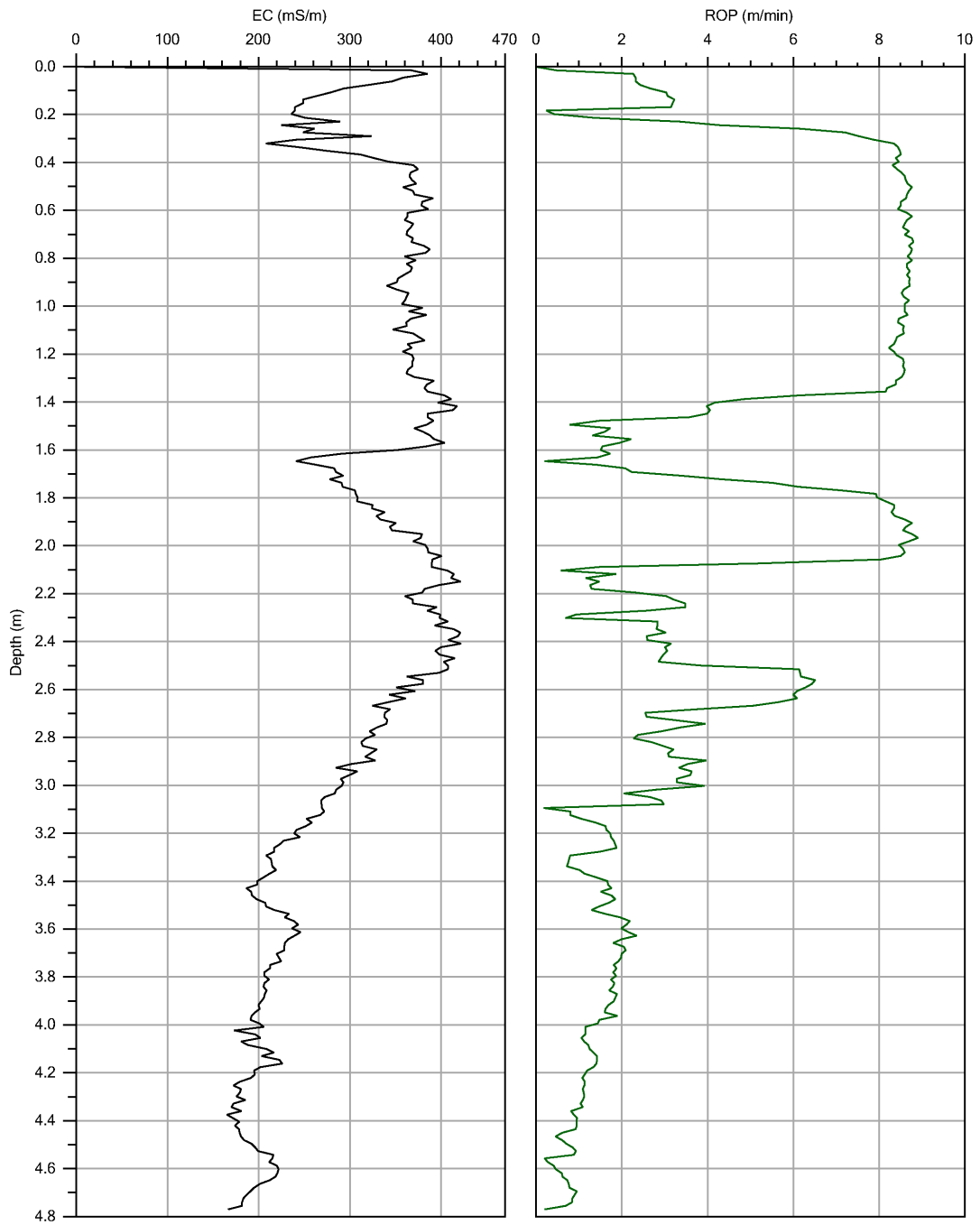
Company:	Intercore	Operator:	Deter	File:	EC-15-2.EC
Project ID:	KJH study site	Client:	U of S	Date:	10/10/2012
				Location:	



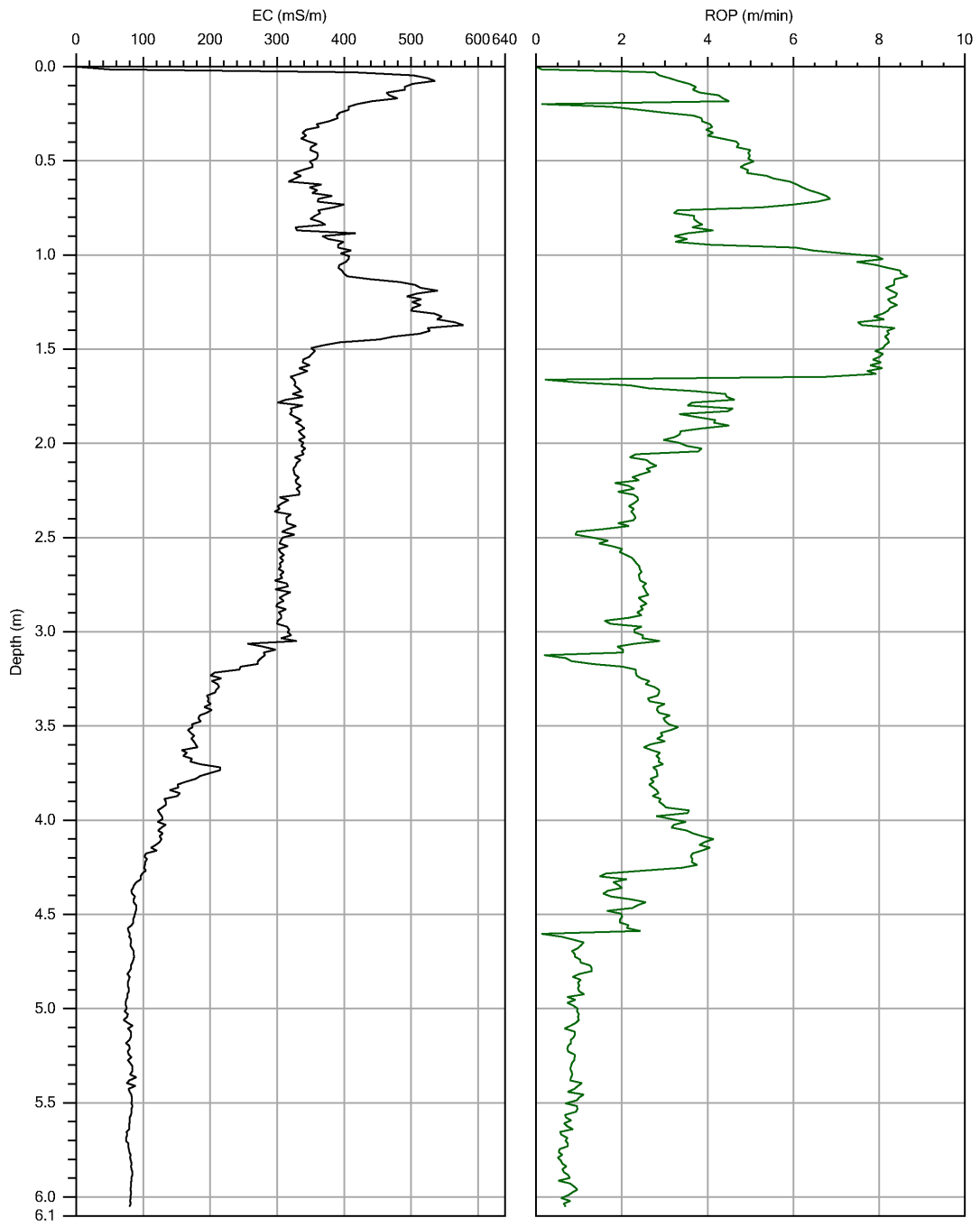
Company:	Intercore	Operator:	Deter	File:	EC-17.EC
Project ID:	KJH study site	Client:	U of S	Date:	10/10/2012
				Location:	



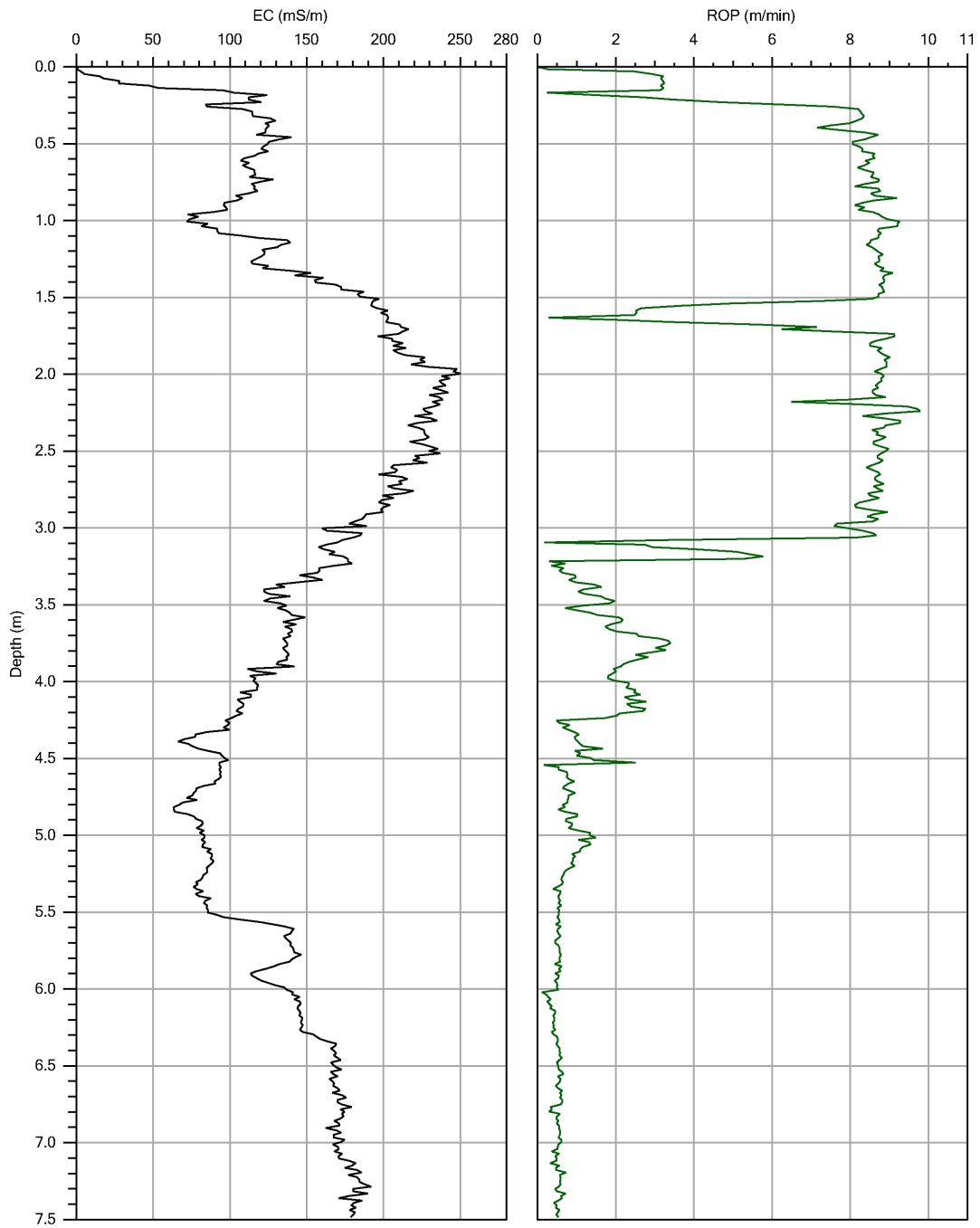
Company:	Intercore	Operator:	Deter	File:	EC-24.EC
Project ID:	KJH study site	Client:	U of S	Date:	11/10/2012
				Location:	



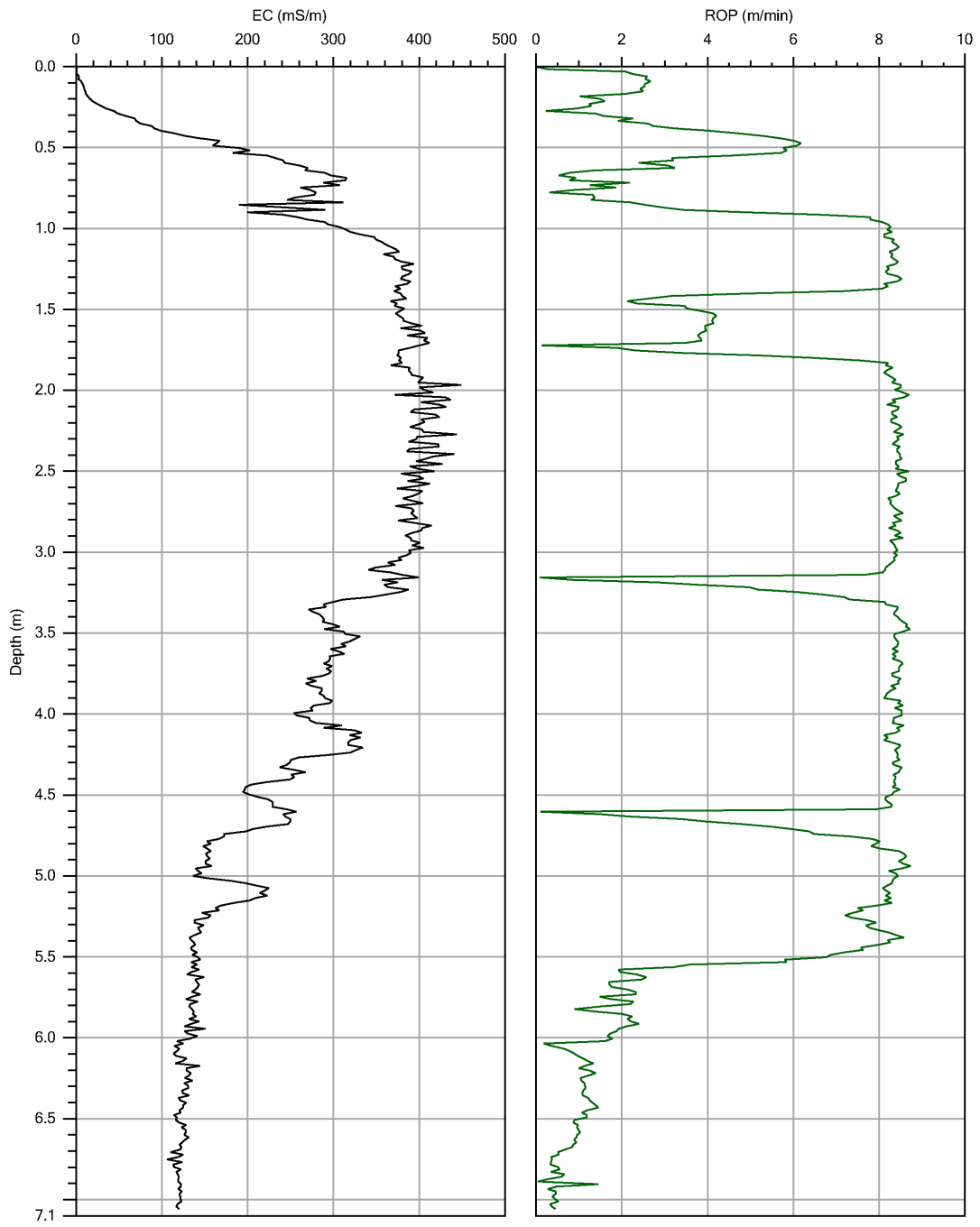
Company:	Intercore	Operator:	Deter	File:	EC-26.EC
Project ID:	KJH study site	Client:	U of S	Date:	11/10/2012
				Location:	



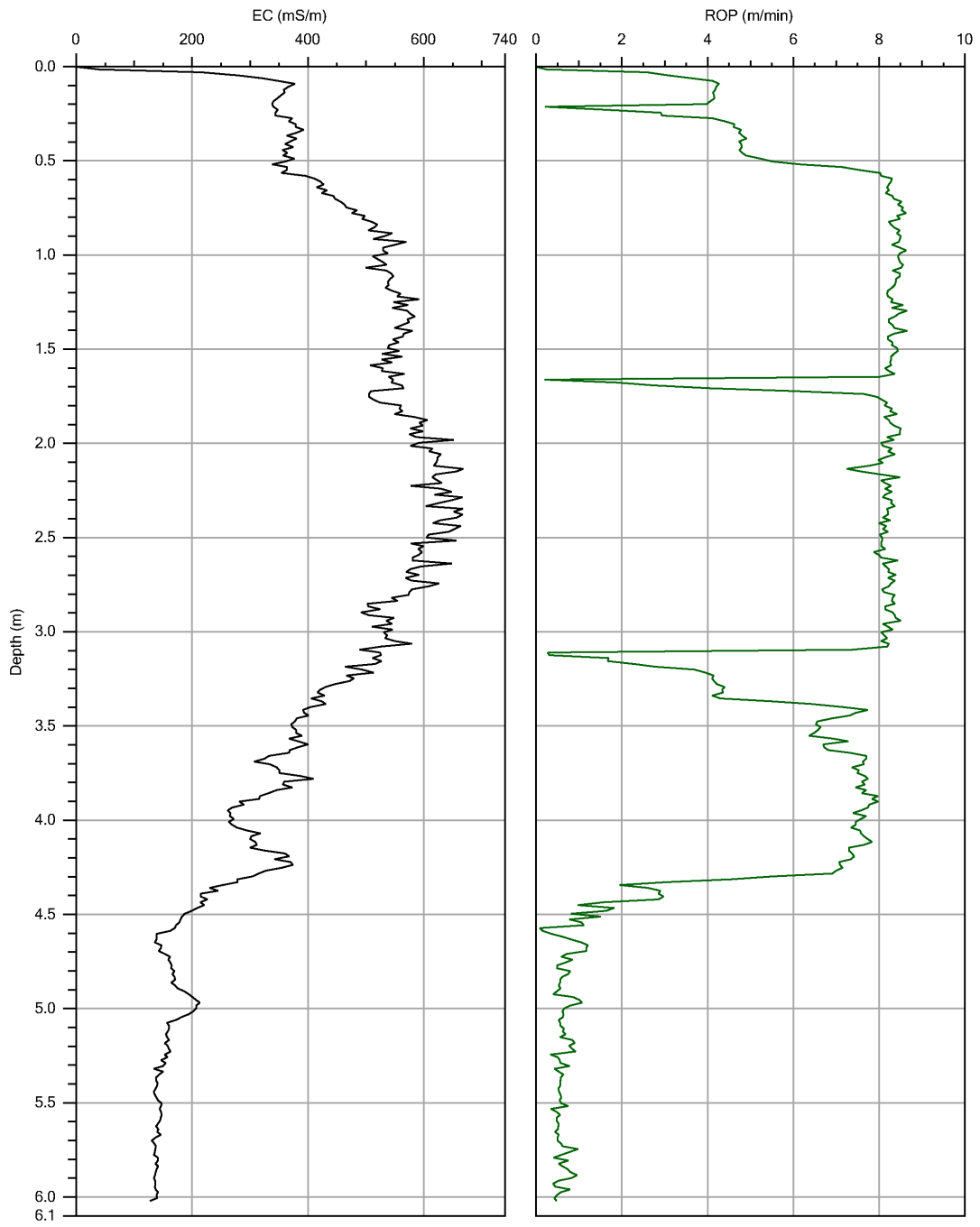
Company:	Intercore	Operator:	Deter	File:	EC-28.EC
Project ID:	KJH study site	Client:	U of S	Date:	11/10/2012
				Location:	



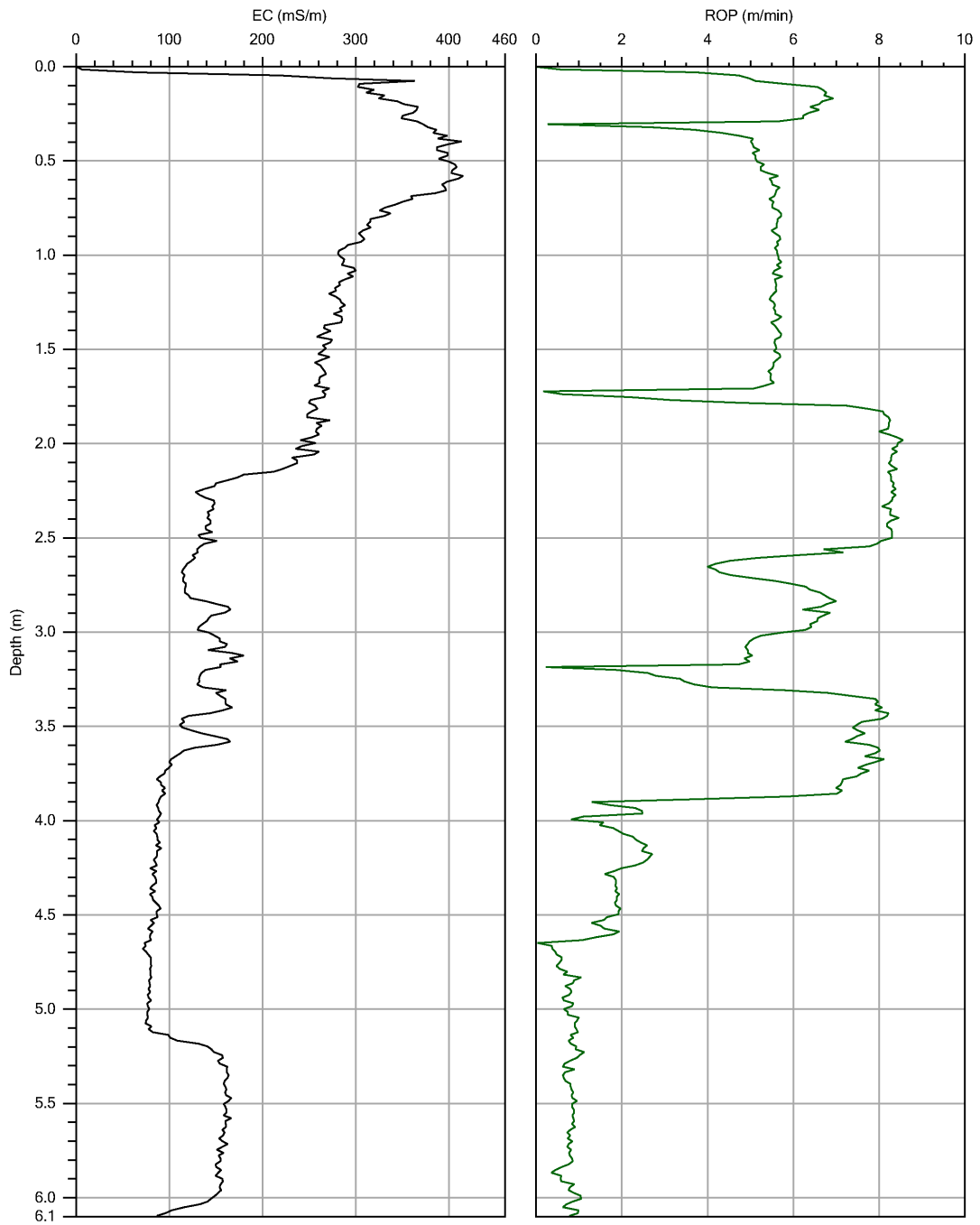
Company:	Intercore	Operator:	Deter	File:	EC-30.EC
Project ID:	KJH study site	Client:	U of S	Date:	11/10/2012
				Location:	



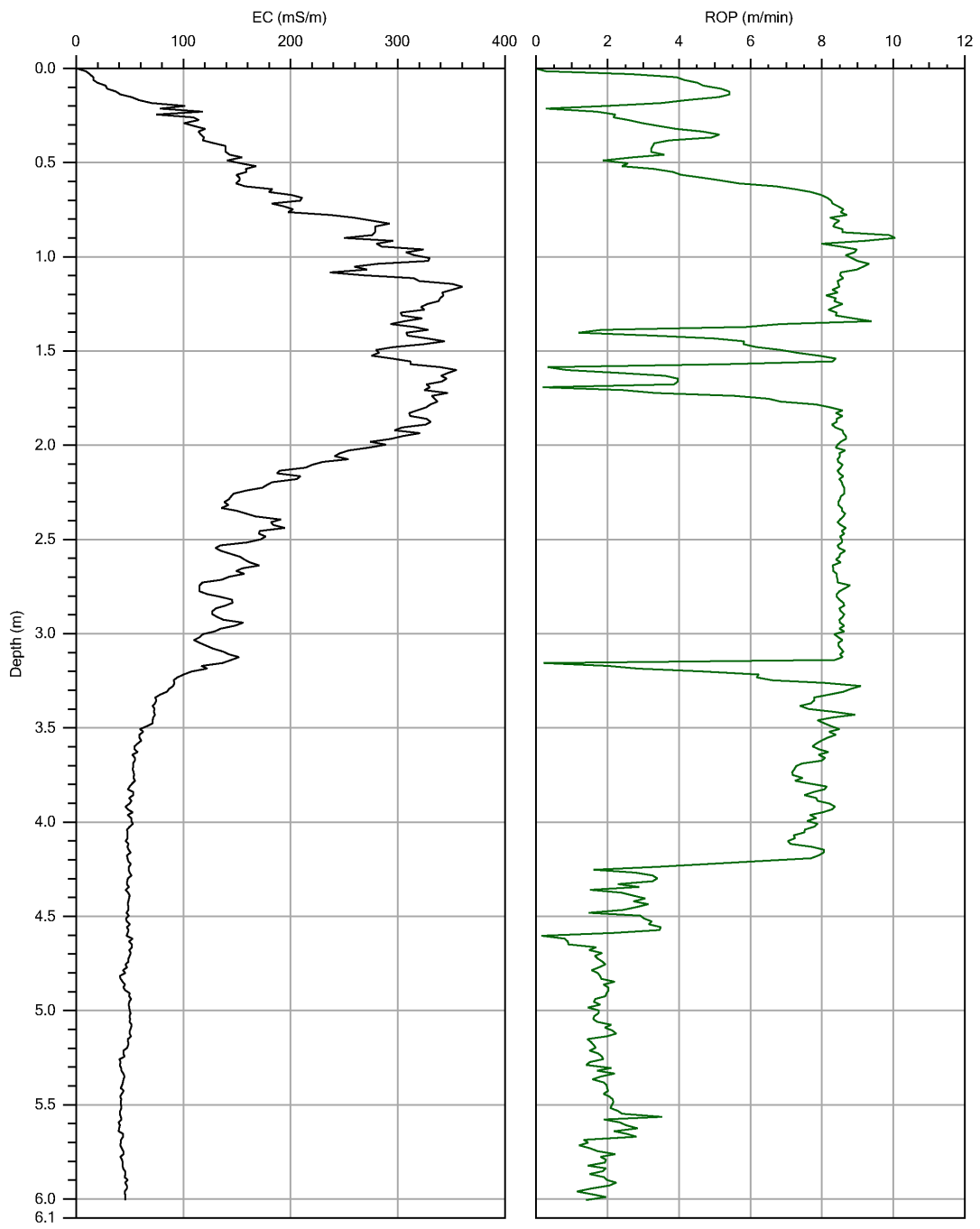
Company:	Intercore	Operator:	Deter	File:	EC-23.EC
Project ID:	KJH study site	Client:	U of S	Date:	11/10/2012
				Location:	



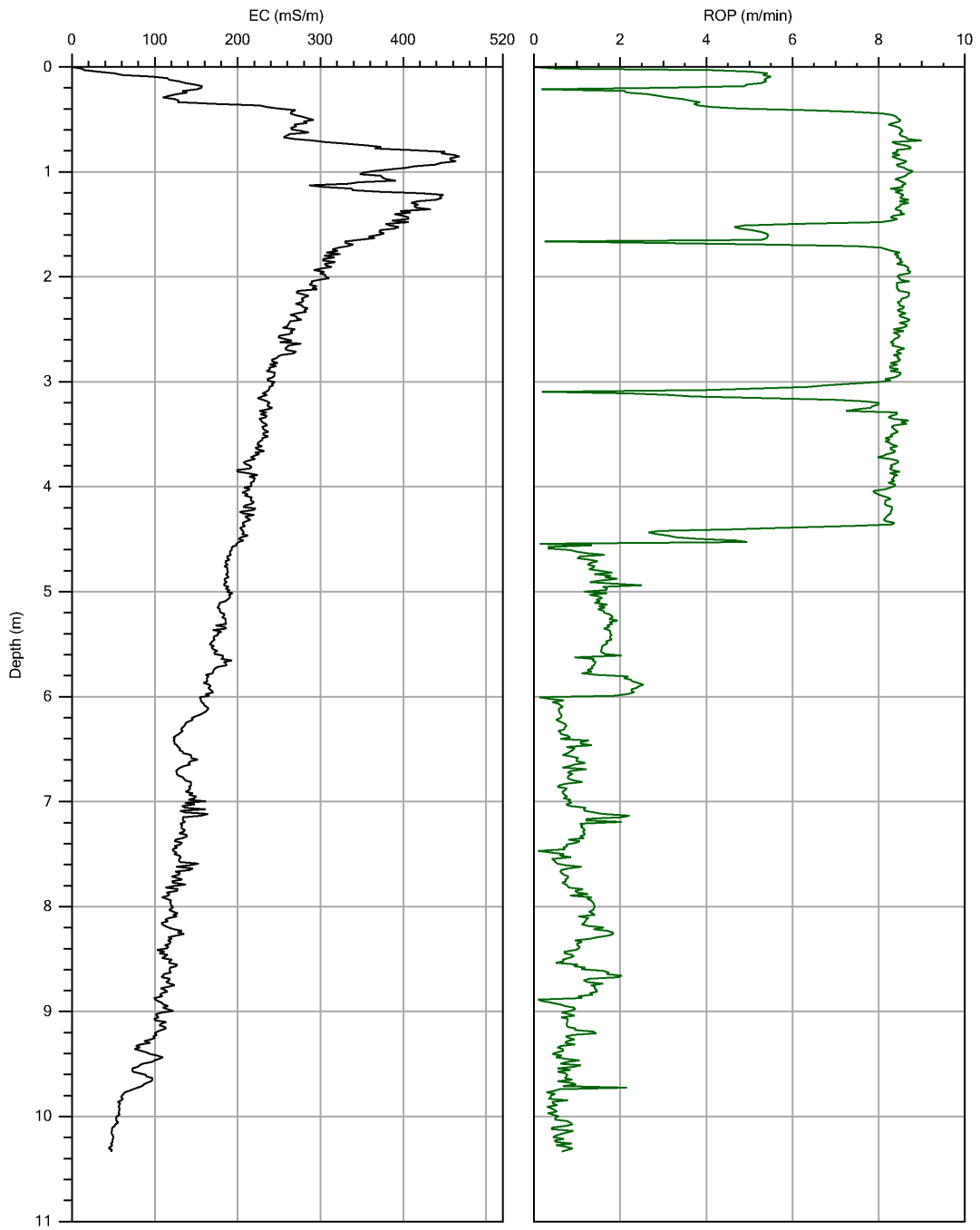
Company:	Intercore	Operator:	Deter	File:	EC-21.EC
Project ID:	KJH study site	Client:	U of S	Date:	11/10/2012
				Location:	



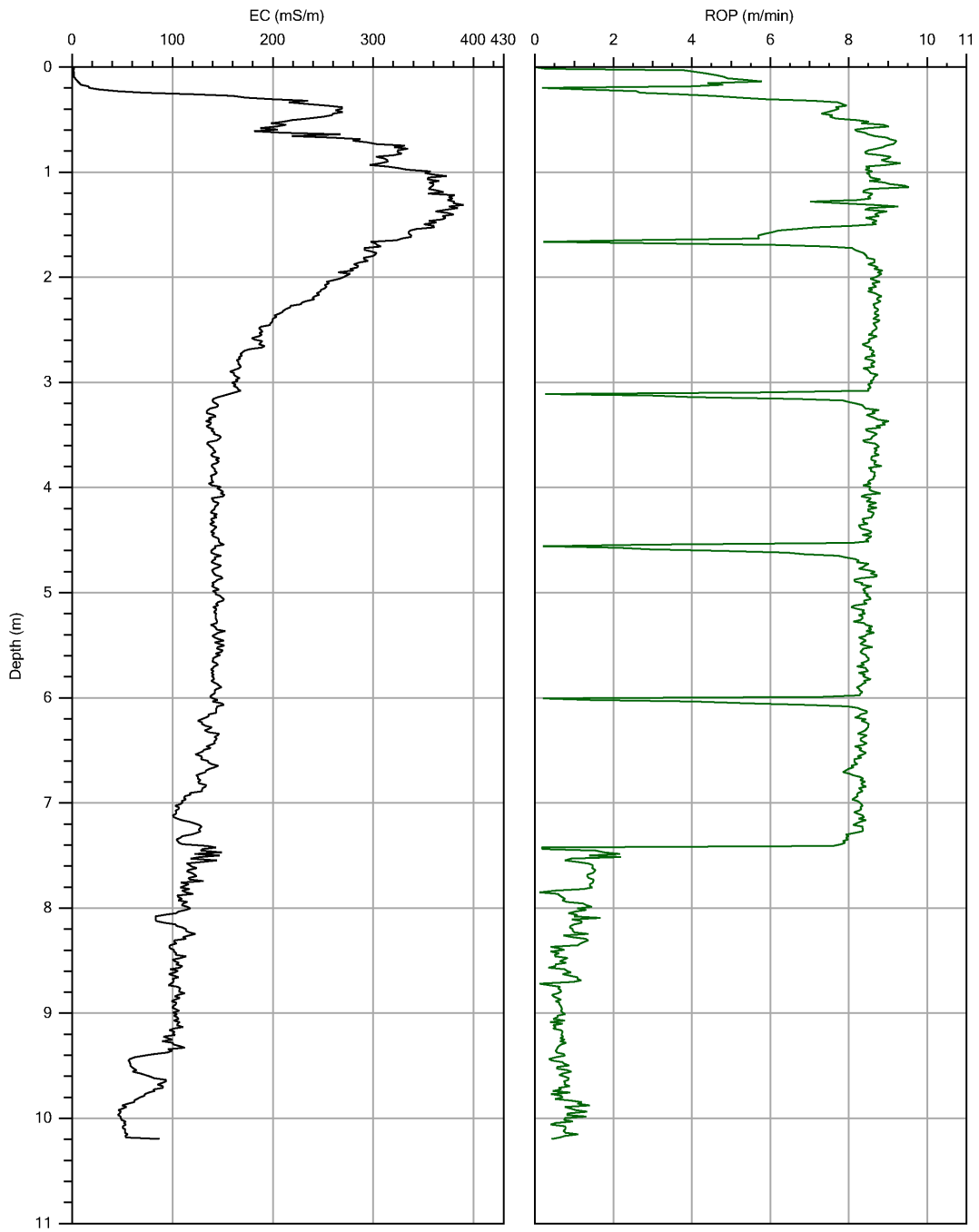
Company:	Intercore	Operator:	Deter	File:	EC-19.EC
Project ID:	KJH study site	Client:	U of S	Date:	11/10/2012
				Location:	



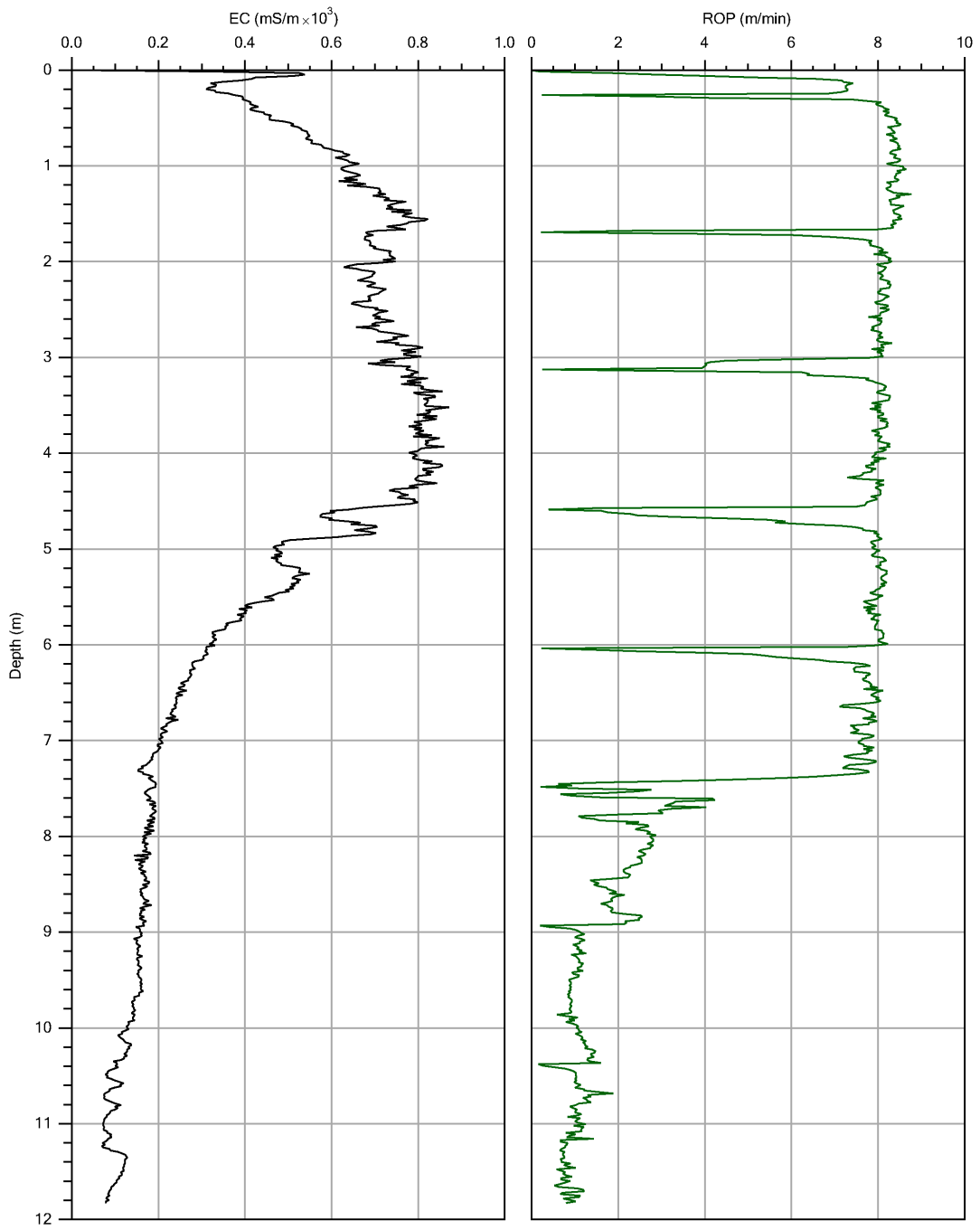
Company:	Intercore	Operator:	Deter	File:	EC-18.EC
Project ID:	KJH study site	Client:	U of S	Date:	11/10/2012
				Location:	



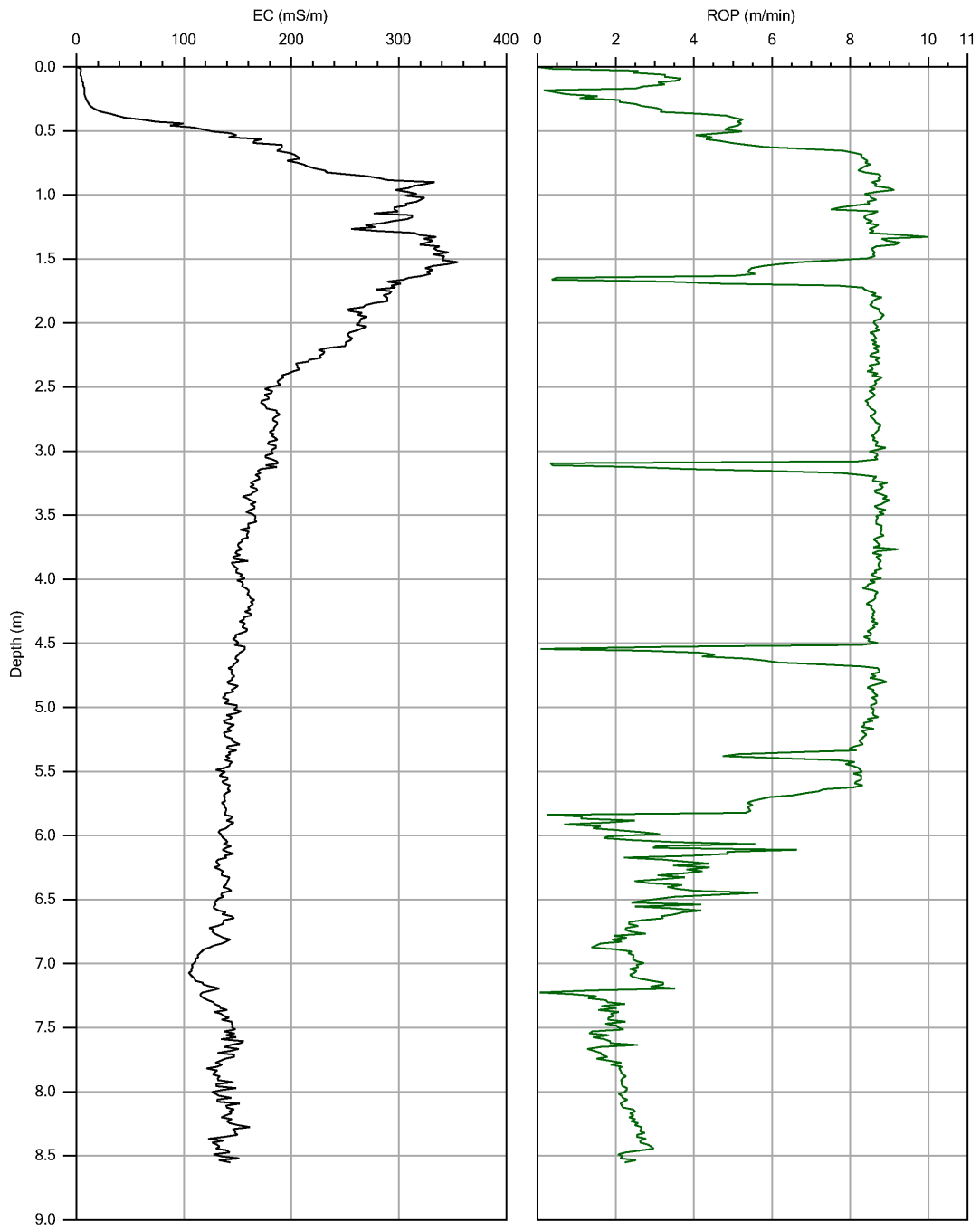
Company:	Intercore	Operator:	Deter	File:	EC-36.EC
Project ID:	KJH study site	Client:	U of S	Date:	11/10/2012
				Location:	



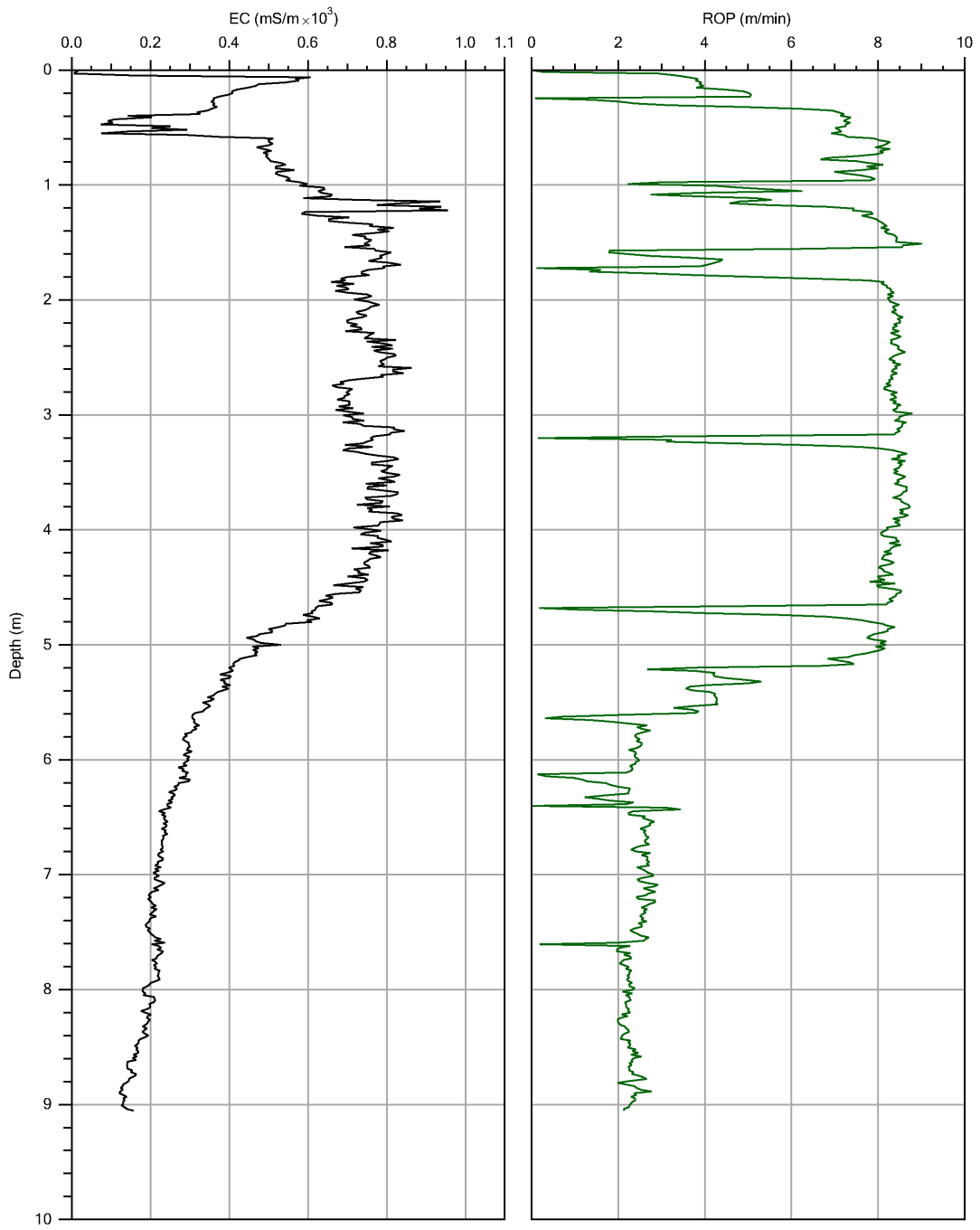
Company:	Intercore	Operator:	Deter	File:	EC-38.EC
Project ID:	KJH study site	Client:	U of S	Date:	11/10/2012
				Location:	



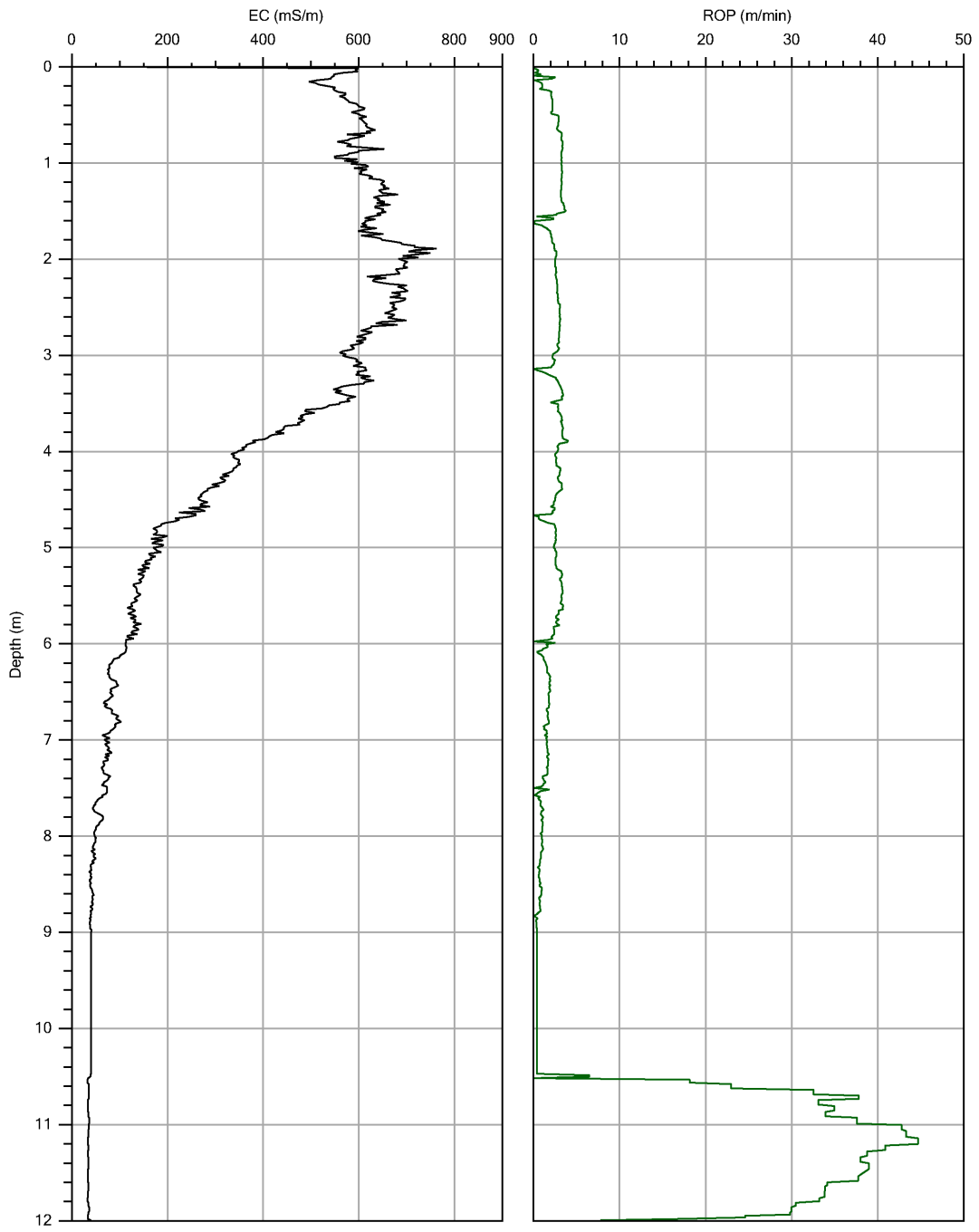
Company:	Intercore	Operator:	Deter	File:	EC-39.EC
Project ID:	KJH study site	Client:	U of S	Date:	11/10/2012
				Location:	



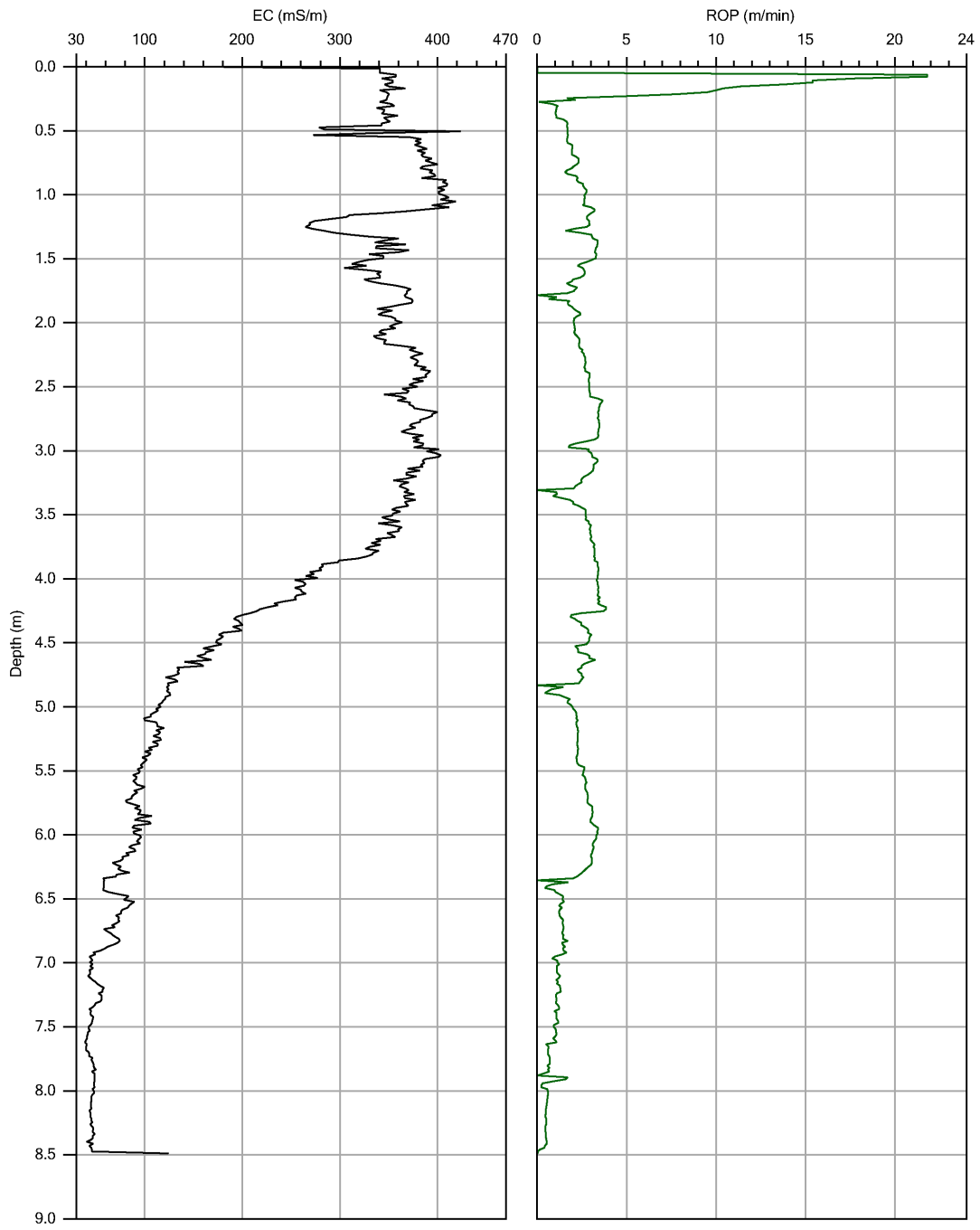
Company:	Intercore	Operator:	Deter	File:	EC-41.EC
Project ID:	KJH study site	Client:	U of S	Date:	11/10/2012
				Location:	



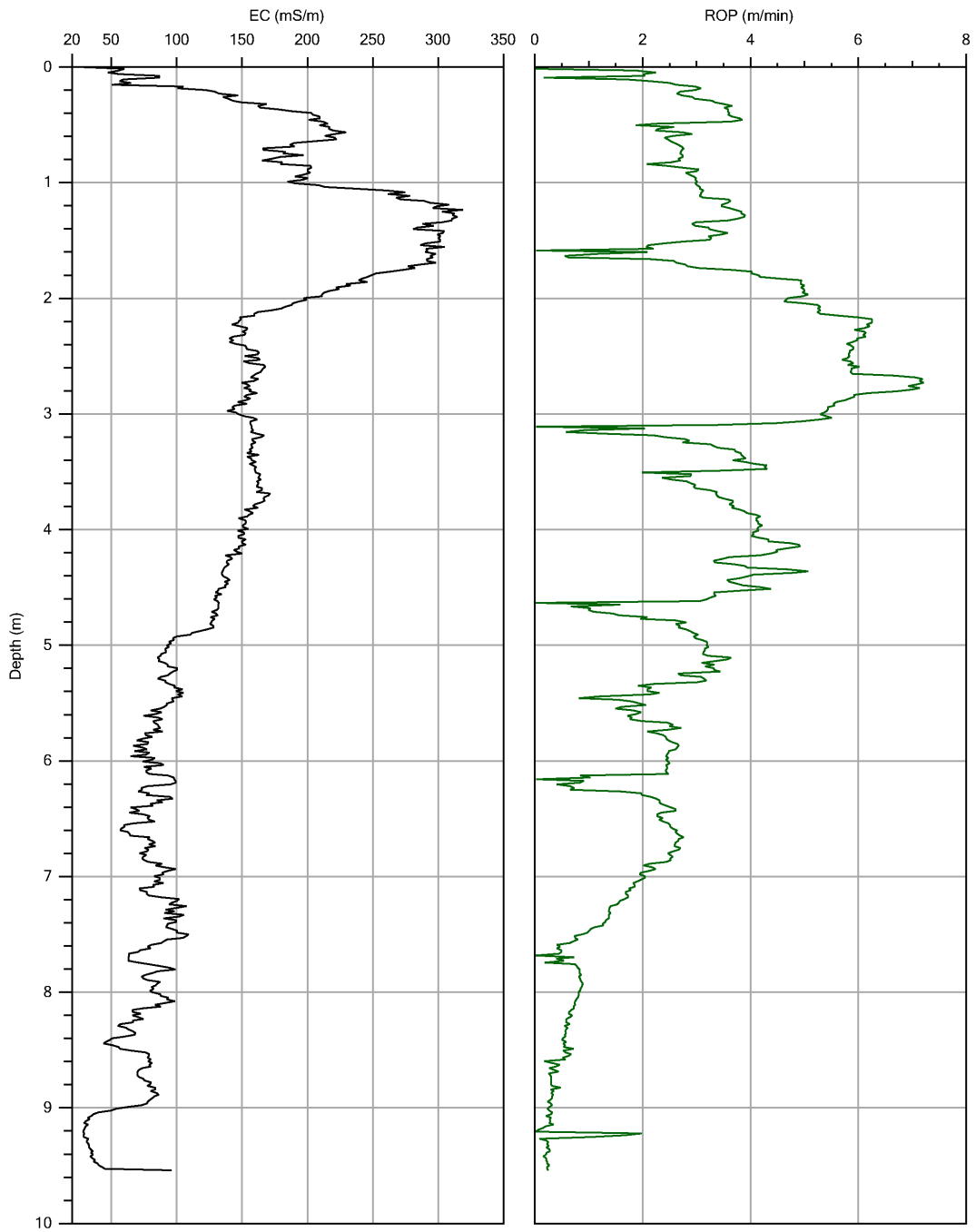
Company:	Intercore	Operator:	Deter	File:	EC-01-2.EC
Project ID:	KJH study site	Client:	U of S	Date:	10/10/2012
				Location:	



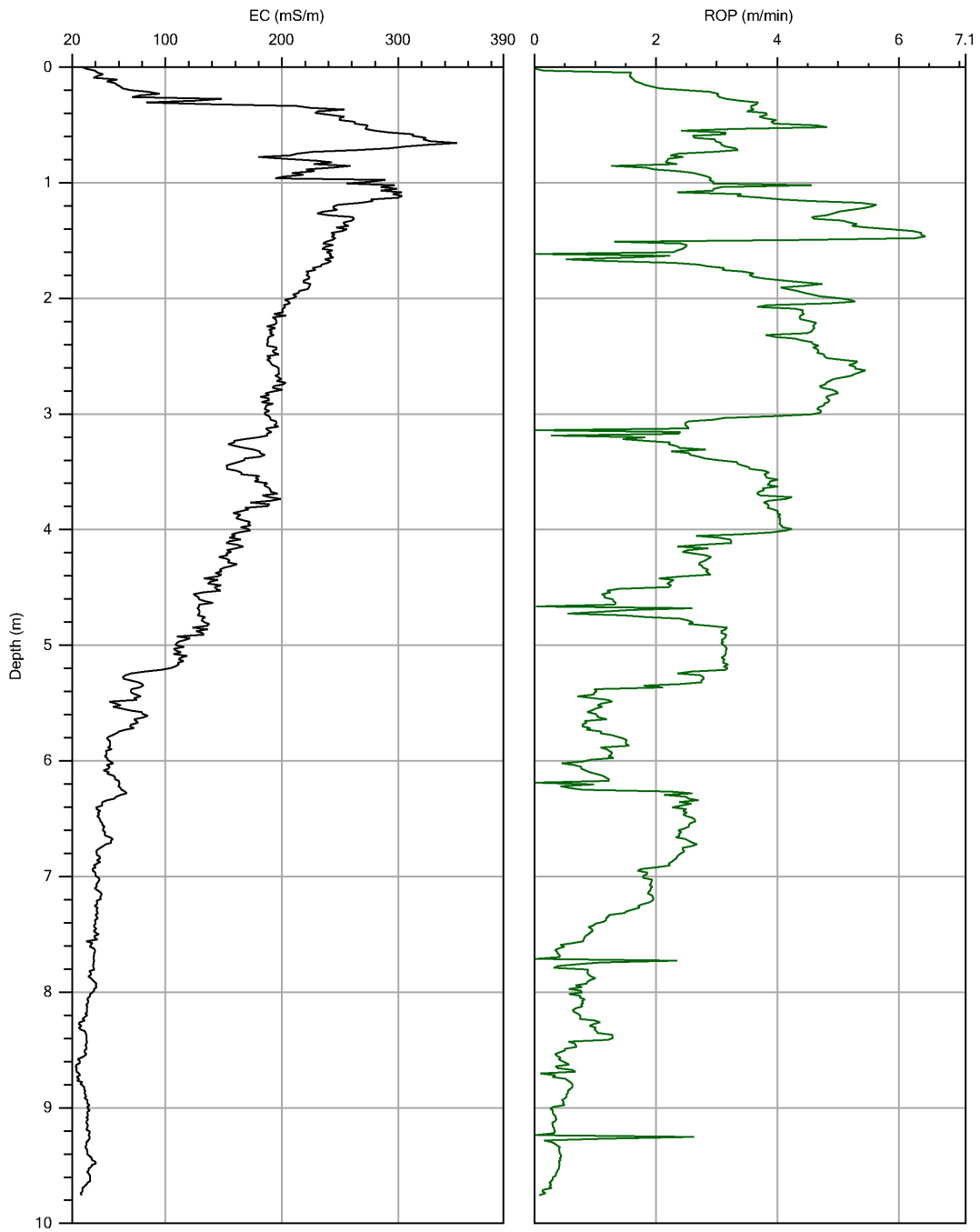
Company:	Intercore	Operator:	Deter	File:	EC03.EC
Project ID:	KJH study site	Client:	U of S	Date:	15/08/2011
				Location:	



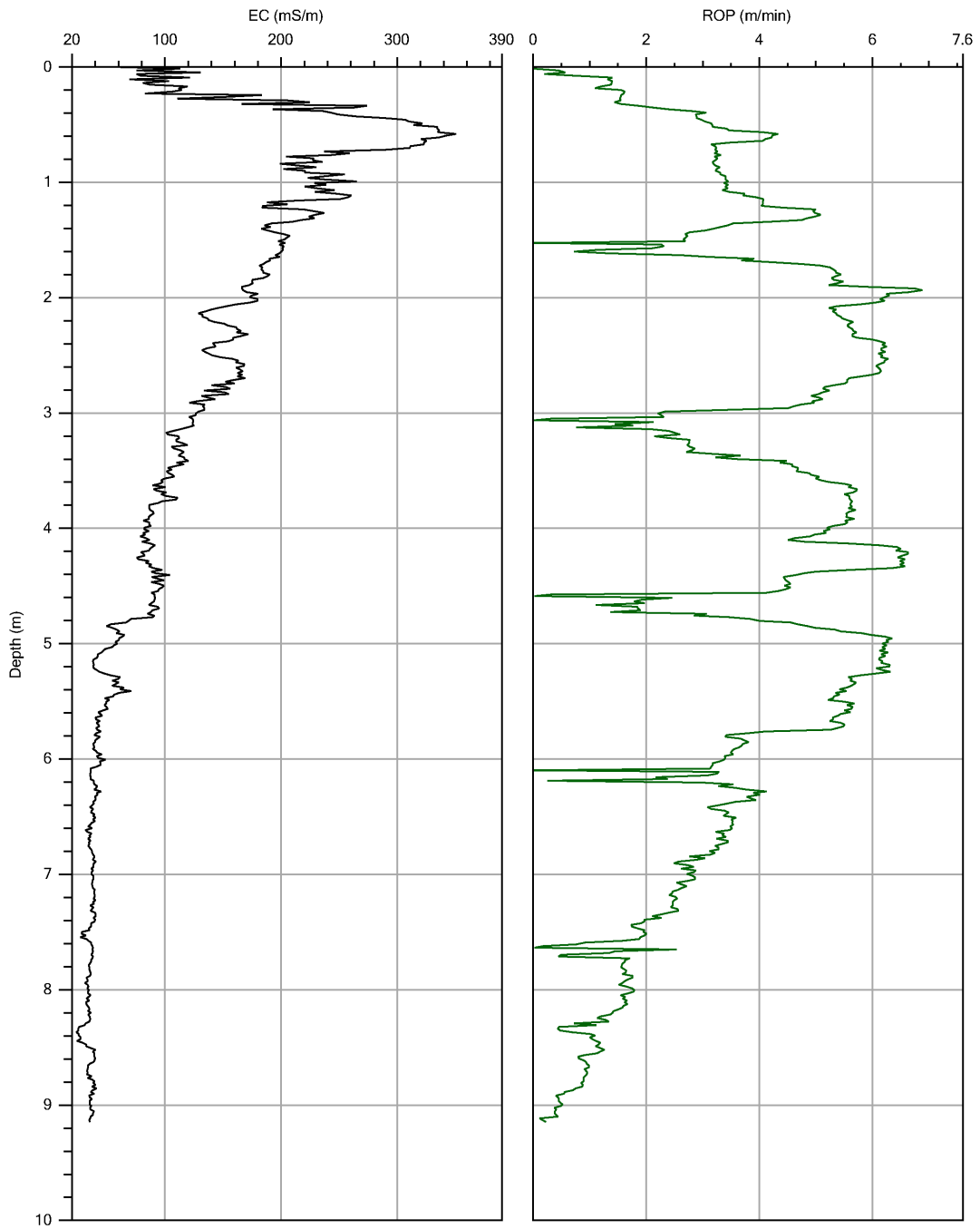
Company:	Intercore	Operator:	Deter	File:	EC05.EC
Project ID:	KJH study site	Client:	U of S	Date:	15/08/2011
				Location:	



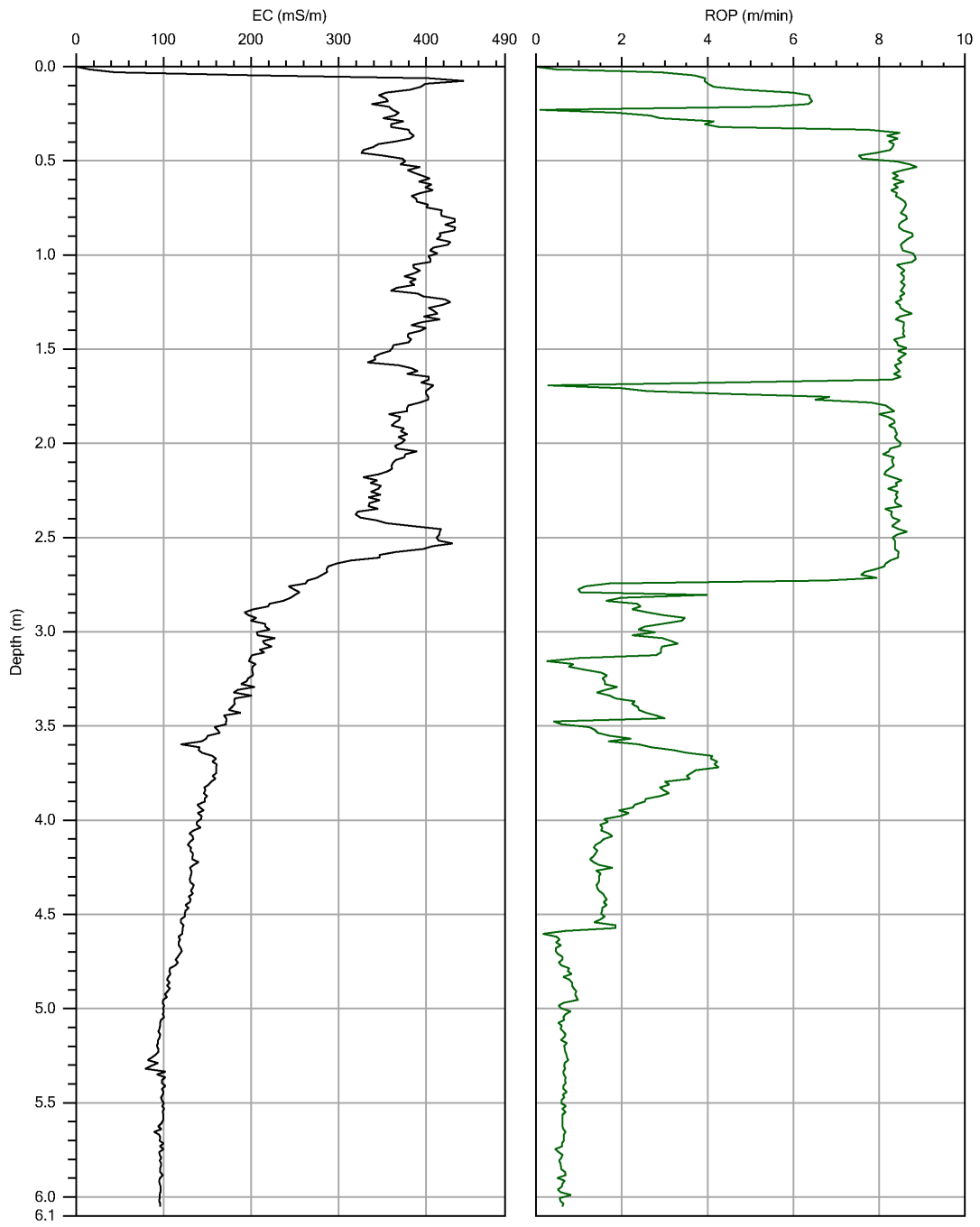
Company:	Intercore	Operator:	Deter	File:	EC08.EC
Project ID:	KJH study site	Client:	U of S	Date:	16/08/2011
				Location:	



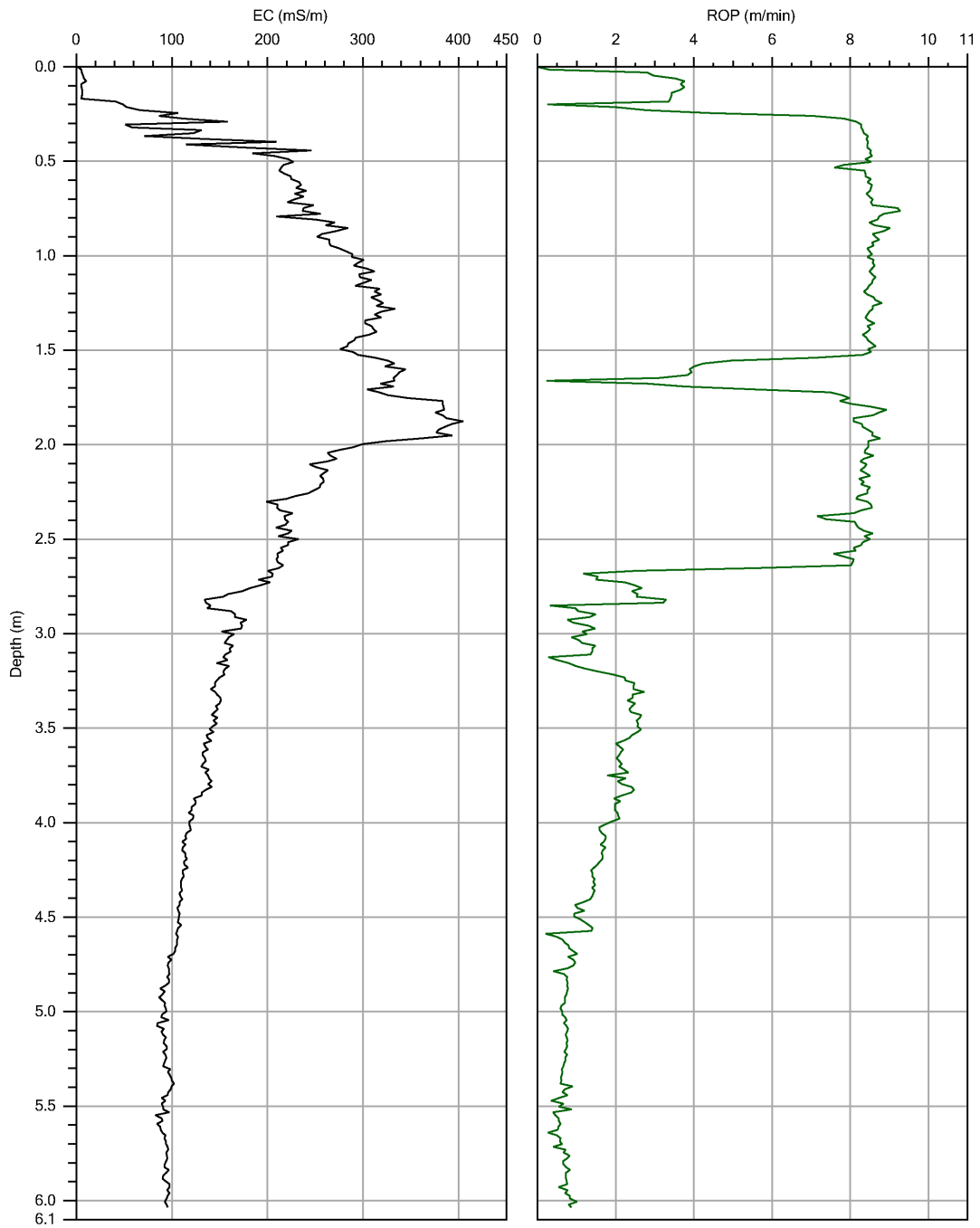
Company:	Intercore	Operator:	Deter	File:	EC11.EC
Project ID:	KJH study site	Client:	U of S	Date:	17/08/2011
				Location:	



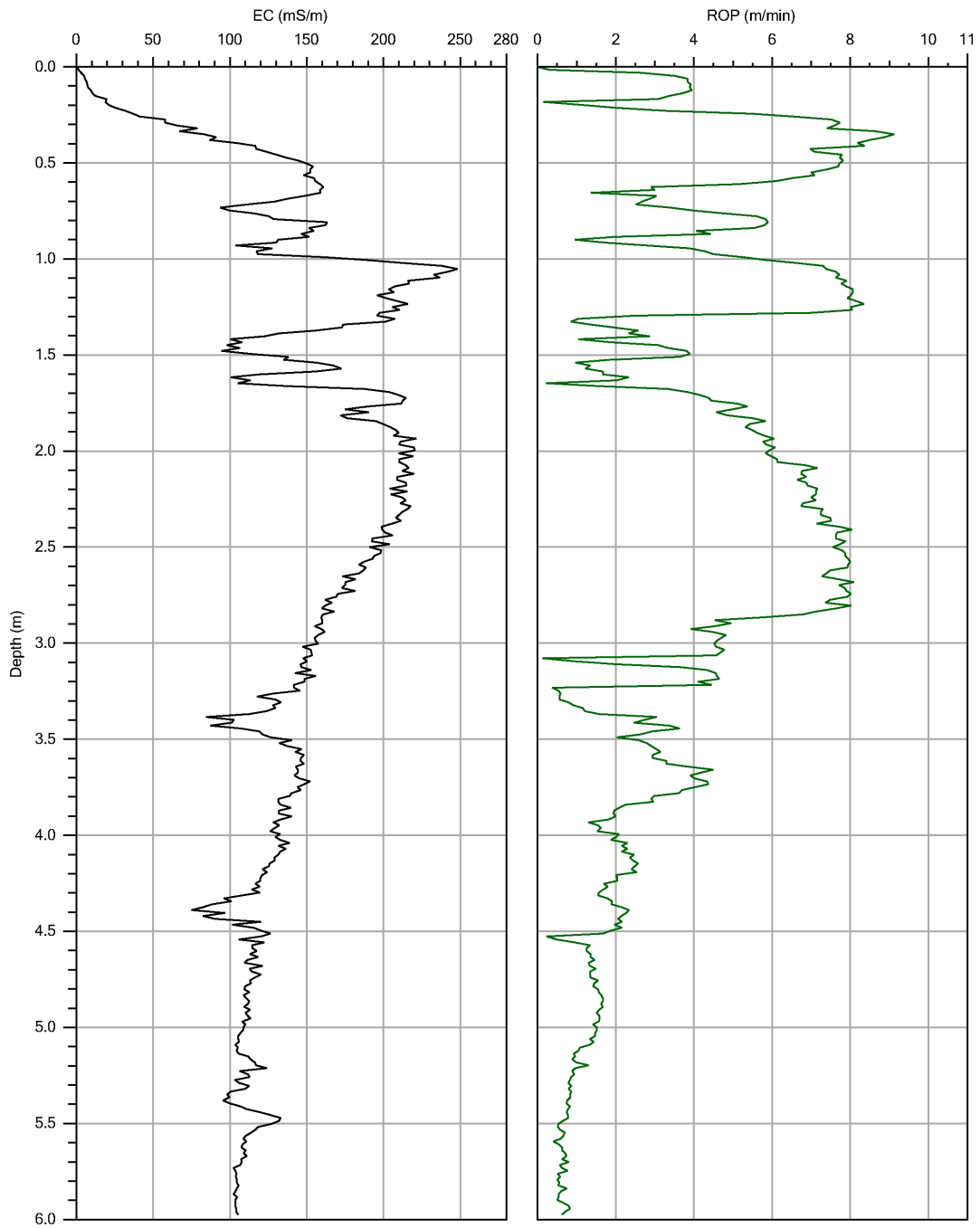
Company:	Intercore	Operator:	Deter	File:	EC14.EC
Project ID:	KJH study site	Client:	U of S	Date:	17/08/2011
				Location:	



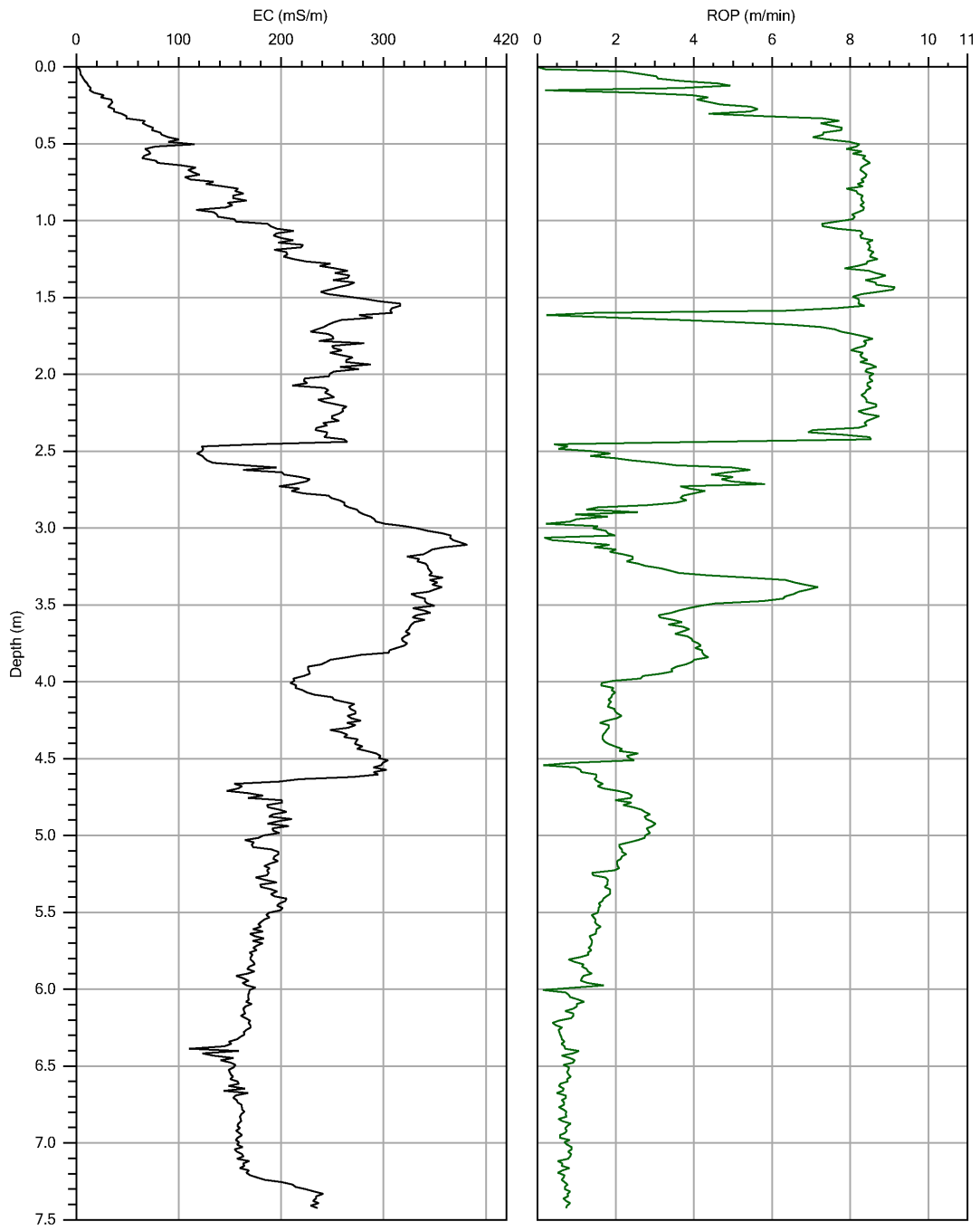
Company:	Intercore	Operator:	Deter	File:	EC-31.EC
Project ID:	KJH study site	Client:	U of S	Date:	11/10/2012
				Location:	



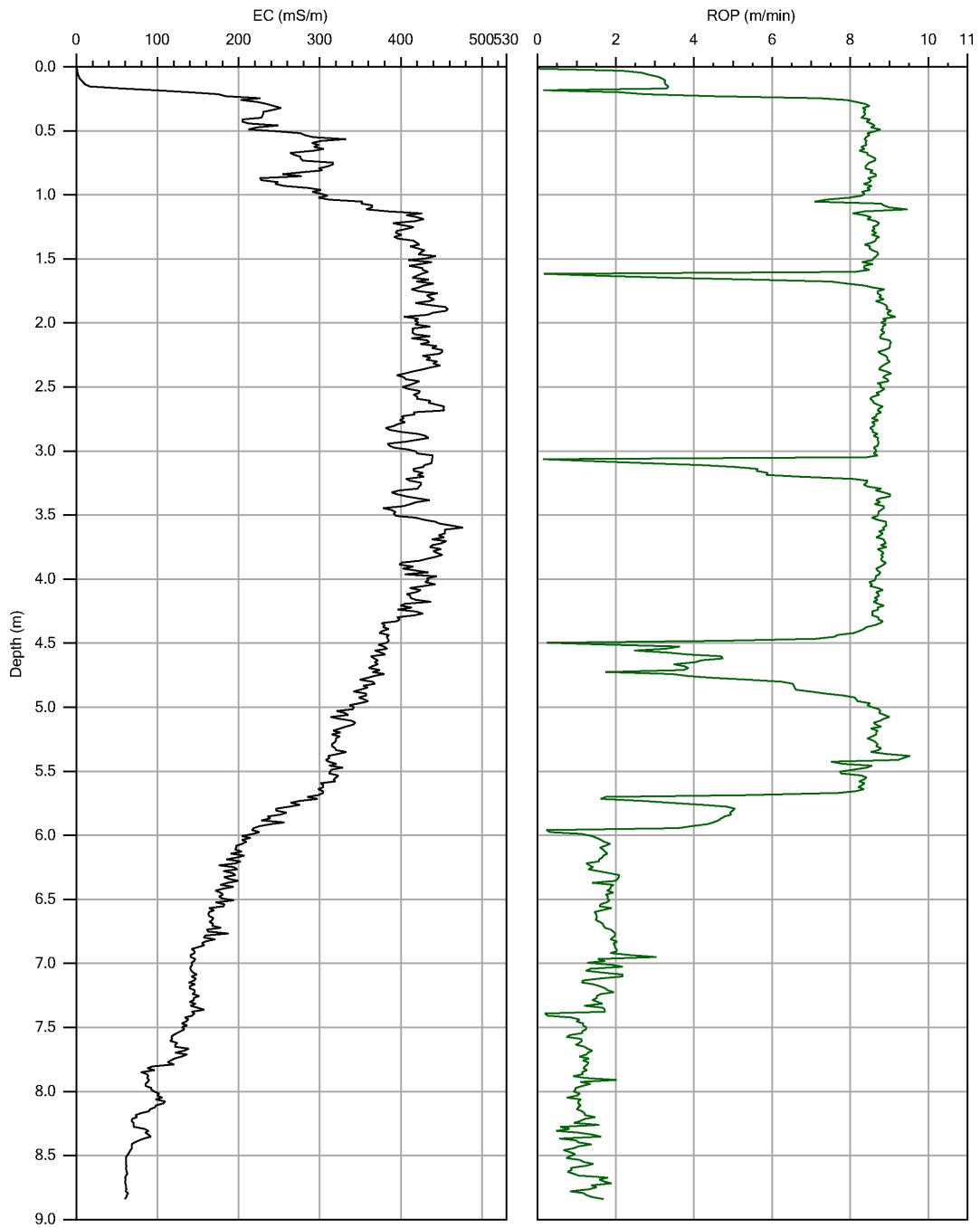
Company:	Intercore	Operator:	Deter	File:	EC-32.EC
Project ID:	KJH study site	Client:	U of S	Date:	11/10/2012
				Location:	



Company:	Intercore	Operator:	Deter	File:	EC-44.EC
Project ID:	KJH study site	Client:	U of S	Date:	11/10/2012
				Location:	



Company:	Intercore	Operator:	Deter	File:	EC-33.EC
Project ID:	KJH study site	Client:	U of S	Date:	11/10/2012
				Location:	



Company:	Intercore	Operator:	Deter	File:	EC-34.EC
Project ID:	KJH study site	Client:	U of S	Date:	11/10/2012
				Location:	

APPENDIX C  
SEDIMENT PROPERTIES

**Table C1:** Soil index parameter results.

Sample No.	Depth (m)	Lithological group	Analysis date dd/mm/yyyy	Water loss during storage (%)	Wet mass prior to analysis (g)	Gravimetric water content (%)	Saturation (%)	Wet density (kg/m <sup>3</sup> )	Dry density (kg/m <sup>3</sup> )	Water-filled porosity (%)
BH1-1	0.15	sand	28/08/2011	nm	72.3	26.10	91.10	1921	1523	43.58
BH1-3	0.46	sand	28/08/2011	nm	77.69	18.86	90.68	2060	1733	35.82
BH1-5	1.52	sand	28/08/2011	nm	67.44	19.01	74.46	1939	1629	39.67
BH1-7	1.98	glaciolacustrine	28/08/2011	nm	66.59	35.81	100.28	1866	1374	49.12
BH1-9	2.29	glaciolacustrine	28/08/2011	nm	74.96	34.39	98.50	1868	1390	48.52
BH1-11	2.59	glaciolacustrine	28/08/2011	nm	78.12	32.04	98.28	1896	1436	46.82
BH1-13	2.90	glaciolacustrine	28/08/2011	nm	60.95	34.68	97.80	1859	1380	48.88
BH1-15	3.20	glaciolacustrine	28/08/2011	nm	68.95	33.21	99.86	1894	1422	47.33
BH1-17	3.51	glaciolacustrine	28/08/2011	nm	71.74	37.38	99.15	1837	1337	50.47
BH1-19	3.81	glaciolacustrine	28/08/2011	nm	63.63	36.42	99.12	1850	1356	49.77
BH1-21	4.11	glaciolacustrine	28/08/2011	nm	69.67	37.39	100.50	1850	1346	50.13
BH1-23	4.42	glaciolacustrine	28/08/2011	nm	50.91	34.98	99.66	1871	1386	48.65
BH1-25	4.72	glaciolacustrine	28/08/2011	nm	65.53	38.36	108.04	1907	1379	48.94
BH1-27	5.03	glaciolacustrine	28/08/2011	nm	70.94	36.12	100.12	1864	1370	49.28
BH1-29	5.33	glaciolacustrine	28/08/2011	nm	57.42	31.37	99.92	1924	1464	45.76
BH1-31	5.64	glaciolacustrine	28/08/2011	nm	66.15	34.26	100.35	1884	1404	48.02
BH1-33	5.94	ablation till	28/08/2011	nm	67.83	38.31	99.27	1830	1323	51.01
BH1-35	6.25	ablation till	28/08/2011	nm	61.61	31.89	99.40	1907	1446	46.44
BH1-37	6.55	ablation till	28/08/2011	nm	61.48	38.50	99.72	1829	1321	51.09
BH1-39	6.86	ablation till	28/08/2011	nm	80.88	23.31	98.44	2032	1648	38.97
BH1-41	7.16	ablation till	28/08/2011	nm	64.41	14.96	94.53	2179	1895	29.80
BH1-43	7.47	ablation till	28/08/2011	nm	58.81	28.19	99.20	1960	1529	43.36
BH2-1	0.30	glaciolacustrine	30/08/2011	nm	65.87	23.46	90.05	1958	1586	41.27
BH2-3	0.61	glaciolacustrine	30/08/2011	nm	51.99	30.86	92.22	1860	1422	47.34
BH2-5	0.91	glaciolacustrine	30/08/2011	nm	60.67	31.84	93.34	1859	1410	47.77
BH2-7	1.22	glaciolacustrine	30/08/2011	nm	70.35	34.91	99.34	1871	1387	48.64
BH2-9	1.52	glaciolacustrine	30/08/2011	nm	58.19	31.76	98.70	1905	1446	46.44
BH2-11	1.83	glaciolacustrine	30/08/2011	nm	54.84	34.98	95.57	1834	1359	49.68
BH2-13	2.13	glaciolacustrine	30/08/2011	nm	66.45	37.95	96.13	1803	1307	51.59
BH2-15	2.44	glaciolacustrine	30/08/2011	nm	83.58	36.11	100.05	1863	1369	49.30
BH2-17	2.74	glaciolacustrine	30/08/2011	nm	60.98	36.91	97.93	1836	1341	50.33

Note:

nm denotes not measured.

**Table C1:** Soil index parameter results.

Sample No.	Depth (m)	Lithological group	Analysis date dd/mm/yyyy	Water loss during storage (%)	Wet mass prior to analysis (g)	Gravimetric water content (%)	Saturation (%)	Wet density (kg/m <sup>3</sup> )	Dry density (kg/m <sup>3</sup> )	Water-filled porosity (%)
BH2-19	3.05	glaciolacustrine	30/08/2011	nm	76.88	35.93	98.77	1859	1368	49.35
BH2-21	3.35	glaciolacustrine	30/08/2011	nm	68.64	33.67	99.02	1884	1409	47.80
BH2-23	3.66	glaciolacustrine	30/08/2011	nm	87.19	39.47	99.60	1821	1306	51.63
BH2-25	3.96	glaciolacustrine	30/08/2011	nm	66.87	34.52	98.98	1872	1392	48.46
BH2-27	4.72	glaciolacustrine	30/08/2011	nm	71.62	36.07	98.13	1845	1356	49.77
BH2-29	5.03	glaciolacustrine	30/08/2011	nm	71.5	36.50	99.13	1848	1354	49.85
BH2-31	5.33	glaciolacustrine	30/08/2011	nm	69.01	31.96	99.30	1906	1444	46.50
BH2-33	5.64	glaciolacustrine	30/08/2011	nm	71.21	29.46	100.67	1953	1508	44.14
BH2-35	5.94	glaciolacustrine	30/08/2011	nm	70.43	28.76	99.81	1956	1519	43.73
BH2-37	6.55	glaciolacustrine	30/08/2011	nm	73.96	30.27	99.99	1939	1488	44.88
BH2-39	6.86	ablation till	30/08/2011	nm	94.5	15.23	95.59	2178	1890	30.01
BH2-41	7.16	ablation till	30/08/2011	nm	106.74	16.74	94.72	2140	1833	32.10
BH2-43	7.77	ablation till	30/08/2011	nm	94.54	18.25	98.38	2131	1802	33.27
BH2-45	8.08	ablation till	30/08/2011	nm	87.97	19.02	98.08	2111	1773	34.32
BH2-47	8.38	subglacial till	30/08/2011	nm	89.93	13.56	95.50	2219	1954	27.64
BH2-49	8.69	subglacial till	30/08/2011	nm	65.34	15.07	96.68	2190	1903	29.52
BH2-51	9.14	subglacial till	30/08/2011	nm	93.44	15.42	95.20	2169	1879	30.39
BH2-53	9.45	subglacial till	30/08/2011	nm	90.54	13.71	93.03	2196	1931	28.46
BH2-55	9.75	subglacial till	30/08/2011	nm	89.34	14.95	97.10	2195	1909	29.28
BH2-57	10.06	subglacial till	30/08/2011	nm	80.34	14.79	94.99	2189	1907	29.37
BH2-59	10.36	subglacial till	30/08/2011	nm	95.55	14.48	93.96	2184	1908	29.33
BH3-1	0.15	glaciolacustrine	26/08/2011	nm	60.58	27.99	91.09	1898	1483	45.07
BH3-3	0.46	glaciolacustrine	26/08/2011	nm	79.76	26.98	91.13	1919	1511	44.02
BH3-5	0.76	glaciolacustrine	26/08/2011	nm	61.06	26.38	93.15	1946	1540	42.96
BH3-7	1.52	sand	26/08/2011	nm	32.74	31.62	95.25	1895	1440	46.67
BH3-9	1.83	sand	26/08/2011	nm	82.78	22.66	90.83	2000	1630	39.62
BH3-11	2.13	sand	26/08/2011	nm	29.96	20.08	82.22	2013	1676	37.92
BH3-13	2.44	glaciolacustrine	26/08/2011	nm	70.42	34.88	96.83	1848	1370	49.24
BH3-15	2.74	glaciolacustrine	26/08/2011	nm	67.17	37.33	96.67	1822	1327	50.86
BH3-17	3.05	glaciolacustrine	26/08/2011	nm	81.43	40.23	98.30	1802	1285	52.40
BH3-19	3.35	glaciolacustrine	26/08/2011	nm	74.87	40.23	98.54	1801	1284	52.44

Note:

nm denotes not measured.

**Table C1:** Soil index parameter results.

Sample No.	Depth (m)	Lithological group	Analysis date dd/mm/yyyy	Water loss during storage (%)	Wet mass prior to analysis (g)	Gravimetric water content (%)	Saturation (%)	Wet density (kg/m <sup>3</sup> )	Dry density (kg/m <sup>3</sup> )	Water-filled porosity (%)
BH3-21	3.66	glaciolacustrine	26/08/2011	nm	64.73	28.36	98.72	1953	1522	43.65
BH3-23	3.96	glaciolacustrine	26/08/2011	nm	71.92	27.55	99.58	1977	1550	42.60
BH3-25	4.27	glaciolacustrine	26/08/2011	nm	46.65	34.81	99.85	1876	1391	48.47
BH3-27	4.72	glaciolacustrine	26/08/2011	nm	73.15	33.70	100.38	1892	1415	47.57
BH3-29	5.03	glaciolacustrine	26/08/2011	nm	63.25	40.16	100.37	1821	1299	51.89
BH3-31	5.33	glaciolacustrine	26/08/2011	nm	75.49	36.31	99.65	1857	1362	49.54
BH3-33	5.64	glaciolacustrine	26/08/2011	nm	77.16	34.42	99.60	1876	1396	48.30
BH3-35	5.94	glaciolacustrine	26/08/2011	nm	59.48	24.61	97.59	2001	1606	40.52
BH3-37	6.40	glaciolacustrine	26/08/2011	nm	54.27	31.60	99.87	1916	1456	46.07
BH3-39	6.71	subglacial till	26/08/2011	nm	95.33	15.26	98.98	2198	1907	29.38
BH3-41	7.01	subglacial till	26/08/2011	nm	68.9	16.46	95.23	2145	1841	31.80
BH3-43	7.32	subglacial till	26/08/2011	nm	86.12	16.33	95.54	2150	1848	31.56
BH3-45	7.92	subglacial till	26/08/2011	nm	76.53	17.18	97.09	2143	1829	32.25
BH3-47	8.23	subglacial till	26/08/2011	nm	86.16	15.36	95.34	2172	1883	30.27
BH3-49	8.53	subglacial till	26/08/2011	nm	65.23	14.77	98.28	2205	1921	28.86
BH3-51	8.84	subglacial till	26/08/2011	nm	65.79	16.17	99.43	2180	1877	30.50
BH4-1	0.15	glaciolacustrine	26/08/2011	nm	128.62	30.33	95.44	1894	1453	46.18
BH4-3	0.46	glaciolacustrine	26/08/2011	nm	176.21	31.89	100.18	1915	1452	46.23
BH4-5	0.76	glaciolacustrine	26/08/2011	nm	247.71	32.78	101.11	1911	1439	46.69
BH4-7	1.52	glaciolacustrine	11/05/2012	0.72	107.74	32.90	100.51	1905	1433	46.92
BH4-9	1.83	glaciolacustrine	11/05/2012	0.73	151.28	32.09	99.88	1909	1445	46.47
BH4-11	2.13	glaciolacustrine	11/05/2012	0.88	183.05	32.48	100.68	1911	1442	46.58
BH4-13	2.44	glaciolacustrine	11/05/2012	0.59	236.15	33.80	96.54	1880	1405	47.95
BH4-15	2.74	glaciolacustrine	11/05/2012	0.81	196.61	37.87	102.04	1858	1348	50.08
BH4-17	3.05	glaciolacustrine	11/05/2012	1.02	218.15	36.55	103.19	1884	1380	48.90
BH4-19	3.35	glaciolacustrine	11/05/2012	0.90	218.54	36.42	104.06	1893	1387	48.62
BH4-21	3.66	glaciolacustrine	11/05/2012	0.90	240.69	37.23	102.01	1865	1359	49.66
BH4-23	3.96	glaciolacustrine	11/05/2012	0.86	226.07	28.31	100.83	1970	1536	43.12
BH4-25	4.27	glaciolacustrine	11/05/2012	0.99	218.75	30.35	101.37	1946	1493	44.71
BH4-27	4.57	glaciolacustrine	11/05/2012	1.24	149.53	34.27	101.73	1898	1413	47.65
BH4-29	4.88	glaciolacustrine	11/05/2012	0.98	190.14	38.97	101.57	1842	1326	50.90

Note:

nm denotes not measured.

**Table C1:** Soil index parameter results.

Sample No.	Depth (m)	Lithological group	Analysis date dd/mm/yyyy	Water loss during storage (%)	Wet mass prior to analysis (g)	Gravimetric water content (%)	Saturation (%)	Wet density (kg/m <sup>3</sup> )	Dry density (kg/m <sup>3</sup> )	Water-filled porosity (%)
BH4-31	5.18	glaciolacustrine	11/05/2012	1.00	209.01	37.02	100.52	1854	1353	49.89
BH4-33	5.49	glaciolacustrine	11/05/2012	1.26	171.78	32.67	101.11	1913	1442	46.61
BH4-35	5.79	glaciolacustrine	11/05/2012	1.61	100.43	35.30	101.33	1883	1391	48.47
BH4-37	6.55	glaciolacustrine	11/05/2012	1.08	210.31	33.25	100.88	1903	1428	47.09
BH4-39	6.86	glaciolacustrine	11/05/2012	0.95	219.29	36.46	100.73	1863	1365	49.44
BH4-41	7.16	ablation till	11/05/2012	1.25	223.86	24.65	98.69	2009	1612	40.29
BH4-43	7.47	subglacial till	11/05/2012	1.64	279.34	14.78	99.40	2211	1926	28.67
BH4-45	7.77	subglacial till	11/05/2012	1.93	266.22	14.91	99.20	2206	1920	28.89
BH4-47	8.08	subglacial till	11/05/2012	1.78	244.25	16.27	99.48	2177	1872	30.66
BH4-49	8.38	glaciolacustrine	11/05/2012	0.82	169.34	38.67	101.18	1842	1328	50.81
BH4-51	8.69	glaciolacustrine	11/05/2012	1.16	121.95	41.72	101.33	1811	1278	52.66
BH4-53	8.99	subglacial till	11/05/2012	1.84	103.22	16.26	100.25	2183	1877	30.47
BH5-3	0.91	glaciolacustrine	16/05/2012	1.57	187.36	24.68	87.97	1915	1536	43.11
BH5-5	1.22	glaciolacustrine	16/05/2012	1.89	142.09	29.21	89.37	1853	1434	46.89
BH5-7	1.52	glaciolacustrine	16/05/2012	1.19	208.17	30.84	96.56	1896	1449	46.32
BH5-9	1.83	glaciolacustrine	16/05/2012	1.62	182.79	32.04	95.44	1869	1416	47.56
BH5-11	2.13	glaciolacustrine	16/05/2012	1.32	213.24	32.02	100.24	1913	1449	46.34
BH5-13	2.44	glaciolacustrine	16/05/2012	1.12	188.2	33.04	100.44	1902	1430	47.05
BH5-15	2.74	glaciolacustrine	16/05/2012	1.50	213.74	33.64	103.20	1918	1435	46.84
BH5-17	3.20	glaciolacustrine	16/05/2012	1.35	153.11	31.42	101.40	1931	1470	45.57
BH5-19	3.51	glaciolacustrine	16/05/2012	1.36	178.16	36.78	95.85	1813	1326	50.90
BH5-21	3.81	glaciolacustrine	16/05/2012	1.31	177.89	39.70	98.94	1809	1295	52.03
BH5-23	4.11	glaciolacustrine	16/05/2012	1.05	229.09	38.29	101.14	1846	1335	50.57
BH5-25	4.42	glaciolacustrine	16/05/2012	1.53	204.92	29.34	100.39	1952	1509	44.11
BH5-27	4.72	glaciolacustrine	16/05/2012	1.50	219.73	27.06	100.71	1988	1564	42.06
BH5-29	5.03	glaciolacustrine	16/05/2012	1.26	220.4	27.61	100.31	1976	1549	42.65
BH5-31	5.33	glaciolacustrine	16/05/2012	1.14	213.07	34.67	100.38	1881	1397	48.27
BH5-33	5.64	glaciolacustrine	16/05/2012	1.77	188.57	39.41	101.17	1834	1315	51.28
BH5-35	5.94	glaciolacustrine	16/05/2012	1.62	191.81	36.26	100.73	1865	1369	49.30
BH5-37	6.40	glaciolacustrine	16/05/2012	1.31	238.77	37.27	100.73	1853	1350	50.00
BH5-39	6.71	glaciolacustrine	16/05/2012	1.47	227.22	34.16	100.93	1893	1411	47.75

Note:

nm denotes not measured.

**Table C1:** Soil index parameter results.

Sample No.	Depth (m)	Lithological group	Analysis date dd/mm/yyyy	Water loss during storage (%)	Wet mass prior to analysis (g)	Gravimetric water content (%)	Saturation (%)	Wet density (kg/m <sup>3</sup> )	Dry density (kg/m <sup>3</sup> )	Water-filled porosity (%)
BH5-41	7.01	glaciolacustrine	16/05/2012	1.56	109.56	34.52	101.86	1896	1409	47.80
BH5-43	7.32	glaciolacustrine	16/05/2012	2.47	185.54	35.02	100.37	1876	1390	48.53
BH5-45	7.77	ablation till	16/05/2012	4.27	231.3	13.03	96.12	2234	1976	26.80
BH5-47	8.08	ablation till	16/05/2012	2.28	205.71	31.87	100.00	1913	1451	46.28
BH5-49	8.38	ablation till	16/05/2012	3.43	225.43	18.84	98.31	2113	1778	34.13
BH5-51	8.69	subglacial till	16/05/2012	3.42	253.24	15.03	99.23	2204	1916	29.03
BH5-53	8.99	subglacial till	16/05/2012	4.76	101.91	14.57	98.83	2214	1932	28.44
BH6-1	0.15	glaciolacustrine	15/05/2012	4.38	145.64	28.61	85.78	1831	1423	47.28
BH6-3	0.46	glaciolacustrine	15/05/2012	2.09	101.95	29.05	89.36	1857	1439	46.70
BH6-5	0.76	glaciolacustrine	15/05/2012	1.39	127.89	32.17	92.05	1835	1388	48.58
BH6-7	1.07	glaciolacustrine	15/05/2012	1.39	86.57	34.98	97.38	1849	1370	49.27
BH6-9	1.68	glaciolacustrine	15/05/2012	0.78	191.73	34.86	94.72	1826	1354	49.86
BH6-11	1.98	glaciolacustrine	15/05/2012	0.88	164.03	36.52	99.77	1853	1357	49.73
BH6-13	2.29	glaciolacustrine	15/05/2012	0.96	193.21	34.37	101.29	1892	1408	47.84
BH6-15	2.59	glaciolacustrine	15/05/2012	0.85	210.44	34.33	102.27	1901	1415	47.58
BH6-17	3.05	glaciolacustrine	15/05/2012	0.89	191.6	35.65	103.71	1899	1400	48.16
BH6-19	3.35	glaciolacustrine	15/05/2012	0.72	213.89	36.99	101.22	1861	1358	49.69
BH6-21	3.66	glaciolacustrine	15/05/2012	0.63	208.69	37.45	101.26	1856	1350	49.99
BH6-23	3.96	glaciolacustrine	15/05/2012	0.73	192.87	36.95	101.68	1865	1362	49.55
BH6-25	4.27	glaciolacustrine	15/05/2012	0.18	207.44	35.30	100.88	1878	1388	48.59
BH6-27	4.57	glaciolacustrine	15/05/2012	1.12	94.51	40.75	102.41	1831	1301	51.81
BH6-29	4.88	glaciolacustrine	15/05/2012	1.02	218.48	39.66	100.64	1826	1307	51.58
BH6-31	5.18	glaciolacustrine	15/05/2012	1.17	149.74	37.99	100.19	1840	1333	50.63
BH6-33	5.49	glaciolacustrine	15/05/2012	0.69	187.96	37.84	99.84	1840	1335	50.57
BH6-35	5.79	glaciolacustrine	15/05/2012	0.83	188.09	36.60	100.09	1855	1358	49.70
BH6-37	6.10	glaciolacustrine	15/05/2012	0.94	171.76	32.69	98.77	1892	1426	47.18
BH6-39	6.40	glaciolacustrine	15/05/2012	0.99	204.97	34.73	100.47	1881	1396	48.30
BH6-41	6.71	ablation till	15/05/2012	0.70	222.28	34.46	100.62	1886	1402	48.06
BH6-43	7.01	ablation till	15/05/2012	0.79	234.44	21.35	99.00	2070	1706	36.81
BH6-45	7.62	subglacial till	15/05/2012	0.97	251.75	13.33	98.12	2239	1976	26.81
BH6-47	7.92	subglacial till	15/05/2012	0.96	296.23	12.11	99.85	2280	2034	24.67

Note:

nm denotes not measured.

**Table C1:** Soil index parameter results.

Sample No.	Depth (m)	Lithological group	Analysis date dd/mm/yyyy	Water loss during storage (%)	Wet mass prior to analysis (g)	Gravimetric water content (%)	Saturation (%)	Wet density (kg/m <sup>3</sup> )	Dry density (kg/m <sup>3</sup> )	Water-filled porosity (%)
BH6-49	8.23	subglacial till	15/05/2012	1.27	228.68	13.94	100.15	2236	1962	27.33
BH6-51	8.53	subglacial till	15/05/2012	1.47	230.5	13.20	97.55	2238	1977	26.76
BH7-1	0.30	glaciolacustrine	16/05/2012	7.77	79.79	23.93	80.94	1886	1522	43.64
BH7-3	0.61	glaciolacustrine	16/05/2012	1.92	132.94	27.38	92.10	1908	1498	44.53
BH7-5	0.91	glaciolacustrine	16/05/2012	1.35	104.9	34.32	99.97	1881	1400	48.14
BH7-7	1.52	glaciolacustrine	16/05/2012	1.20	158.91	35.11	98.49	1858	1375	49.06
BH7-9	1.83	glaciolacustrine	16/05/2012	1.21	169.47	34.14	97.60	1862	1388	48.59
BH7-11	2.13	glaciolacustrine	16/05/2012	1.10	191.71	35.62	99.98	1867	1376	49.02
BH7-13	2.44	glaciolacustrine	16/05/2012	3.10	93.26	34.26	98.95	1874	1396	48.30
BH7-15	2.74	glaciolacustrine	16/05/2012	1.54	195.66	36.69	100.97	1862	1362	49.55
BH7-17	3.05	glaciolacustrine	16/05/2012	0.96	195.53	38.69	100.94	1839	1326	50.89
BH7-19	3.35	glaciolacustrine	16/05/2012	1.06	211.57	36.82	99.56	1848	1351	49.98
BH7-21	3.66	glaciolacustrine	16/05/2012	1.04	208.67	39.75	100.66	1827	1307	51.58
BH7-23	3.96	glaciolacustrine	16/05/2012	1.23	208.34	41.56	100.96	1809	1278	52.66
BH7-25	4.27	glaciolacustrine	16/05/2012	1.53	167.07	34.23	100.85	1890	1408	47.86
BH7-27	4.88	glaciolacustrine	16/05/2012	1.32	94.36	36.16	101.09	1869	1373	49.16
BH7-29	5.18	glaciolacustrine	16/05/2012	1.12	184.01	37.42	101.06	1854	1349	50.03
BH7-31	5.49	glaciolacustrine	16/05/2012	1.24	184.61	33.45	100.86	1900	1424	47.27
BH7-33	5.79	glaciolacustrine	16/05/2012	1.23	190.08	37.28	100.41	1851	1348	50.07
BH7-35	6.40	glaciolacustrine	16/05/2012	1.83	129.84	40.83	99.42	1802	1279	52.62
BH7-37	6.71	glaciolacustrine	16/05/2012	0.98	228.67	32.87	100.31	1902	1432	46.98
BH7-39	7.01	ablation till	16/05/2012	1.22	216.33	30.14	100.37	1939	1490	44.81
BH7-41	7.32	ablation till	16/05/2012	1.39	223.21	20.20	100.24	2102	1749	35.24
BH7-43	7.62	subglacial till	16/05/2012	3.73	194.8	13.04	87.91	2182	1931	28.50
BH7-45	7.92	subglacial till	16/05/2012	3.04	246.53	12.38	98.84	2267	2018	25.27
BH7-47	8.23	subglacial till	16/05/2012	2.63	261.5	11.36	99.95	2301	2066	23.49
BH7-49	8.53	subglacial till	16/05/2012	2.11	256.94	15.95	99.26	2183	1883	30.26
BH7-51	8.84	subglacial till	16/05/2012	2.29	261.12	13.56	99.01	2238	1971	27.00
BH7-53	9.14	subglacial till	16/05/2012	3.69	219.23	13.52	98.76	2238	1971	26.98
BH7-55	9.45	subglacial till	16/05/2012	3.59	260.81	12.52	99.12	2265	2013	25.43
BH7-57	9.75	subglacial till	16/05/2012	2.34	279.94	12.76	96.41	2243	1990	26.31

Note:

nm denotes not measured.

**Table C1:** Soil index parameter results.

Sample No.	Depth (m)	Lithological group	Analysis date dd/mm/yyyy	Water loss during storage (%)	Wet mass prior to analysis (g)	Gravimetric water content (%)	Saturation (%)	Wet density (kg/m <sup>3</sup> )	Dry density (kg/m <sup>3</sup> )	Water-filled porosity (%)
BH7-59	10.06	subglacial till	16/05/2012	2.71	271.38	13.33	99.25	2246	1981	26.61
BH7-61	10.36	subglacial till	16/05/2012	2.84	209.54	12.92	95.54	2233	1978	26.75
BH8-1	0.46	glaciolacustrine	22/05/2012	nm	56.17	25.49	nm	nm	nm	nm
BH8-3	0.76	glaciolacustrine	22/05/2012	1.77	71.69	28.13	92.17	1900	1483	45.09
BH8-5	1.07	glaciolacustrine	22/05/2012	1.32	162.1	30.89	95.43	1888	1443	46.57
BH8-7	1.37	glaciolacustrine	22/05/2012	1.20	167.47	35.18	99.84	1871	1384	48.75
BH8-9	1.68	glaciolacustrine	22/05/2012	0.91	194.87	31.71	101.88	1933	1467	45.66
BH8-11	1.98	glaciolacustrine	22/05/2012	0.94	228.77	27.00	103.32	2011	1583	41.36
BH8-13	2.29	glaciolacustrine	22/05/2012	0.83	209.04	35.66	104.30	1905	1404	47.99
BH8-15	2.59	glaciolacustrine	22/05/2012	0.63	207.67	37.95	103.93	1876	1360	49.65
BH8-17	3.05	glaciolacustrine	22/05/2012	0.90	170.44	39.57	103.42	1854	1328	50.81
BH8-19	3.35	glaciolacustrine	22/05/2012	1.32	185.77	34.74	103.86	1911	1418	47.47
BH8-21	3.66	glaciolacustrine	22/05/2012	1.02	210.95	37.16	104.84	1892	1379	48.91
BH8-23	3.96	glaciolacustrine	22/05/2012	0.75	215.83	36.82	102.86	1878	1373	49.15
BH8-25	4.27	glaciolacustrine	22/05/2012	1.35	89.66	38.44	104.77	1877	1356	49.78
BH8-27	4.57	ablation till	22/05/2012	2.68	71.94	20.23	104.89	2134	1775	34.26
BH8-29	4.88	ablation till	22/05/2012	1.12	216.35	25.61	105.18	2047	1630	39.64
BH8-31	5.18	subglacial till	22/05/2012	1.71	204.29	14.87	103.98	2237	1948	27.87
BH8-33	5.49	subglacial till	22/05/2012	1.83	105.08	14.96	105.56	2244	1952	27.69
BH8-35	6.25	subglacial till	22/05/2012	1.93	201.59	14.09	104.35	2259	1980	26.65
BH8-37	6.55	subglacial till	22/05/2012	1.42	236.11	13.77	103.91	2264	1990	26.30
BH8-39	7.01	subglacial till	22/05/2012	1.62	221.27	13.40	109.13	2301	2029	24.85
BH8-41	7.32	subglacial till	22/05/2012	2.11	224.82	13.58	106.43	2282	2009	25.59
BH8-43	7.62	subglacial till	22/05/2012	1.47	218.7	13.59	105.07	2276	2004	25.78
BH8-45	7.92	subglacial till	22/05/2012	2.80	225.3	12.72	104.08	2291	2032	24.73
BH8-47	8.23	subglacial till	22/05/2012	1.65	244.39	13.95	107.80	2282	2002	25.85
BH8-49	8.53	subglacial till	22/05/2012	2.87	169.22	14.94	108.16	2263	1969	27.09
BH9-1	0.61	glaciolacustrine	24/05/2012	2.56	70.21	18.72	76.76	1933	1628	39.69
BH9-3	0.91	glaciolacustrine	24/05/2012	1.43	92.46	26.29	92.58	1931	1529	43.36
BH9-5	1.22	glaciolacustrine	24/05/2012	0.67	208.79	33.09	97.40	1876	1409	47.80
BH9-7	1.52	glaciolacustrine	24/05/2012	0.67	179.14	33.30	98.08	1878	1409	47.82

Note:

nm denotes not measured.

**Table C1:** Soil index parameter results.

Sample No.	Depth (m)	Lithological group	Analysis date dd/mm/yyyy	Water loss during storage (%)	Wet mass prior to analysis (g)	Gravimetric water content (%)	Saturation (%)	Wet density (kg/m <sup>3</sup> )	Dry density (kg/m <sup>3</sup> )	Water-filled porosity (%)
BH9-9	1.83	glaciolacustrine	24/05/2012	0.70	174.96	35.07	100.93	1882	1393	48.40
BH9-11	2.13	glaciolacustrine	24/05/2012	0.69	177.11	36.73	99.77	1852	1355	49.83
BH9-13	2.44	glaciolacustrine	24/05/2012	0.80	201.1	33.91	102.56	1911	1427	47.15
BH9-15	2.74	glaciolacustrine	24/05/2012	0.78	207.39	35.75	101.92	1883	1387	48.62
BH9-17	3.05	glaciolacustrine	24/05/2012	0.87	187.84	37.88	100.63	1847	1340	50.39
BH9-19	3.35	glaciolacustrine	24/05/2012	0.73	233.04	26.77	100.78	1994	1573	41.76
BH9-21	3.66	glaciolacustrine	24/05/2012	0.79	210.73	29.30	100.77	1957	1513	43.95
BH9-23	3.96	glaciolacustrine	24/05/2012	1.06	182.55	36.29	100.66	1865	1369	49.31
BH9-25	4.27	glaciolacustrine	24/05/2012	0.95	192.73	35.96	101.20	1873	1377	48.98
BH9-27	4.57	glaciolacustrine	24/05/2012	0.76	160.23	38.51	100.21	1835	1325	50.93
BH9-29	4.88	glaciolacustrine	24/05/2012	0.71	208.67	33.28	100.53	1902	1427	47.14
BH9-31	5.18	glaciolacustrine	24/05/2012	0.63	214.12	36.22	100.33	1862	1367	49.37
BH9-33	5.49	glaciolacustrine	24/05/2012	0.66	206.58	32.81	100.90	1909	1438	46.75
BH9-35	5.79	glaciolacustrine	24/05/2012	0.68	198.14	33.38	100.56	1899	1424	47.26
BH9-37	6.10	ablation till	24/05/2012	0.51	213.57	24.99	99.29	2010	1608	40.45
BH9-39	6.40	ablation till	24/05/2012	0.49	244.52	23.63	99.72	2036	1647	39.01
BH9-41	6.71	ablation till	24/05/2012	0.56	213.48	27.37	99.90	1977	1552	42.51
BH9-43	7.01	ablation till	24/05/2012	0.79	219.64	19.20	98.48	2109	1769	34.46
BH10-1	0.30	glaciolacustrine	24/05/2012	3.36	95.51	20.77	85.47	1973	1634	39.50
BH10-3	0.61	glaciolacustrine	24/05/2012	5.47	81.92	24.42	nm	nm	nm	nm
BH10-5	0.91	glaciolacustrine	24/05/2012	1.72	84.3	27.84	87.54	1859	1454	46.13
BH10-7	1.22	glaciolacustrine	24/05/2012	1.13	163.98	30.85	93.96	1874	1432	46.97
BH10-9	1.52	glaciolacustrine	24/05/2012	0.87	180.34	31.83	93.76	1864	1414	47.62
BH10-11	1.83	glaciolacustrine	24/05/2012	0.91	198.9	33.84	101.24	1899	1419	47.44
BH10-13	2.13	glaciolacustrine	24/05/2012	0.87	177.61	36.74	99.29	1847	1351	49.98
BH10-15	2.44	glaciolacustrine	24/05/2012	0.72	233.86	33.20	101.98	1914	1437	46.78
BH10-17	2.74	glaciolacustrine	24/05/2012	0.79	235.53	36.43	102.03	1876	1375	49.08
BH10-19	3.20	glaciolacustrine	24/05/2012	1.90	88.21	31.72	101.29	1927	1463	45.83
BH10-21	3.51	glaciolacustrine	24/05/2012	1.14	120.23	35.39	102.06	1887	1394	48.37
BH10-23	3.81	glaciolacustrine	24/05/2012	0.98	200.55	35.59	101.00	1876	1384	48.75
BH10-25	4.11	glaciolacustrine	24/05/2012	0.87	215.82	34.06	101.76	1901	1418	47.47

Note:

nm denotes not measured.

**Table C1:** Soil index parameter results.

Sample No.	Depth (m)	Lithological group	Analysis date dd/mm/yyyy	Water loss during storage (%)	Wet mass prior to analysis (g)	Gravimetric water content (%)	Saturation (%)	Wet density (kg/m <sup>3</sup> )	Dry density (kg/m <sup>3</sup> )	Water-filled porosity (%)
BH10-27	4.42	glaciolacustrine	24/05/2012	1.60	108.08	36.55	102.38	1876	1374	49.11
BH10-29	4.88	glaciolacustrine	24/05/2012	1.35	106.04	30.78	101.53	1943	1486	44.98
BH10-31	5.18	glaciolacustrine	24/05/2012	1.15	171.06	37.22	100.98	1857	1353	49.87
BH10-33	5.49	ablation till	24/05/2012	0.82	200.9	35.91	101.04	1871	1377	49.00
BH10-35	5.79	ablation till	24/05/2012	1.09	216.94	30.66	99.59	1927	1475	45.38
BH10-37	6.10	ablation till	24/05/2012	1.27	191.02	22.94	98.16	2034	1655	38.72
BH10-39	6.40	ablation till	24/05/2012	1.17	160.44	37.69	98.45	1828	1328	50.83
BH10-41	6.71	ablation till	24/05/2012	1.22	242.41	19.15	99.89	2120	1779	34.11
BH10-43	7.01	ablation till	24/05/2012	1.47	271.68	16.40	93.66	2134	1833	32.10
BH10-45	7.32	ablation till	24/05/2012	0.89	262.17	28.25	99.96	1964	1532	43.27
BH11-5	0.76	subglacial till	09/05/2012	3.66	141.26	15.01	90.67	2148	1868	30.82
BH11-7	1.07	subglacial till	09/05/2012	2.17	188.45	15.46	97.78	2186	1893	29.88
BH11-9	1.37	subglacial till	09/05/2012	3.88	147.58	14.90	95.01	2183	1900	29.65
BH11-11	1.68	subglacial till	09/05/2012	2.81	237.17	15.53	93.80	2160	1870	30.75
BH11-13	1.98	subglacial till	09/05/2012	4.61	141.84	15.35	91.95	2148	1862	31.03
BH11-15	2.29	subglacial till	09/05/2012	2.28	263.29	14.54	94.80	2188	1911	29.24
BH11-17	2.59	subglacial till	09/05/2012	2.00	281.78	15.47	98.54	2190	1896	29.76
BH11-19	2.90	subglacial till	09/05/2012	2.41	237.04	16.11	98.27	2174	1872	30.66
BH11-21	3.20	sand	09/05/2012	2.47	268.91	18.26	100.88	2147	1816	32.76
BH11-23	3.51	sand	09/05/2012	3.15	179.18	20.29	101.04	2111	1755	35.00
BH11-25	3.81	sand	09/05/2012	2.92	203.26	20.49	99.18	2088	1733	35.80
BH11-27	4.11	sand	09/05/2012	2.46	215.16	20.93	101.29	2096	1733	35.82
BH11-29	4.42	subglacial till	09/05/2012	3.73	269.89	14.69	102.08	2230	1944	27.99
BH11-31	4.72	subglacial till	09/05/2012	5.51	136.51	16.73	98.99	2164	1854	31.33
BH11-33	5.03	subglacial till	09/05/2012	4.43	157.98	18.12	89.78	2069	1752	35.12
BH11-35	5.33	subglacial till	09/05/2012	4.98	156.72	16.31	101.55	2191	1884	30.22
BH11-37	5.64	subglacial till	09/05/2012	3.26	180.15	17.68	101.22	2162	1837	31.96
BH11-39	5.94	subglacial till	09/05/2012	1.25	269.61	17.22	100.94	2167	1849	31.53
BH11-41	6.25	subglacial till	09/05/2012	1.28	293.27	18.77	101.07	2136	1799	33.39
BH11-43	6.55	subglacial till	09/05/2012	1.60	199.07	17.39	98.95	2152	1833	32.11
BH11-45	6.86	subglacial till	09/05/2012	1.36	216.61	16.84	98.02	2157	1846	31.64

Note:  
nm denotes not measured.

**Table C1:** Soil index parameter results.

Sample No.	Depth (m)	Lithological group	Analysis date dd/mm/yyyy	Water loss during storage (%)	Wet mass prior to analysis (g)	Gravimetric water content (%)	Saturation (%)	Wet density (kg/m <sup>3</sup> )	Dry density (kg/m <sup>3</sup> )	Water-filled porosity (%)
BH11-47	7.16	subglacial till	09/05/2012	3.33	126.13	14.82	97.37	2196	1913	29.16
BH11-49	7.47	subglacial till	09/05/2012	1.66	283.89	15.48	99.20	2194	1900	29.63
BH11-51	7.77	subglacial till	09/05/2012	1.46	167.46	22.78	101.96	2068	1685	37.61
BH11-53	8.08	subglacial till	09/05/2012	1.22	181.53	26.52	102.60	2012	1590	41.10
BH11-55	8.38	glaciolacustrine	09/05/2012	1.18	195.83	33.79	100.40	1892	1414	47.62
BH11-57	8.69	glaciolacustrine	09/05/2012	1.24	170.68	34.45	101.41	1892	1408	47.87
BH11-59	8.99	glaciolacustrine	09/05/2012	1.20	110.41	37.37	101.04	1855	1350	50.00
BH12-5	0.76	ablation till	11/05/2012	0.96	171.66	22.12	96.75	2039	1670	38.16
BH12-7	1.07	ablation till	11/05/2012	0.77	264.71	19.95	96.26	2077	1731	35.87
BH12-9	1.37	ablation till	11/05/2012	0.84	225.86	20.91	96.60	2060	1704	36.88
BH12-11	1.68	subglacial till	11/05/2012	0.79	157.4	16.70	92.70	2121	1817	32.70
BH12-13	1.98	subglacial till	11/05/2012	0.77	190.22	16.72	93.55	2128	1823	32.48
BH12-15	2.29	subglacial till	11/05/2012	1.43	168.37	15.66	93.53	2152	1861	31.09
BH12-17	2.59	subglacial till	11/05/2012	1.17	258.85	16.69	100.32	2173	1862	31.02
BH12-19	2.90	subglacial till	11/05/2012	0.97	261.17	16.34	97.80	2164	1860	31.12
BH12-21	3.20	subglacial till	11/05/2012	0.97	276.6	15.73	98.95	2186	1889	30.05
BH12-23	3.51	subglacial till	11/05/2012	0.86	285.02	17.05	101.31	2173	1856	31.25
BH12-25	3.81	subglacial till	11/05/2012	0.99	295.55	14.68	102.34	2232	1946	27.93
BH12-27	4.11	subglacial till	11/05/2012	1.70	266.46	15.28	100.22	2205	1912	29.17
BH12-29	4.42	subglacial till	11/05/2012	1.07	265.5	15.22	99.72	2202	1912	29.20
BH12-31	4.72	subglacial till	11/05/2012	1.22	266.93	17.44	101.89	2168	1846	31.62
BH12-33	5.03	subglacial till	11/05/2012	1.64	200.98	17.11	94.85	2127	1816	32.73
BH12-35	5.33	subglacial till	11/05/2012	0.92	274.49	18.10	100.43	2145	1816	32.74
BH12-37	5.64	subglacial till	11/05/2012	1.06	263.24	20.99	101.94	2099	1735	35.76
BH12-39	5.94	subglacial till	11/05/2012	1.92	213.3	16.51	100.50	2181	1872	30.66
BH12-41	6.25	subglacial till	11/05/2012	1.47	197.43	18.48	100.13	2134	1802	33.27
BH12-43	6.55	subglacial till	11/05/2012	1.69	151.49	15.55	99.13	2192	1897	29.76
BH12-45	6.86	subglacial till	11/05/2012	1.07	194.21	20.75	99.93	2089	1730	35.92
BH12-47	7.16	subglacial till	11/05/2012	1.73	162.52	16.30	100.15	2182	1876	30.51
BH12-49	7.47	glaciolacustrine	11/05/2012	1.33	107.06	33.53	99.39	1887	1413	47.67
BH13-1	0.46	glaciolacustrine	23/05/2012	4.20	86.85	30.46	97.09	1905	1460	45.91

Note:  
nm denotes not measured.

**Table C1:** Soil index parameter results.

Sample No.	Depth (m)	Lithological group	Analysis date dd/mm/yyyy	Water loss during storage (%)	Wet mass prior to analysis (g)	Gravimetric water content (%)	Saturation (%)	Wet density (kg/m <sup>3</sup> )	Dry density (kg/m <sup>3</sup> )	Water-filled porosity (%)
BH13-3	0.76	glaciolacustrine	23/05/2012	1.18	164.22	26.38	93.64	1939	1534	43.18
BH13-5	1.07	ablation till	23/05/2012	2.07	227.24	17.70	93.83	2106	1789	33.73
BH13-7	1.37	ablation till	23/05/2012	1.41	244.7	13.27	94.45	2218	1958	27.47
BH13-9	1.68	ablation till	23/05/2012	1.13	231.41	21.08	99.55	2081	1718	36.36
BH13-11	1.98	ablation till	23/05/2012	1.41	189.56	20.99	99.02	2078	1718	36.38
BH13-13	2.29	ablation till	23/05/2012	1.55	206.44	14.81	97.18	2197	1913	29.14
BH13-15	2.59	ablation till	23/05/2012	1.00	204.29	21.06	100.56	2087	1724	36.13
BH13-17	2.90	subglacial till	23/05/2012	1.38	245.04	14.67	99.04	2211	1928	28.59
BH13-19	3.20	subglacial till	23/05/2012	1.91	227.53	15.05	97.46	2192	1905	29.45
BH13-21	3.51	subglacial till	23/05/2012	1.99	215.62	14.68	96.49	2195	1914	29.11
BH13-23	3.81	subglacial till	23/05/2012	2.22	244.57	14.16	96.58	2208	1934	28.38
BH13-25	4.11	subglacial till	23/05/2012	1.65	253.61	15.76	101.03	2199	1900	29.65
BH13-27	4.42	subglacial till	23/05/2012	1.66	240.67	14.33	100.22	2227	1948	27.86
BH13-29	4.72	subglacial till	23/05/2012	2.02	193.86	14.27	100.64	2231	1953	27.68
BH13-31	5.03	subglacial till	23/05/2012	2.90	223.12	13.11	91.69	2209	1953	27.68
BH13-33	5.33	subglacial till	23/05/2012	2.22	242.21	12.74	98.42	2256	2001	25.89
BH13-35	5.64	subglacial till	23/05/2012	1.97	301.98	14.13	99.35	2227	1951	27.72
BH13-37	5.94	subglacial till	23/05/2012	1.82	281.84	14.70	100.17	2217	1933	28.40
BH13-39	6.25	subglacial till	23/05/2012	2.66	149.7	15.55	99.61	2195	1900	29.64
BH13-41	6.55	subglacial till	23/05/2012	2.39	181.72	14.70	97.62	2202	1920	28.89
BH13-43	6.86	subglacial till	23/05/2012	2.61	243.53	14.20	93.06	2186	1914	29.11
BH13-45	7.32	subglacial till	23/05/2012	1.41	265.37	15.53	101.66	2208	1912	29.20
BH14-5	1.22	ablation till	10/05/2012	1.22	177.98	18.29	89.24	2057	1739	35.58
BH14-7	1.52	ablation till	10/05/2012	1.87	186.21	16.45	91.55	2120	1821	32.57
BH14-9	1.83	ablation till	10/05/2012	3.22	115.95	15.97	91.90	2132	1838	31.91
BH14-11	2.13	subglacial till	10/05/2012	1.14	257.82	15.18	96.44	2182	1894	29.83
BH14-13	2.44	subglacial till	10/05/2012	1.06	286.49	15.34	98.75	2193	1901	29.58
BH14-15	2.74	subglacial till	10/05/2012	0.81	291.26	15.63	98.63	2186	1890	29.99
BH14-17	3.05	subglacial till	10/05/2012	2.21	193.72	14.71	90.93	2155	1879	30.42
BH14-19	3.35	subglacial till	10/05/2012	1.18	309.26	16.04	99.93	2186	1884	30.22
BH14-20	3.51	subglacial till	10/05/2012	3.43	127.06	15.97	92.36	2138	1844	31.72

Note:  
nm denotes not measured.

**Table C1:** Soil index parameter results.

Sample No.	Depth (m)	Lithological group	Analysis date dd/mm/yyyy	Water loss during storage (%)	Wet mass prior to analysis (g)	Gravimetric water content (%)	Saturation (%)	Wet density (kg/m <sup>3</sup> )	Dry density (kg/m <sup>3</sup> )	Water-filled porosity (%)
BH14-23	3.96	sand	10/05/2012	5.97	75.01	13.60	nm	nm	nm	nm
BH14-25	4.27	subglacial till	10/05/2012	1.39	263.7	13.81	99.65	2237	1965	27.22
BH14-27	4.57	subglacial till	10/05/2012	1.90	273.94	15.43	102.74	2217	1921	28.85
BH14-29	4.88	subglacial till	10/05/2012	1.21	281.5	17.81	102.06	2163	1836	32.02
BH14-31	5.18	subglacial till	10/05/2012	1.17	316	14.69	100.46	2221	1936	28.29
BH14-33	5.49	subglacial till	10/05/2012	2.06	246.32	15.36	98.59	2195	1903	29.52
BH14-35	5.79	subglacial till	10/05/2012	2.09	298.48	14.18	101.93	2242	1964	27.26
BH14-37	6.10	subglacial till	10/05/2012	1.67	223.6	22.58	100.98	2064	1684	37.63
BH14-39	6.40	subglacial till	10/05/2012	1.56	203.59	18.29	101.76	2151	1818	32.66
BH14-41	6.71	subglacial till	10/05/2012	1.10	181.42	25.37	102.24	2026	1616	40.14
BH14-43	7.01	subglacial till	10/05/2012	1.85	236.02	17.39	99.89	2156	1837	31.97
BH14-45	7.32	glaciolacustrine	10/05/2012	0.83	290	25.29	102.27	2028	1618	40.06
BH15-5	1.07	glaciolacustrine	10/05/2012	3.20	71.55	31.18	88.18	1820	1387	48.63
BH15-7	1.37	glaciolacustrine	10/05/2012	1.36	141.98	32.53	97.45	1885	1422	47.33
BH15-9	1.68	glaciolacustrine	10/05/2012	2.05	172.17	24.95	99.04	2008	1607	40.49
BH15-11	1.98	glaciolacustrine	10/05/2012	3.51	112.97	26.50	98.47	1979	1564	42.07
BH15-13	2.29	glaciolacustrine	10/05/2012	1.71	174.41	32.88	100.79	1907	1435	46.84
BH15-15	2.59	glaciolacustrine	10/05/2012	1.41	217.08	35.41	100.64	1874	1384	48.74
BH15-17	3.66	glaciolacustrine	10/05/2012	1.50	208.35	26.88	99.02	1976	1558	42.31
BH15-19	3.96	ablation till	10/05/2012	2.04	173.61	26.63	98.51	1976	1560	42.21
BH15-21	4.27	ablation till	10/05/2012	3.24	143.96	35.04	99.17	1866	1382	48.81
BH15-23	4.57	ablation till	10/05/2012	2.77	218.33	22.75	100.03	2053	1673	38.06
BH15-25	4.88	ablation till	10/05/2012	2.57	190.16	32.12	100.19	1911	1446	46.43
BH15-27	5.18	ablation till	10/05/2012	2.91	208	15.61	95.81	2168	1875	30.54
BH15-29	5.49	ablation till	10/05/2012	2.33	199.37	26.61	100.83	1995	1576	41.65
BH15-31	5.79	subglacial till	10/05/2012	2.68	255.2	15.09	96.55	2186	1899	29.66
BH15-33	6.10	subglacial till	10/05/2012	3.14	317.67	10.19	110.35	2383	2162	19.91
BH15-35	6.40	subglacial till	10/05/2012	3.66	241.64	14.63	103.02	2239	1953	27.67
BH15-37	6.71	subglacial till	10/05/2012	3.17	300.94	13.61	103.49	2266	1995	26.12
BH15-39	7.01	subglacial till	10/05/2012	5.35	212.7	14.61	101.71	2232	1947	27.89
BH15-41	7.32	subglacial till	10/05/2012	5.05	238.56	14.25	102.18	2244	1964	27.27

Note:

nm denotes not measured.

**Table C1:** Soil index parameter results.

Sample No.	Depth (m)	Lithological group	Analysis date dd/mm/yyyy	Water loss during storage (%)	Wet mass prior to analysis (g)	Gravimetric water content (%)	Saturation (%)	Wet density (kg/m <sup>3</sup> )	Dry density (kg/m <sup>3</sup> )	Water-filled porosity (%)
BH15-43	7.62	subglacial till	10/05/2012	4.38	181.26	14.66	100.38	2222	1938	28.22
BH15-45	7.92	subglacial till	10/05/2012	4.13	251.18	14.37	102.09	2238	1957	27.53
BH15-47	8.23	subglacial till	10/05/2012	4.16	315.08	12.98	101.53	2268	2008	25.63
BH15-49	8.53	subglacial till	10/05/2012	4.61	266.48	13.68	100.97	2247	1977	26.79
BH15-51	8.84	subglacial till	10/05/2012	7.14	154.59	13.59	94.17	2207	1943	28.03
BH16-3	1.07	glaciolacustrine	23/05/2012	1.24	212.06	29.69	101.39	1958	1510	44.09
BH16-5	1.37	glaciolacustrine	23/05/2012	1.71	176.13	31.21	99.54	1919	1463	45.82
BH16-7	1.98	glaciolacustrine	23/05/2012	1.12	214.29	33.61	101.41	1905	1425	47.21
BH16-9	2.29	glaciolacustrine	23/05/2012	1.03	208.78	33.15	101.14	1907	1432	46.96
BH16-11	2.59	glaciolacustrine	23/05/2012	1.66	134.27	32.70	97.95	1883	1419	47.44
BH16-13	2.90	glaciolacustrine	23/05/2012	1.06	217.41	34.59	102.69	1903	1414	47.64
BH16-15	3.35	glaciolacustrine	23/05/2012	1.01	203.19	33.28	103.33	1924	1443	46.54
BH16-17	3.66	glaciolacustrine	23/05/2012	1.23	185.08	35.37	102.03	1887	1394	48.37
BH16-19	3.96	glaciolacustrine	23/05/2012	1.04	218.57	32.95	102.32	1919	1444	46.53
BH16-21	4.27	glaciolacustrine	23/05/2012	1.02	253.55	29.92	102.05	1958	1507	44.19
BH16-23	4.57	ablation till	23/05/2012	1.53	222.01	29.19	101.31	1962	1518	43.76
BH16-25	4.88	ablation till	23/05/2012	2.15	285.92	16.71	101.17	2180	1868	30.81
BH16-27	5.18	subglacial till	23/05/2012	2.17	291.05	12.97	100.38	2261	2002	25.87
BH16-29	5.49	subglacial till	23/05/2012	1.78	305.98	14.23	99.46	2225	1948	27.86
BH16-31	5.79	subglacial till	23/05/2012	2.03	260.26	14.91	100.98	2218	1931	28.50
BH16-33	6.10	subglacial till	23/05/2012	2.58	271.81	14.09	99.66	2229	1954	27.65
BH16-35	6.40	subglacial till	23/05/2012	2.29	276.56	15.10	99.12	2202	1913	29.14
BH16-37	6.71	subglacial till	23/05/2012	2.47	281.56	13.39	99.68	2248	1982	26.58
BH16-39	7.01	subglacial till	23/05/2012	2.12	305.53	13.56	97.30	2228	1962	27.32
BH16-41	7.32	subglacial till	23/05/2012	2.57	298.7	12.42	97.97	2262	2012	25.47
BH17-1	0.30	glaciolacustrine	24/05/2012	2.42	107.35	26.05	99.61	1995	1582	41.39
BH17-3	0.61	glaciolacustrine	24/05/2012	2.13	216.33	24.71	101.72	2034	1631	39.60
BH17-5	0.91	glaciolacustrine	24/05/2012	1.61	183.5	33.25	100.88	1905	1430	47.05
BH17-7	1.22	glaciolacustrine	24/05/2012	1.73	204.83	33.17	101.37	1909	1433	46.92
BH17-11	2.13	glaciolacustrine	24/05/2012	1.89	213.58	36.55	101.84	1873	1372	49.20
BH17-13	2.44	glaciolacustrine	24/05/2012	2.40	168.34	37.22	98.90	1838	1339	50.39

Note:

nm denotes not measured.

**Table C1:** Soil index parameter results.

Sample No.	Depth (m)	Lithological group	Analysis date dd/mm/yyyy	Water loss during storage (%)	Wet mass prior to analysis (g)	Gravimetric water content (%)	Saturation (%)	Wet density (kg/m <sup>3</sup> )	Dry density (kg/m <sup>3</sup> )	Water-filled porosity (%)
BH17-15	2.74	ablation till	24/05/2012	2.62	243.46	18.91	100.64	2130	1791	33.66
BH17-17	3.05	ablation till	24/05/2012	n/a	185.71	24.67	102.02	2037	1634	39.48
BH17-19	3.35	ablation till	24/05/2012	3.07	254.19	18.22	98.73	2131	1803	33.23
BH17-21	3.66	ablation till	24/05/2012	3.52	262.57	19.75	99.83	2108	1760	34.80
BH17-23	3.96	ablation till	24/05/2012	3.31	269.25	19.49	101.29	2124	1778	34.16
BH17-25	4.27	ablation till	24/05/2012	2.67	285.94	16.83	102.30	2185	1870	30.75
BH17-27	4.57	subglacial till	24/05/2012	4.34	216.57	14.04	100.10	2234	1959	27.45
BH17-29	4.88	subglacial till	24/05/2012	3.80	220.12	14.21	98.65	2221	1945	27.96
BH17-31	5.18	subglacial till	24/05/2012	4.00	234.16	13.91	99.82	2238	1964	27.24
BH17-33	5.49	subglacial till	24/05/2012	6.01	180.13	14.86	99.13	2208	1923	28.79
BH18-1	0.46	glaciolacustrine	15/05/2012	9.87	76.94	19.97	83.70	1970	1642	39.18
BH18-3	0.76	glaciolacustrine	15/05/2012	10.43	60.93	28.20	87.25	1850	1443	46.55
BH18-5	1.07	glaciolacustrine	15/05/2012	1.70	189.89	28.99	96.17	1919	1488	44.90
BH18-7	1.37	glaciolacustrine	15/05/2012	1.21	242.29	31.56	96.36	1886	1434	46.89
BH18-9	1.83	glaciolacustrine	15/05/2012	2.16	170.85	33.68	99.72	1887	1412	47.71
BH18-11	2.13	glaciolacustrine	15/05/2012	1.37	185.12	37.46	101.20	1855	1350	50.01
BH18-13	2.44	glaciolacustrine	15/05/2012	6.93	74	31.25	97.91	1903	1450	46.31
BH18-15	2.74	ablation till	15/05/2012	1.45	209.26	33.95	101.07	1896	1415	47.59
BH18-17	3.05	ablation till	15/05/2012	12.88	189.94	25.47	100.22	2008	1600	40.72
BH18-19	3.35	ablation till	15/05/2012	1.95	205.71	29.37	100.91	1956	1512	44.01
BH18-21	3.66	subglacial till	15/05/2012	2.35	264.91	17.06	98.64	2154	1840	31.84
BH18-23	3.96	subglacial till	15/05/2012	3.02	259.74	15.94	100.78	2194	1892	29.91
BH18-25	4.27	subglacial till	15/05/2012	2.48	262.31	15.63	99.05	2191	1895	29.80
BH18-27	4.57	subglacial till	15/05/2012	2.72	252.83	14.81	97.53	2201	1917	29.01
BH18-29	4.88	subglacial till	15/05/2012	2.48	253.5	14.81	98.39	2206	1922	28.82
BH18-31	5.18	subglacial till	15/05/2012	2.76	241.45	15.16	97.49	2191	1903	29.53
BH18-33	5.49	subglacial till	15/05/2012	3.38	208.11	14.48	93.54	2181	1905	29.44
BH18-35	5.79	subglacial till	15/05/2012	2.24	292.54	13.78	99.30	2235	1965	27.23
BH18-37	6.10	subglacial till	15/05/2012	3.56	202.84	13.84	98.75	2232	1961	27.38
BH18-39	6.40	subglacial till	15/05/2012	2.84	206.34	14.00	99.09	2230	1956	27.54
BH18-41	6.71	subglacial till	15/05/2012	11.57	90.46	12.53	88.15	2211	1965	27.23

Note:  
nm denotes not measured.

**Table C1:** Soil index parameter results.

Sample No.	Depth (m)	Lithological group	Analysis date dd/mm/yyyy	Water loss during storage (%)	Wet mass prior to analysis (g)	Gravimetric water content (%)	Saturation (%)	Wet density (kg/m <sup>3</sup> )	Dry density (kg/m <sup>3</sup> )	Water-filled porosity (%)
BH19-1	0.15	glaciolacustrine	22/05/2012	2.16	126.16	23.00	86.28	1933	1571	41.80
BH19-3	0.46	glaciolacustrine	22/05/2012	4.91	86.52	31.80	95.43	1874	1422	47.34
BH19-5	0.76	glaciolacustrine	22/05/2012	2.15	185.98	33.41	100.19	1896	1421	47.37
BH19-7	1.52	glaciolacustrine	22/05/2012	6.14	69.05	33.57	101.03	1901	1423	47.29
BH19-9	1.83	glaciolacustrine	22/05/2012	2.65	190.08	38.72	100.33	1834	1322	51.02
BH19-11	2.13	glaciolacustrine	22/05/2012	2.13	203.79	38.92	101.16	1843	1326	50.87
BH19-13	2.44	glaciolacustrine	22/05/2012	2.09	152.07	38.47	101.15	1847	1334	50.59
BH19-15	2.74	glaciolacustrine	22/05/2012	1.49	198.5	36.96	101.68	1868	1364	49.48
BH19-17	3.05	glaciolacustrine	22/05/2012	1.64	220.68	38.55	100.89	1842	1330	50.76
BH19-19	3.35	glaciolacustrine	22/05/2012	1.80	227.58	37.77	101.07	1853	1345	50.18
BH19-21	3.66	glaciolacustrine	22/05/2012	1.28	244.97	38.80	101.39	1844	1328	50.80
BH19-23	3.96	glaciolacustrine	22/05/2012	1.56	223.81	38.25	100.93	1846	1335	50.55
BH19-25	4.27	glaciolacustrine	22/05/2012	1.59	245.51	36.11	101.78	1877	1379	48.93
BH19-27	4.57	glaciolacustrine	22/05/2012	2.01	195.23	38.06	101.61	1854	1343	50.25
BH19-29	4.88	glaciolacustrine	22/05/2012	1.89	169.95	38.54	101.36	1847	1333	50.63
BH19-31	5.18	glaciolacustrine	22/05/2012	1.52	234.38	40.02	101.54	1831	1308	51.56
BH19-33	5.49	glaciolacustrine	22/05/2012	2.04	219.98	38.52	101.24	1846	1333	50.64
BH19-35	5.79	glaciolacustrine	22/05/2012	1.68	234.78	38.69	102.15	1851	1334	50.58
BH19-37	6.10	glaciolacustrine	22/05/2012	1.11	206.15	38.09	101.60	1852	1341	50.32
BH19-39	6.40	glaciolacustrine	22/05/2012	1.53	197.42	36.53	101.61	1871	1370	49.25
BH19-41	6.71	glaciolacustrine	22/05/2012	5.37	93.9	40.42	101.62	1827	1301	51.81
BH19-43	7.01	glaciolacustrine	22/05/2012	1.29	174.8	39.79	101.21	1830	1309	51.50
BH19-45	7.32	glaciolacustrine	22/05/2012	1.81	167.58	31.56	99.92	1918	1458	45.99
BH19-47	7.77	glaciolacustrine	22/05/2012	2.02	158.24	36.91	100.67	1859	1357	49.72
BH19-49	8.08	glaciolacustrine	22/05/2012	1.41	199.78	33.71	100.81	1898	1419	47.43
BH19-51	8.38	glaciolacustrine	22/05/2012	1.82	207.46	32.92	101.00	1909	1436	46.80
BH19-53	8.69	glaciolacustrine	22/05/2012	1.19	201.05	36.58	101.14	1866	1366	49.40
BH19-55	8.99	glaciolacustrine	22/05/2012	1.49	226.9	35.47	101.52	1882	1389	48.55
BH19-57	9.60	glaciolacustrine	22/05/2012	1.76	199.45	33.21	101.39	1909	1433	46.92
BH19-59	9.91	ablation till	22/05/2012	2.08	191.08	32.25	101.50	1922	1453	46.17
BH19-61	10.21	ablation till	22/05/2012	2.08	249.49	25.68	100.76	2010	1599	40.77

Note:  
nm denotes not measured.

**Table C1:** Soil index parameter results.

Sample No.	Depth (m)	Lithological group	Analysis date dd/mm/yyyy	Water loss during storage (%)	Wet mass prior to analysis (g)	Gravimetric water content (%)	Saturation (%)	Wet density (kg/m <sup>3</sup> )	Dry density (kg/m <sup>3</sup> )	Water-filled porosity (%)
BH19-63	10.52	subglacial till	22/05/2012	11.96	105.44	13.18	98.96	2248	1986	26.43
BH20-1	0.46	glaciolacustrine	06/12/2011	1.70	75.4	26.09	93.17	1940	1538	43.02
BH20-3	0.76	glaciolacustrine	06/12/2011	1.96	71.05	26.01	84.98	1879	1491	44.78
BH20-5	1.07	glaciolacustrine	06/12/2011	0.99	97.18	31.09	94.74	1878	1433	46.94
BH20-7	1.37	glaciolacustrine	06/12/2011	1.59	77.4	31.55	97.34	1896	1441	46.61
BH20-9	1.68	glaciolacustrine	06/12/2011	1.81	76.1	36.07	98.67	1854	1362	49.55
BH20-11	1.98	glaciolacustrine	06/12/2011	1.67	68.3	38.29	99.21	1834	1326	50.88
BH20-13	2.29	glaciolacustrine	06/12/2011	2.47	70.91	38.91	99.48	1834	1320	51.09
BH20-15	2.59	glaciolacustrine	06/12/2011	1.86	78.04	38.58	99.97	1839	1327	50.84
BH20-17	3.20	glaciolacustrine	06/12/2011	1.26	78.61	42.91	98.97	1784	1248	53.77
BH20-19	3.51	glaciolacustrine	06/12/2011	1.64	77.5	40.41	100.27	1821	1297	51.98
BH20-21	3.81	glaciolacustrine	06/12/2011	1.63	70.53	41.39	100.02	1810	1280	52.58
BH20-23	4.11	glaciolacustrine	06/12/2011	1.28	92.53	41.19	101.25	1821	1290	52.24
BH20-25	4.42	glaciolacustrine	06/12/2011	2.01	77.98	43.10	99.98	1791	1252	53.64
BH20-27	4.72	glaciolacustrine	06/12/2011	2.62	89.63	38.57	100.38	1839	1327	50.85
BH20-29	5.03	glaciolacustrine	06/12/2011	2.52	76.14	40.89	100.49	1818	1290	52.21
BH20-31	5.33	glaciolacustrine	06/12/2011	2.40	85.58	39.90	101.17	1834	1311	51.46
BH20-33	5.64	glaciolacustrine	06/12/2011	2.07	88.06	36.76	101.33	1867	1365	49.45
BH20-35	5.94	glaciolacustrine	06/12/2011	2.13	99.81	36.52	101.18	1868	1368	49.32
BH20-37	6.25	glaciolacustrine	06/12/2011	2.64	72.81	38.65	102.49	1857	1339	50.39
BH20-39	6.55	glaciolacustrine	06/12/2011	2.43	85.74	40.89	101.06	1820	1292	52.15
BH20-41	6.86	glaciolacustrine	06/12/2011	2.12	95.47	38.11	99.65	1835	1329	50.78
BH20-43	7.16	glaciolacustrine	06/12/2011	1.89	89.2	38.72	100.53	1836	1324	50.97
BH20-45	7.47	glaciolacustrine	06/12/2011	2.39	85.7	39.16	100.78	1834	1318	51.19
BH20-47	7.77	glaciolacustrine	06/12/2011	3.17	68.53	36.49	100.49	1863	1365	49.45
BH20-49	8.08	glaciolacustrine	06/12/2011	2.67	96.42	29.40	100.38	1953	1510	44.09
BH20-51	8.38	glaciolacustrine	06/12/2011	2.52	84.46	37.13	100.70	1857	1355	49.83
BH20-53	8.69	glaciolacustrine	06/12/2011	3.21	86.92	30.91	100.33	1932	1475	45.35
BH20-55	8.99	glaciolacustrine	06/12/2011	2.47	95.06	36.93	100.98	1861	1359	49.66
BH20-57	9.35	glaciolacustrine	06/12/2011	2.66	87.76	37.20	100.30	1853	1351	49.97
BH20-58	9.45	glaciolacustrine	06/12/2011	3.29	74.99	31.61	99.76	1921	1460	45.93

Note:  
nm denotes not measured.

**Table C1:** Soil index parameter results.

Sample No.	Depth (m)	Lithological group	Analysis date dd/mm/yyyy	Water loss during storage (%)	Wet mass prior to analysis (g)	Gravimetric water content (%)	Saturation (%)	Wet density (kg/m <sup>3</sup> )	Dry density (kg/m <sup>3</sup> )	Water-filled porosity (%)
BH20-61	9.81	glaciolacustrine	06/12/2011	3.40	69.72	40.84	101.00	1821	1293	52.11
BH20-63	10.06	glaciolacustrine	06/12/2011	2.17	88.85	35.82	101.21	1877	1382	48.82
BH20-65	10.36	ablation till	06/12/2011	3.05	92.41	31.26	100.34	1928	1469	45.60
BH21-3	0.30	glaciolacustrine	16/05/2012	8.33	88.59	25.74	101.79	2019	1605	40.54
BH21-5	0.61	glaciolacustrine	16/05/2012	6.54	96.42	32.11	101.54	1923	1456	46.09
BH21-7	0.91	glaciolacustrine	16/05/2012	4.20	163.94	32.48	100.27	1909	1441	46.63
BH21-9	1.83	glaciolacustrine	16/05/2012	4.36	188.34	35.63	101.07	1878	1385	48.72
BH21-11	2.13	glaciolacustrine	16/05/2012	3.96	173.53	35.85	101.12	1881	1385	48.71
BH21-13	2.44	glaciolacustrine	16/05/2012	4.58	190.43	36.31	100.96	1868	1371	49.23
BH21-15	2.74	glaciolacustrine	16/05/2012	7.18	156.76	37.41	100.80	1853	1348	50.06
BH21-17	3.05	glaciolacustrine	16/05/2012	5.37	195.05	38.76	100.95	1841	1326	50.87
BH21-19	3.35	glaciolacustrine	16/05/2012	5.34	181.55	37.72	100.98	1853	1345	50.17
BH21-21	3.66	glaciolacustrine	16/05/2012	3.86	180.12	37.72	100.32	1846	1340	50.36
BH21-23	3.96	glaciolacustrine	16/05/2012	4.95	166.21	36.72	101.04	1866	1365	49.44
BH21-25	4.57	glaciolacustrine	16/05/2012	6.08	176.47	36.02	101.11	1874	1378	48.97
BH21-27	4.88	glaciolacustrine	16/05/2012	5.98	177.64	36.55	101.73	1873	1372	49.20
BH21-29	5.18	glaciolacustrine	16/05/2012	7.52	71.88	34.09	101.85	1901	1417	47.50
BH21-31	5.49	glaciolacustrine	16/05/2012	8.08	76.5	35.33	100.27	1873	1384	48.74
BH21-33	5.79	glaciolacustrine	16/05/2012	5.82	205.12	34.21	102.72	1908	1421	47.36
BH21-35	6.25	glaciolacustrine	16/05/2012	5.74	88.43	36.50	101.06	1866	1367	49.36
BH21-37	6.55	glaciolacustrine	16/05/2012	3.12	194.21	34.77	100.01	1877	1393	48.43
BH21-39	6.86	glaciolacustrine	16/05/2012	3.63	204.05	34.73	100.05	1877	1394	48.39
BH21-41	7.16	glaciolacustrine	16/05/2012	3.43	186.28	35.22	100.87	1879	1389	48.54
BH21-43	7.47	glaciolacustrine	16/05/2012	2.40	228.6	33.92	100.46	1891	1412	47.70
BH21-45	7.77	glaciolacustrine	16/05/2012	3.37	195.11	28.62	99.34	1955	1520	43.70
BH21-47	8.08	glaciolacustrine	16/05/2012	3.15	185.9	33.32	100.13	1896	1422	47.34
BH21-49	8.38	glaciolacustrine	16/05/2012	3.32	198.82	35.01	100.09	1874	1388	48.59
BH21-51	8.84	glaciolacustrine	16/05/2012	3.02	190.61	36.94	100.40	1854	1354	49.85
BH21-53	9.14	glaciolacustrine	16/05/2012	3.63	181	38.37	99.60	1831	1323	50.99
BH21-55	9.45	glaciolacustrine	16/05/2012	3.09	177.13	36.93	100.43	1854	1354	49.84
BH21-57	9.75	glaciolacustrine	16/05/2012	2.98	185.31	38.45	100.27	1837	1327	50.86

Note:

nm denotes not measured.

**Table C1:** Soil index parameter results.

Sample No.	Depth (m)	Lithological group	Analysis date dd/mm/yyyy	Water loss during storage (%)	Wet mass prior to analysis (g)	Gravimetric water content (%)	Saturation (%)	Wet density (kg/m <sup>3</sup> )	Dry density (kg/m <sup>3</sup> )	Water-filled porosity (%)
BH21-59	10.06	glaciolacustrine	16/05/2012	3.12	175.5	34.49	98.42	1865	1387	48.63
BH21-61	10.36	glaciolacustrine	16/05/2012	2.65	218.16	35.13	100.50	1877	1389	48.56
BH21-63	10.67	glaciolacustrine	16/05/2012	3.07	191.24	34.06	99.33	1879	1402	48.09
BH21-65	10.97	ablation till	16/05/2012	3.27	208.78	37.42	100.53	1850	1346	50.14
BH21-67	11.43	ablation till	16/05/2012	4.59	182.43	30.11	99.56	1933	1486	44.97
BH21-69	11.73	ablation till	16/05/2012	4.66	220.67	20.15	98.49	2090	1739	35.59
BH21-71	12.04	ablation till	16/05/2012	5.56	205.32	17.75	98.20	2137	1815	32.78
BH22-1	0.30	glaciolacustrine	07/12/2011	0.75	130.37	24.26	80.44	1866	1502	44.39
BH22-3	0.61	glaciolacustrine	07/12/2011	1.21	81.63	29.80	92.10	1870	1441	46.63
BH22-7	1.52	glaciolacustrine	07/12/2011	1.32	79.16	35.97	96.40	1829	1345	50.18
BH22-9	1.83	glaciolacustrine	07/12/2011	0.77	88.49	38.26	99.46	1832	1325	50.91
BH22-11	2.13	glaciolacustrine	07/12/2011	0.83	76.83	41.93	99.90	1799	1268	53.04
BH22-13	2.44	glaciolacustrine	07/12/2011	1.12	80.28	35.84	100.53	1870	1377	49.01
BH22-15	3.05	glaciolacustrine	07/12/2011	1.01	85.44	38.19	100.29	1841	1333	50.65
BH22-17	3.35	glaciolacustrine	07/12/2011	0.86	85.31	39.77	99.82	1823	1304	51.70
BH22-19	3.66	glaciolacustrine	07/12/2011	0.75	65.66	39.71	100.55	1826	1307	51.58
BH22-21	3.96	glaciolacustrine	07/12/2011	0.62	61.62	40.29	100.54	1823	1299	51.88
BH22-23	4.27	glaciolacustrine	07/12/2011	0.59	68.54	37.27	102.06	1869	1361	49.58
BH22-25	4.57	glaciolacustrine	07/12/2011	0.41	69.09	39.83	100.62	1828	1307	51.58
BH22-27	4.88	glaciolacustrine	07/12/2011	0.61	91.43	39.60	100.77	1830	1311	51.45
BH22-29	5.18	glaciolacustrine	07/12/2011	0.71	87.24	40.54	100.67	1818	1293	52.10
BH22-31	5.49	glaciolacustrine	07/12/2011	0.69	81.43	39.45	100.64	1834	1315	51.30
BH22-33	5.79	glaciolacustrine	07/12/2011	0.67	82.28	40.38	100.84	1820	1297	51.98
BH22-35	6.10	glaciolacustrine	07/12/2011	0.64	101.46	37.81	101.53	1854	1346	50.16
BH22-37	6.40	glaciolacustrine	07/12/2011	0.28	88.65	39.88	100.71	1825	1304	51.69
BH22-39	6.71	glaciolacustrine	07/12/2011	0.69	77.04	38.80	101.09	1840	1326	50.90
BH22-41	7.01	glaciolacustrine	07/12/2011	1.00	89.72	40.46	100.93	1820	1296	52.01
BH22-43	7.32	glaciolacustrine	07/12/2011	1.07	79.71	40.71	100.71	1816	1291	52.20
BH22-47	7.92	glaciolacustrine	07/12/2011	1.14	82	28.66	100.91	1967	1529	43.39
BH22-49	8.23	glaciolacustrine	07/12/2011	0.77	95.46	29.90	100.53	1944	1496	44.57
BH22-51	8.53	glaciolacustrine	07/12/2011	0.99	81.33	37.22	100.23	1850	1348	50.06
BH22-53	8.84	glaciolacustrine	07/12/2011	0.81	83.81	41.39	100.82	1810	1280	52.58

Note:  
nm denotes not measured.

**Table C2:** Soil grain size results.

Lithological group	Sample No.	Depth (m)	Core log description	% sand (4.75-0.074 mm)	% silt (0.074-0.005 mm)	% clay (<0.005 mm)
glaciolacustrine	BH2-19	3.05	clay, some silt	0	60	40
glaciolacustrine	BH16-15	3.35	interbedded silt and clay	1	37	62
glaciolacustrine	BH21-13	2.44	clayey silt	0	75	25
glaciolacustrine	BH21-53	9.14	clay, trace silt	0	12	88
ablation till	BH13-9	1.68	clayey till, diamicton	18	44	38
subglacial till	BH2-55	9.75	clayey till, diamicton	42	31	27
subglacial till	BH13-23	3.81	clayey till, diamicton	37	36	27
subglacial till	BH16-29	5.49	clayey till, diamicton	39	34	26

APPENDIX D  
PORE-WATER CHEMISTRY

**Table D:** Soil pore-water chemistry results and direct-push EC selections.

Sample No.	Middle depth (m)	Lithological group	Squeeze date dd/mm/yyyy	Water loss during storage (%)	Wet mass prior to analysis (g)	EC corrected for water loss (mS/cm)	Cl <sup>-</sup> corrected for water loss (mg/L)	Temperature corrected 5-pt average D-P EC (mS/cm)
BH1-4	0.72	sand	29/05/2012	nm	nm	32.30	7240	4.95
BH1-5	1.63	sand	29/05/2012	nm	nm	31.90	7300	5.40
BH1-7	2.09	glaciolacustrine	29/05/2012	nm	nm	27.50	6530	6.51
BH1-14	3.15	glaciolacustrine	29/05/2012	nm	nm	22.40	5230	4.90
BH1-18	3.76	glaciolacustrine	29/05/2012	nm	nm	20.60	4830	3.95
BH1-26	4.98	glaciolacustrine	28/05/2012	nm	nm	8.88	2230	2.18
BH1-30	5.59	glaciolacustrine	28/05/2012	nm	nm	6.93	1550	1.95
BH1-31	5.75	glaciolacustrine	28/05/2012	nm	nm	6.47	1470	1.81
BH1-33	6.05	ablation till	28/05/2012	nm	nm	8.47	1040	1.81
BH1-36	6.51	ablation till	25/05/2012	nm	nm	5.00	919	0.90
BH1-39	6.96	ablation till	25/05/2012	nm	nm	8.12	785	1.35
BH1-43	7.57	ablation till	28/05/2012	nm	nm	6.84	610	0.82
BH2-6	1.17	glaciolacustrine	24/05/2012	nm	nm	27.90	3990	6.83
BH2-11	1.94	glaciolacustrine	25/05/2012	nm	nm	24.10	4060	5.47
BH2-17	2.85	glaciolacustrine	25/05/2012	nm	nm	29.00	9380	6.84
BH2-26	4.22	glaciolacustrine	24/05/2012	nm	nm	27.10	9080	4.75
BH2-29	5.14	glaciolacustrine	25/05/2012	nm	nm	22.50	6560	3.17
BH2-30	5.29	glaciolacustrine	25/05/2012	nm	nm	17.90	5270	2.98
BH2-31	5.44	glaciolacustrine	24/05/2012	nm	nm	15.20	3960	2.58
BH2-33	5.75	glaciolacustrine	25/05/2012	nm	nm	10.10	2390	1.98
BH2-35	6.05	glaciolacustrine	25/05/2012	nm	nm	7.00	295	1.81
BH2-37	6.66	glaciolacustrine	25/05/2012	nm	nm	6.60	549	1.63
BH2-39	6.96	ablation till	25/05/2012	nm	nm	3.99	434	1.39
BH2-43	7.88	ablation till	24/05/2012	nm	nm	5.59	nm	1.06
BH2-44	8.03	ablation till	24/05/2012	nm	nm	2.97	208	1.11
BH2-49	8.79	subglacial till	24/05/2012	nm	nm	5.49	135	0.69
BH2-53	9.56	subglacial till	31/05/2012	nm	nm	3.50	106	0.61
BH2-57	10.17	subglacial till	24/05/2012	nm	nm	3.02	95.5	0.64
BH3-3	0.56	glaciolacustrine	31/05/2012	nm	nm	30.70	9310	5.17
BH3-6	1.02	sand	31/05/2012	nm	nm	36.00	11700	6.61
BH3-7	1.63	sand	30/05/2012	nm	nm	30.10	9080	5.07
BH3-9	1.94	sand	30/05/2012	nm	nm	32.2	9900	4.92
BH3-11	2.24	sand	30/05/2012	nm	nm	35	11400	6.29

Note:

nm denotes not measured.

**Table D:** Soil pore-water chemistry results and direct-push EC selections.

Sample No.	Middle depth (m)	Lithological group	Squeeze date dd/mm/yyyy	Water loss during storage (%)	Wet mass prior to analysis (g)	EC corrected for water loss (mS/cm)	Cl <sup>-</sup> corrected for water loss (mg/L)	Temperature corrected 5-pt average D-P EC (mS/cm)
BH3-13	2.55	glaciolacustrine	30/05/2012	nm	nm	22.20	5540	5.96
BH3-19	3.46	glaciolacustrine	30/05/2012	nm	nm	21.60	5040	4.82
BH3-23	4.07	glaciolacustrine	30/05/2012	nm	nm	17.30	2430	3.66
BH3-27	4.83	glaciolacustrine	30/05/2012	nm	nm	5.45	1190	1.70
BH3-29	5.14	glaciolacustrine	30/05/2012	nm	nm	3.80	690	1.42
BH3-31	5.44	glaciolacustrine	30/05/2012	nm	nm	5.12	384	1.44
BH3-33	5.75	glaciolacustrine	29/05/2012	nm	nm	5.26	233	1.30
BH3-35	6.05	glaciolacustrine	29/05/2012	nm	nm	4.93	142	1.01
BH3-37	6.51	glaciolacustrine	29/05/2012	nm	nm	3.11	129	0.86
BH3-39	6.81	subglacial till	29/05/2012	nm	nm	4.77	119	0.82
BH3-43	7.42	subglacial till	31/05/2012	nm	nm	2.04	86.9	0.52
BH3-45	8.03	subglacial till	29/05/2012	nm	nm	2.64	147	0.72
BH3-51	8.95	subglacial till	29/05/2012	nm	nm	5.04	99.0	0.70
BH4-7	1.63	glaciolacustrine	04/06/2012	1.73	186.48	55.10	19400	9.36
BH4-15	2.85	glaciolacustrine	04/06/2012	1.90	203.57	32.40	8530	6.19
BH4-27	4.68	glaciolacustrine	04/06/2012	1.89	151.06	33.10	8430	5.78
BH4-31	5.29	glaciolacustrine	04/06/2012	2.13	224.60	21.10	3740	3.12
BH4-35	5.90	glaciolacustrine	04/06/2012	2.29	174.88	10.00	1090	2.05
BH4-37	6.66	glaciolacustrine	04/06/2012	2.95	230.87	5.79	491	1.42
BH4-39	6.96	glaciolacustrine	01/06/2012	1.32	231.86	4.83	425	0.92
BH4-41	7.27	ablation till	01/06/2012	1.93	259.08	4.16	310	0.90
BH4-46	8.03	subglacial till	01/06/2012	3.50	208.60	5.89	214	0.84
BH4-49	8.49	glaciolacustrine	01/06/2012	1.63	172.20	3.32	155	0.73
BH4-51	8.79	glaciolacustrine	01/06/2012	2.17	116.85	3.42	181	0.74
BH4-53	9.10	subglacial till	01/06/2012	3.42	250.36	6.27	169	0.70
BH5-7	1.63	glaciolacustrine	06/06/2012	1.79	176.33	9.67	147	2.93
BH5-14	2.70	glaciolacustrine	06/06/2012	1.55	234.64	13.70	1400	2.42
BH5-23	4.22	glaciolacustrine	06/06/2012	1.66	205.33	8.37	697	2.14
BH5-31	5.44	glaciolacustrine	05/06/2012	2.55	251.68	7.70	723	2.17
BH5-35	6.05	glaciolacustrine	05/06/2012	1.81	171.66	4.34	561	1.48
BH5-36	6.36	glaciolacustrine	05/06/2012	2.05	183.70	4.04	347	1.55
BH5-37	6.51	glaciolacustrine	05/06/2012	1.90	244.73	4.12	325	1.53
BH5-39	6.81	glaciolacustrine	05/06/2012	2.64	227.72	3.86	285	1.53

Note:

nm denotes not measured.

**Table D:** Soil pore-water chemistry results and direct-push EC selections.

Sample No.	Middle depth (m)	Lithological group	Squeeze date dd/mm/yyyy	Water loss during storage (%)	Wet mass prior to analysis (g)	EC corrected for water loss (mS/cm)	Cl <sup>-</sup> corrected for water loss (mg/L)	Temperature corrected 5-pt average D-P EC (mS/cm)
BH5-41	7.12	glaciolacustrine	05/06/2012	2.12	216.23	3.65	219	1.72
BH5-43	7.42	glaciolacustrine	05/06/2012	1.71	204.68	2.69	157	1.24
BH5-45	7.88	ablation till	05/06/2012	5.66	225.11	5.19	189	0.93
BH5-47	8.18	ablation till	05/06/2012	1.93	203.86	2.97	128	0.64
BH5-49	8.49	ablation till	05/06/2012	3.60	244.70	3.80	132	0.71
BH5-53	9.10	subglacial till	05/06/2012	4.24	235.66	4.93	148	0.69
BH6-7	1.17	glaciolacustrine	06/06/2012	2.41	138.69	43.60	15000	9.35
BH6-17	3.15	glaciolacustrine	06/06/2012	2.22	186.51	37.60	12200	8.93
BH6-25	4.37	glaciolacustrine	06/06/2012	2.26	190.21	36.80	12400	7.03
BH6-29	4.98	glaciolacustrine	06/06/2012	1.67	206.86	20.70	6110	3.50
BH6-33	5.59	glaciolacustrine	06/06/2012	1.71	205.27	10.50	2880	2.09
BH6-34	5.75	glaciolacustrine	06/06/2012	1.72	220.57	8.70	2260	1.90
BH6-35	5.90	glaciolacustrine	06/06/2012	2.19	212.16	8.50	1700	1.85
BH6-37	6.20	glaciolacustrine	06/06/2012	2.58	176.44	7.41	851	1.21
BH6-39	6.51	glaciolacustrine	06/06/2012	1.66	220.03	5.11	527	0.71
BH6-41	6.81	ablation till	06/06/2012	1.40	236.72	3.76	311	0.68
BH6-45	7.73	subglacial till	06/06/2012	3.50	254.60	5.66	326	0.68
BH6-49	8.34	subglacial till	06/06/2012	3.67	275.12	4.95	174	0.60
BH6-52	8.79	subglacial till	06/06/2012	4.09	234.21	5.30	159	0.59
BH7-7	1.63	glaciolacustrine	05/06/2012	3.51	131.60	17.40	2110	3.26
BH7-17	3.15	glaciolacustrine	05/06/2012	2.12	175.28	10.00	1160	3.08
BH7-27	4.98	glaciolacustrine	04/06/2012	1.80	194.63	8.80	1050	2.03
BH7-31	5.59	glaciolacustrine	04/06/2012	1.99	229.19	6.31	778	1.61
BH7-34	6.05	glaciolacustrine	04/06/2012	1.84	177.22	6.12	489	1.62
BH7-35	6.51	glaciolacustrine	04/06/2012	3.21	179.64	6.27	352	1.22
BH7-36	6.66	glaciolacustrine	04/06/2012	2.70	209.78	4.77	348	1.17
BH7-37	6.81	glaciolacustrine	04/06/2012	1.55	227.75	4.34	280	1.06
BH7-41	7.42	ablation till	04/06/2012	3.32	238.08	4.05	189	0.66
BH7-49	8.64	subglacial till	04/06/2012	4.12	252.17	4.03	155	0.69
BH7-55	9.56	subglacial till	04/06/2012	5.42	257.75	5.07	153	0.53
BH7-61	10.47	subglacial till	04/06/2012	4.66	253.04	5.21	118	0.50
BH8-12	2.24	glaciolacustrine	01/06/2012	3.06	233.40	39	10600	7.33
BH8-16	2.85	glaciolacustrine	01/06/2012	3.33	184.06	26	6760	5.92

Note:

nm denotes not measured.

**Table D:** Soil pore-water chemistry results and direct-push EC selections.

Sample No.	Middle depth (m)	Lithological group	Squeeze date dd/mm/yyyy	Water loss during storage (%)	Wet mass prior to analysis (g)	EC corrected for water loss (mS/cm)	Cl <sup>-</sup> corrected for water loss (mg/L)	Temperature corrected 5-pt average D-P EC (mS/cm)
BH8-19	3.46	glaciolacustrine	01/06/2012	3.63	191.63	23.80	6030	5.64
BH8-23	4.07	glaciolacustrine	01/06/2012	3.97	202.30	22.50	5630	3.69
BH8-25	4.37	glaciolacustrine	01/06/2012	3.40	190.76	14.60	3590	2.33
BH8-27	4.68	ablation till	01/06/2012	7.91	132.42	6.19	1310	1.52
BH8-29	4.98	ablation till	31/05/2012	3.75	246.79	4.39	867	1.15
BH8-31	5.29	subglacial till	31/05/2012	6.17	260.60	2.96	408	1.23
BH8-33	5.59	subglacial till	31/05/2012	7.43	203.09	3.23	169	1.16
BH8-35	6.36	subglacial till	31/05/2012	8.09	176.54	4.16	118	1.00
BH8-39	7.12	subglacial till	31/05/2012	6.80	277.27	1.94	86.7	0.98
BH8-49	8.64	subglacial till	31/05/2012	6.20	239.93	2.19	105	0.51
BH11-22	3.46	sand	19/03/2013	5.76	261.99	18.40	2480	4.23
BH11-23	3.61	sand	19/03/2013	5.74	250.96	18.70	2480	4.07
BH12-6	1.02	ablation till	18/03/2013	7.54	225.77	34.70	16900	5.89
BH12-9	1.48	ablation till	18/03/2013	6.05	217.56	37.00	18700	6.63
BH12-11	1.80	subglacial till	18/03/2013	7.27	275.63	37.60	18100	4.36
BH12-13	2.09	subglacial till	18/03/2013	7.77	222.98	41.30	18300	5.96
BH12-16	2.55	subglacial till	18/03/2013	5.90	254.20	47.30	16000	6.70
BH12-18	2.85	subglacial till	18/03/2013	7.18	234.03	45.40	13400	5.58
BH12-20	3.15	subglacial till	18/03/2013	7.65	258.70	36.20	7200	4.67
BH12-22	3.46	subglacial till	18/03/2013	7.25	248.31	33.90	5830	3.58
BH12-26	4.07	subglacial till	18/03/2013	8.19	236.11	27.80	4250	3.38
BH13-4	1.02	ablation till	14/03/2013	9.57	194.81	39.80	17900	6.52
BH13-6	1.33	ablation till	14/03/2013	10.38	230.47	41.80	19800	8.31
BH13-8	1.63	ablation till	14/03/2013	7.48	220.12	42.60	20700	5.60
BH13-10	1.94	ablation till	14/03/2013	7.38	198.66	42.10	19800	5.25
BH13-14	2.55	ablation till	14/03/2013	7.59	237.81	39.90	14800	5.20
BH13-17	3.00	subglacial till	14/03/2013	9.55	227.90	30.80	9580	4.99
BH13-19	3.31	subglacial till	14/03/2013	10.22	221.25	25.20	7470	4.52
BH13-21	3.61	subglacial till	14/03/2013	10.71	199.95	21.50	6550	3.12
BH13-22	3.76	subglacial till	14/03/2013	10.85	240.28	18.80	5720	2.83
BH13-24	4.07	subglacial till	14/03/2013	10.15	231.42	14.30	4500	2.23
BH13-26	4.37	subglacial till	14/03/2013	9.91	270.14	11.7	3360	1.70
BH13-28	4.68	subglacial till	14/03/2013	11.39	269.87	8.93	2390	1.42

Note:  
nm denotes not measured.

**Table D:** Soil pore-water chemistry results and direct-push EC selections.

Sample No.	Middle depth (m)	Lithological group	Squeeze date dd/mm/yyyy	Water loss during storage (%)	Wet mass prior to analysis (g)	EC corrected for water loss (mS/cm)	Cl <sup>-</sup> corrected for water loss (mg/L)	Temperature corrected 5-pt average D-P EC (mS/cm)
BH13-32	5.29	subglacial till	14/03/2013	11.48	293.50	6.80	1500	1.22
BH14-10	2.09	subglacial till	19/03/2013	10.36	212.64	23.70	9180	3.90
BH14-13	2.55	subglacial till	19/03/2013	8.89	225.67	26.80	8420	3.69
BH14-16	3.00	subglacial till	19/03/2013	9.92	211.20	27.10	6750	3.25
BH14-18	3.31	subglacial till	19/03/2013	7.84	219.11	24.20	4770	2.67
BH14-21	3.76	sand	19/03/2013	8.37	245.51	18.90	3210	2.32
BH14-23	4.07	sand	19/03/2013	9.10	256.21	18.40	2850	2.22
BH14-24	4.22	sand	19/03/2013	10.18	260.72	18.50	3040	1.92
BH14-28	4.83	subglacial till	19/03/2013	6.89	246.41	9.43	1700	1.54
BH14-31	5.29	subglacial till	19/03/2013	8.37	257.96	7.44	1300	1.35

Note:

nm denotes not measured.

APPENDIX E  
HYDRAULIC CONDUCTIVITY RESULTS

**Table E1:** Saturated hydraulic conductivity results from bail testing of piezometers.

Piezometer ID	Lithology screened	Sandpack interval (mbg)	Borehole radius (m)	Static level (mbg)	Level at time=0 s (mbg)	Observed drawdown (m)	From log H/Ho plots			Analysis method	Hydraulic conductivity (m/s)	
							H1	H2	T1 (s)			T2 (s)
MW1	GL	2.74 - 3.50	0.041	1.642	1.904	0.262	0.6	0.3	140000	420000	Hvorslev	3.1E-09
MW2	GL	3.66 - 4.42	0.041	1.516	1.772	0.256	0.9	0.3	20000	320000	Hvorslev	4.5E-09
2008-08†	till	7.04 - 9.08	0.064	1.102	2.126	1.024	0.9	0.1	0	980000	Hvorslev	1.2E-09
2008-09†	till	3.05 - 4.91	0.064	0.744	1.412	0.667	0.9	0.4	0	26000	Hvorslev	1.8E-08
2009-06†	GL	2.4 - 7.3	0.076	2.742	3.107	0.365	0.8	0.3	0	180	Bouwer-Rice†	5.1E-06
2010-02A	GL	11.0 - 13.5	0.102	0.313	0.485	0.172	0.4	0.2	6000	13500	Hvorslev	3.8E-08
2010-02B	GL	2.1 - 6.05	0.102	0.623	1.006	0.383	0.8	0.5	0	120	Hvorslev	1.2E-06
2010-03B†	GL	5.5 - 9.04	0.102	1.406	2.388	0.982	1	0.37	0	8100	Hvorslev	4.0E-08
2010-04†	GL/till	3.4 - 7.6	0.102	0.383	1.201	0.818	0.66	0.41	6480	17280	Hvorslev	1.3E-08
2010-06†	GL/till	2.4 - 6.1	0.076	1.628	2.259	0.631	0.8	0.2	0	6115	Hvorslev	7.8E-08

Note:

1. Casing radius for all piezometers was 0.0254 m.

2. GL denotes glaciolacustrine.

† Observed drawdown higher than 0.25 m expected because watera tubing removed from piezometers prior to introducing bailer.

‡ Additional parameters used in analysis: effective casing radius=0.054 m; parameter c from Bouwer and Rice [1976]=3.

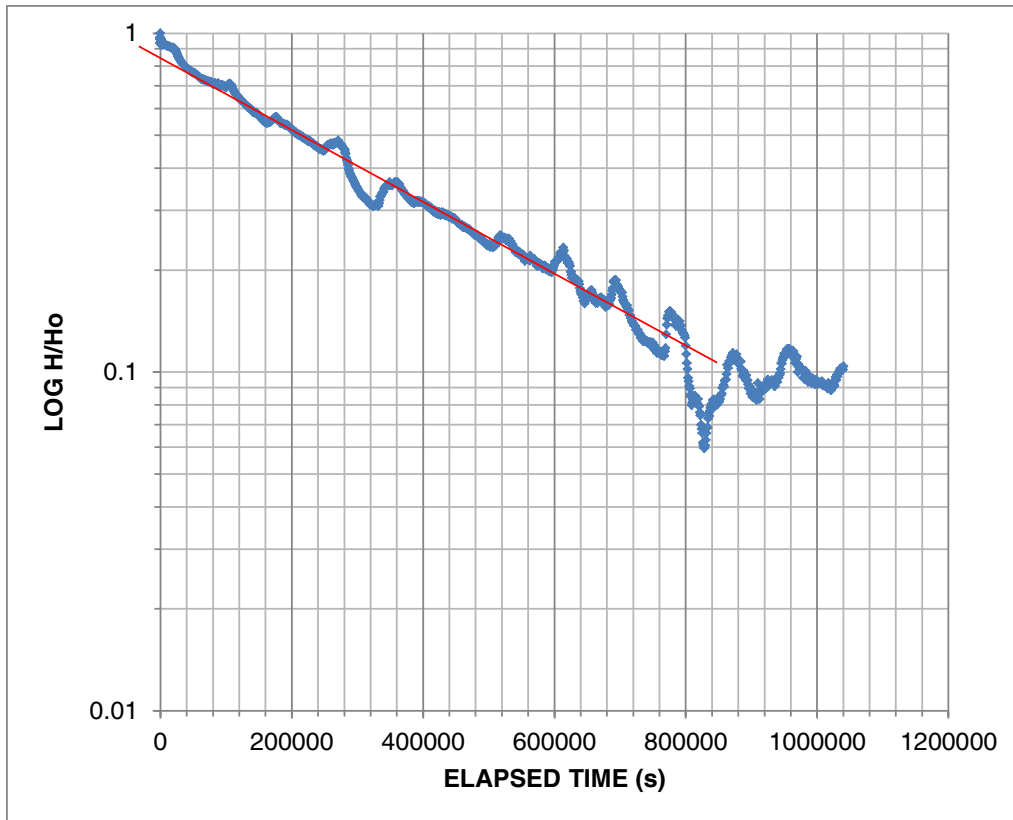


Figure E1:  
MW01

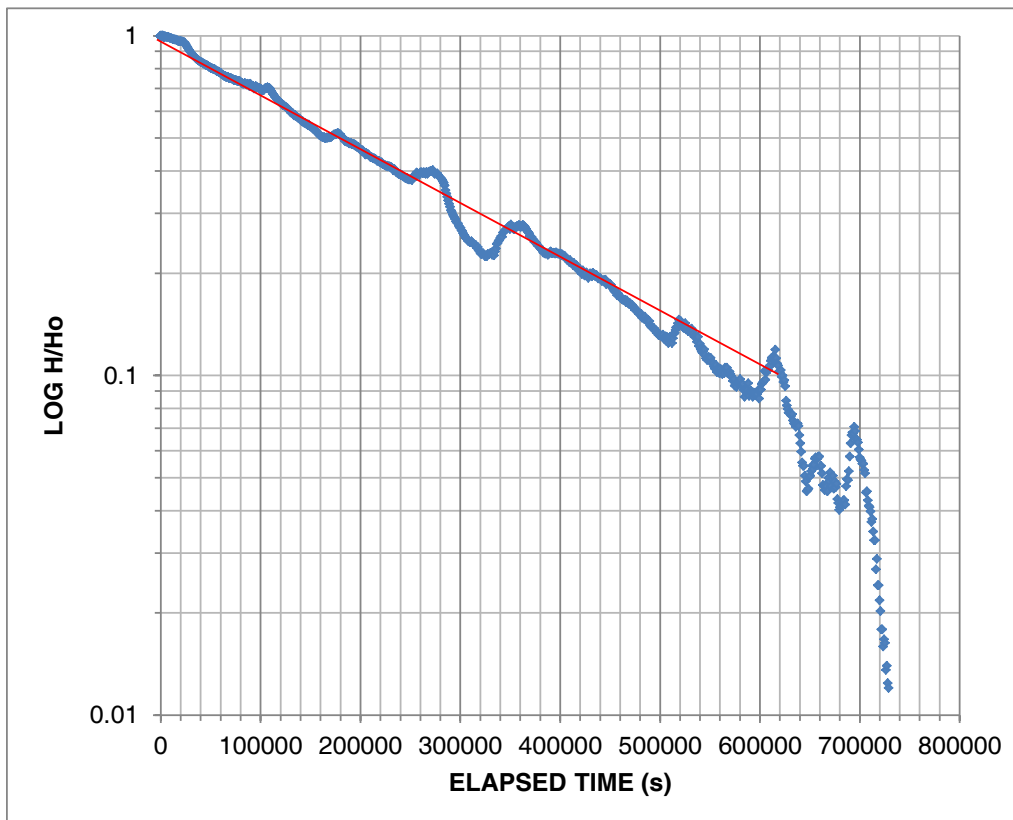


Figure E2:  
MW02

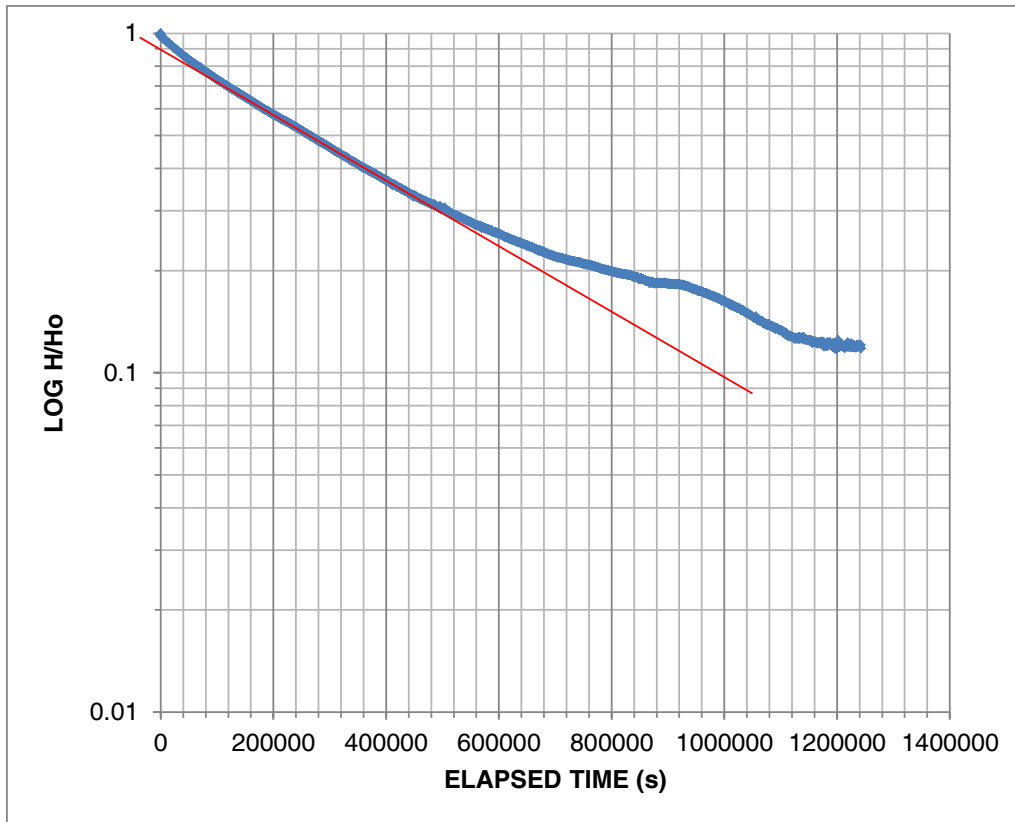


Figure E3:  
2008-08

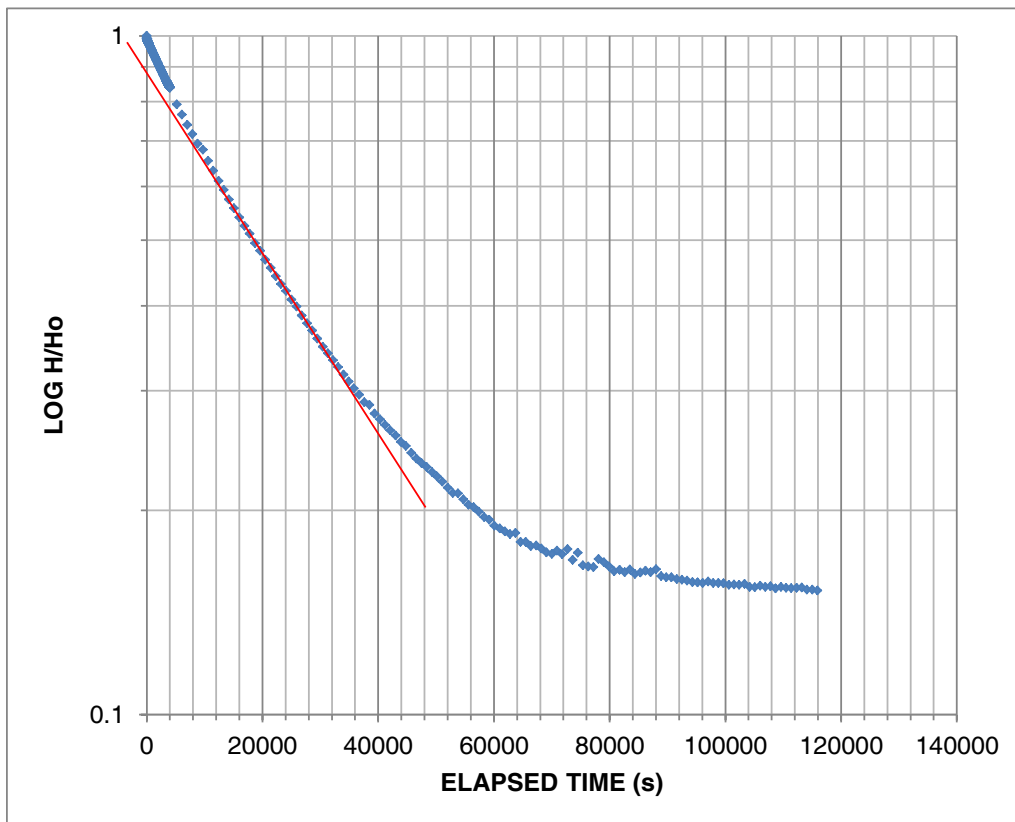


Figure E4:  
2008-09

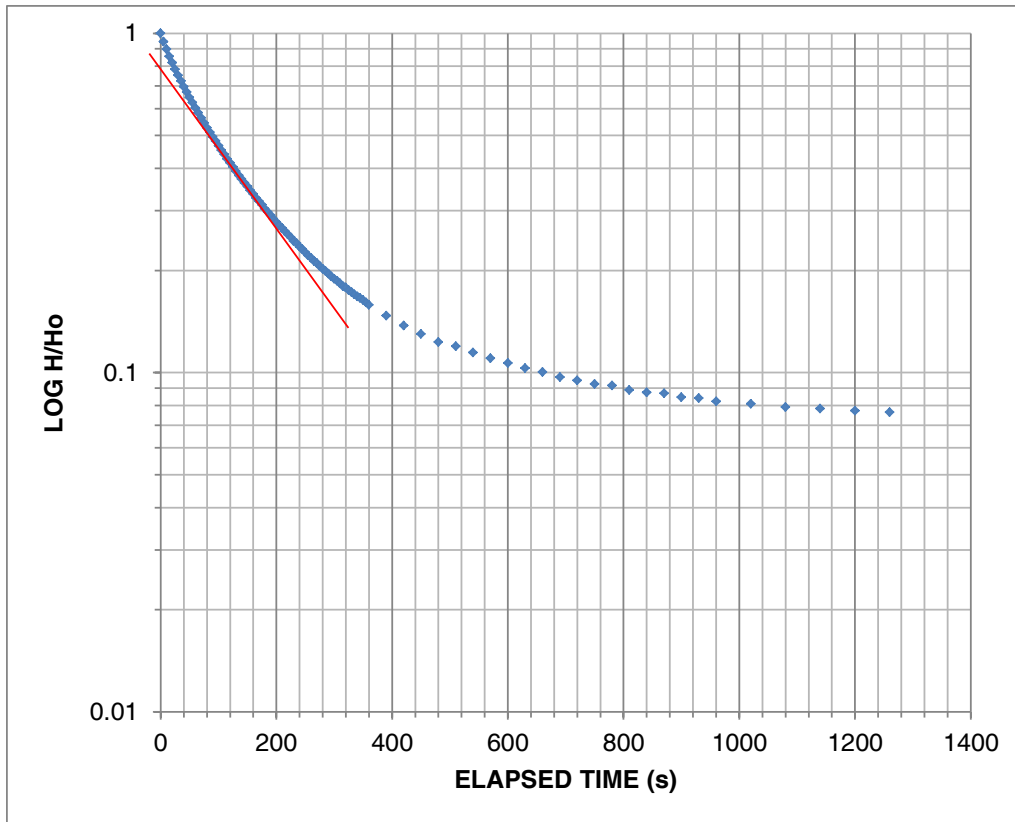


Figure E5:  
2009-06

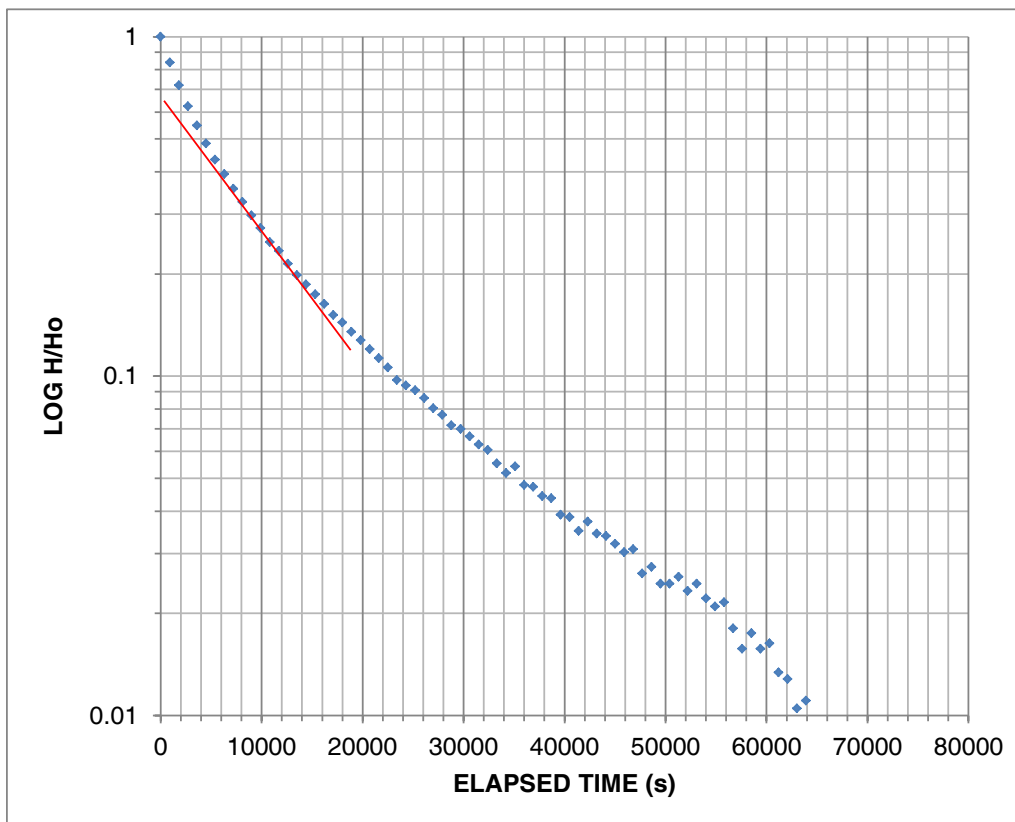


Figure E6:  
2010-02A

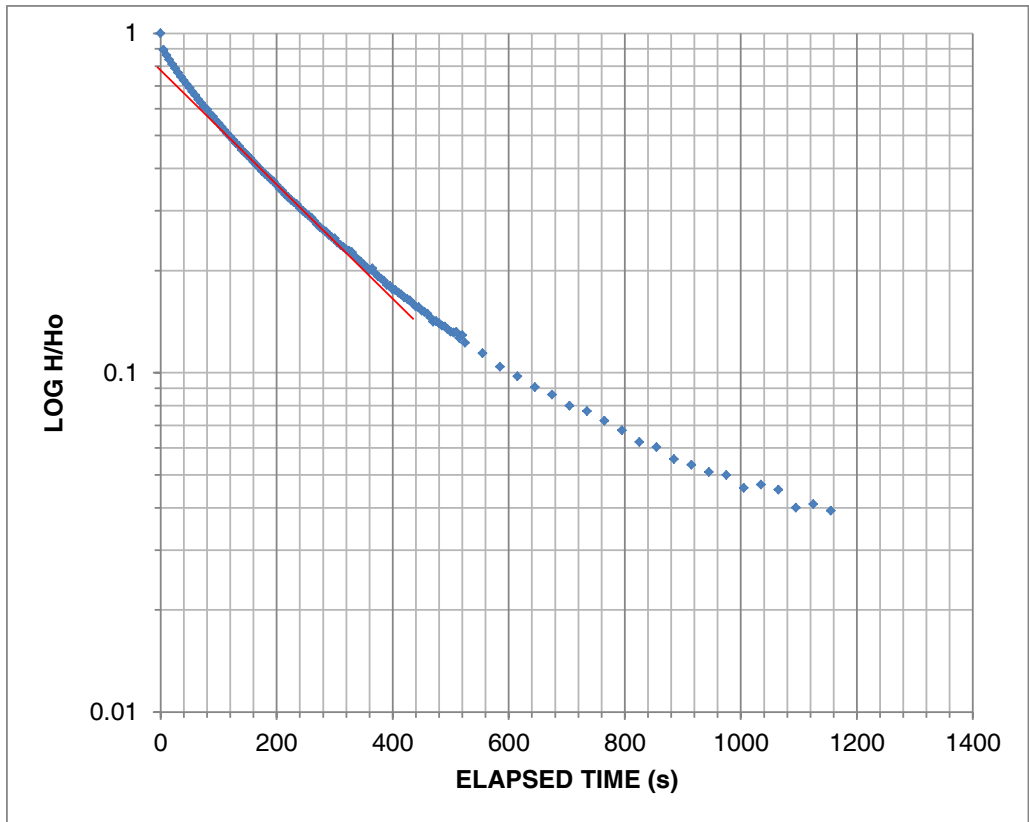


Figure E7:  
2010-02B

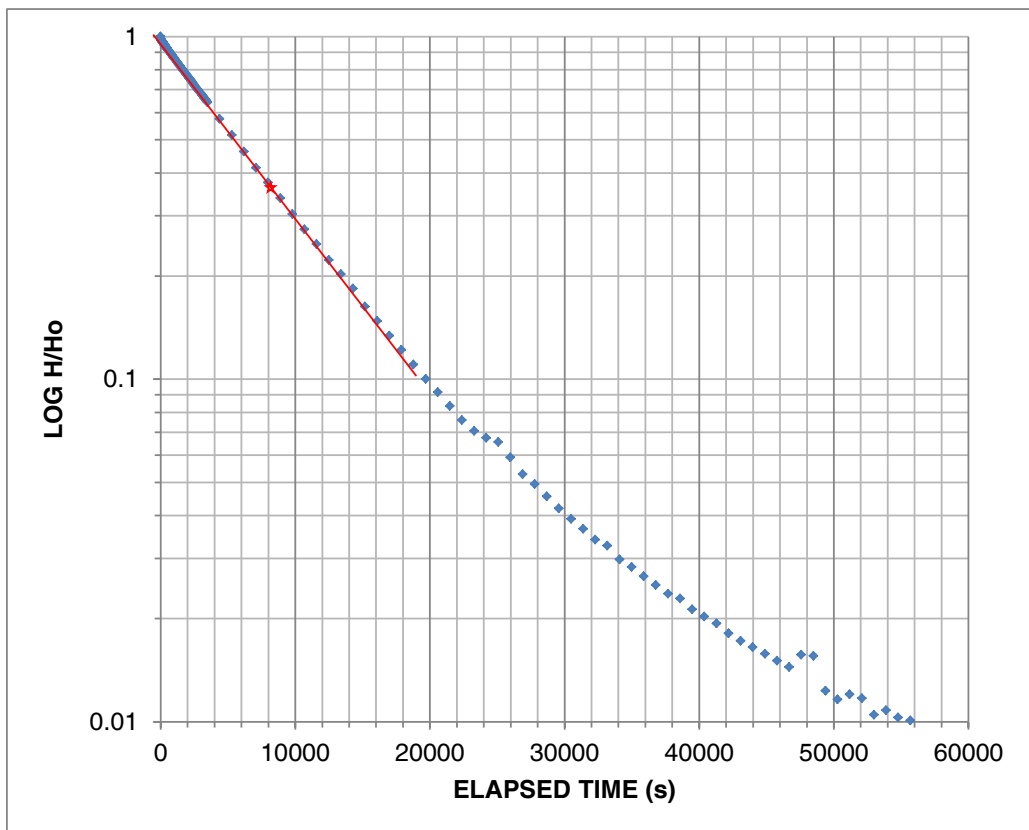


Figure E8:  
2010-03B

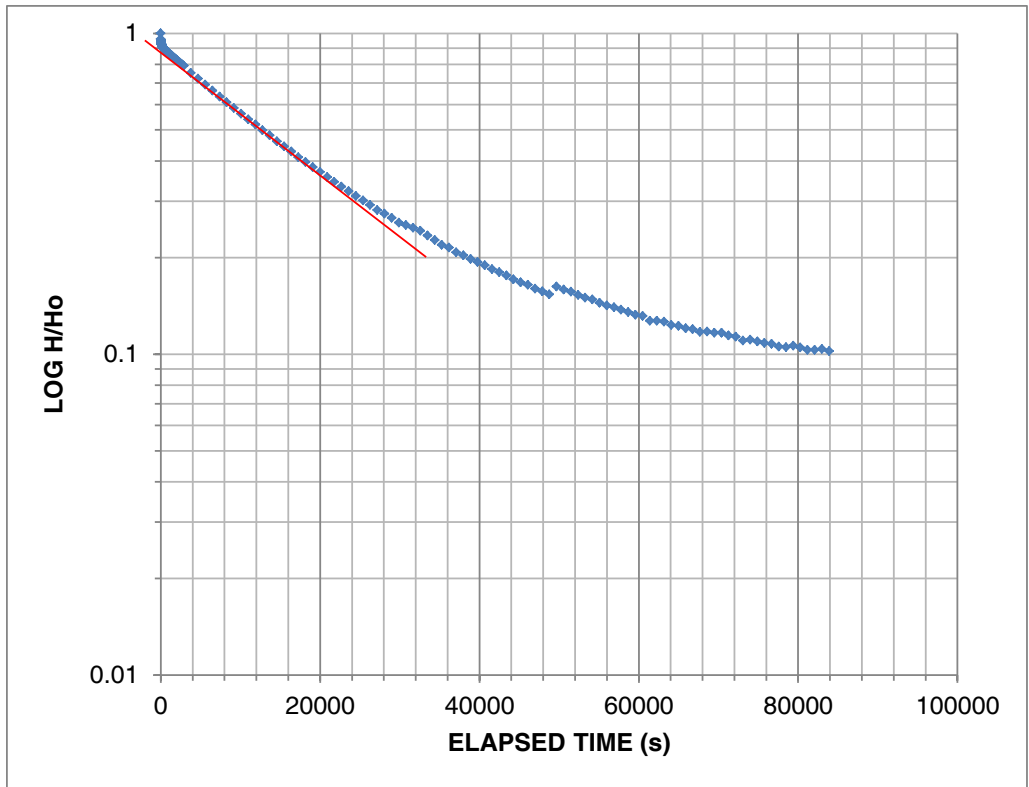


Figure E9:  
2010-04

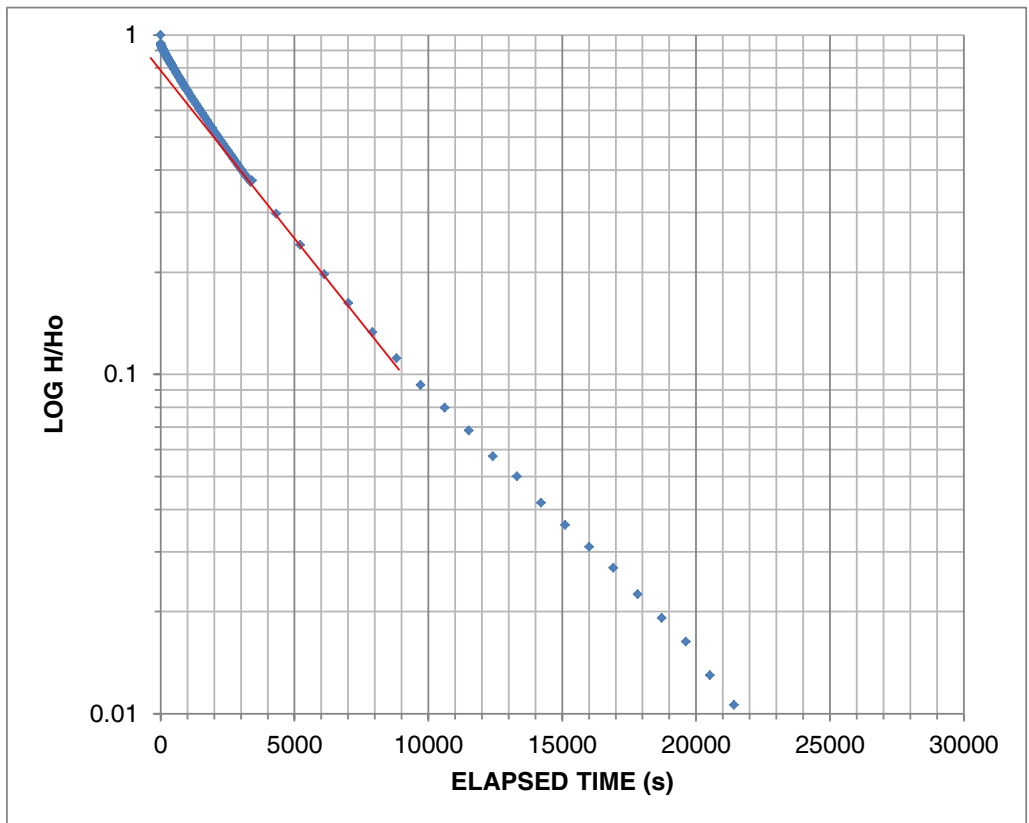
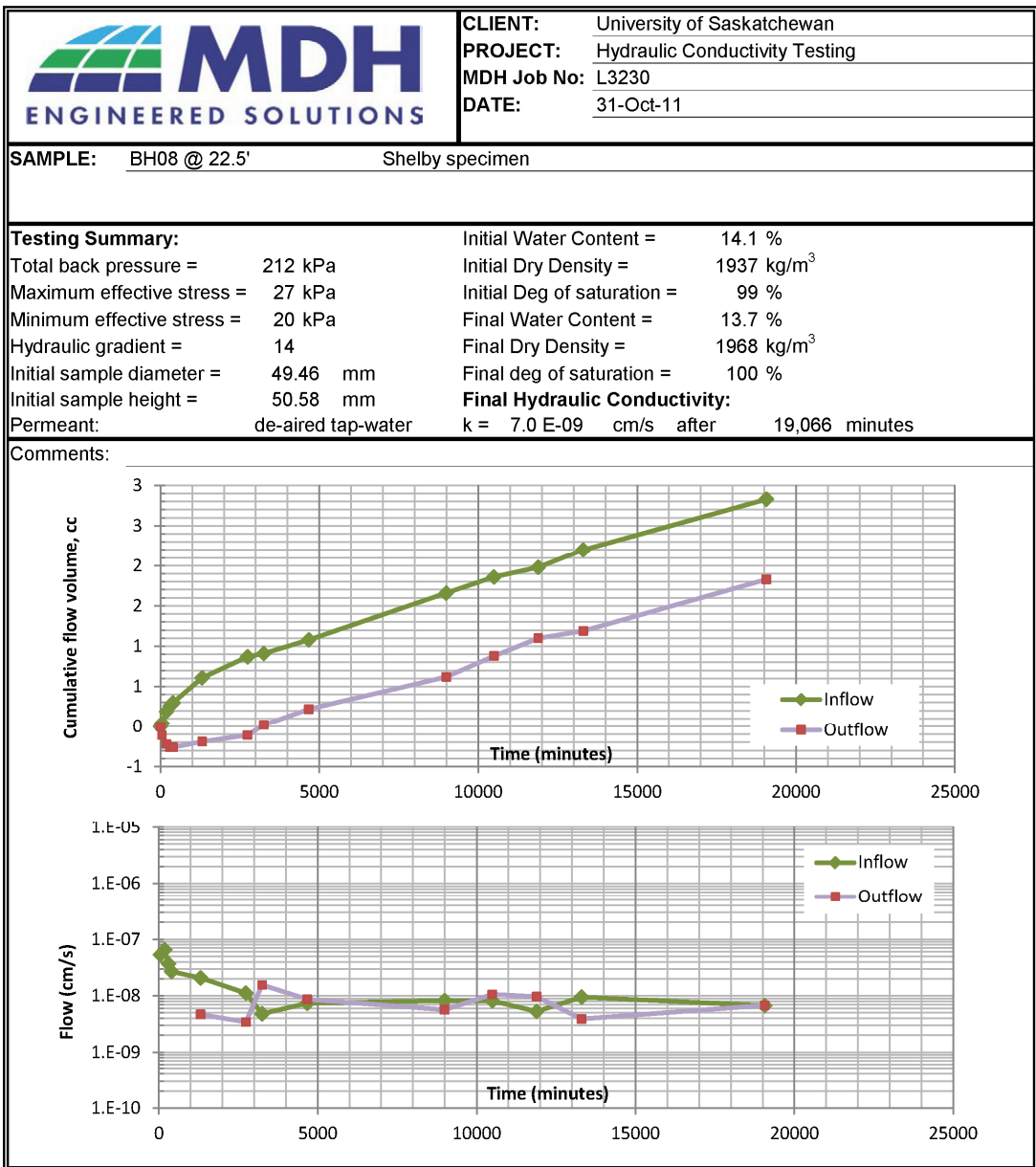


Figure E10:  
2010-06

# TRIAxIAL HYDRAULIC CONDUCTIVITY TEST REPORT

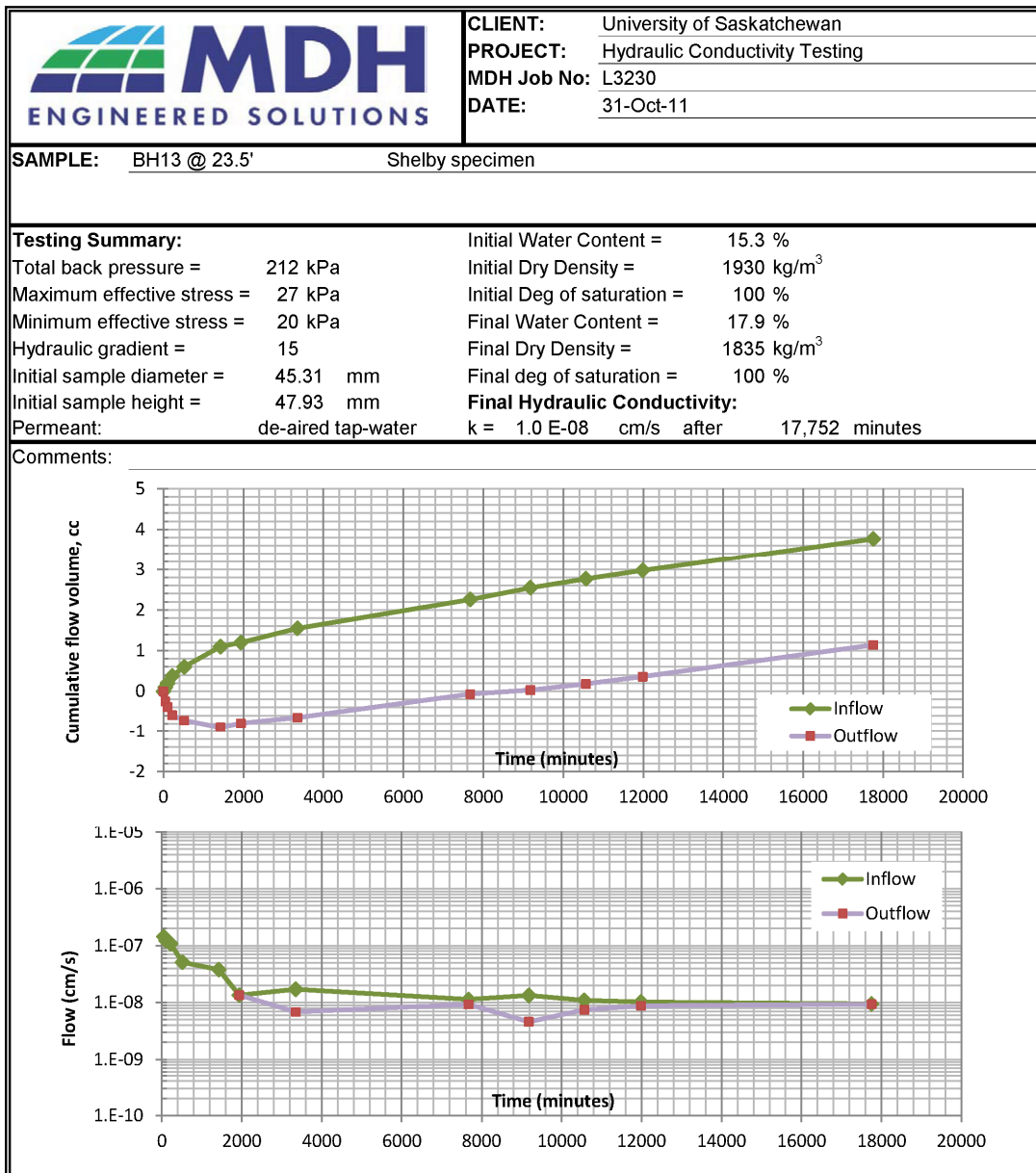
Test reference: ASTM D 5084



The testing services reported here have been performed in accordance with accepted local industry standards.  
 The results presented are for the sole use of the designated client only.  
 This report constitutes a testing service only. It does not represent any interpretation or opinion regarding specification compliance or material suitability.  
 Engineering interpretation will be provided by MDH Engineered Solutions Corp upon request.

# TRIAxIAL HYDRAULIC CONDUCTIVITY TEST REPORT

Test reference: ASTM D 5084



The testing services reported here have been performed in accordance with accepted local industry standards.

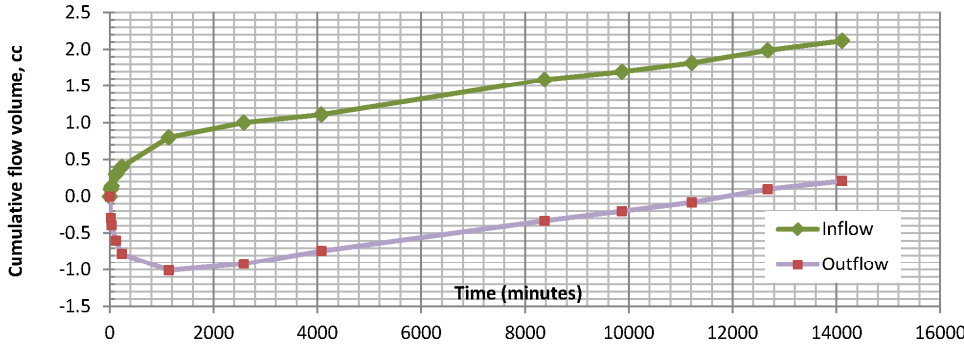
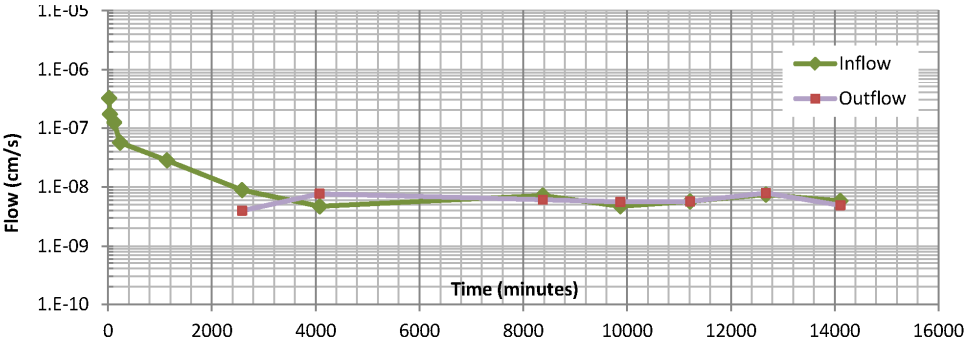
The results presented are for the sole use of the designated client only.

This report constitutes a testing service only. It does not represent any interpretation or opinion regarding specification compliance or material suitability.

Engineering interpretation will be provided by MDH Engineered Solutions Corp upon request.

# TRIAxIAL HYDRAULIC CONDUCTIVITY TEST REPORT

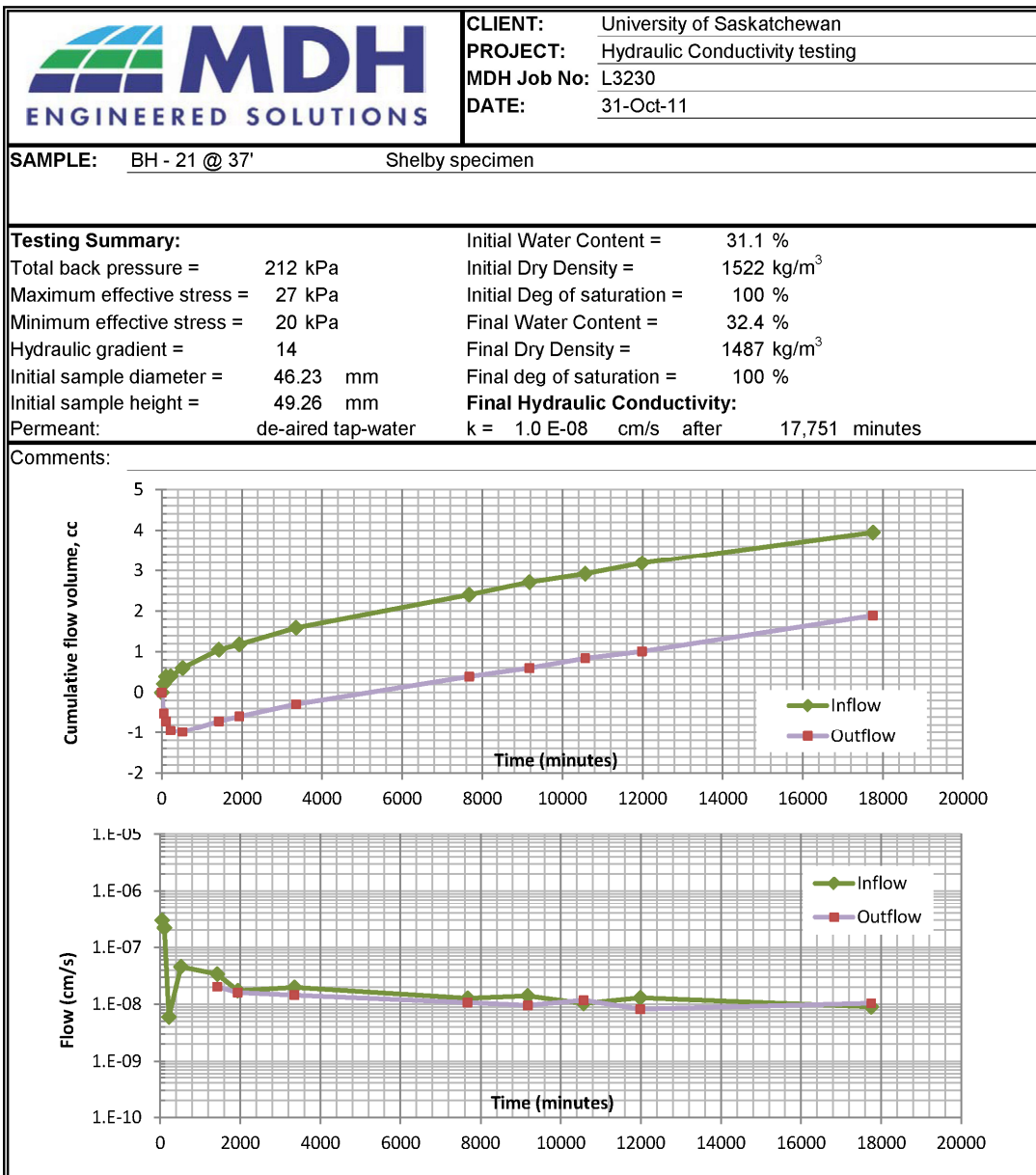
Test reference: ASTM D 5084

	<b>CLIENT:</b> University of Saskatchewan																
	<b>PROJECT:</b> Hydraulic Conductivity testing																
	<b>MDH Job No:</b> L3230																
	<b>DATE:</b> 15-Nov-11																
<b>SAMPLE:</b> BH21 @ 28' Shelby specimen																	
<b>Testing Summary:</b> <table style="width: 100%; border: none;"> <tr> <td style="width: 50%;">Total back pressure = 212 kPa</td> <td style="width: 50%;">Initial Water Content = 37.5 %</td> </tr> <tr> <td>Maximum effective stress = 27 kPa</td> <td>Initial Dry Density = 1331 kg/m<sup>3</sup></td> </tr> <tr> <td>Minimum effective stress = 20 kPa</td> <td>Initial Deg of saturation = 100 %</td> </tr> <tr> <td>Hydraulic gradient = 14</td> <td>Final Water Content = 38.0 %</td> </tr> <tr> <td>Initial sample diameter = 49.08 mm</td> <td>Final Dry Density = 1355 kg/m<sup>3</sup></td> </tr> <tr> <td>Initial sample height = 52.09 mm</td> <td>Final deg of saturation = 100 %</td> </tr> <tr> <td>Permeant: de-aired tap-water</td> <td><b>Final Hydraulic Conductivity:</b></td> </tr> <tr> <td></td> <td>k = 6.0 E-09 cm/s after 14,108 minutes</td> </tr> </table>		Total back pressure = 212 kPa	Initial Water Content = 37.5 %	Maximum effective stress = 27 kPa	Initial Dry Density = 1331 kg/m <sup>3</sup>	Minimum effective stress = 20 kPa	Initial Deg of saturation = 100 %	Hydraulic gradient = 14	Final Water Content = 38.0 %	Initial sample diameter = 49.08 mm	Final Dry Density = 1355 kg/m <sup>3</sup>	Initial sample height = 52.09 mm	Final deg of saturation = 100 %	Permeant: de-aired tap-water	<b>Final Hydraulic Conductivity:</b>		k = 6.0 E-09 cm/s after 14,108 minutes
Total back pressure = 212 kPa	Initial Water Content = 37.5 %																
Maximum effective stress = 27 kPa	Initial Dry Density = 1331 kg/m <sup>3</sup>																
Minimum effective stress = 20 kPa	Initial Deg of saturation = 100 %																
Hydraulic gradient = 14	Final Water Content = 38.0 %																
Initial sample diameter = 49.08 mm	Final Dry Density = 1355 kg/m <sup>3</sup>																
Initial sample height = 52.09 mm	Final deg of saturation = 100 %																
Permeant: de-aired tap-water	<b>Final Hydraulic Conductivity:</b>																
	k = 6.0 E-09 cm/s after 14,108 minutes																
<b>Comments:</b> <div style="display: flex; flex-direction: column; align-items: center;">   </div>																	

The testing services reported here have been performed in accordance with accepted local industry standards.  
 The results presented are for the sole use of the designated client only.  
 This report constitutes a testing service only. It does not represent any interpretation or opinion regarding specification compliance or material suitability.  
 Engineering interpretation will be provided by MDH Engineered Solutions Corp upon request.

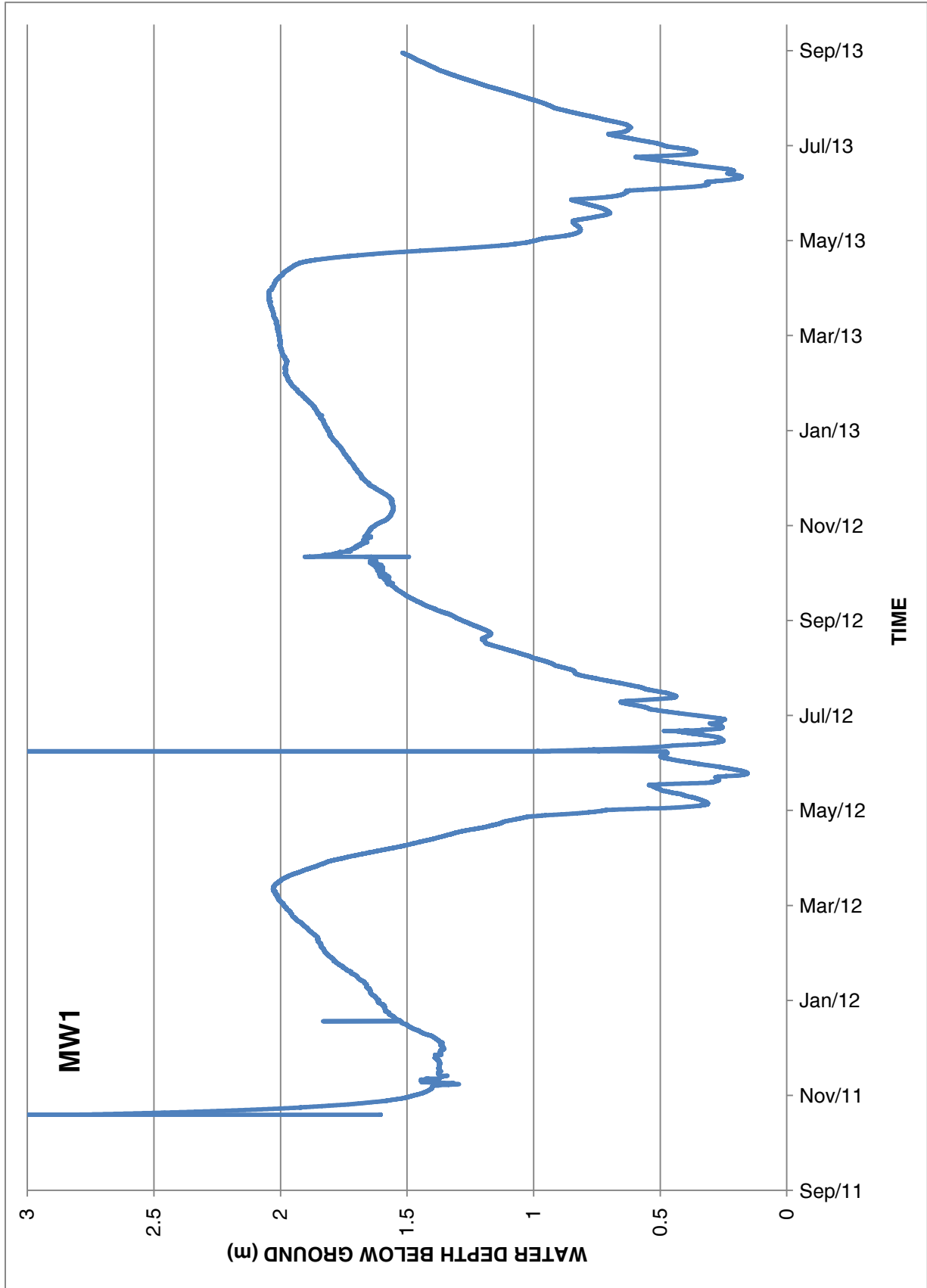
# TRIAxIAL HYDRAULIC CONDUCTIVITY TEST REPORT

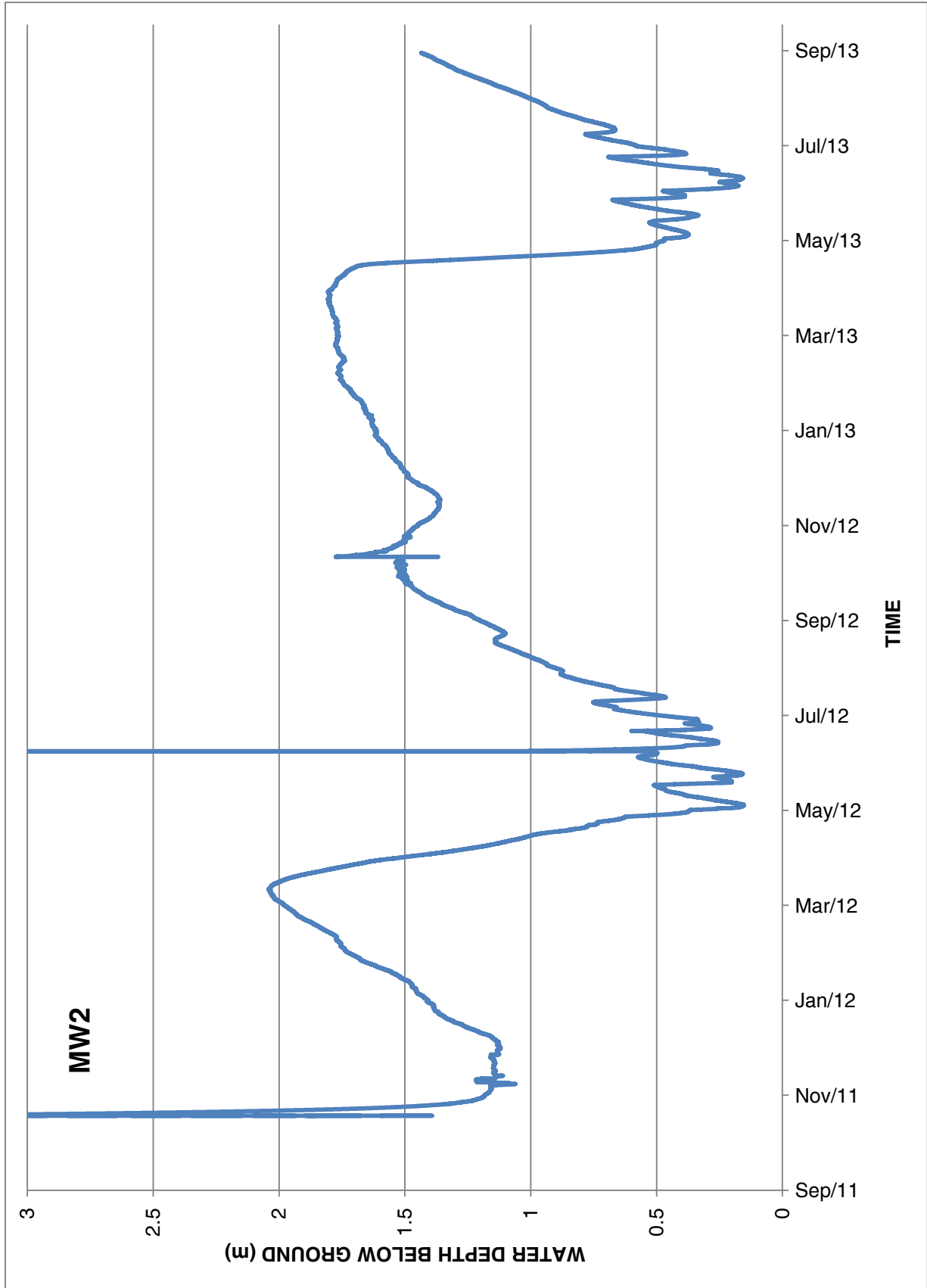
Test reference: ASTM D 5084

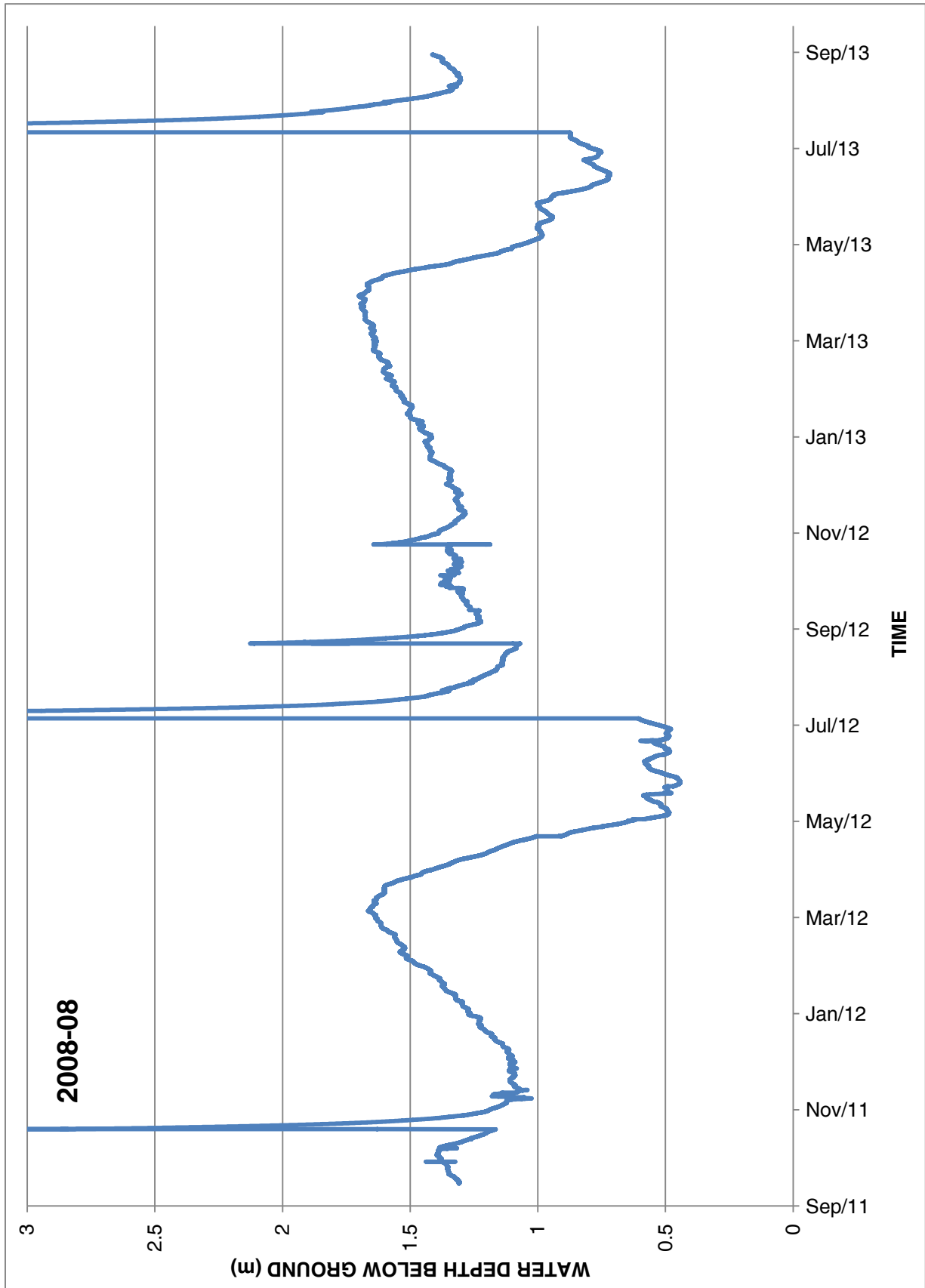


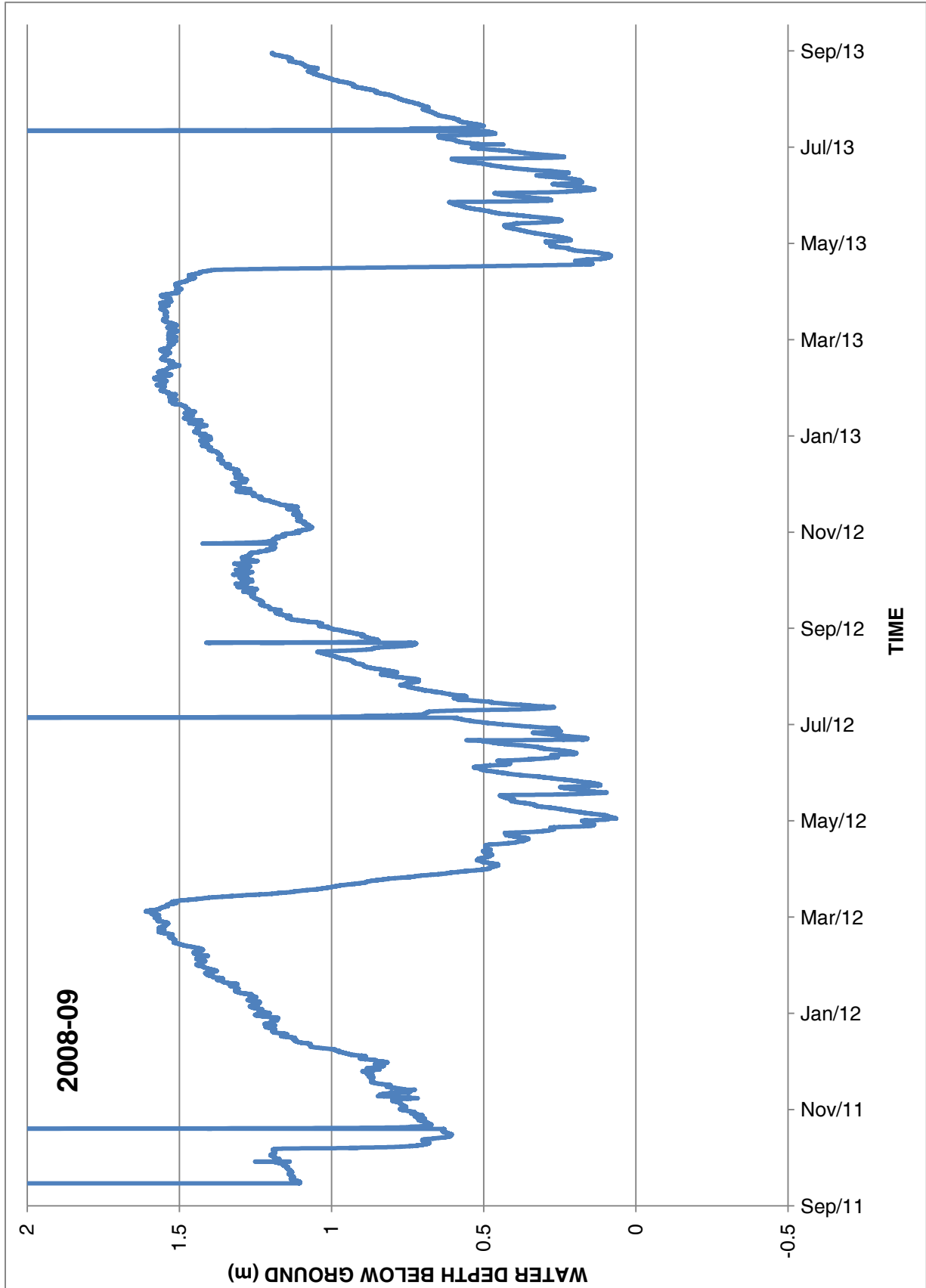
The testing services reported here have been performed in accordance with accepted local industry standards.  
 The results presented are for the sole use of the designated client only.  
 This report constitutes a testing service only. It does not represent any interpretation or opinion regarding specification compliance or material suitability.  
 Engineering interpretation will be provided by MDH Engineered Solutions Corp upon request.

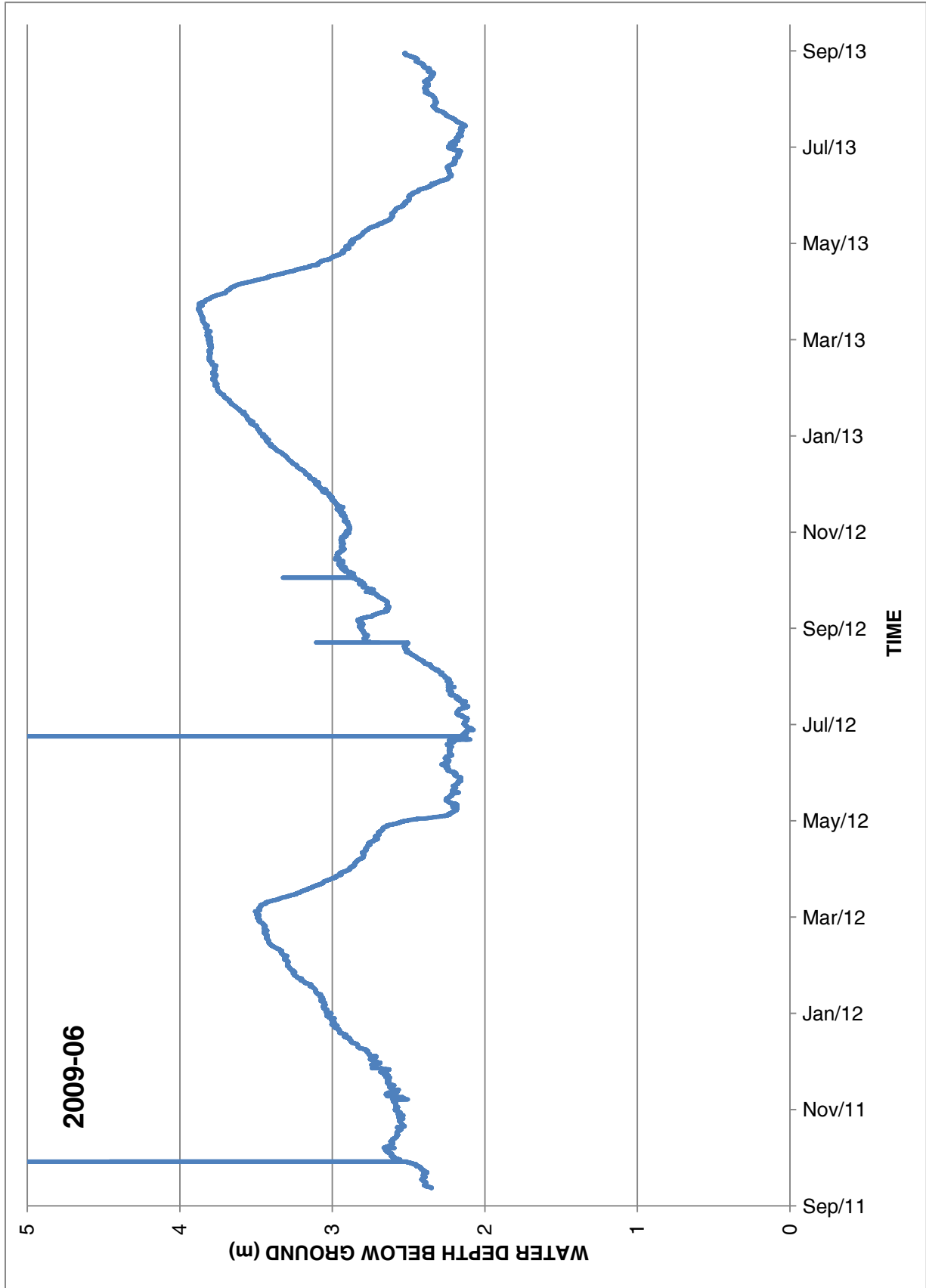
APPENDIX F  
GROUNDWATER HYDROGRAPHS

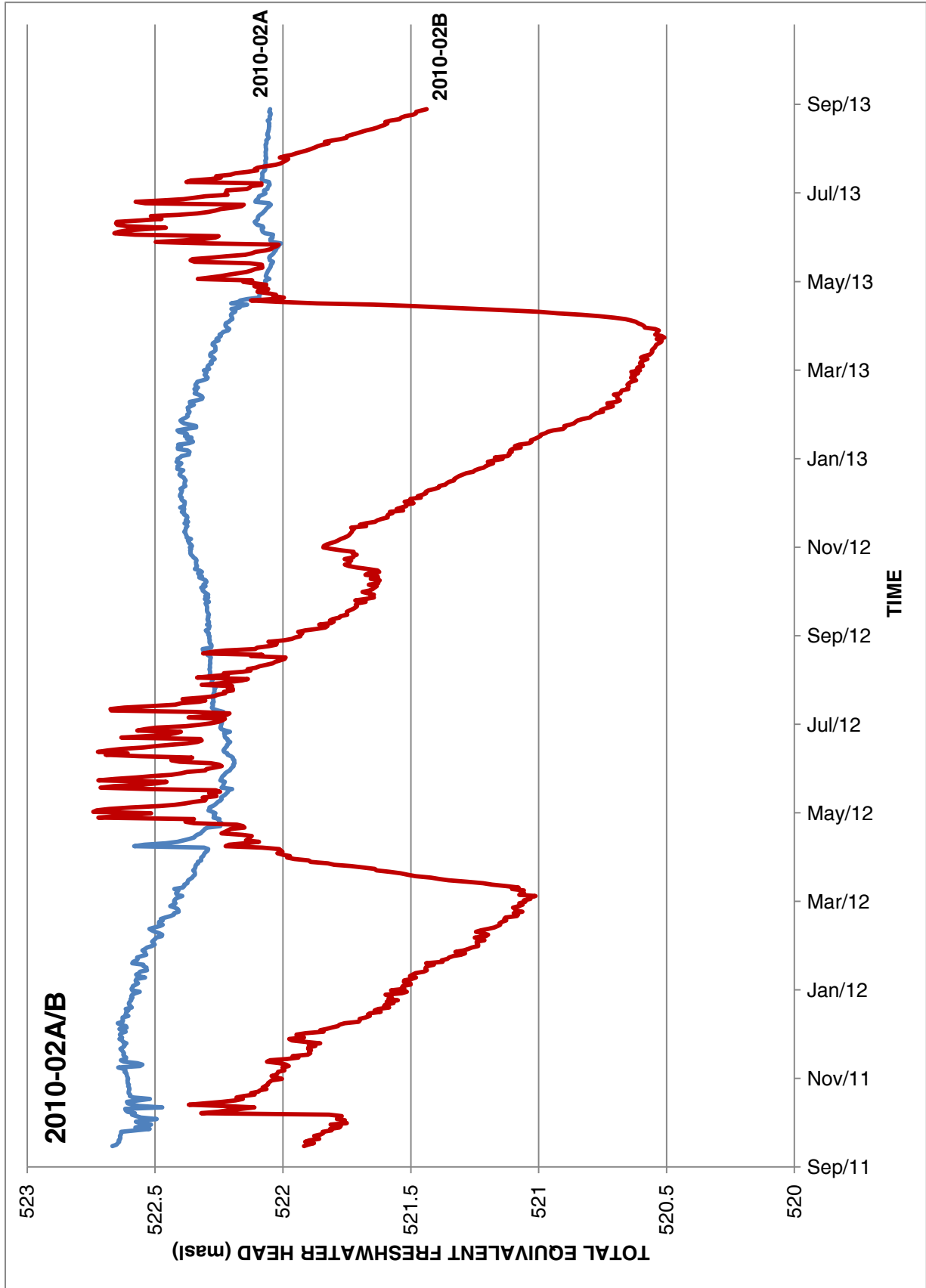


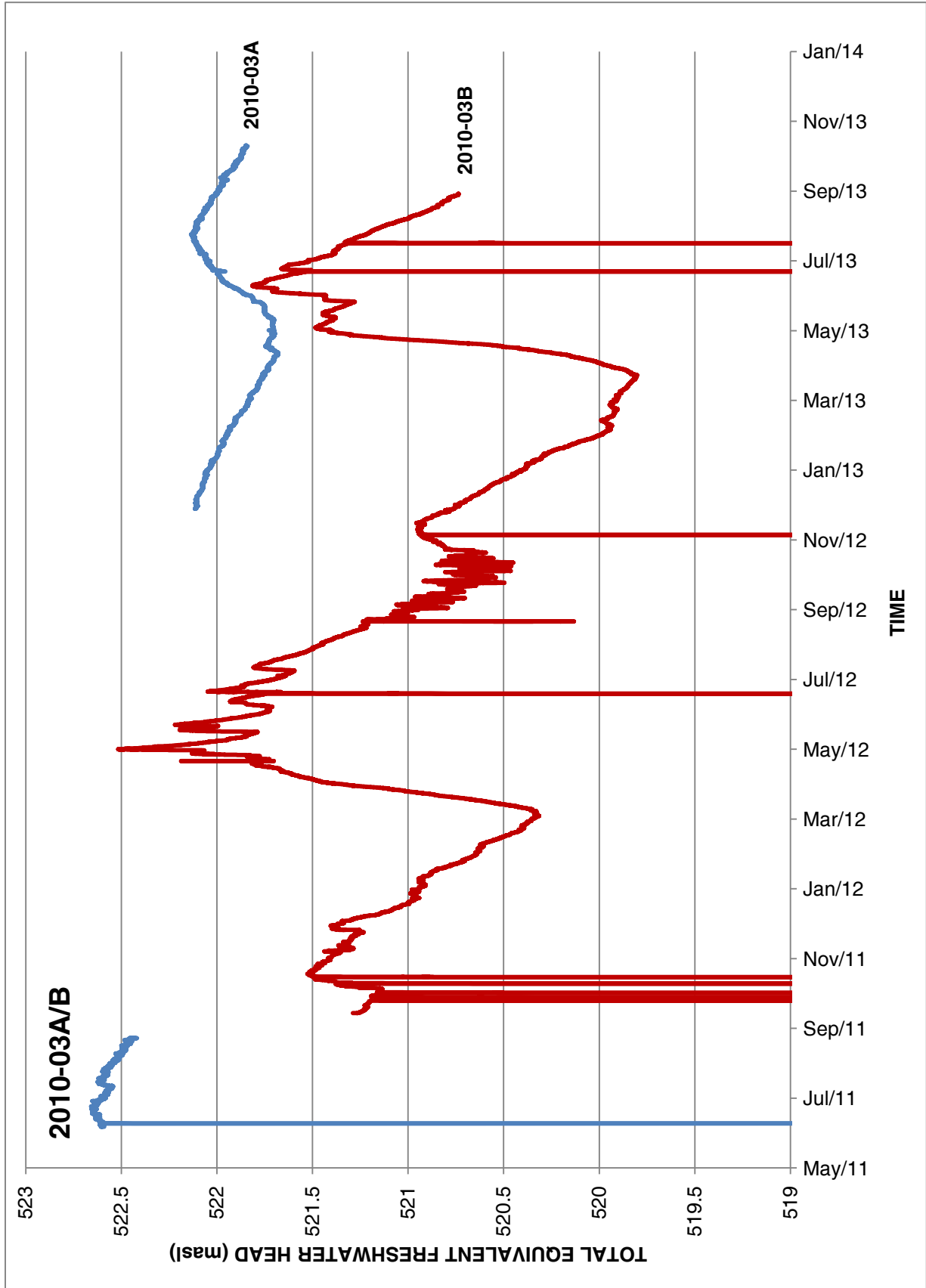


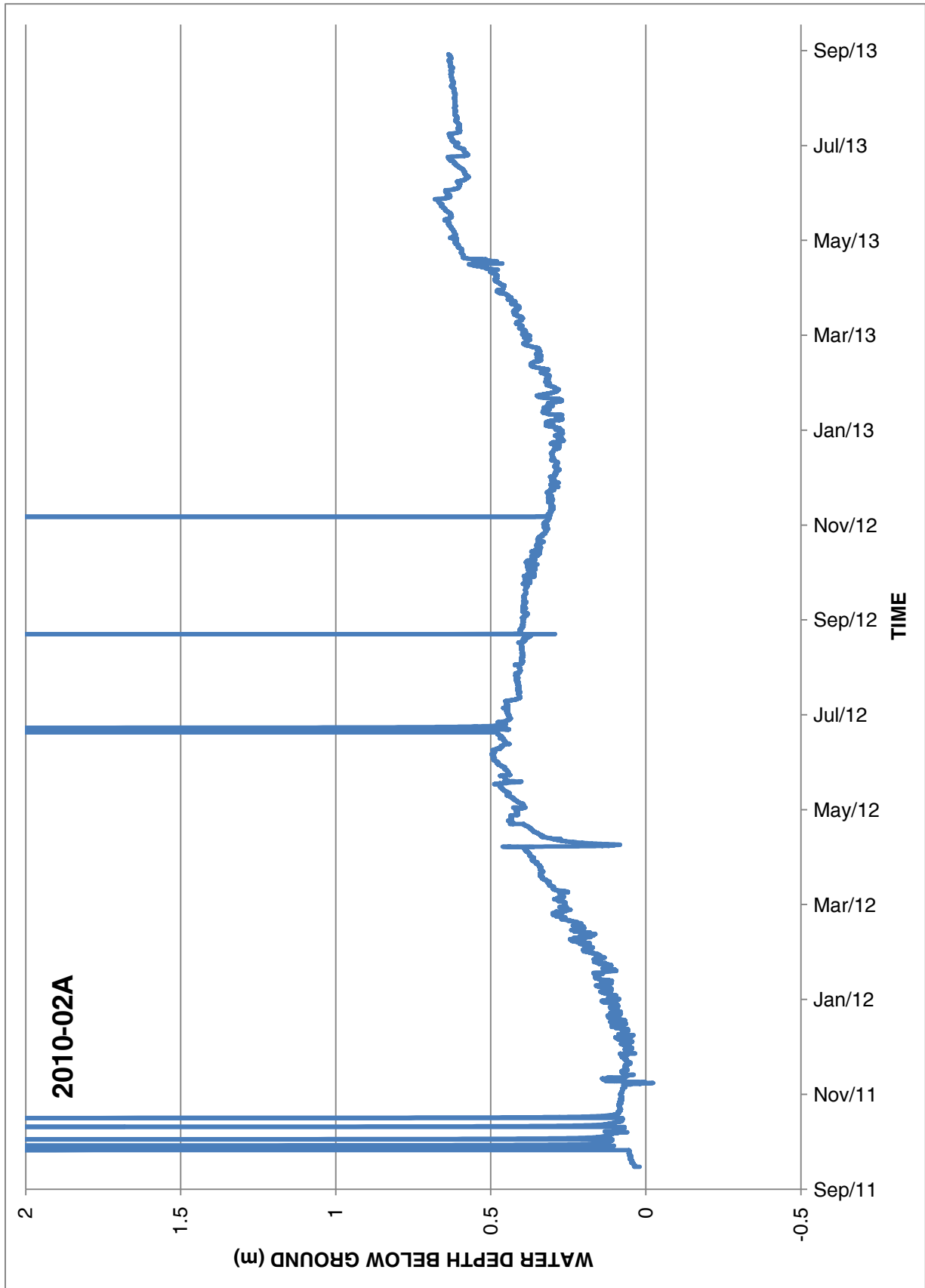


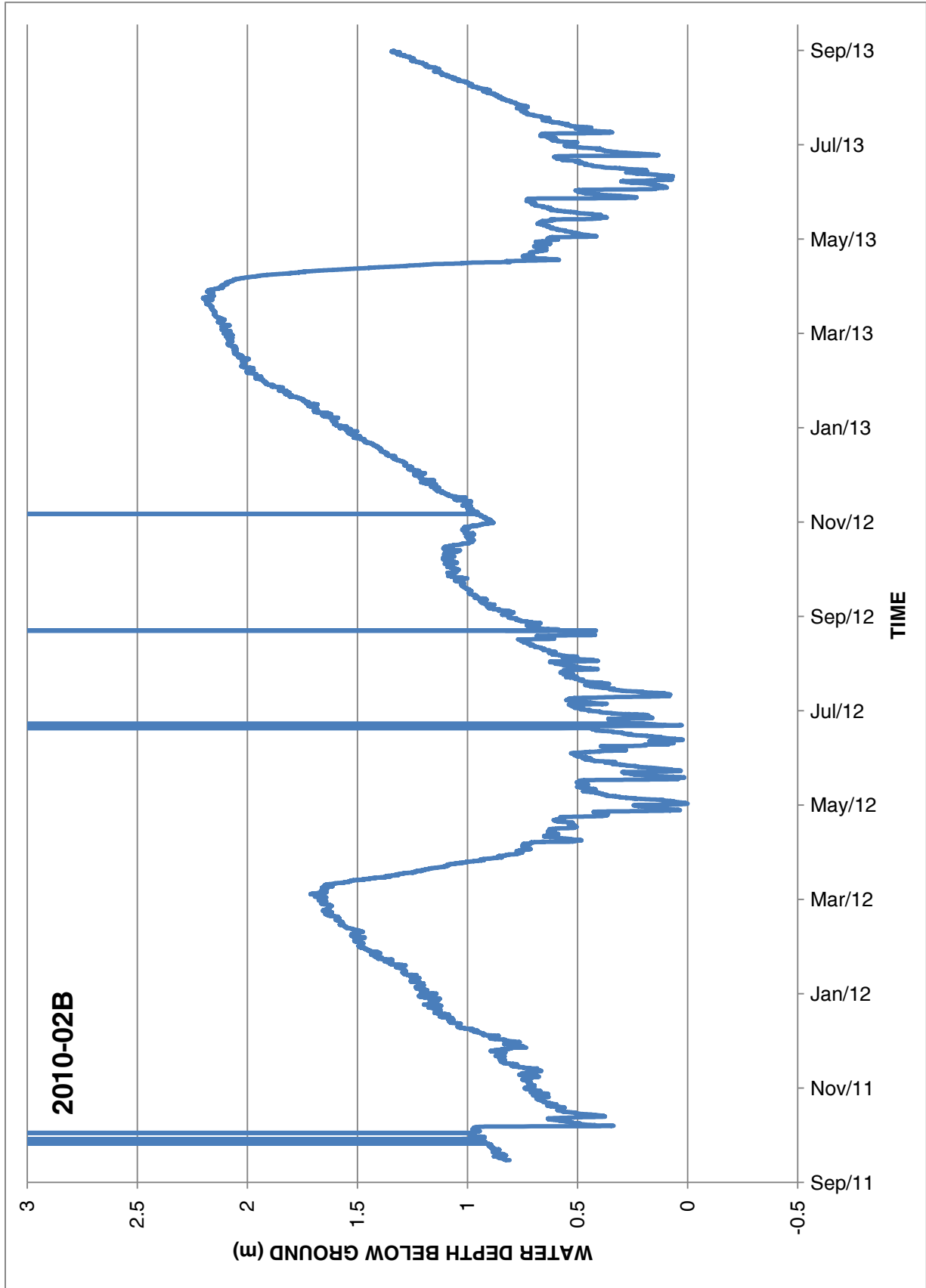


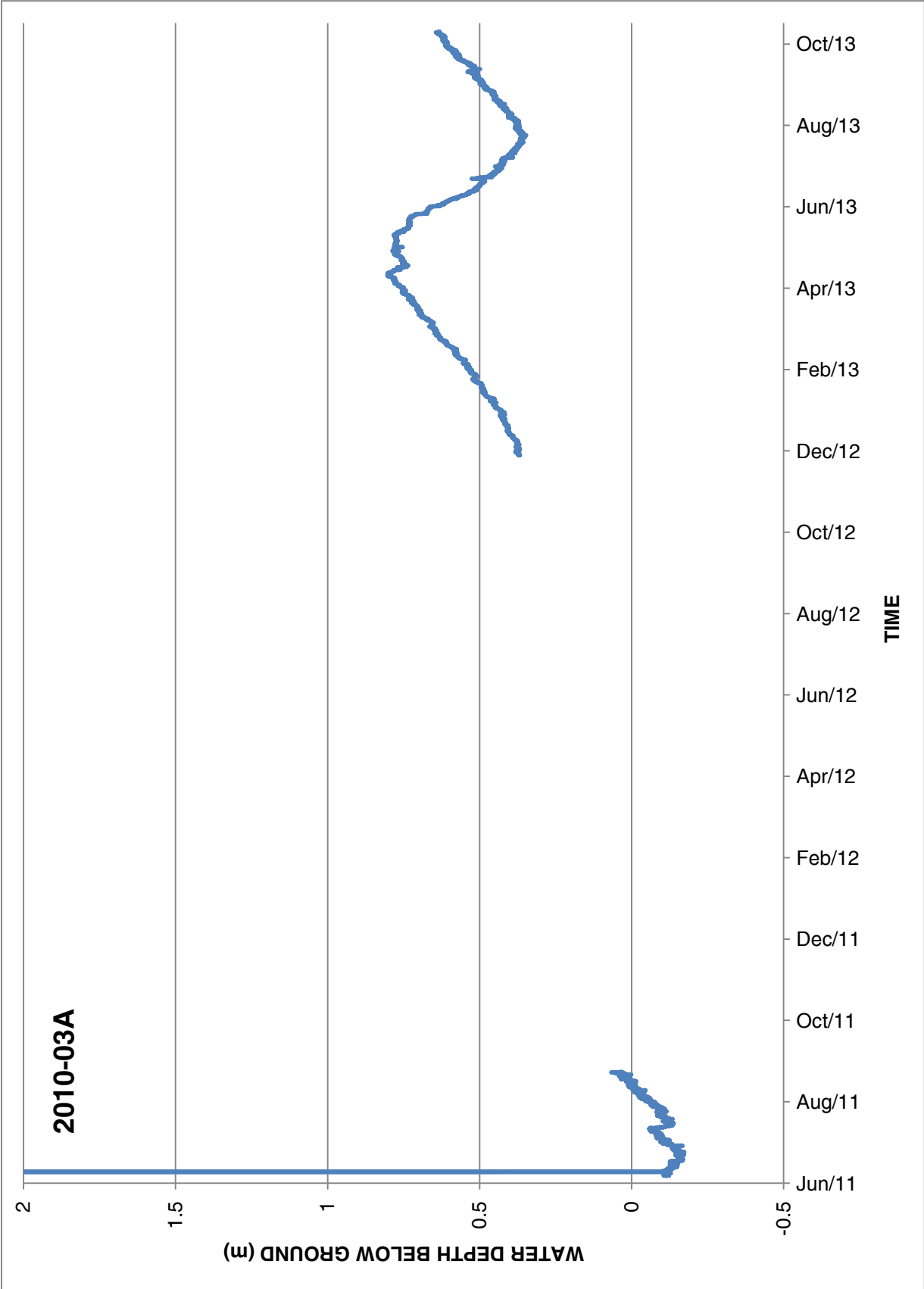


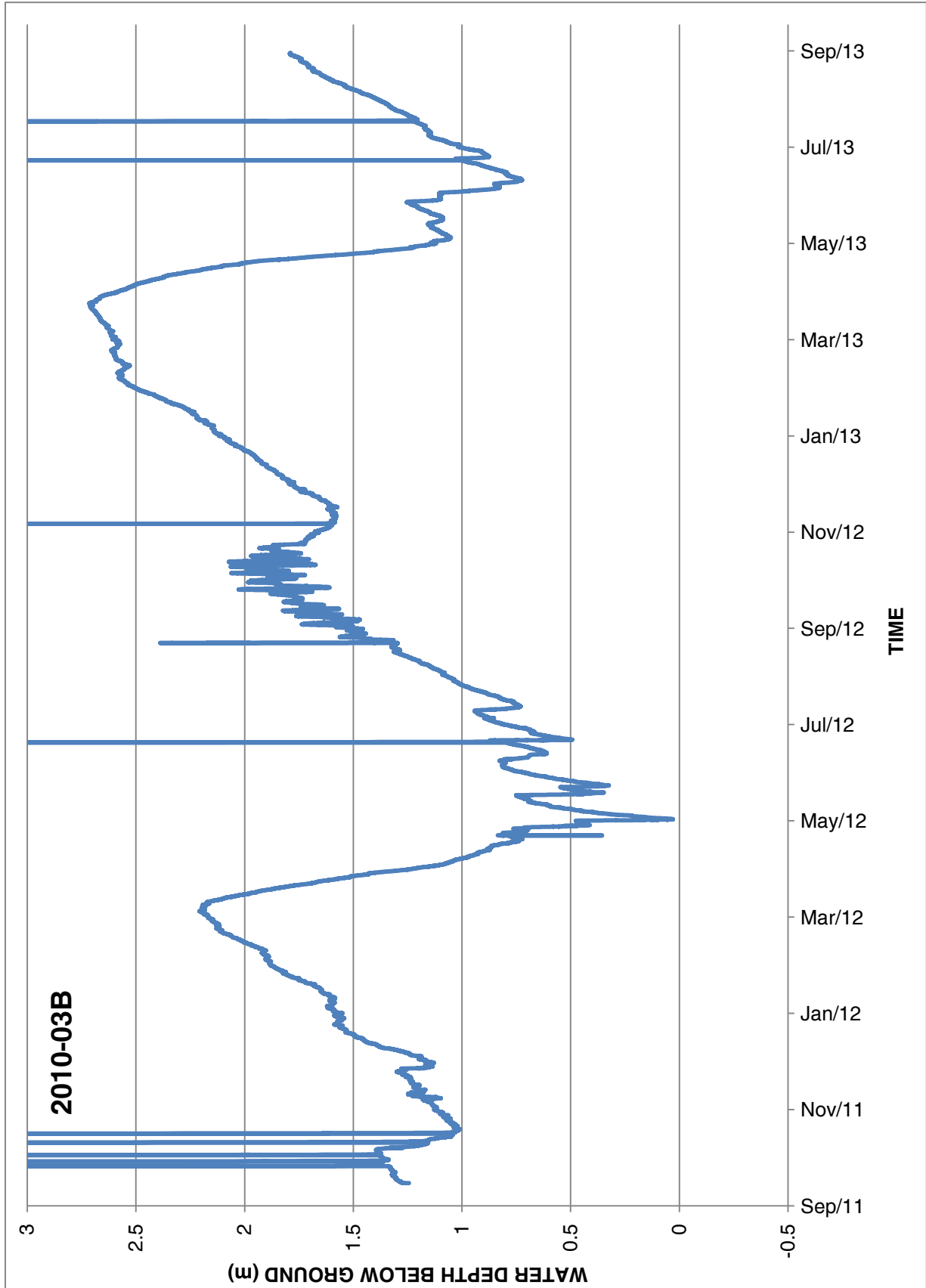


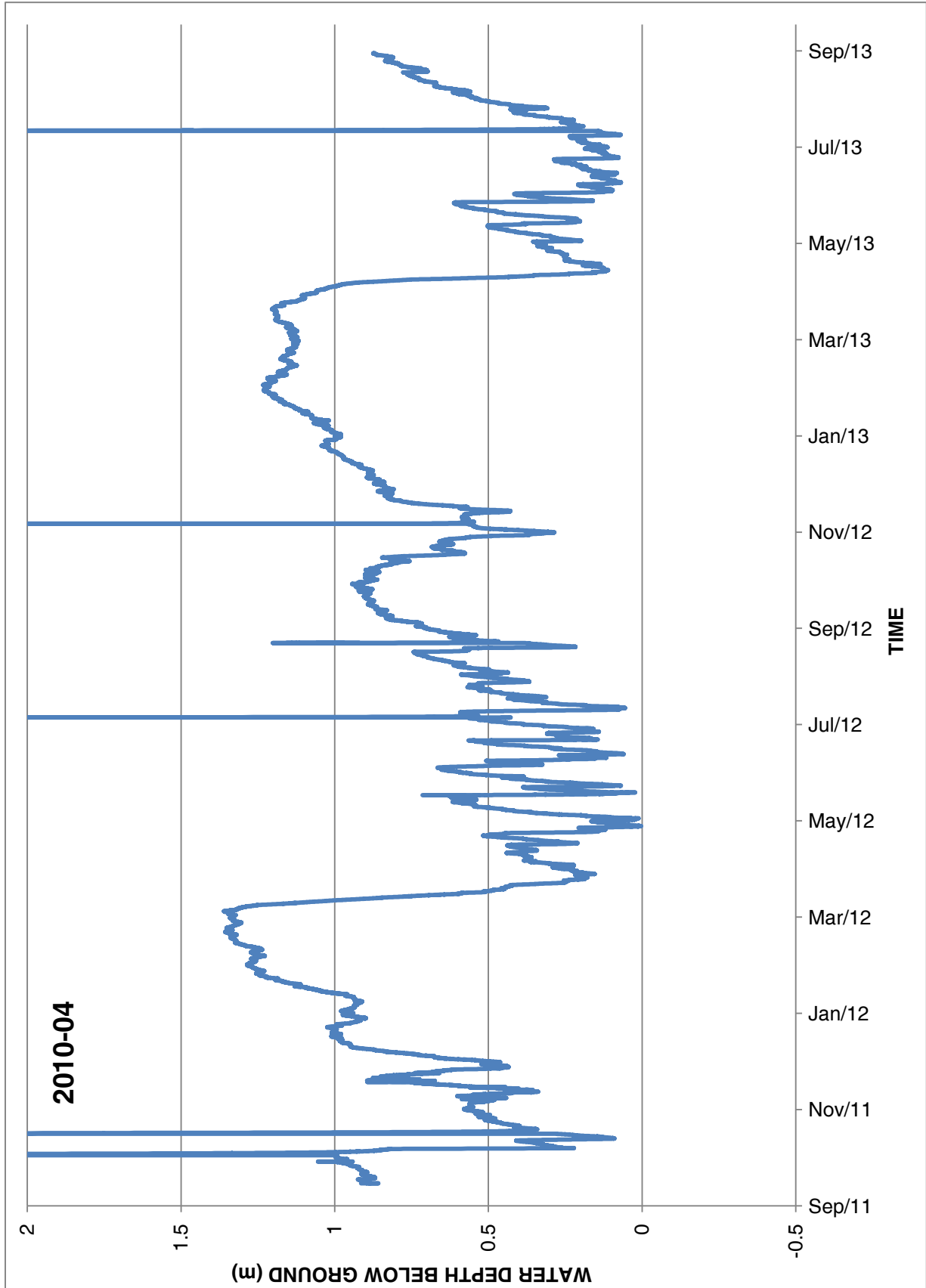


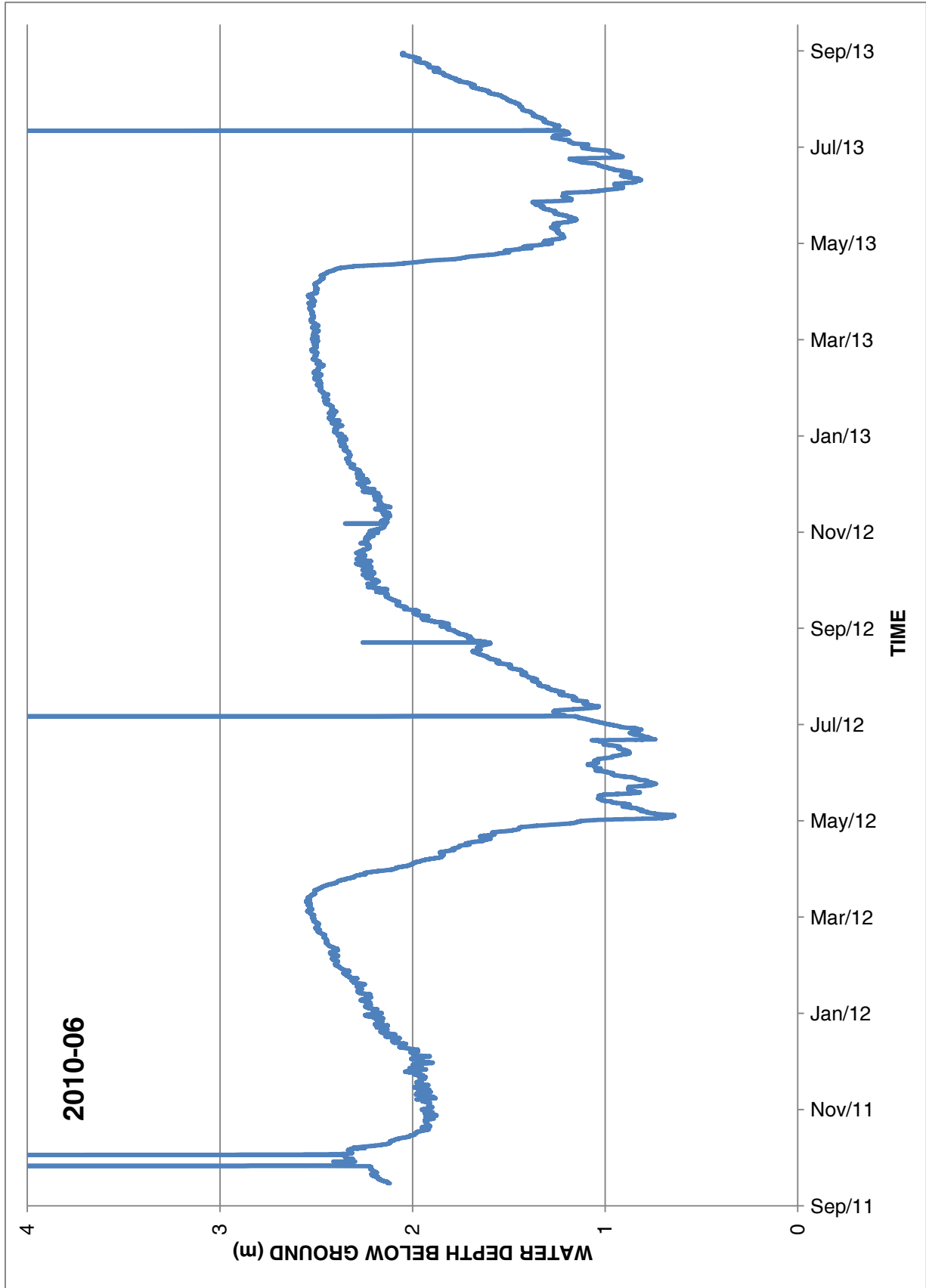


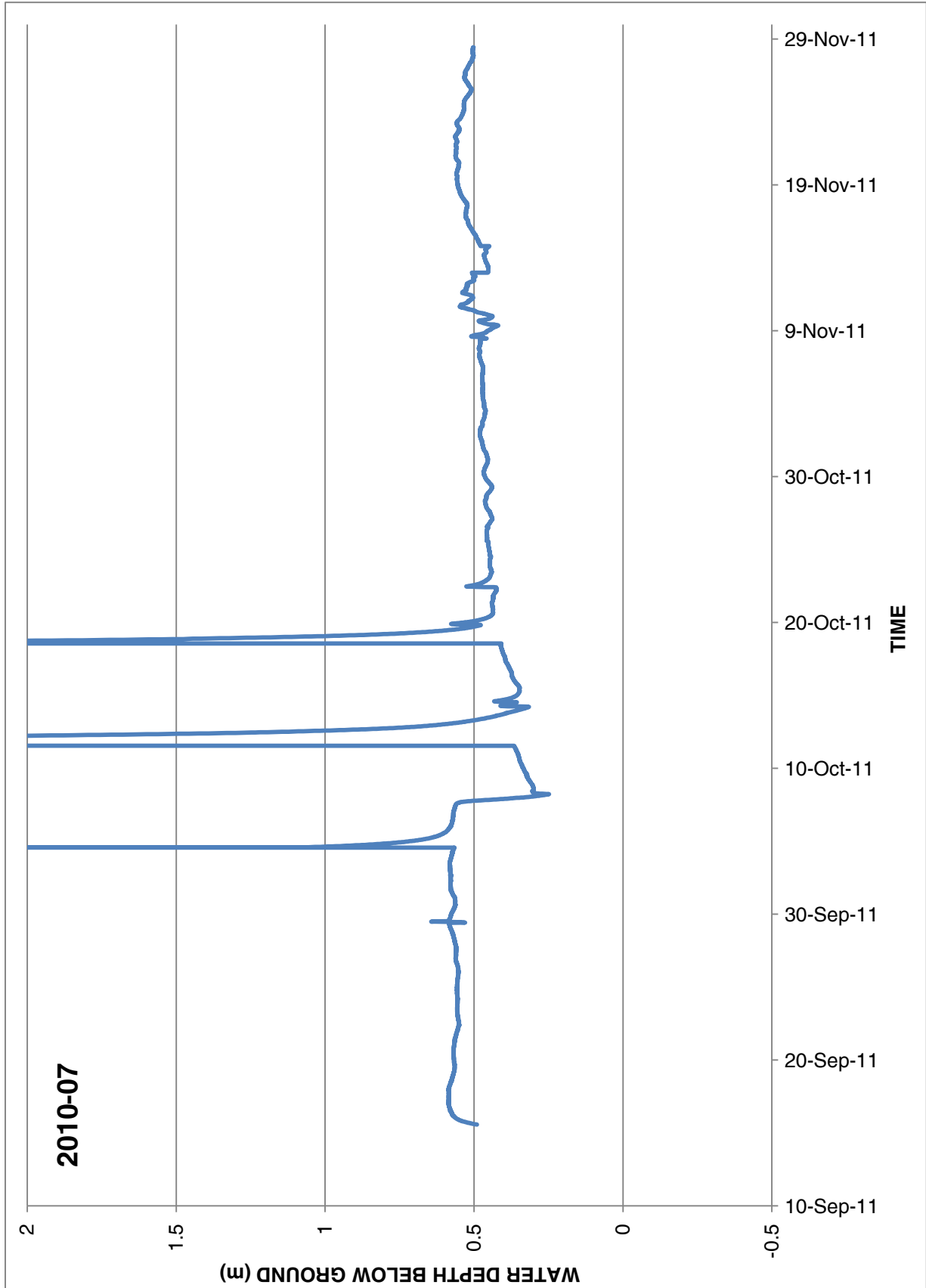












APPENDIX G  
SURFACE WATER CHEMISTRY

**Table G1:** Surface water EC and Cl results.

Location	Sample ID	Sample Date dd/mm/yyyy	EC ( $\mu$ S/cm)	Cl (mg/L)
mill outflow	mill out	29/06/2012	na	170000
		duplicate	na	169000
		28/08/2012	na	179000
		31/10/2012	na	186000
brine source	BP	02/06/2011	23100	7140
		duplicate	na	7860
		21/10/2011	12250	3560
		30/04/2012	location dry	
		29/06/2012	17770	5290
		28/08/2012	location dry	
		31/10/2012	location dry	
wetland 1A	SW-1-1	02/06/2011	20900	6920
		21/10/2011	location dry	
		30/04/2012	location dry	
		29/06/2012	location dry	
		27/08/2012	location dry	
		31/10/2012	location dry	
	SW-1-2	02/06/2011	9730	2270
		21/10/2011	20600	6010
		30/04/2012	11910	3170
		29/06/2012	8720	2010
		duplicate	8720	1990
		27/08/2012	18930	4790
	SW-1-3	02/06/2011	21200	6830
		21/10/2011	36000	11700
		30/04/2012	20200	6330
		29/06/2012	18170	5730
28/08/2012		31000	9910	
		31/10/2012	39000	16200

Notes:

1. na denotes not available.
2. Only select samples collected May 7, 2012 following an extended rain event.

**Table G1:** Surface water EC and Cl results.

Location	Sample ID	Sample Date dd/mm/yyyy	EC ( $\mu$ S/cm)	Cl (mg/L)
wetland 1A continued	SW-1-6	21/10/2011	31900	10200
		30/04/2012	26200	8550
		duplicate	na	8010
		29/06/2012	22100	6710
		27/08/2012	31700	9990
		duplicate	31700	10000
		31/10/2012	location dry	
	SW-1-7	21/10/2011	31900	10200
		30/04/2012	26300	8630
		29/06/2012	21500	6570
		27/08/2012	32500	10300
		31/10/2012	location dry	
	SW-1-9	30/04/2012	20800	6490
		29/06/2012	31500	10200
28/08/2012		48000	16700	
31/10/2012		57600	24300	
wetland 1B	SW-1-4	02/06/2011	13330	3310
		duplicate	na	3270
		21/10/2011	18490	5020
		30/04/2012	14390	3780
		03/07/2012	13450	4150
		28/08/2012	15860	3980
		31/10/2012	17280	4670
	SW-1-5	02/06/2011	6540	1340
		21/10/2011	10070	2170
		30/04/2012	7440	1590
		03/07/2012	6470	1400
		28/08/2012	8660	1980
		30/10/2012	12280	3000
	SW-1-8	30/04/2012	8350	1870
		07/05/2012	6820	1310
		03/07/2012	6900	1440
		27/08/2012	8660	1840
		30/10/2012	13730	3350

## Notes:

1. na denotes not available.
2. Only select samples collected May 7, 2012 following an extended rain event.

**Table G1:** Surface water EC and Cl results.

Location	Sample ID	Sample Date dd/mm/yyyy	EC ( $\mu$ S/cm)	Cl (mg/L)
wetland 1B continued	SW-1-10	03/07/2012	7160	1350
		28/08/2012	8580	1640
		30/10/2012	14080	3250
wetland 2	SW-2	02/06/2011	7230	1680
		21/10/2011	14760	3960
		30/04/2012	10300	2780
		03/07/2012	11360	2830
		27/08/2012	14900	3830
		30/10/2012	20200	5730
	SW-2-2	30/04/2012	14200	3950
		duplicate		3660
		03/07/2012	15770	4390
		27/08/2012	23200	6870
		30/10/2012	location dry	
wetland 3	SW-3	08/06/2011	7270	1680
		duplicate	na	1700
		21/10/2011	14250	3800
		30/04/2012	10340	2730
		03/07/2012	12500	2950
		duplicate	12540	3200
		27/08/2012	15180	4000
		30/10/2012	19390	5530
wetland 4	SW-4	08/06/2011	7430	1790
		21/10/2011	13690	3710
		30/04/2012	9800	2620
		03/07/2012	11940	3010
		duplicate	11940	2910
		27/08/2012	14620	3810
		30/10/2012	17960	5140
		wetland 5	SW-5-1	08/06/2011
duplicate	na			6150
21/10/2011	37300			11700
30/04/2012	26000			8430
29/06/2012	27500			8310
27/08/2012	37700			11700
31/10/2012	location dry			

## Notes:

1. na denotes not available.
2. Only select samples collected May 7, 2012 following an extended rain event.

**Table G1:** Surface water EC and Cl results.

Location	Sample ID	Sample Date dd/mm/yyyy	EC ( $\mu$ S/cm)	Cl (mg/L)
wetland 5 continued	SW-5-2	08/06/2011	19860	6000
		20/10/2011	37700	12000
		30/04/2012	28200	9080
		29/06/2012	24800	7410
		27/08/2012	34900	10100
		duplicate	34900	10800
		31/10/2012	58000	23100
	SW-5-3	20/10/2011	39400	12400
		30/04/2012	26300	8290
		29/06/2012	24800	7350
		duplicate	24800	7260
		27/08/2012	35000	10800
		31/10/2012	44700	15300
	SW-5-4	21/10/2011	40600	12900
		duplicate	na	12900
		30/04/2012	32000	10500
		29/06/2012	27500	8270
		27/08/2012	37500	11700
		30/10/2012	42300	14200
		duplicate	42300	14400
	other wetlands	SW-6	08/06/2011	8830
21/10/2011			9400	2180
30/04/2012			9120	2250
29/06/2012			8000	1790
27/08/2012			9060	2080
30/10/2012			11150	2790
SW-6-2		21/10/2011	9320	2140
		30/04/2012	8900	2190
		03/07/2012	8050	1810
		27/08/2012	8780	2020
		30/10/2012	10320	2550
SW-7		02/06/2011	558	16.3
		duplicate	na	18.2
		21/10/2011	630	22.5
		30/04/2012	439	7.22
		29/06/2012	466	16.9
		27/08/2012	504	23.7
		30/10/2012	location dry	

## Notes:

1. na denotes not available.
2. Only select samples collected May 7, 2012 following an extended rain event.

**Table G1:** Surface water EC and Cl results.

Location	Sample ID	Sample Date dd/mm/yyyy	EC ( $\mu$ S/cm)	Cl (mg/L)
other wetlands continued	SW-8	02/06/2011	559	22.8
		21/10/2011	location dry	
		29/06/2012	1188	14.8
		27/08/2012	location dry	
		30/10/2012	location dry	
	SW-8-2	21/10/2011	575	22.8
		30/04/2012	509	11.5
		29/06/2012	461	14.7
		27/08/2012	524	24.3
		30/10/2012	location dry	
	SW-9	02/06/2011	4040	1100
		21/10/2011	12140	2540
		duplicate	na	2470
		30/04/2012	9550	2120
		duplicate	na	1950
		07/05/2012	5880	1100
		03/07/2012	6000	369
		27/08/2012	7800	1510
	30/10/2012	14870	3670	
	SW-10	02/06/2011	2760	279
21/10/2011		4230	331	
duplicate		na	323	
30/04/2012		3840	242	
03/07/2012		4240	353	
27/08/2012		5090	420	
31/10/2012		6620	623	
SW-11	02/06/2011	4150	396	
	21/10/2011	7190	758	
	30/04/2012	4650	388	
	03/07/2012	5360	506	
	27/08/2012	6510	584	
	duplicate	6500	592	
	31/10/2012	8090	809	

Notes:

1. na denotes not available.
2. Only select samples collected May 7, 2012 following an extended rain event.

**Table G1:** Surface water EC and Cl results.

Location	Sample ID	Sample Date dd/mm/yyyy	EC ( $\mu$ S/cm)	Cl (mg/L)
other wetlands continued	SW-12	02/06/2011	965	66.3
		21/10/2011	1241	138
		duplicate	na	136
		30/04/2012	1353	117
		03/07/2012	1511	130
		duplicate	1511	130
		27/08/2012	1641	160
		31/10/2012	location dry	
	SW-13	08/06/2011	965	73.9
		duplicate	na	71.8
		21/10/2011	996	125
		30/04/2012	957	93.7
		03/07/2012	1054	103
		27/08/2012	1067	129
		30/10/2012	1632	237
SW-14	08/06/2011	476	34.3	
	21/10/2011	location dry		
	30/04/2012	712	44.3	
	03/07/2012	912	98.2	
	duplicate	913	97.9	
	27/08/2012	926	111	
	30/10/2012	location dry		
SW-15	08/06/2011	309	18.4	
	21/10/2011	location dry		
	30/04/2012	498	21.2	
	03/07/2012	606	48.5	
	27/08/2012	645	45.5	
	30/10/2012	location dry		
SW-16	08/06/2011	2230	420	
	21/10/2011	3200	492	
	duplicate	na	497	
	30/04/2012	2340	397	
	03/07/2012	1124	157	
	27/08/2012	1399	225	
	30/10/2012	location dry		

## Notes:

1. na denotes not available.
2. Only select samples collected May 7, 2012 following an extended rain event.

**Table G1:** Surface water EC and Cl results.

Location	Sample ID	Sample Date dd/mm/yyyy	EC ( $\mu$ S/cm)	Cl (mg/L)
other wetlands continued	SW-17	08/06/2011	6000	1610
		duplicate	na	1620
		20/10/2011	10750	2930
		30/04/2012	7410	2010
		29/06/2012	7960	2050
		27/08/2012	10120	2710
		31/10/2012	13690	4040
	SW-18	08/06/2011	1415	274
		20/10/2011	3240	745
		30/04/2012	2180	506
		29/06/2012	2540	559
		27/08/2012	3640	823
		31/10/2012	4950	1300
	SW-19	08/06/2011	2360	207
		21/10/2011	3740	397
		30/04/2012	2480	214
		29/06/2012	3040	300
		27/08/2012	3540	359
		30/10/2012	4820	582
	SW-20	22/07/2011	392	61.2
		duplicate	na	60.7
20/10/2011		location dry		
30/04/2012		location dry		
29/06/2012		222	16.2	
27/08/2012		location dry		
30/10/2012		location dry		
SW-21	22/07/2011	355	52.2	
	20/10/2011	location dry		
	30/04/2012	location dry		
	29/06/2012	302	45.2	
	27/08/2012	location dry		
	30/10/2012	location dry		

Notes:

1. na denotes not available.
2. Only select samples collected May 7, 2012 following an extended rain event.

**Table G1:** Surface water EC and Cl results.

Location	Sample ID	Sample Date dd/mm/yyyy	EC ( $\mu$ S/cm)	Cl (mg/L)
other wetlands continued	SW-22	22/07/2011	7800	1960
		20/10/2011	10360	2450
		30/04/2012	5360	1210
		29/06/2012	6100	1500
		27/08/2012	7070	1730
		duplicate	7090	1730
		30/10/2012	location dry	
	SW-23	22/07/2011	1905	356
		20/10/2011	3950	604
		30/04/2012	2720	476
		29/06/2012	2550	557
		27/08/2012	2990	691
		30/10/2012	location dry	
	SW-24	21/10/2011	10070	2050
30/04/2012		5320	939	
03/07/2012		6570	1380	
27/08/2012		7970	1770	
31/10/2012		13010	3440	
SW-25	21/10/2011	11510	2600	
	duplicate	na	2610	
	30/04/2012	5000	975	
	03/07/2012	6940	1510	
	27/08/2012	8950	2040	
	30/10/2012	14220	3800	
SW-26	21/10/2011	8390	1270	
	30/04/2012	3980	541	
	03/07/2012	5420	1050	
	27/08/2012	6380	1300	
	30/10/2012	9340	2270	
SW-27	21/10/2011	1959	210	
	30/04/2012	1997	183	
	03/07/2012	1926	165	
	31/10/2012	2930	398	

## Notes:

1. na denotes not available.
2. Only select samples collected May 7, 2012 following an extended rain event.

**Table G1:** Surface water EC and Cl results.

Location	Sample ID	Sample Date dd/mm/yyyy	EC ( $\mu$ S/cm)	Cl (mg/L)
other wetlands continued	SW-28	30/04/2012	1078	68.4
		duplicate	na	66.9
		29/06/2012	1660	110
		27/08/2012	1769	126
		31/10/2012	2240	178
		duplicate	2240	184
	SW-29	30/04/2012	3600	603
		03/07/2012	5150	1310
		27/08/2012	6020	1570
		30/10/2012	location dry	
	SW-30	30/04/2012	2980	338
		03/07/2012	3970	660
		27/08/2012	5540	1010
		30/10/2012	location dry	
	SW-31	07/05/2012	6470	1600
		03/07/2012	location dry	
		27/08/2012	location dry	
		30/10/2012	location dry	
	SW-32	07/05/2012	6180	1510
03/07/2012		location dry		
27/08/2012		location dry		
30/10/2012		location dry		
SW-33	07/05/2012	6110	1280	
	03/07/2012	5770	1240	
	27/08/2012	8850	2060	
	30/10/2012	12240	3060	
SW-34	07/05/2012	6700	1240	
	duplicate	na	1230	
	03/07/2012	6450	1240	
	27/08/2012	location dry		
	30/10/2012	location dry		
SW-35	07/05/2012	6010	1100	
	03/07/2012	6100	1140	
	27/08/2012	7840	1610	
	30/10/2012	location dry		

## Notes:

1. na denotes not available.
2. Only select samples collected May 7, 2012 following an extended rain event.

**Table G1:** Surface water EC and Cl results.

Location	Sample ID	Sample Date dd/mm/yyyy	EC ( $\mu$ S/cm)	Cl (mg/L)
other wetlands continued	SW-36	29/06/2012	2380	208
		27/08/2012	location dry	
		30/10/2012	location dry	
	SW-37	03/07/2012	2760	377
		27/08/2012	location dry	
		30/10/2012	location dry	
	SW-38	03/07/2012	7540	1440
		27/08/2012	location dry	
		30/10/2012	location dry	
	SW-39	03/07/2012	7770	915
		27/08/2012	location dry	
		30/10/2012	location dry	
SW-40	03/07/2012	8170	1610	
	27/08/2012	location dry		
	30/10/2012	location dry		

Notes:

1. na denotes not available.
2. Only select samples collected May 7, 2012 following an extended rain event.

**Table G2:** Surface water chemistry results August 2012.

Sample ID	Sample Date dd/mm/yyyy	Temp (°C)	pH (unitless)	Alkalinity as CaCO <sub>3</sub>	Ca	Mg	Na	K	Cl	SO <sub>4</sub>
mill out	28/08/2012	22	8.01	43	1420	601	118000	44500	179000	2930
SW-8-2	27/08/2012	22	9.62	183	23	20	42	44	24	58
SW-14	27/08/2012	22	7.26	258	61	31	48	61	111	23
SW-28	27/08/2012	22	7.36	272	64	101	142	74	126	479

Note:

1. concentration in mg/L unless otherwise noted.

**Table G3:** Surface water Cl and Br results.

Sample ID	Sample Date dd/mm/yyyy	Cl (mg/L)	Br (mg/L)	Cl/Br mass ratio
mill out	29/06/2012	170000	96.7	1758
SW-1-7	21/10/2011	10200	9.35	1091
duplicate	21/10/2011	na	9.01	
SW-1-4	21/10/2011	5020	5.15	975
SW-2	21/10/2011	3960	3.52	1125
SW-4	21/10/2011	3710	3.7	1003
SW-5-4	21/10/2011	12900	11.2	1157
SW-8-2	21/10/2011	22.8	0.06	380
duplicate	21/10/2011	na	0.05	
SW-14	27/08/2012	111	0.27	411
SW-28	27/08/2012	126	0.33	382

Note:

na denotes not available.

APPENDIX H  
GROUNDWATER CHEMISTRY

**Table H1:** Groundwater chemistry results from piezometer sampling.

Location	Sample Date dd/mm/yyyy	Temperature (°C)	EC (µS/cm)	Cl (mg/L)
MW1	19/10/2011	9.5	20500	4740
	duplicate	na	na	4670
	13/06/2012	6.9	21600	4870
	duplicate	na	na	4890
	18/10/2012	8.2	20100	4840
MW2	19/10/2011	11.2	24900	8140
	13/06/2012	6.9	26500	8210
	18/10/2012	8.1	24800	8030
	duplicate	na	na	8020
2008-08	20/10/2011	7.8	11350	1840
	31/10/2012	5.0	10570	1960
2008-09	20/10/2011	9.5	31800	9210
	31/10/2012	5.6	27600	10800
2010-02A	13/11/2012	5.1	14060	6160
2010-02B	13/11/2012	6.1	41200	23700
2010-03A	13/11/2012	4.8	2630	109
2010-03B	13/11/2012	6.0	12220	1950
2010-04	13/11/2012	6.7	24500	8190
2010-06	13/11/2012	6.5	21800	7050

Note:

na denotes not available.